Mechanisms of H_2O_2-induced signal transduction

Heather Ruth Latimer

Thesis submitted for the degree of Doctor of Philosophy

Institute for Cell and Molecular Biosciences

Faculty of Medical Sciences

Newcastle University

September 2016

Declaration

I certify that this thesis is my own work, except where acknowledged. Work in this thesis has not been previously submitted for another degree or qualification at this or any other university.

The work in this thesis is also supported by the publication:

Latimer, H.R. and Veal, E.A. (2016) 'Peroxiredoxins in Regulation of MAPK Signalling Pathways; Sensors and Barriers to Signal Transduction', *Mol Cells*, 39(1), pp. 40-5.

Acknowledgements

Firstly, I would like to greatly thank my supervisor, Elizabeth Veal, for her invaluable help, advice and support over the past four years. I would also like to thank all the past and present members of the Morgan, Quinn and Whitehall labs for their help, but most importantly their friendship. It has made my time at Newcastle University such an enjoyable experience and it wouldn't have been the same without you all. A huge thank you to Alex, Alison, Csenge, Ellen, Faye C, Faye M, Johny, Lewis, Melanie, Pippa and Zoe. A special mention to Clare, who has been a great friend from day one of our undergraduate course. I would also like to thank the Biotechnology and Biological Sciences Research Council (BBSRC) for funding this research, Emily Holmes (University of Manchester) for performing the mitochondrial enrichment, and Tobias Dansen (Utrecht University) for carrying out the mass spectrometry and computational analysis. I am extremely lucky to have the support from my Grandma, Grandpa, Nana and Grandad, who have helped me through the most stressful times of my studies with their love and encouragement. Finally, I would like to thank my Mum, my Dad and my sister Bethany, who have had to deal with the ups and downs that have accompanied the past few years. I honestly couldn't have achieved everything that I have without your continuous love, support and encouragement.

Abstract

Reactive oxygen species (ROS), including H_2O_2, are produced as unavoidable by-products of aerobic respiration, leading to oxidative stress and the initiation and development of many diseases, particularly age-associated diseases. Cells have evolved antioxidant and repair enzymes to protect against ROS, including the 2-Cys peroxiredoxins (Prx) family, a group of extremely abundant, highly conserved peroxidases. H_2O_2 initiates protective cell responses that include increasing expression of these enzymes. Counterintuitively, typical 2-Cys Prx have also been shown to have important roles in promoting stress-induced signal transduction, and as molecular chaperones, independent of their thioredoxin peroxidase activity.

Although H_2O_2's function as a signalling molecule is now well-established, the targets of H_2O_2 signals and the mechanisms by which these targets are regulated are poorly characterised. Studies in yeast models have provided some of the best evidence to date for the positive signalling roles of low levels of H_2O_2 to drive adaptive responses to limit damage. For example, in the fission yeast *Schizosaccharomyces pombe*, different levels of H_2O_2 activate distinct signal transduction pathways and transcriptional responses that protect cells against the toxic effects of increased ROS. Previous work has established that the single typical 2-Cys Prx, Tpx1, is essential for H_2O_2-induced gene expression. In *S. pombe*, Tpx1 is needed to promote the H_2O_2-induced activation of the AP-1-like transcription factor Pap1 and the p38/JNK related mitogen activated protein kinase (MAPK), Sty1, by mechanisms involving oxidation of cysteine residues. The overall aim of this project was to use biochemical and genetic approaches to investigate the molecular mechanisms underlying H_2O_2-sensing in the genetically amenable model organism, *S. pombe*.

In this study we have identified that Tpx1 stimulates inactivation of the protein tyrosine phosphatase (PTP) Pyp1, to promote activation of the Sty1 pathway in response to low concentrations of H_2O_2. We have identified that Pyp1 undergoes multiple post-translational modifications, including oxidation and

phosphorylation in response to H_2O_2. We have examined the role of these modifications in regulating H_2O_2-induced activation of Sty1, identifying that H_2O_2-induced formation of a disulphide with thioredoxin, and stress-induced phosphorylation by the MAPKK Wis1, are important for maintaining Pyp1 function in cells exposed to increasingly stressful conditions. Moreover, we have also investigated the relationship between related PTP in the control of H_2O_2-induced Sty1 activation, identifying an unexpected role for Pyp1 in promoting the expression of the stress-induced PTP, Pyp2.

Oxidation of the catalytic cysteine in the glycolytic GAPDH enzyme, Tdh1, has previously been shown to be important for H_2O_2-induced activation of Sty1. Indeed, GAPDH's susceptibility to H_2O_2-induced oxidation of its catalytic cysteine has been proposed to have evolved as an important protective response to H_2O_2. Here we show that although a second cysteine in the active site of Tdh1 is important for the H_2O_2-induced oxidation of Tdh1 and oxidative stress resistance, this oxidation is not important for the H_2O_2-induced activation of Sty1.

Having found that Tpx1 is required for the oxidation of Pap1, Sty1, Pyp1 and Tdh1, we have also investigated whether Tpx1 act as direct H_2O_2 transducers to promote the oxidation of these and other proteins. This has provided further insight into the mechanisms involved in activation of Pap1, and also identified many potential new candidates for Tpx1-dependent regulation by H_2O_2. These include a conserved MAPK activated kinase, Srk1, that we show inhibits cell cycle progression by a mechanism that is partially dependent on Tpx1.

In summary, this study has identified new mechanisms involved in protective responses to increases in H_2O_2. In particular, it has provided new insight into how cells regulate the activity of stress-activated MAPK and GAPDH to coordinate appropriate responses to rises in ROS.

Contents

List of Figures

List of Tables

List of Appendices

List of Abbreviations

1°	Primary
2°	Secondary
2-Cys Prx	2-cysteine peroxiredoxin
°C	Degrees celcius
Δ	Gene deletion strains
Amp^+	Ampicillin resistant
AMS	4-acetamido-4'-maleimidylstilbene-2,2'-disulphonic acid
AP	Alkaline phosphatase
AP-1	Activating protein-1
ASK1	Apoptosis signal-regulating kinase
Asn	Asparagine
Asp	Aspartic acid
Atf1	Activating transcription factor 1
ATP	Adenosine triphosphate
β-ME	β-mercaptoethanol
BSA	Bovine serum albumin
b-ZIP	Basic leucine zipper
C. albicans	*Candida albicans*
cAMP	Cyclic adenosine monophosphate
C. elegans	*Caenorhabditis elegans*
CESR	Core environmental stress response
CRD	Cysteine rich domain
Cys	Cysteine
Cys-SH	Reduced cysteine
Cys-SOH	Cysteine sulphenic acid
Cys-SO_2H	Cysteine sulphinic acid
Cys-SO_3H	Cysteine sulphonic acid
DAPI	4',6-diamidino-2-phenylindole
DMSO	Dimethyl sulphoxide
DNA	Deoxyribonucleic acid

D. melanogaster	*Drosophila melanogaster*
E. coli	*Escherichia coli*
EDTA	Ethylenediaminetetraacetic acid
EMM	Edinburgh minimal media
EMM½G	Edinburgh minimal media with half glutamate
ER	Endoplasmic reticulum
ERK	Extracellular signal-regulated kinase
ETC	Electron transport chain
EtOH	Ethanol
FITC	Fluorescence immunoglobulin conjugate
G	Gram
GAPDH	Glyceraldehyde-3-phosphate dehydrogenase
GFP	Green fluorescent protein
Gpx	Glutathione peroxidase
Grx	Glutaredoxin
GSH	Reduced glutathione
GSSG	Oxidised glutathione dimer
GST	Glutathione-*S*-transferase
G3P	Glyceraldehyde-3-phosphate
HMW	High molecular weight
HO·	Hydroxyl radical
Hog1	High osmolarity glycerol 1
HRP	Horse radish peroxidase
H_2O_2	Hydrogen peroxide
IAA	Iodoacetamide
iBAC	Intensity based absolute quantification
IMS	Intermembrane space
IPTG	Isopropyl β-D-1-thiogalactopyranoside
JNK	c-Jun N-terminal kinase
Kan	Kanamycin
Kb	Kilobase
kDa	Kilodalton

LB	Luria broth
LFQ	Label free quantification
LiAc	Lithium acetate
LMW	Low molecular weight
M	Molar
MAPKAP	Mitogen activation protein kinase-activated protein
MAPK	Mitogen activated protein kinase
MAPKK	Mitogen activated protein kinase kinase
MAPKKK	Mitogen activated protein kinase kinase kinase
MeOH	Methanol
MIA	Mitochondrial intermembrane space assembly machinery
MTS	Mitochondrial targeting sequence
µg	Microgram
MKP	Mitogen activation protein kinase phosphatase
µM	Micromolar
mg	Milligram
mM	Millimolar
mtDNA	Mitochondrial DNA
MTS	Mitochondrial targeting sequence
NAC	*N*-acetyl cysteine
NADPH	Nicotinamide adenine dinucleotide phosphate
NEM	*N*-Ethylmaleimide
NES	Nuclear export signal
nM	Nanomolar
$O_2 \cdot^-$	Superoxide anion
OD	Optical density
OH·	Hydroxyl radical
ORF	Open reading frame
OS	Oxidative stress
OSR	Oxidative stress response
oxLDL	Oxidised low density lipoprotein
PAGE	Polyacrylamide gel electrophoresis

PANTHER	Protein Analysis THrough Evolutionary Relationships
Pap1	*Pombe* AP-1 like
PCR	Polymerase chain reaction
PDI	Protein disulphide isomerase
PEG	Polyethene glycol
PIP_3	Phosphatidylinositol 3,4,5 trisphosphate
PLB	Pombe lysis buffer
PMSF	Phenylmethylsulfonyl fluoride
PP2C	Protein phosphatase 2C
PPP	Pentose phosphate pathway
Prx	Peroxiredoxin
Ptc1/2/3/4	Protein phosphatase 2C 1/2/3/4
PTEN	Phosphatase and tensin homolog
PTK	Protein tyrosine kinase
PTP	Protein tyrosine phosphatase
Pyp1/2	Protein tyrosine phosphatase 1/2
RNS	Reactive nitrogen species
RNA	Ribonucleic acid
ROS	Reactive oxygen species
rpm	Revolutions per minute
SAPK	Stress activated protein kinase
S. cerevisiae	*Saccharomyces cerevisiae*
SDS	Sodium dodecyl sulphate
SDS-PAGE	Sodium dodecyl sulphate polyacrylamide gel electrophoresis
Ser	Serine
SH	Thiol
SOD	Superoxide dismutase
SOH	Sulphenic acid
SOOH	Sulphinic acid
SOOOH	Sulphonic acid
S. pombe	*Schizosaccharomyces pombe*
Srk1	Sty1-regulated kinase

Srx	Sulphiredoxin
ssDNA	Salmon sperm DNA
t-BOOH	*tert*-butyl hydroperoxide
TBST	Tris-buffered saline tween
TCA	Tricholoracetic acid
Tdh1	Triose-phosphate dehydrogenase 1
Thr	Threonine
TNF-α	Tumour necrosis factor-α
TOM	Translocase of the outer membrane
Tpx	Thioredoxin peroxidase
Trr	Thioredoxin reductase
Trx	Thioredoxin
Tsa	Thiol-specific antioxidant
TTC	2,3,5-triphenyltetrazolium
Tyr	Tyrosine
UV	Ultraviolet
Wis1	Win1 suppressor 1
WT	Wild-type
X-gal	5-bromo-4-chloro-3-indolyl β-D-galactopyranoside
Yap1	Yeast AP-1
YE5S	Yeast extract media with five supplements

CHAPTER 1

1. Introduction

1.1 Sources of reactive oxygen species

Reactive oxygen species (ROS) are damaging, highly reactive, reduced forms of oxygen, produced in a wide range of physiological processes. Exposure of cells to high levels of ROS causes damage to intracellular constituents, including DNA, proteins and lipids, leading to pathology associated with various diseases and ageing (Gutteridge and Halliwell, 1999). Consequently, there is a strong evolutionary pressure to evolve mechanisms to protect against ROS-induced damage. These include increasing the expression of ROS-detoxifying enzymes and repair mechanisms in response to increased ROS levels. However, in multicellular organisms they can also include activating cell death mechanisms to prevent organismal damage. In eukaryotes, many of these processes are mediated by activation of conserved mitogen activated protein kinase (MAPK) signalling pathways. However, more recently, other positive signalling roles have been identified for low levels of certain ROS in regulating a variety of cellular processes, including cell division, migration, differentiation, and the initiation of the oxidative stress response to protect against damage (For a review see (Veal and Day, 2011)). Therefore, the study of the cellular response and the protective mechanisms following ROS-induced damage is important in understanding the cause and development of many diseases. In addition, further studies into the biphasic response to H_2O_2 is important to further elucidate the mechanisms by which cells respond to ROS, where low and high levels of H_2O_2 have different biological effects, discussed further in section 1.2.2 (For reviews see (Finkel, 2011; Veal and Day, 2011)).

The partial reduction of molecular oxygen generates metabolites of oxygen, for example, superoxide anion ($O_2^{\bullet -}$), hydroxyl radicals ($OH^{\bullet}$), and hydrogen peroxide (H_2O_2), which are more reactive than

oxygen, discussed in section 1.1.1. ROS can be produced in the mitochondria as by-products of aerobic respiration. Mitochondrion are the primary site of aerobic metabolism, and proposed to be the most important intracellular source of ROS due to partially reduced oxygen species leaking out of the electron transport chain (ETC) during respiration (Gutteridge and Halliwell, 1999; Bokov *et al.*, 2004). However, ROS can also be produced during oxidative protein folding in the endoplasmic reticulum (ER) (Winterbourn and Hampton, 2008), and through many metabolic redox reactions including fatty acid oxidation, as by-products of metabolic reduction reactions, such as cytochrome P450 (Gutteridge and Halliwell, 1999), and through enzymatic sources including NADPH oxidases (Winterbourn and Hampton, 2008). NADPH oxidases reduce oxygen to superoxide, and due to their wide tissue distribution, provided some of the first evidence that ROS could function as signalling molecules (Winterbourn and Hampton, 2008).

Although the major sources of ROS occur as a result of normal metabolic processes, ROS can also be generated exogenously following exposure to xenobiotics or irradiation by UV light and X-rays (Gutteridge and Halliwell, 1999).

1.1.1 Reactive oxygen species

The superoxide anion ($O_2^{\bullet -}$) is produced in aerobic cells following the addition of one electron to oxygen, reducing O_2 to $O_2^{\bullet -}$. A major source of $O_2^{\bullet -}$ is due to the leakage of electrons from the ETC, for example by cytochrome *c* oxidase in the mitochondria. Biochemical reactions catalysed by enzymes such as NADPH oxidase in phagocytic immune cells also produce $O_2^{\bullet -}$ (Halliwell and Gutteridge, 1985).

Following the formation of $O_2^{\bullet -}$, the addition of a second electron produces the peroxide ion ($O_2^{\bullet 2-}$). However, at physiological pH, $O_2^{\bullet 2-}$ will become protonated, forming hydrogen peroxide (H_2O_2) and oxygen. H_2O_2 is produced in the cytoplasm through a dismutation reaction, catalysed by superoxide dismutase (SOD), but can also be produced non-enzymatically, for example by phagocytic immune cells in response to invasion by foreign particles (Halliwell and Gutteridge, 1984a). High concentrations of H_2O_2 cause oxidative damage through DNA damage, protein oxidation, and lipid peroxidation,

however at low concentrations, H_2O_2 is also utilised as an effective signalling molecule, regulating a variety of cellular processes.

There are numerous reactions which produce hydroxyl radicals (OH·); (i) heat treatment or ionising radiation produces two OH· from H_2O_2, (ii) H_2O_2 is degraded to OH· in the metal-catalysed Fenton reaction, and (iii) combining the superoxide-catalysed reduction of Fe(III) to Fe(II) and oxygen, in the Haber-Weiss reaction, with the Fenton reaction, produces OH·. OH· are extremely reactive, participating in three types of reaction; (i) hydrogen atom abstraction, (ii) addition onto other molecules, and (iii) electron transfer, and thus readily react with biological molecules close to their site of generation. For example, OH· can initiate lipid peroxidation by hydrogen atom abstraction. As the reaction of H_2O_2 with metal salts, Cu(I) and Fe(II), produces highly reactive OH·, the level of free metals and H_2O_2 are tightly regulated (Halliwell and Gutteridge, 1984b).

1.2 Biological roles of ROS

1.2.1 The role of ROS-induced damage in ageing and disease

ROS can cause structural damage to DNA, proteins and lipids, but also cause modifications in redox-sensitive signalling pathways, implicated in the inhibition of apoptosis and tumourigenesis. In addition, oxidative damage to DNA can lead to carcinogenesis, and indeed, oxidative modifications have been implicated in the initiation, promotion and progression of many malignancies (Cooke *et al.*, 2003; Valko *et al.*, 2004). Oxidative stress is defined as an imbalance between the generation and destruction of ROS, and has been implicated in numerous human disease states, including atherosclerosis, cancer, cardiovascular disease, chronic inflammatory diseases, diabetes and neurodegenerative disease (For reviews see (Berlett and Stadtman, 1997; Cooke *et al.*, 2003; Ischiropoulos and Beckman, 2003; Valko *et al.*, 2004)).

Harman's 'oxidative stress theory of ageing' proposes that due to the production of ROS within living cells, macromolecules accumulate oxidative damage, ultimately promoting ageing within the organism (Harman, 1956). As the organism aged, the accumulated damage was predicted to impair cellular functions, finally leading to age-related diseases (Harman, 1956). Various studies have provided evidence in support of Harman's theory that levels of oxidative damage increase with age. It has been demonstrated that some long-lived animals have reduced levels of oxidative damage, correlating to increased resistance to oxidative stress (Dudas and Arking, 1995). Indeed, studies in *Caenorhabditis elegans* and *Drosophila melanogaster* have provided evidence for a link between life span and increased stress resistance (For a review see (Finkel and Holbrook, 2000)). However, the role of ROS in ageing is still not clear, and many recent studies are inconsistent with Harman's theory, suggesting that changes in ROS levels do not alter longevity as expected. Calorie restriction induces mitochondrial metabolism and extends life span in many species and model organisms, including mice, *Saccharomyces cerevisiae*, and *D. melanogaster*. Interestingly, in *C. elegans*, mitochondrial mutants have increased generation of superoxide, which is both necessary and sufficient for longevity, suggesting that superoxide can trigger cellular changes or mechanisms to attenuate the effects of ageing (Yang and Hekimi, 2010). The theory of 'mitohormesis' proposes that increased mitochondrial ROS production is required for extended lifespan, and can over-activate protective mechanisms, such as antioxidants. Furthermore, when antioxidants prevent the ROS signal, lifespan is reduced, indicating that ROS are essential for health and longevity. However, mitohormesis cannot explain why overexpression of protective mechanisms is not sufficient to extend lifespan, or why overexpression of protective mechanisms suppresses lifespan extension in models with increased levels of ROS. The role of mitochondrial ROS in the onset of ageing and age-related diseases is still unclear; whilst old data supported Harman's oxidative stress theory of ageing, more recent studies are inconsistent with this concept and indicate that ROS can extend lifespan in lower organisms such as worms or flies. In addition, the source of ROS involved in lifespan extension seems organism-specific; superoxide

appears to be the key ROS to extend lifespan in worms, whereas H_2O_2 appears to be key to extend lifespan in flies (For reviews see (Ristow and Zarse, 2010; Sanz, 2016)).

1.2.2 Physiological roles of low levels of ROS

In addition to the evidence suggesting that ROS can promote longevity, discussed in section 1.2.1, there is now substantial evidence that ROS have positive functions in many normal physiological processes. For example, although it has long been appreciated that NADPH oxidases are important in immune cells to generate superoxide and kill target cells, the discovery that they are also expressed in other tissues first suggested another physiological role for these ROS-generating systems (Geiszt and Leto, 2004). Further evidence in support of this was provided by the finding that NADPH oxidases are activated in response to growth factors and that low levels of ectopic H_2O_2 are able to stimulate the growth of cultured mammalian cells (Geiszt and Leto, 2004). In particular, recent years have provided increasing evidence for positive roles for low levels of H_2O_2 (Veal *et al.*, 2007; Winterbourn, 2008). There is now a general acceptance that, although high levels of H_2O_2 are harmful and can lead to cell damage, low levels of H_2O_2 can be beneficial to drive responses important for normal health and longevity, and in the initiation of many biological responses (For reviews see (Finkel, 2011; Veal and Day, 2011)). Several studies have provided evidence to support the important role of low levels of ROS in downstream signalling. For instance, treatment of bovine chondrocytes with the cytokines interleukin 1 (IL-1) and tumour necrosis factor α (TNFα) stimulates the production of ROS, which induces the expression of the MAPK, c-Jun N-terminal kinases (JNK), leading to a rapid induction of JNK activity (Lo *et al.*, 1996). Furthermore, serotonin causes an increase in the formation of the superoxide anion, and is able to stimulate the phosphorylation and activation of the MAPK, extracellular signal-regulated kinase (ERK), ERK1 and ERK2, in smooth muscle cells (Lee *et al.*, 1999). The addition of platelet derived growth factor (PDGF) in vascular smooth muscle cells produces a rapid rise in ROS levels, essential for downstream PDGF signalling (Sundaresan *et al.*, 1995). ROS defences must therefore maintain the concentration of ROS at a level to permit signalling, and initiate responses

important for adaptation to stress conditions, but prevent any associated damage. However, the molecular mechanism by which cells sense and respond to ROS is poorly understood. Understanding these mechanisms will allow us to further understand how physiological responses are regulated.

1.3 ROS-removing activities

In all cells there is a balance between the production of ROS, and the destruction of ROS by endogenous defence systems, including both enzymatic and non-enzymatic defences. Enzymatic defences consist of small molecules and antioxidant enzymes, including peroxiredoxins (Prx). Non-enzymatic defences consist of dietary antioxidants, such as Vitamin C (ascorbic acid) and Vitamin E (α-tocopherol), which function as scavenging molecules to detoxify free radicals and ROS (Chaudiere and Ferrari-Iliou, 1999). A low level of continuous antioxidant expression maintains intracellular redox homeostasis. In response to ROS, there is an increase in the production of antioxidant enzymes to remove ROS before they are able to cause oxidative damage (Gutteridge and Halliwell, 1999; Bokov *et al.*, 2004). As will be discussed, along with protecting against damage, these antioxidants inevitably interfere with the signalling functions of ROS. However, strikingly, in the case of one group of thioredoxin peroxidases, that will be discussed in detail, rather than inhibiting signal transduction, this can be a positive role in transducing the H_2O_2 signal (see section 1.5).

1.3.1 Superoxide dismutase

Superoxide dismutase (SOD) catalyses the dismutation of superoxide ($O_2^{\bullet -}$) to H_2O_2 and oxygen. SODs are highly concentrated in the cell, highlighting their importance to detoxify highly reactive superoxide (Chaudiere and Ferrari-Iliou, 1999). There are multiple SOD isoforms, grouped according to their metal centre and amino acid constituency (Valko *et al.*, 2006). There are at least two intracellular SODs in most eukaryotic cells; (i) Mn SOD functions in the mitochondria, and (ii) Cu/Zn SOD, the major isoform,

which functions in the cytoplasm to protect the cell from superoxide (Jamieson, 1998; Chaudiere and Ferrari-Iliou, 1999).

Similar to higher eukaryotes, the fission yeast *Schizosaccharomyces pombe* contains two types of SOD. The expression of the *S. pombe* mitochondrial Mn SOD is induced by superoxide generators, high osmolarity and heat. The expression of the *S. pombe* cytoplasmic Cu/Zn SOD is regulated by various metal ions and by the transcription factor Pap1, however superoxide-generating menadione did not affect the expression of Cu/Zn SOD (Lee *et al.*, 2002b).

1.3.2 Catalase

Catalase functions to detoxify H_2O_2 into oxygen and water, through a dismutation reaction. Catalase is a homotetrameric heme-containing enzyme, with one of the highest catalytic rates of all enzymes (Valko *et al.*, 2006). The majority of catalase localises to the peroxisomes in mammalian cells, where there are high H_2O_2 concentrations, however catalase also localises to the mitochondrial matrix (Chaudiere and Ferrari-Iliou, 1999).

Disrupting the catalase gene in *S. pombe* causes this mutant to completely lack catalase activity, and become more sensitive to H_2O_2 than the parent strain. Catalase in *S. pombe* plays an important role in resistance to high concentrations of H_2O_2, but offers little protection from H_2O_2 generated in small amounts under normal growth conditions (Mutoh *et al.*, 1999).

1.3.3 Glutathione peroxidase

Using reducing power provided by NADPH, glutathione (GSH) and glutathione reductase, glutathione peroxidases (Gpx) reduce H_2O_2 and other hydroperoxides, providing an enzymatic defence against oxidative stress (Michiels *et al.*, 1994). Mammalian cells contain classical Gpx and phospholipid hydroperoxide Gpx (PHGpx) (Roveri *et al.*, 1994). On the other hand, the budding yeast *S. cerevisiae*, does not contain any classical Gpx, but contains three PHGpx, encoded by GPX1-3 (Inoue *et al.*, 1999; Avery and Avery, 2001). Purified glutaredoxins, Grx1 and Grx2, in *S. cerevisiae* have glutathione

peroxidase activity, suggesting that Grx1 and Grx2 share an overlapping function with Gpx1-3 in protecting against H_2O_2 (Collinson *et al.*, 2002; Collinson and Grant, 2003). One Gpx has been identified in *S. pombe*, Gpx1, homologous with many glutathione peroxidase genes. Gpx1 acts as a thioredoxin-dependent peroxidase, especially in stationary phase, and is crucial to the long-term survival of fission yeast (Lee *et al.*, 2008).

1.3.3.1 Glutathione

Reduced glutathione (GSH) is a tripeptide (γ-L-glutamylcystinylglycine), with roles in a variety of cellular processes, including the detoxification of carcinogens, mutagens and ROS (Meister, 1988; Sies, 1993), but also as a cofactor for many enzymatic antioxidants, such as glutathione S-transferases (GST), glutathione peroxidases (Gpx) and glutaredoxins (Grx). Therefore, the cellular levels of GSH are tightly controlled to avoid a redox imbalance. A cysteine residue in the low molecular weight thiol, GSH, reacts with oxidants to produce a thiyl radical (GS·), which dimerises to produce the non-reactive, oxidised glutathione dimer (GSSG) (For reviews see (Hayes *et al.*, 1996; Jamieson, 1998; Chaudiere and Ferrari-Iliou, 1999; Valko *et al.*, 2004; Valko *et al.*, 2006)). Glutathione is able to affect the redox status of cysteine residues, by reacting with protein thiol groups and forming a mixed disulphide bond between the protein and GSH. Previous studies have demonstrated that S-glutathionylation acts to protect proteins from irreversible oxidation and inactivation (Grant, 2001). Glutathione has also been shown to regulate redox signalling events, through alterations in the levels of total GSH, and the GSH/GSSG ratio (Valko *et al.*, 2006). The high prevalence of GSH over GSSG causes the intracellular milieu to be a reducing environment, however the presence of ROS alters this redox homeostasis.

The glutaredoxin system consists of glutaredoxin (Grx), a small heat-stable oxidoreductase, which is oxidised by substrates, and reduced by glutathione, using electrons donated by NADPH. Following the reduction of Grx, oxidised glutathione is then regenerated by glutathione reductase, in an NADPH-dependent reaction (Fernandes and Holmgren, 2004). Grx can function as a protein disulphide reductase, reducing disulphide bonds in proteins such as ribonucleotide reductase (RNR) and

glutathione (Wheeler and Grant, 2004). Deletion of Grx in *S. cerevisiae* and *S. pombe* causes cells to become hypersensitive to H_2O_2 and *t*-BOOH, suggesting that Grx protects against oxidative stress (Collinson *et al.*, 2002; Wheeler and Grant, 2004).

1.3.4 Thioredoxin peroxidase

Peroxiredoxins (Prx) are a family of extremely abundant, highly conserved thioredoxin peroxidase antioxidant enzymes (Wood *et al.*, 2003a; Wood *et al.*, 2003b; Rhee *et al.*, 2005), involved in the detoxification of H_2O_2, peroxynitrite and other hydroperoxides. Prx have been identified in yeast, mammals, bacteria, algae, higher plants and parasites (For reviews see (Hofmann *et al.*, 2002; Wood *et al.*, 2003a; Wood *et al.*, 2003b; Rhee *et al.*, 2005)). Prx are primarily located in the cytoplasm, however they have also been shown to be present in the mitochondria, peroxisomes and nucleus in eukaryotes (Wood *et al.*, 2003b). Similar to Gpx, Prx utilise redox-active cysteine residues for the reduction and detoxification of peroxides, including H_2O_2, however the oxidised Prx and Gpx are reduced by different electron donors.

There are three classes of structurally different Prx, grouped according to the number of cysteine residues involved in their catalytic mechanism: typical 2-Cys, atypical 2-Cys, and 1-Cys Prx (Wood *et al.*, 2003b). All three classes of Prx share the same initial catalytic mechanism, involving a reaction between the peroxidatic cysteine residue of the Prx and the peroxide, generating a sulphenic acid (Wood *et al.*, 2003b). The largest group of Prx, typical 2-Cys Prx, employ two catalytically-active cysteine residues in their role to reduce H_2O_2 (Figure 1.1). Under non-stressed conditions, non-covalent dimers of typical 2-Cys Prx interact to form decamers. Once the peroxidatic cysteine thiol has become oxidised by H_2O_2 to a sulphenic acid, the sulphenic acid then reacts with the resolving cysteine of a neighbouring Prx molecule and becomes stabilised due to the formation of an intermolecular disulphide bond. The 2-Cys Prx is restored to its original active redox state through the thioredoxin system; the disulphide bond between the two catalytic cysteines becomes reduced by thioredoxin (Trx) (Wood *et al.*, 2003b).

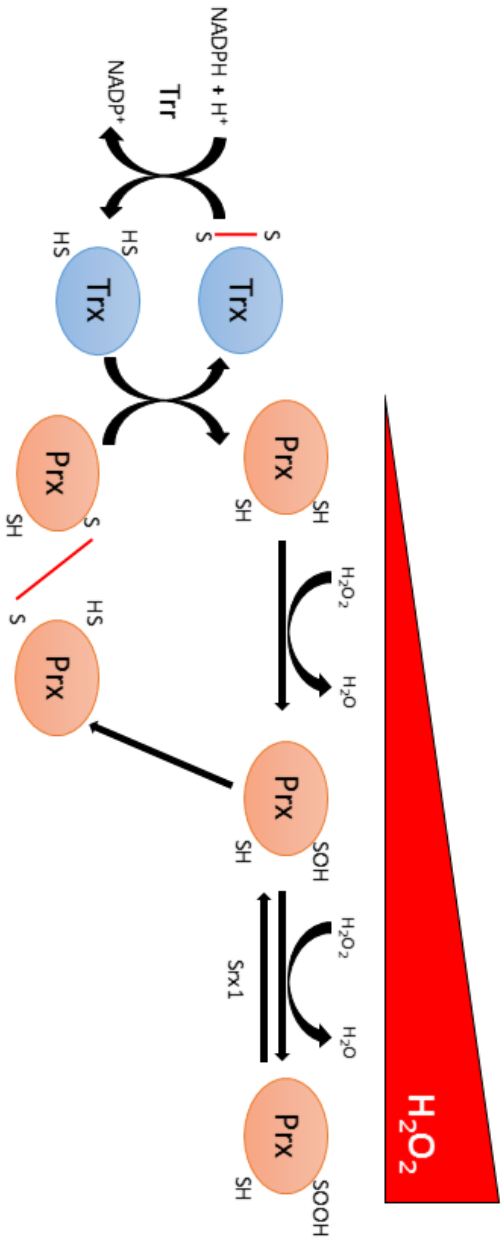

Figure 1.1 Catalytic mechanism of typical 2-Cys peroxiredoxins (2-Cys Prx). The peroxidatic cysteine residue becomes oxidised by H_2O_2 to form a sulphenic acid derivative (-SOH). Prx then form homodimers due to a disulphide bond (red bar) forming between the peroxidatic cysteine and the resolving cysteine of a neighbouring Prx. The disulphide bond between the catalytic cysteine residues can be reduced by thiols, such as thioredoxin (Trx), by thioredoxin reducatase (Trr) using electrons from NADPH, restoring the activity of 2-Cys Prx. At high concentrations of H_2O_2, the peroxidatic cysteine can become hyperoxidised to a sulphinic acid (-SOOH), inactivating the thioredoxin peroxidase activity of 2-Cys Prx. The sulphinic form of the Prx cannot be reduced by Trx, but instead is reduced by the sulphiredoxin (Srx1) (Adapted from Taylor, 2009).

In response to higher concentrations of H_2O_2, the sulphenic acid derivative of eukaryotic, but not prokaryotic, 2-Cys Prx becomes oxidised further to sulphinic and sulphonic acid derivatives, termed hyperoxidised. This hyperoxidation inactivates the thioredoxin peroxidase activity of the 2-Cys Prx (Woo *et al.*, 2003; Wood *et al.*, 2003b). Most prokaryotic 2-Cys Prx are much more resistant to hyperoxidation, as exemplified by the *Salmonella typhimurium* Prx, AhpC, which requires 100-fold more H_2O_2 than human Prx1 (Wood *et al.*, 2003b). The hyperoxidised cysteine cannot be reduced by thioredoxin, however enzymes have been identified in *S. pombe*, *S. cerevisiae* (Biteau *et al.*, 2003), higher plants (Liu *et al.*, 2006), cyanobacteria (Boileau *et al.*, 2011), and mammalian cells (Budanov *et al.*, 2004) which are able to catalyse the reduction of the sulphinic acid. These tightly regulated enzymes are termed sulphiredoxins (Srx1), and catalyse the reduction of the sulphinic acid in typical 2-Cys Prx, dependent on ATP hydrolysis, Mg^{2+} or Mn^{2+}, and a thiol reductant. Srx1 specifically catalyses the reduction of hyperoxidised cysteine residues in typical 2-Cys Prx, as sulphinic acids in other proteins, such as atypical 2-Cys Prx, 1-Cys Prx and GAPDH, cannot be reduced by Srx1 (Woo *et al.*, 2005).

1.3.4.1 Thioredoxin

Thioredoxin (Trx) is a small oxidoreductase with broad substrate specificity, and contains the "thioredoxin motif" (active site sequence, CGPC). Trx acts to maintain a reduced intracellular state, allowing it to function as a protein disulphide reductase to repair many oxidatively damaged proteins, including transcription factors and signalling molecules. Trx is also a vital cofactor for many enzymes, including methionine sulphoxide reductase (Mxr1), which is important for repairing oxidative damage. In addition, Trx can act as an electron donor, reducing disulphide bonds in the catalytic cycle of ribonucleotide reductase (RNR), and can act as hydrogen donor for PAPS reductase, which converts 3'-phosphoadenosine 5'-phosphosulphate (PAPS) to sulphite (Gonzalez Porque *et al.*, 1970a; Gonzalez Porque *et al.*, 1970b). The role of Trx as an electron donor and in reducing disulphide bonds has been shown to be a key event in the regulation of important processes including signal transduction,

apoptosis and gene expression. Trx reduces oxidised cysteine residues through interaction with conserved cysteine residues in its active site sequence. Following the reduction of its substrate, Trx becomes oxidised through the formation of an intramolecular disulphide bond, which is reduced by thioredoxin reductase (Trr) and NADPH, reactivating Trx. The major substrate for Trx is the thioredoxin peroxidase/peroxiredoxin, allowing Trx to act as an antioxidant enzyme and protect the cell from ROS-induced damage (For a review see (Holmgren *et al.*, 2005)).

S. cerevisiae contains two cytoplasmic Trx, TRX1 and TRX2, which are dispensable during normal growth conditions, and one mitochondrial Trx, TRX3 (Gan, 1991; Muller, 1991). TRX2 acts as the predominant antioxidant during stationary phase growth to protect against oxidative stress, as deletion of TRX2 causes cells to become hypersensitive to hydroperoxides (Garrido and Grant, 2002). However, the thioredoxin isoenzymes have redundant activities as antioxidants, which is required for both the survival of yeast cells, along with protection against oxidative stress during stationary phase growth (Garrido and Grant, 2002).

The genome of *S. pombe* encodes one cytoplasmic Trx, Trx1, and one mitochondrial Trx, Trx2 (Lee *et al.*, 2002). In fission yeast, the expression of Trx1 is moderately induced by H_2O_2 and other environmental stresses, while Trx2 is not. Consequently, *trx1*$^+$ is considered to be part of the core environmental stress response (CESR) in *S. pombe* (Chen *et al.*, 2003). In addition, *S. pombe* contains a novel thioredoxin-like protein, Txl1, which participates in the cellular protection against oxidative stress induced by alkyl hydroperoxide. The domain organisation of *S. pombe* Txl1 is identical to the human orthologue and other reported orthologues, having a thioredoxin-like N-terminal domain, followed by a C-terminal domain, which has been suggested to be a regulatory domain (Jin *et al.*, 2002).

The thioredoxin system consists of a Tpx/Prx, Trx, Trr and NADPH, functioning to control redox homeostasis (Holmgren and Lu, 2010). The thioredoxin system is present within all domains of life,

conserved from bacteria and yeast to higher eukaryotes. The high conservation suggests the thioredoxin system may therefore regulate a variety of cellular processes and disease states.

1.4 Mechanisms of ROS-induced signal transduction

1.4.1 Oxidative modification of proteins

Cellular signal transduction pathways can become initiated by the oxidation of thiol-containing proteins, causing reversible oxidative post-translational modifications such as S-glutathionylation, S-nitrosylation, and the formation of intramolecular and intermolecular disulphide bonds, often resulting in a change to the activity of the protein. Irreversible oxidative modification of cysteine residues progresses from reduced cysteine thiols to sulphinic and sulphonic acid derivatives, demonstrated to lead to protein damage (Claiborne *et al.*, 1999; Cabiscol *et al.*, 2000). The accumulation of these oxidatively modified proteins has been associated with numerous age-related diseases (Valko *et al.*, 2006). Redox signalling initiates the activation of stress responses, resulting in a variety of downstream effects, including increased expressed of antioxidants and repair proteins, and initiating the activation of peroxide-induced signal transduction (For reviews see (Aslund and Beckwith, 1999; Linke and Jakob, 2003; Jacob *et al.*, 2004; Janssen-Heininger *et al.*, 2008)). Redox signalling can also be used to regulate normal cellular processes such as cell proliferation and growth in non-stressed cells (For reviews see (Jacob *et al.*, 2004; Biswas *et al.*, 2006; Winterbourn and Hampton, 2008)).

1.4.2 Signalling functions of H_2O_2

H_2O_2 has a relatively long half-life and is a fairly unreactive molecule. H_2O_2 is non-polar and lipid soluble, allowing it to diffuse throughout the cell, as well as being able to cross cellular membranes, where it can act locally. H_2O_2 can selectively oxidise deprotonated cysteine residues, as exemplified by Prx, discussed in section 1.3.4 (Winterbourn and Hampton, 2008). The oxidation state of cysteines

can be transferred from a redox-active sensor protein, such as Prx, to target oxidation-sensitive signalling proteins, making H_2O_2 well suited as a signalling molecule, discussed further in section 1.5. Thiol-containing proteins demonstrate different sensitivities for reaction with H_2O_2, determined by the pK_a of the protein, and its abundance within the cell. At cellular pH, most protein thiols are protonated and resistant to oxidation (pK_a approximately 8.5). Cysteine thiols that are more susceptible to oxidation by H_2O_2, particularly catalytic cysteine residues (Winterbourn and Hampton, 2008), have a pK_a between 4.5 and 7, favouring the formation of a thiolate anion under physiological conditions (Winterbourn and Metodiewa, 1999; Chen *et al.*, 2009). The thiolate anion can be reversibly oxidised to a sulphenic acid, then further irreversibly oxidised to a sulphinic or sulphonic acid (Winterbourn and Hampton, 2008). Therefore, cysteine thiols with a low pK_a, and which are relatively abundant in the cell, will react more readily with H_2O_2. For example, Prx have a low pK_a (5-6) and are highly abundant within the cell, making them one of relatively few thiol-containing proteins which are able to be directly targeted by H_2O_2 (Winterbourn and Hampton, 2008). These characteristics make H_2O_2 well suited as a signalling molecule.

An important question facing the H_2O_2-signalling field is how less reactive proteins, such as protein tyrosine phosphatases (PTP), become oxidised by H_2O_2 when abundant, more reactive Prx are present. One possibility is that low peroxide concentrations are scavenged by Prx, whereas higher levels cause localised inactivation of Prx, allowing regulatory and signalling proteins to be targeted (Wood *et al.*, 2003b; Rhee, 2006; Veal *et al.*, 2007). In some instances, Prx are able to act as sensors, and become oxidised by H_2O_2 to then oxidise other proteins (Winterbourn and Hampton, 2008).

1.5 Roles of peroxiredoxin and thioredoxin in regulating protein thiol oxidation

Alongside their role as antioxidant enzymes, Prx also have key roles in ROS responses, as molecular chaperones and in H_2O_2 signal transduction (Jang *et al.*, 2004; Veal *et al.*, 2004; Olahova *et al.*, 2008). Prx can act as H_2O_2 sensors to transmit the H_2O_2 signal by promoting the oxidation of less reactive

protein-thiols, thus regulating the activity of diverse proteins. In addition, hyperoxidation of the catalytic cysteine residue of eukaryotic 2-Cys Prx, due to exposure to higher levels of H_2O_2, results in inactivation of the thioredoxin peroxidase activity (Woo *et al.*, 2003; Wood *et al.*, 2003a; Wood *et al.*, 2003b), which acts as a molecular switch to initiate the activation of different signalling pathways (Veal *et al.*, 2004; Bozonet *et al.*, 2005; Vivancos *et al.*, 2005). Recent work has suggested that the roles of Prx in signalling and as chaperones, rather than in the detoxification of H_2O_2, might underlie their role in oxidative stress resistance (Brown *et al.*, 2013), and in longevity (Hanzen *et al.*, 2016). Multiple studies have provided evidence for roles for Prx as both a protective antioxidant enzyme and as a regulator of oxidant-sensitive signal transduction, examples of which are discussed further in this section.

Tpx1 (Thioredoxin peroxidase 1) is the single typical 2-Cys Prx in *S. pombe*, and contains redox-active cysteine residues at positions 48 (peroxidatic) and 169 (resolving). Tpx1 in *S. pombe* transmits a redox signal to the AP-1 like transcription factor Pap1, and the MAPK Sty1, causing oxidation of their redox-active cysteine residues (Quinn *et al.*, 2002). Orthologues of Tpx1 in pathogenic fungi and nematode worms have been shown to be required for activation of p38 MAPK homologues in response to oxidative stress, indicating that this signalling function of Prx is conserved (Conway and Kinter, 2006; Olahova *et al.*, 2008; da Silva Dantas *et al.*, 2010). At higher concentrations of H_2O_2, the peroxidatic cysteine residue can be hyperoxidised, inhibiting the thioredoxin peroxidase activity of Tpx1, which can be restored through sulphiredoxin (Woo *et al.*, 2003; Wood *et al.*, 2003b; Bozonet *et al.*, 2005; Vivancos *et al.*, 2005). This catalytic cycle of the *S. pombe* Prx is similar to other eukaryotic Prx (Rhee and Woo, 2011), making *S. pombe* an excellent model organism to study the functions of 2-Cys Prx in ROS responses. Much of our current understanding of how Prx are involved in H_2O_2 signalling and the function of hyperoxidation comes from studies in *S. pombe*, owing to the advantage of *S. pombe* containing a single representative of the typical 2-Cys Prx family, Tpx1. Studies have shown that Tpx1 is essential for adaptive transcriptional responses to H_2O_2 (Veal *et al.*, 2004; Bozonet *et al.*, 2005; Vivancos *et al.*, 2005). Similar to other eukaryotic 2-Cys Prx, Tpx1 is sensitive to inactivation of its

thioredoxin peroxidase activity by hyperoxidation, which also allows thioredoxins to reduce other oxidised proteins and promote cell survival. It has been revealed in *S. pombe* that, despite thioredoxin, Trx1, acting to reduce many oxidised proteins, Tpx1 disulphides are the main substrate for Trx1. However, as Trr1 levels are limiting, Trx1 becomes completely oxidised, and Trx1 substrates remain oxidised (Day *et al.*, 2012; Brown *et al.*, 2013). Studies from our laboratory have suggested that hyperoxidation of Tpx1 to a form that is resistant to Trx1-mediated reduction is important for cell survival under high ROS conditions in *S. pombe* (Day *et al.*, 2012). In addition, hyperoxidised Prx have been shown to have pro-survival functions, for example hyperoxidation promotes the chaperone activity of 2-Cys Prx in *S. cerevisiae* and human cells (Jang *et al.*, 2004; Moon *et al.*, 2005). A model was proposed whereby the peroxidase activity of 2-Cys Prx is coupled to thioredoxin, allowing the H_2O_2-dependent regulation of many Trx1 substrates. In fact, recent work within our laboratory has proven that Prx are able to inhibit thioredoxin family proteins through oxidation in response to H_2O_2 (Brown *et al.*, 2013).

1.5.1 Protein thiol oxidation in the endoplasmic reticulum

There are multiple dedicated cellular pathways that ensure the correct formation of disulphide bonds, essential for the function and stability of a number of proteins. When introducing disulphide bonds into a protein containing more than two cysteines, there is a possibility that incorrect disulphide bonds can be formed. Aberrant disulphide bonds can be rearranged by isomerisation through disulphide exchange reactions to attain the native protein conformation. Disulphide bonds are formed in secreted proteins in the endoplasmic reticulum (ER), and in bacterial secreted proteins. Protein disulphide isomerase (PDI), a multi-domain, multi-functional protein, belonging to the thioredoxin superfamily, is responsible for introducing and rearranging disulphide bonds in secretory proteins in the ER (For reviews see (Ferrari and Soling, 1999; Freedman *et al.*, 2002)). PDI, the first protein folding catalyst to be identified, contains two thioredoxin-like catalytic domains, separated by two non-catalytic domains. The two catalytic domains contain low affinity binding sites for non-native proteins,

whereas one of the non-catalytic domains contains a higher affinity binding site, allowing PDI-catalysed disulphide bond isomerisation (Darby *et al.*, 1998; Klappa *et al.*, 1998). Upon binding of the substrate to PDI, a disulphide bond forms between the substrate and PDI. Through a disulphide bond relay, the PDI-substrate disulphide bond is reduced by ER sulphydryl oxidases, such as Ero1, releasing reduced PDI and the oxidised substrate. One of four typical 2-Cys Prx in mammalian cells, PrxIV, is the only mammalian Prx known to be secreted from the cell, due to the presence of a putative secretory signal (Haridas *et al.*, 1998). More recently, PrxIV has been shown to have a role in disulphide bond formation in the ER. The production of H_2O_2 by the activity of Ero1 in the ER leads to oxidative stress, and ultimately to apoptosis. Increased Ero1 activity and production of H_2O_2 leads to preferential hyperoxidation of the ER-localised Prx, PrxIV, and suggests that the oxidation status of PrxIV acts as a marker for ER oxidative stress (Tavender and Bulleid, 2010). In response to H_2O_2, PrxIV becomes oxidised through the formation of a disulphide bond. Members of the PDI family directly reduce the PrxIV disulphide bond, restoring the catalytic activity of PrxIV, causing oxidation of PDI. Oxidation of PDI by PrxIV is a highly efficient process, allowing oxidation by H_2O_2 to be coupled to disulphide bond formation, and may increase the efficiency of disulphide formation by Ero1 (Tavender *et al.*, 2010).

DsbA, a soluble periplasmic protein in *Escherichia coli*, belongs to the thioredoxin superfamily (Guddat *et al.*, 1998), and contains a characteristic fold which functions as a scaffold for a variety of redox reactions. The nascent polypeptide chain interacts with oxidised DsbA in the periplasm (Kadokura and Beckwith, 2009). Via a nucleophilic substitution reaction, cysteine residues of a substrate attack the oxidised cysteine 30 of the CXXC motif in DsbA, displacing cysteine 33, forming a mixed disulphide bond between DsbA and the substrate (Darby and Creighton, 1995; Kadokura and Beckwith, 2009; Perez-Jimenez *et al.*, 2009). Via another nucleophilic attack by substrate thiols, the mixed disulphide bond is reduced, resulting in reduced DsbA and an oxidised substrate.

1.5.2 Protein thiol oxidation in the mitochondria

A redox-regulated import pathway can be utilised to import proteins into the intermembrane space (IMS) of the mitochondria. Alongside the introduction of disulphide bonds in secreted proteins in the ER, and in bacterial secreted proteins, disulphide bonds are also formed in the mitochondrial IMS. The IMS, although a reducing environment like the cytosol, and therefore not favourable for disulphide bond formation, contains a subset of mitochondrial proteins with disulphide linkages, such as the superoxide dismutase Sod1, the copper chaperone for Sod1, Ccs2, and the subunit 12 of the cytochrome *c* oxidase (Herrmann and Kohl, 2007; Stojanovski *et al.*, 2008; Koehler and Tienson, 2009). The disulphide bonds function in both structural and catalytic roles, but also serve as a mechanism for the import and assembly of proteins into the IMS. Owing to the importance of disulphide bond formation in the IMS, data has suggested that the redox properties of the IMS are in fact different from the reducing environment of the cytosol, and are more similar to the oxidising environment of the ER and the bacterial periplasm (For reviews see (Sevier and Kaiser, 2006; Riemer *et al.*, 2009)). The mitochondrial IMS contains a family of low molecular mass, intermembrane proteins with catalytic cysteine residues organised in twin CX_3C or twin CX_9C motifs. Proteins with twin CX_3C motifs belong to a family of small Tim proteins, which function as chaperones in the IMS (Herrmann and Hell, 2005; Stojanovski *et al.*, 2008; Koehler and Tienson, 2009). The family of Tim proteins are conserved from yeast to mammals and plants, but are not found in prokaryotes (Bauer *et al.*, 1999). Structural studies of the small Tim proteins and Cox17, the best studied member of the family of proteins with twin CX_9C motifs, demonstrates that two anti-parallel α-helices are linked by two disulphide bonds, to form a hairpin-like structure. The catalytic cysteine residues are essential for the assembly of the small Tim proteins, with the disulphide bonds crucial for folding and stabilisation of the structure.

Tim40 is an essential, evolutionary conserved, IMS protein, tethered to the inner mitochondrial membrane in yeast, mediating the import of small Tim proteins and other twin CX_9C proteins (Chacinska *et al.*, 2004; Naoe *et al.*, 2004; Gabriel *et al.*, 2007; Terziyska *et al.*, 2007). The IMS domain

of Tim40 consists of six conserved cysteine residues in twin CX_9C motifs and an N-terminal CPC motif, which form three intramolecular disulphide bonds in the oxidised state, essential for Tim40 function (Naoe *et al.*, 2004; Grumbt *et al.*, 2007). One disulphide bond connects the two cysteines in the CPC motif, with two disulphide bonds forming between the two cysteines of each CX_9C motif. Whereas the disulphide bonds in the CX_9C motifs form to stabilise the protein, the CPC motif is easily accessible to reducing agents, and is most likely to form a transient disulphide bond with substrates (Grumbt *et al.*, 2007).

Small incoming cysteine-containing mitochondrial precursor proteins, such as small Tim proteins, form disulphide bonds with the mitochondrial intermembrane space assembly machinery (MIA). The precursor protein, in an unfolded, reduced state, becomes translocated across the outer membrane through the translocase of the outer membrane (TOM) complex (Kurz *et al.*, 1999). Only reduced precursor proteins, and not oxidised proteins, are competent for import into the mitochondria (Lu *et al.*, 2004; Tokatlidis, 2005; Morgan and Lu, 2008). Recent work has implicated the cytosolic thioredoxin system in maintaining small Tim proteins in a reduced, import-competent form in the cytosol, facilitating their mitochondrial import (Durigon *et al.*, 2012). Once in the IMS, oxidoreductases such as Tim40, introduces disulphide bonds into target proteins, trapping them in the IMS (Grumbt *et al.*, 2007; Milenkovic *et al.*, 2007; Sideris and Tokatlidis, 2007; Banci *et al.*, 2009; Milenkovic *et al.*, 2009), providing a mechanism whereby protein import and oxidative folding are coupled together. A disulphide relay exists in the IMS, whereby Tim40 forms a mixed disulphide bond with the precursor protein, resulting in oxidation of cysteine residues in the precursor protein and reduction of cysteine residues in Tim40 (Mesecke *et al.*, 2005; Grumbt *et al.*, 2007; Muller *et al.*, 2008). Tim40 releases its substrate by an unknown mechanism, predicted to involve the rearrangement of disulphide bonds, resulting in the mature conformation of the substrate (Sideris and Tokatlidis, 2007; Milenkovic *et al.*, 2009). Tim40 is reoxidised by Erv1, an IMS sulphydryl oxidase, which transfers electrons from Tim40 to cytochrome *c* and the ETC (Farrell and Thorpe, 2005; Bihlmaier *et al.*, 2007; Dabir *et al.*, 2007). The

IMS is important for disease processes, including apoptosis and neurodegeneration, therefore new roles in the regulation of redox chemistry in the mitochondria seem likely to be relevant.

1.5.3 Protein thiol oxidation in the cytoplasm

Prx have been shown to have multiple roles in H_2O_2 signalling, either as activators or inhibitors of H_2O_2 signal transduction. Several studies have provided evidence to suggest that Prx inhibit the activation of ROS-activated signalling pathways, including MAPK pathways, which are involved in a wide range of processes, such as apoptosis and the oxidative stress response (Kang *et al.*, 2004; Choi *et al.*, 2005; Yang *et al.*, 2007; Cao *et al.*, 2009; Woo *et al.*, 2010; Kil *et al.*, 2012). On the other hand, several studies have identified a positive role for Prx in H_2O_2 signal transduction, with increasing evidence that the ability of Prx to promote ROS-signalling are not only observed in unicellular eukaryotes, but are also present in animals. A study in mammalian cells showed that Prx2 acts as a H_2O_2 receptor, to transmit oxidative signals to the redox-regulated transcription factor STAT3 (Sobotta *et al.*, 2015). Additionally, several studies have shown that Prx are required for activation of p38 MAPK homologues in response to stress, indicating that this signalling function of Prx is conserved. For example, the single 2-Cys Prx in *S. pombe*, Tpx1, is required for H_2O_2 signal transduction to the p38/JNK related MAPK Sty1, suggesting a conserved function for Prx in promoting H_2O_2 signal transduction (Veal *et al.*, 2004). Tpx1 has been demonstrated to play an important role in H_2O_2-induced signal transduction in *S. pombe*, and indeed, more recent studies have shown that Prx can promote H_2O_2 signalling in other systems. Prdx1 in macrophage-derived foam cells has been shown to have a dual role as an antioxidant enzyme, and as an activator of p38 MAPK, providing evidence for conservation of the role of Prx in activation of MAPK pathways. In response to oxidised low density lipoprotein (oxLDL), a number of proteins, including Prdx1 become upregulated, required for activation of the p38 MAPK, and promoting cell survival (Conway and Kinter, 2006). This is consistent with findings in *S. pombe*, whereby in response to low levels of H_2O_2, antioxidant enzymes are upregulated during the transcriptional response, allowing *S. pombe* to grow while exposed to low levels of H_2O_2 (Chen *et al.*, 2003; Chen *et al.*, 2008).

In addition, Prdx1 is able to specifically regulate H_2O_2-induced p38 MAPK activation in mammalian cells (Jarvis *et al.*, 2012), and the 2-Cys Prx, Tsa1, in *C. albicans* is required for H_2O_2-induced activation of the p38/JNK related Hog1 MAPK pathway (da Silva Dantas *et al.*, 2010). In *C. elegans*, the 2-Cys Prx, PRDX-2, is required for arsenite-induced activation of the p38 related MAPK, PMK-1 (Olahova *et al.*, 2008), and is required for PMK-1 activation following treatment with metformin, which induces production of ROS (De Haes *et al.*, 2014). There have been a number of mechanisms described underlying the role of Prx in promoting p38/JNK MAPK activation in response to H_2O_2, including as direct redox-transducers, as H_2O_2-dependent thioredoxin inhibitors, and through the signalling activities of hyperoxidised Prx. These will be discussed further in this section.

Studies from our laboratory provided some of the first evidence for a H_2O_2-induced direct disulphide bond between a Prx and a MAPK, supporting a model where Prx have a role in H_2O_2-induced signal transduction through regulation of MAPK oxidation (Veal *et al.*, 2004). Following oxidative stress, the single typical 2-Cys Prx, Tpx1, forms a disulphide bond with the Sty1 MAPK, proposed to promote H_2O_2-induced Sty1 activation in *S. pombe* (Veal *et al.*, 2004). In fact, there are multiple Tpx1-dependent, H_2O_2-induced oxidised forms of Sty1, suggesting that additional redox-sensitive cysteine residues in Sty1 may be involved in its regulation (Veal *et al.*, 2004). A disulphide bond forms between cysteine 153 and cysteine 158 of Sty1, required for oxidative stress resistance and H_2O_2-induced gene expression, however oxidation of these cysteine residues is not required for Sty1 phosphorylation (Day and Veal, 2010). In addition, cysteine 153 and cysteine 158 of Sty1 are important for maintaining *atf1*$^+$ mRNA stability following high concentrations of H_2O_2 (Day and Veal 2010).

Studies in *S. cerevisiae* identified a disulphide bond between Yap1, the Pap1 homologue, and the thioredoxin peroxidase, Gpx3, or the Tpx1 orthologue, Tsa1, required for H_2O_2-induced oxidation of Yap1 (Delaunay *et al.*, 2000; Veal *et al.*, 2003). However, Gpx1, the Gpx3 homologue in *S. pombe* is not essential for the oxidation and activation of Pap1 (Bozonet, 2006), and no disulphide bond can be detected between Tpx1 and Pap1 (Bozonet *et al.*, 2005; Vivancos *et al.*, 2005).

Studies in mammalian cells have also demonstrated that Prdx1, a cytosolic typical 2-Cys Prx, plays a role in the regulation of MAPK signalling pathways. Prdx1 transmits the peroxide signal to the MAPKKK, ASK1, resulting in phosphorylation of both the p38 and JNK MAPK. In response to H_2O_2, oxidised ASK1 preferentially transmits the peroxide signal to p38 and JNK, resulting in MAPK phosphorylation. To maintain this oxidised form of ASK1, a Prdx1-ASK1 intermolecular disulphide bond forms in response to peroxide, resulting in complete activation of the ASK1 pathway (Jarvis *et al.*, 2012) (Figure 1.2A). In this instance, Prdx1 is acting as a peroxide receptor, receiving and transducing the peroxide signal to ASK1 via a disulphide-exchange mechanism, consistent with Prx function in yeast.

In addition, the thioredoxin, Trx1, was identified as an interactor of ASK1 through a two hybrid screen. The redox status of the cell is believed to control and regulate multiple signalling pathways, and as Trx1 contributes to the intracellular redox homeostasis of the cell, it has been implicated in an intermediate of ROS-mediated signalling. The reduced form of Trx1 directly binds to the N-terminus of ASK1, inhibiting the kinase activity of ASK1 under reducing conditions (Saitoh *et al.*, 1998). Upon exposure to peroxide or TNF-α, Trx1 becomes oxidised through the formation of intramolecular disulphide bonds, causing its dissociation from ASK1 (Saitoh *et al.*, 1998). The oligomerisation of ASK1 allows autophosphorylation of a threonine residue in the activation loop of ASK1 to increase its kinase activity (Gotoh and Cooper, 1998; Tobiume *et al.*, 2001), leading to increased p38 and JNK phosphorylation, and ultimately apoptosis (Ichijo *et al.*, 1997). The binding of reduced Trx1 to ASK1 was initially proposed to inhibit the multimerisation of ASK1, and therefore inhibit its kinase activity. H_2O_2-induced Trx1 oxidation and subsequent dissociation from ASK1 led to the activation and phosphorylation of ASK1.

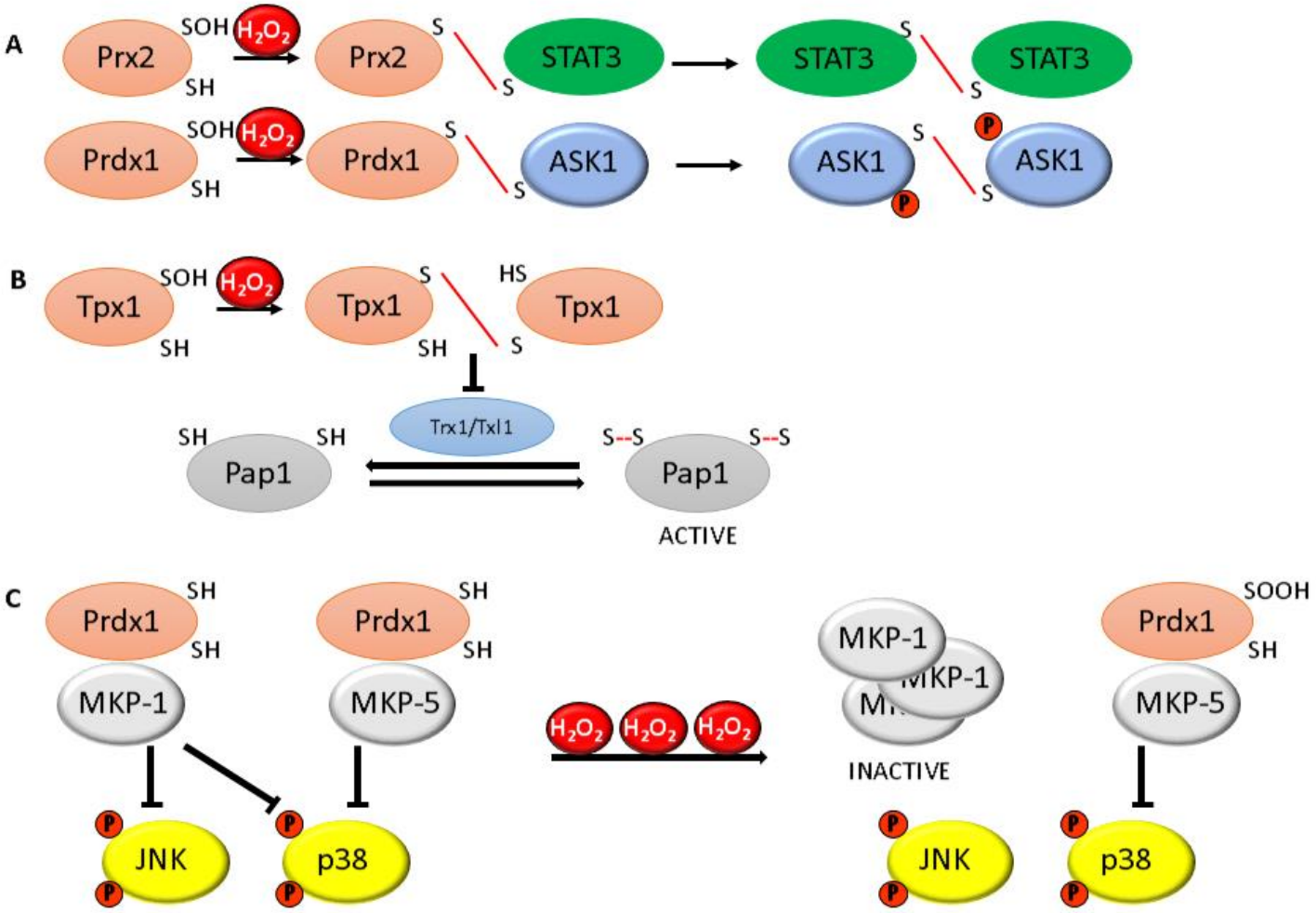
A
Prx2
SOH
SH
H_2O_2
Prx2
S
S
STAT3
STAT3
S
S
STAT3
Prdx1
SOH
SH
H_2O_2
Prdx1
S
S
ASK1
ASK1
S
P
S
ASK1
B
Tpx1
SOH
SH
H_2O_2
Tpx1
S
SH
HS
S
Tpx1
Trx1/Txl1
SH
Pap1
SH
S--S
Pap1
S--S
ACTIVE
C
Prdx1
SH
SH
MKP-1
Prdx1
SH
SH
MKP-5
H_2O_2 H_2O_2 H_2O_2
MKP-1
MKP-1
INACTIVE
Prdx1
SOOH
SH
MKP-5
P
JNK
P
P
p38
P
P
JNK
P
P
p38
P

Figure 1.2 Mechanisms underlying the role of Prx in promoting p38/JNK MAPK activation in response to H_2O_2. (**A**) Prx2 forms transient Prx2-STAT3 disulphides, followed by STAT3-STAT3 oligomers, promoting STAT3 activation. Similarly, Prdx1 is able to activate ASK1 through the formation of Prdx1-ASK1 disulphides, followed by ASK1-ASK1 oligomers. (**B**) As Tpx1-Tpx1 disulphides are the predominant substrate for Trx1 in *S. pombe*, this prevents the thioredoxin activity of Trx1 and Txl1 towards other substrates, such as Pap1. (**C**) At low concentrations of H_2O_2, Prdx1 associates with two MAPK phosphatases, MKP-1 and MKP-5, in human malignant breast epithelial cells. However, when Prdx1 is hyperoxidised in response to high concentrations of H_2O_2, Prdx1 dissociates from MKP-1, leading to the oligomerisation and inactivation of MKP-1, inhibiting the phosphorylation of both p38α and JNK. However, Prdx1 is still able to associate with MKP-5, even when Prdx1 is hyperoxidised, protecting MKP-5 from oligomerisation and inactivation, therefore promoting MKP-5 activity towards p38α MAPK (Adapted from Latimer and Veal, 2016).

More recently, a new model was proposed, suggesting that exposure to H_2O_2 induced both phosphorylation and oxidation of ASK1, modifications which are independent of each other, but both essential for signalling through the ASK1 pathway. H_2O_2-induced ASK1 oligomerisation involves the formation of intermolecular disulphide bonds between cysteine residues in ASK1, stabilising the ASK1-ASK1 interactions required for autophosphorylation (Nadeau *et al.*, 2007), and essential for full p38 and JNK activation, and apoptosis. This suggests that Trx1 negatively regulates the ASK1 signalling pathway by directly reducing the oxidised, oligomeric forms of ASK1, preventing autophosphorylation (Nadeau *et al.*, 2007). In addition, the interaction between ASK1 and Trx1 has also been proposed to involve a disulphide bond between specific cysteine residues in both proteins. Under unstressed conditions, the ASK1 signalosome is inactive, consisting of ASK1 oligomers, with cysteine 32 of Trx1 bound to ASK1, masking cysteine 250 of ASK1. Following exposure to H_2O_2, ASK1 becomes phosphorylated and the ASK1 signalosome activated, causing Trx1 to dissociate, exposing cysteine 250 of ASK1. This cysteine residue is essential for H_2O_2-induced JNK activation, and although the role of cysteine 250 is unknown, it is speculated that cysteine 250 may associate with specific H_2O_2 interactors to activate and phosphorylate JNK (Nadeau *et al.*, 2007). These studies suggest that many activating stimuli of MAPK pathways are able to increase the oxidation of thioredoxin, indicating that ASK1 is acting as a sensor of thioredoxin oxidation. Trx1 has been shown to be required for the H_2O_2-induced activation of the p38/JNK related Hog1 MAPK in *C. albicans* (da Silva Dantas *et al.*, 2010). This suggests that oxidised thioredoxin may play a positive role in MAPK activation. Due to the association between ASK1 and Trx1 in the mammalian p38/JNK MAPK pathway (Saitoh *et al.*, 1998), and the conservation between *S. pombe* and mammalian p38/JNK MAPK pathways, it seems possible that the thioredoxin system may regulate H_2O_2-dependent signal transduction in *S. pombe* also. Indeed, studies from our laboratory in *S. pombe* have shown an *in vivo* role for the thioredoxin-like protein, Txl1, as an inhibitor of H_2O_2 signalling, and that the redox-coupling between Trx1 and the thioredoxin peroxidase activity of Tpx1 is central for the initiation of responses to H_2O_2 (Day *et al.*, 2012; Brown *et al.*, 2013).

Similar to the Prdx1-ASK1 disulphide bond which forms in response to H_2O_2, Prx2 promotes activation of the STAT3 transcription factor through the transient formation of Prx2-STAT3 disulphides, followed by disulphide-linked STAT3 oligomers (Sobotta *et al.*, 2015) (Figure 1.2A). The thioredoxin system then mediates STAT3 reduction. These results suggest that peroxidase-based redox relays are common in mammalian cells, which may be conserved as H_2O_2-sensing mechanisms in other domains of life.

Thioredoxin is directly responsible for the reduction of Prx disulphides, therefore the role of Prx and the thioredoxin system are intimately linked in their signalling role. In *S. pombe*, Tpx1-Tpx1 disulphides are the main substrate for Trx1, preventing the thioredoxin activity of Trx1 and Txl1 towards other substrates, such as the AP-1 like transcription factor Pap1 (Brown *et al.*, 2013) (Figure 1.2B). However, as thioredoxin reductase (Trr1) levels are limiting, Trx1 becomes completely oxidised, and Tpx1 and Trx1 substrates remain oxidised (Day *et al.*, 2012; Brown *et al.*, 2013). Following exposure of cells to high concentrations of H_2O_2, Tpx1 can become hyperoxidised, allowing thioredoxins to reduce other oxidised proteins, and promote cell survival (Day *et al.*, 2012). It has been demonstrated that the presence of H_2O_2-induced Tpx1 disulphides inhibits Txl1, which underlays the role of Tpx1 in the H_2O_2-induced activation of Pap1 (Brown *et al.*, 2013). Owing to the important role of Trx1 in the reduction of active, oxidised ASK1 oligomers, there is a possibility that Prx might promote MAPK activation in yeast and animals by inhibiting the activity of thioredoxin towards other oxidised proteins.

Eukaryotic 2-Cys Prx are sensitive to hyperoxidation of the peroxidatic cysteine residue in response to high concentrations of H_2O_2, to form a sulphinic acid derivative, inactivating its thioredoxin peroxidase activity (Woo *et al.*, 2003). This hyperoxidation is proposed to increase the molecular chaperone ability of Prx (Jang *et al.*, 2004). Studies in *S. pombe* have shown that hyperoxidation of the 2-Cys Prx, Tpx1, allows thioredoxins to reduce other oxidised proteins, and promote cell survival (Day *et al.*, 2012). Unlike activation of the transcription factor Pap1, which requires the thioredoxin peroxidase activity of Tpx1, activation of the transcription factor Atf1 is independent of the thioredoxin peroxidase activity of Tpx1 (Bozonet *et al.*, 2005; Vivancos *et al.*, 2005). Atf1 becomes activated by the MAPK Sty1,

which becomes increasingly activated as concentrations of H_2O_2 increase up to 10.0 mM, suggesting that hyperoxidised Tpx1 is able to promote Sty1 activation (Veal *et al.*, 2004).

Prdx1 regulates the p38α MAPK phosphatases (MKP), MKP-1 and MKP-5, in a H_2O_2 dose-dependent manner, using the peroxidatic cysteine (C52) of Prdx1 as a H_2O_2 sensor in human malignant breast epithelial cells, allowing Prdx1 to specifically regulate H_2O_2-induced p38α MAPK signalling (Turner-Ivey *et al.*, 2013) (Figure 1.2C). Prdx1 binds to both MKP-1 and MKP-5, but following exposure to high concentrations of H_2O_2, where the peroxidatic cysteine became hyperoxidised, Prdx1 dissociates from MKP-1. This prevents the formation of Prdx1:MKP-1 complexes, leading to the oligomerisation and inactivation of MKP-1, inhibiting the phosphorylation of both p38α and JNK. Conversely, maintenance of the Prdx1:MKP-5 complex at high H_2O_2 concentrations, even when Prdx1 is hyperoxidised, protected MKP-5 from oligomerisation and inactivation, therefore promoting MKP-5 activity towards p38α MAPK. MKP-1 and MKP-5 favour different MAPK substrates, and therefore this differential binding and inactivation can be used by the cell to specifically target MAPK. For example, MKP-1 inactivation under high H_2O_2 concentrations allows JNK activity over p38α, whereas maintained MKP-5 activation prevents p38α activation in H_2O_2-induced cellular senescence (Turner-Ivey *et al.*, 2013). The ability of Prdx1 to protect MKP-1 and MKP-5 from inactivation is consistent with the proposed chaperone function of Prdx1.

Alongside Prx, other enzymes, including protein tyrosine phosphatases (PTP), contain catalytic cysteine residues that are susceptible to inactivation by reaction with H_2O_2 (den Hertog *et al.*, 2005; Winterbourn and Hampton, 2008). In eukaryotes, PTP are important regulators of signal transduction, which become initiated by stimuli including growth factors and cytokines. All cysteine-based phosphatases, including PTP, contain a highly conserved active site motif (HCXXGXXR[S/T], where X represents any amino acid), in which the catalytic cysteine residue has a low pK_a, and is therefore highly susceptible to H_2O_2-induced oxidation and inactivation (For reviews see (Rhee *et al.*, 2005; Winterbourn and Hampton, 2008)). The catalytic mechanism of PTP involves a two-step process,

beginning with nucleophilic attack by the Sγ of the catalytic cysteine on the phosphorus of the phosphotyrosyl substrate, resulting in formation of a phospho-cysteine intermediate. In the second step, the transient phospho-enzyme intermediate is hydrolysed by an activated H_2O. H_2O_2-induced oxidation of the active site cysteine to sulphenic acid results in inhibition of the PTP activity because the modified cysteine can no longer function as a phosphate acceptor in the first step of the PTP-catalysed reaction.

H_2O_2-induced oxidation of certain susceptible cysteine residues in PTP (Winterbourn and Hampton, 2008) has been established as an integral part of signal transduction, whereby the oxidative inactivation of PTP increases the steady state levels of phosphorylation, facilitating signal transduction (For reviews see (Rhee *et al.*, 2000; Rhee *et al.*, 2003)). Owing to the roles of these phosphatases in the control and regulation of cell signalling pathways, these enzymes have evolved mechanisms to prevent irreversible oxidation of the catalytic cysteine to the sulphinic and sulphonic acid derivatives. For instance, in the case of PTEN (phosphatase and tensin homolog) and Cdc25, an intracellular disulphide bond between the cysteine residue at the active site and a nearby "backdoor" cysteine, typically between 9 and 12 Å from the catalytic cysteine, forms to stabilise the oxidised PTP (Savitsky and Finkel, 2002; Kwon *et al.*, 2004). In contrast, for PTP1B, sulphenylamide traps the singly oxidised form of the cysteine, making it resistant to further ROS-induced oxidation (Salmeen *et al.*, 2003). Alternatively, following exposure of cells to the superoxide anion, the catalytic cysteine of PTP1B can become glutathionylated, preventing irreversible oxidation of the sulphenic acid derivative (Barrett *et al.*, 1999).

The tumour suppressor PTEN regulates cell migration, growth and survival, and reverses the action of phosphoinositide 3-kinase, which is an important activator of the protein kinase Akt. Activated Akt promotes cell survival by phosphorylating the pro-apoptotic factors BAD and caspase-9, therefore unregulated Akt activation can result in tumour formation (Lee *et al.*, 2002). PTEN negatively regulates the phosphoinositide 3-kinase-Akt signalling pathway by blocking Akt activation and reducing cell

survival, therefore acting as both a regulator of signal transduction and a tumour suppressor (Lee *et al.*, 2002). PTEN is negatively regulated by phosphorylation of serine 380, threonine 382 and threonine 383 under non-stressed conditions (Cho *et al.*, 2004). PTEN becomes oxidised and inactivated in a time- and H_2O_2 concentration-dependent manner, leading to uncontrolled Akt activation and inhibition of apoptosis, contributing to tumour formation (Lee *et al.*, 2002). Following exposure to H_2O_2, cysteine 124 in the active site of PTEN forms a disulphide bond with cysteine 71, which is reduced predominantly by thioredoxin (Lee *et al.*, 2002). Thioredoxin has also been implicated in the reactivation of oxidised PTP1B. The catalytic cysteine of PTP1B becomes oxidised, with a disulphide-linked PTP1B-TRX1 detected at 0.2 mM H_2O_2, which can be reduced by thioredoxin (Kwon *et al.*, 2004; Schwertassek *et al.*, 2014). The oxidation of thioredoxin would therefore be predicted to inhibit the reduction of oxidised, inactive PTP, increasing the duration of MAPK activation.

GAPDH catalyses the conversion of glyceraldehyde-3-phosphate to 1,3-bisphosphoglycerate during the sixth step of glycolysis. Alongside its glycolytic activity, GAPDH has been shown to be a multifunctional protein with diverse activities in signal transduction, transcriptional and post-transcriptional regulation of gene expression, DNA repair and apoptosis (For a review see (Sirover, 2011)). GAPDH activity is sensitive to inactivation by reversible or irreversible oxidation of the catalytic cysteine following exposure to H_2O_2 stress, as exemplified by studies in mammalian cells and the budding yeast *S. cerevisiae* (Brodie and Reed, 1987; Brodie and Reed, 1990; Grant *et al.*, 1999). The sensitivity of GAPDH to inactivation by oxidation was originally demonstrated in *S. cerevisiae*, whereby one of the GAPDH isoforms, Tdh3, undergoes reversible S-thiolation of cysteine residue(s), reversibly inhibiting its enzyme activity, but also protecting the enzyme from irreversible oxidation and inactivation (Grant *et al.*, 1999). This study also provided evidence that S-thiolation of GAPDH is a regulated process, affecting survival during oxidative stress conditions, where two GAPDH isoforms play complementary roles depending on their ability to become oxidised (Grant *et al.*, 1999). Studies in human lung carcinoma cells have also demonstrated that GAPDH becomes reversibly oxidised by H_2O_2 (Brodie and Reed, 1987). One way in which GAPDH oxidation protects cells against ROS is by

inhibiting glycolysis and allowing increased NADPH production by the pentose phosphate pathway (PPP), maintaining the cytoplasmic NADPH/NADP equilibrium to counteract oxidative stress (Ralser *et al.*, 2007). Previous work in *S. pombe* has revealed that one of two GAPDH isoforms, Tdh1, interacts with upstream components of the p38 related Sty1 MAPK pathway, and was required for the H_2O_2-induced activation of Sty1 (Morigasaki *et al.*, 2008). It has also been proposed that GAPDH oxidation was important for the H_2O_2-induced increase in Sty1 phosphorylation (Morigasaki *et al.*, 2008). Unpublished work from our laboratory has suggested that Tpx1 acts as a peroxide-sensitive molecular scaffold, facilitating the oxidation of Tdh1. Tpx1 is required for the hyperoxidation and inactivation of Tdh1 in response to high concentrations of H_2O_2, important for the activation of Sty1 (Day and Veal unpublished data).

Taken together, evidence from a variety of studies, discussed in this section, hint at the different mechanisms utilised by Prx in regulating protein thiol oxidation and H_2O_2 signalling, depending on the concentration of H_2O_2, and the oxidation status of the Prx. An outstanding question in the field is how to resolve the multiple roles of Prx and Trx in regulating H_2O_2-induced signalling pathways, through transducing H_2O_2 signals via H_2O_2-induced oxidation, and modulating the activity of various proteins.

1.6 Regulation of transcriptional responses in response to H_2O_2 in *S. pombe*

Unicellular eukaryotes, including *S. pombe* and *S. cerevisiae*, respond to external stress by inducing the expression of protective and detoxifying enzymes that allow cell survival. During the core environmental stress response (CESR), there is a change in gene expression, inducing genes involved in antioxidant production and transcriptional regulation, and repressing genes involved in protein metabolism and cellular signalling (Chen *et al.*, 2003). In *S. pombe*, the CESR is primarily mediated by the MAPK Sty1, and the transcription factor Atf1 (Chen *et al.*, 2003), to induce a specific set of stress-activated genes that confer protection against a variety of stress conditions.

1.6.1 *S. pombe* as a model eukaryote to understand cellular responses to H_2O_2

Although, as discussed in section 1.2, low levels of H_2O_2 have been shown to be mitogenic, promote cell migration in wound healing, and a host of other physiological responses, the most conserved response to rises in H_2O_2 is to activate mechanisms to protect against potential damage. Indeed, the evolutionary pressure to prevent this damage has led to the evolution of conserved pathways to increase the expression of ROS-detoxifying enzymes to protect against this damage. In animals these pathways are also involved in limiting damage by promoting apoptotic cell death.

Although H_2O_2 initiates responses that are important for cell adaptation to stress conditions, the targets of H_2O_2 signals and the mechanisms by which these targets are regulated are poorly characterised. Yeast is an excellent model to investigate these signalling roles, due to the reduced gene redundancy and ease of genetic manipulation. Indeed, studies in yeast models have provided some of the best evidence to date for the positive signalling roles of low levels of H_2O_2 to drive adaptive responses to limit damage (For a review see (Finkel, 2011; Veal and Day, 2011; Veal *et al.*, 2014)).

1.6.2 Pap1

AP-1 (Activating protein-1) transcription factors are members of the b-Zip transcription factor family, which become activated in response to a variety of signals including oxidative stress, osmotic stress and growth factors (Karin, 1995; Wisdom, 1999), and activate a number of stress responsive genes (Kyriakis and Avruch, 2001). The *S. pombe* homologue of the mammalian b-Zip transcription factor, AP-1 (c-Jun), was identified as Pap1, which shares 65% identity with *S. cerevisiae* Yap1. Pap1 was shown to have a role in the regulation of genes involved in the oxidative stress response following exposure to a variety of oxidants (Toda *et al.*, 1991; Toone and Jones, 1998). Pap1 contains a b-Zip domain, and two cysteine rich domains (CRD); the N-terminal CRD contains four redox-sensitive cysteine residues, whilst the C-terminal CRD contains three redox-sensitive cysteine residues and a nuclear export signal (NES) which is recognised by the nuclear export factor, Crm1. In response to oxidative stress, three cysteines residues in Pap1 are critical for the regulation of Pap1 nuclear

localisation and activation (Kudo *et al.*, 1999). Following exposure to H_2O_2, cysteine 278 and cysteine 501 in the CRD of Pap1 become reversibly oxidised, forming a disulphide bond (Castillo *et al.*, 2002; Vivancos *et al.*, 2004). The *S. pombe* homologue of a bacterial two-component response regulator, Prr1, also plays a role in the oxidative stress response, alongside Pap1, whereby formation of disulphide bonds in Pap1 promotes the interaction between Pap1 and Prr1, important for the activation of H_2O_2-induced Pap1/Prr1 target genes (Calvo *et al.*, 2012). In addition, Prr1 is important for the maximal activity of most Pap1-dependent genes (Chen *et al.*, 2003).

The major cytoplasmic thioredoxin, Trx1, and the proteasome-associated thioredoxin family protein, Txl1, in *S. pombe* maintains Pap1 in a reduced state under non-stressed conditions (Day *et al.*, 2012), where it shuttles between the cytoplasm and the nucleus. Upon exposure to a low level (μM) of H_2O_2, Pap1 becomes activated and accumulates in the nucleus (Chen *et al.*, 2008). Pap1 becomes reversibly oxidised on several cysteine residues (cysteines 278, 285, 501 and 532) forming intramolecular disulphide bonds (Calvo *et al.*, 2013). Mutation of three of these cysteine residues (cysteines 278, 285 and 532) prevents Pap1 activation and causes cells to become sensitive to H_2O_2 (Calvo *et al.*, 2013). The oxidation and activation of Pap1, dependent on the 2-Cys Prx, Tpx1, prevents Pap1 associating with the nuclear export protein Crm1 (Bozonet *et al.*, 2005; Vivancos *et al.*, 2005), inhibiting its nuclear export, therefore causing Pap1 to accumulate in the nucleus, and activate the expression of H_2O_2-induced Pap1 target genes by binding to AP-1 recognition elements within the promoters of its targets genes (Toda *et al.*, 1991), and through the strengthened interaction with another transcriptional activator Prr1 (Calvo *et al.*, 2012). Along with Pap1 oxidation, exposure to H_2O_2 causes the oxidation of Trx1, due to its role in the catalytic detoxification of H_2O_2 by Tpx1, leading to the accumulation of oxidised Pap1 and Pap1-dependent gene expression (Day *et al.*, 2012). H_2O_2-induced activation of Pap1 is dependent on the thioredoxin peroxidase activity of Tpx1. However, after exposure to concentrations of H_2O_2 at which Tpx1 is hyperoxidised, its thioredoxin peroxidase activity is inhibited, preventing Pap1 activation (Bozonet *et al.*, 2005; Vivancos *et al.*, 2005), and allowing Trx1 to be targeted towards other oxidised substrate proteins to promote cell survival (Day *et al.*, 2012).

It has recently been shown that the thioredoxin peroxidase activity of Tpx1 inhibits the Txl1-mediated reduction of oxidised Pap1. In cells lacking thioredoxin reductase, Pap1 is constitutively oxidised (Vivancos *et al.*, 2004; Brown *et al.*, 2013), indicating that proteins belonging to the thioredoxin family are responsible for the reduction of oxidised Pap1. Taking all this together, loss of the thioredoxin peroxidase activity of Tpx1 protects Trx1 and Txl1 from oxidation, and prevents Pap1 activation. Multiple strands of evidence indicate that Txl1 is directly involved in the reduction of Pap1 (Brown *et al.*, 2013) (Figure 1.3). Firstly, Txl1 and Pap1 form mixed disulphides when Pap1 activation is inhibited (Brown *et al.*, 2013). Secondly, in Δ*trr1* cells, Trx1 is excluded from the nucleus, and Pap1 is constitutively oxidised (Day *et al.*, 2012; Brown *et al.*, 2013). There is also evidence to suggest that in order for Pap1 to become oxidised, it must be present in a soluble form within the cell. Trx1 and Txl1 have semi-redundant functions in maintaining Pap1 in a soluble form, as in Δ*trx1*Δ*txl1* cells, there is a pool of insoluble Pap1, resistant to H_2O_2-induced oxidation (Brown *et al.*, 2013).

In *S. cerevisiae*, the homologue of Pap1, Yap1, forms an intermolecular disulphide bond with the thioredoxin peroxidase, Gpx3, or the Tpx1 orthologue, Tsa1, required for the H_2O_2-induced oxidation and activation of Yap1 (Delaunay *et al.*, 2000; Veal et al., 2003). However, Gpx1, the Gpx3 homologue in *S. pombe* is not essential for the oxidation and activation of Pap1 (Bozonet, 2006), and no disulphide bond can be detected between Tpx1 and Pap1 (Bozonet *et al.*, 2005; Vivancos *et al.*, 2005). Interestingly, hyperoxidation of Tpx1 also prevents Pap1 oxidation; in this state, Trx1 and Txl1 are able to reduce other substrates, such as Pap1 (Brown *et al.*, 2013), rather than a Tpx1-Tpx1 disulphide.

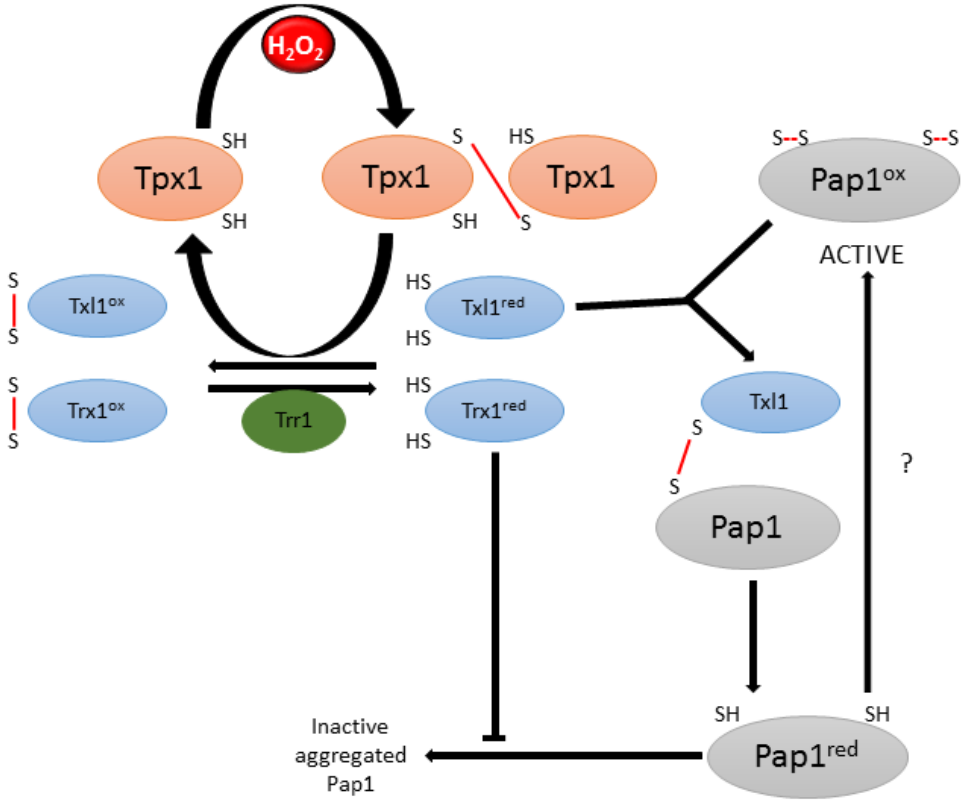

Figure 1.3 The H_2O_2-dependent regulation of Trx1 and Txl1 by Tpx1, and how this contributes to the regulation of Pap1. During the catalytic cycle of the 2-Cys Prx, Tpx1, Tpx1 disulphides are formed in response to H_2O_2. Tpx1 disulphides are reduced by members of the thioredoxin family, including Trx1 and Txl1, which become oxidised. Trx1 and Txl1 are reduced by Trr1, whose levels are limiting in *S. pombe*, to restore the oxidised thioredoxin family proteins which can then act upon Tpx1 disulphides and other oxidised proteins. This oxidation of Trx1 and Txl1 is important to prevent Txl1 from reducing active, oxidised Pap1. Data has suggested that in order for Pap1 to become oxidised and activated in response to H_2O_2, Pap1 must be in a soluble form, dependent on Trx1 and/or Txl1. It is still unclear what initiates oxidation of Pap1 (?) (Adapted from Brown, *et al.*, 2013).

1.6.3 p38/JNK related mitogen activated protein kinase (MAPK) pathways

Mitogen activated protein kinase (MAPK) pathways are essential for eukaryotic cells to respond and adapt to external environmental conditions, such as increased levels of ROS, and are highly conserved from yeast to humans (Figure 1.4). MAPK pathways consist of three tiers of protein kinases, which become activated in a cascade through serial phosphorylation in response to a range of stimuli including osmotic stress, oxidative stress, heat shock and DNA damage (For a review see (Marshall, 1994)). The activated MAPK phosphorylates a range of downstream protein targets, including transcription factors and phosphatases, which control cellular processes and bring about an appropriate response, often involving a change in gene expression towards stress adaptation (For a review see (Sabio and Davis, 2014)).

Higher eukaryotes have several MAPK pathways which can become activated in response to signals such as cytokines, to regulate certain cellular processes (Duch *et al.*, 2012). Greater redundancy and complexity of mammalian p38/JNK MAPK pathways makes studying these pathways more difficult, therefore the *S. pombe* p38/JNK related MAPK pathway, Sty1, provides a better model for the study of how mammalian p38 and JNK pathways are activated by oxidative stress. Additionally, the *S. pombe* Sty1 pathway is activated following a range of stress conditions, whereas the *S. cerevisiae* Hog1 MAPK pathway is primarily activated in response to osmotic stress, therefore Sty1 provides a better model to study the activation of mammalian MAPK by oxidative stress.

MAPK have been shown to have important roles in regulating many biological processes (Wagner and Nebreda, 2009). In humans p38 MAPK have been shown to contribute to the development of cancer (Wagner and Nebreda, 2009), and in *S. pombe*, the Sty1 MAPK is important for cell growth and survival under stress conditions (Zuin *et al.*, 2010). Understanding how MAPK are activated in response to particular stimuli will be of great value in developing drugs to selectively inhibit MAPK activity or in response to specific stimuli.

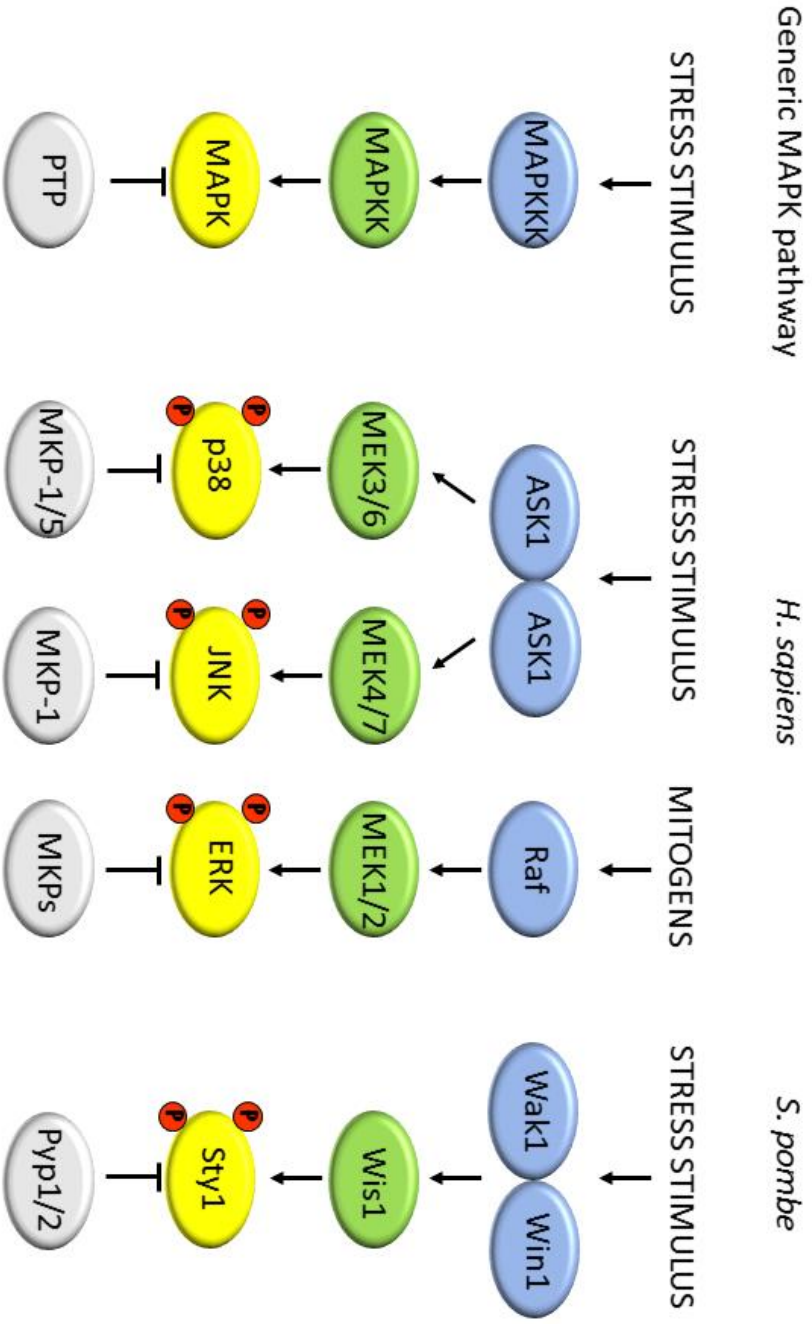

Figure 1.4 MAPK pathways are conserved, and mediate responses to a variety of stimuli. Mitogen activated protein kinase (MAPK) signalling pathways are conserved from yeast to humans, and activated following a range of stress conditions. Oxidative stress, osmotic stress, and UV irradiation can activate the p38 and JNK MAPK pathways in mammals, and the Sty1 MAPK pathway in *S. pombe*, whereas growth factors activate the ERK MAPK pathway in mammals. MAPK pathways consist of a MAPKKK, MAPKK and MAPK, which become sequentially activated by phosphorylation. MAPK can then phosphorylate downstream targets, including transcription factors, to promote changes in gene expression in response to a particular stimulus. There are three groups of MAPK, p38, JNK (c-Jun N-terminal kinase) and ERK (extracellular signal-regulated kinase), which become activated by specific MAPKK and MAPKKK, bringing substrate specificity to the pathway. To attenuate MAPK activity, protein tyrosine phosphatases (PTPs) dephosphorylate the MAPK. The p38/JNK related MAPK in *S. pombe*, Sty1 is activated by Wis1, which in turn is phosphorylated by Wak1 and Win1. Sty1 dephosphorylation is catalysed by two PTPs, Pyp1 and Pyp2 (Adapted from Latimer and Veal, 2016).

1.6.3.1 Activation of the MAPK pathway, Sty1, in S. pombe

S. pombe contains a single homologue of the p38 and JNK MAPK, Sty1 (Spc1 or Phh1). Similar to mammalian MAPK pathways, the Sty1 MAPK pathway in *S. pombe* is activated by a range of extracellular stimuli, including oxidative stress. Sty1 is crucial to bring about an appropriate response following exposure to multiple stress conditions, promoting the expression of repair and detoxification enzymes (Degols *et al.*, 1996). Following exposure to oxidative or osmotic stress stimuli, Sty1 becomes activated through increased phosphorylation of both threonine 171 and tyrosine 173 residues (Shiozaki and Russell, 1995) by a single MAPKK Wis1 (Warbrick and Fantes, 1991) (Figure 1.5). A multistep histidine-to-aspartate phosphorelay system, related to the bacterial two-component systems, regulates activation of the Sty1 MAPK pathway, which becomes activated in response to oxidative stress (Figure 1.5).

Activated Sty1 phosphorylates a range of downstream protein targets, including the *S. pombe* b-Zip transcription factor, Atf1, which becomes phosphorylated and activated following exposure to osmotic, oxidative and heat stress (Shiozaki and Russell, 1996; Wilkinson *et al.*, 1996). Activated Sty1 rapidly and transiently translocates to the nucleus, where it directly phosphorylates Atf1 at up to 11 sites, stabilising the protein, and causing expression of Atf1-induced genes, including the antioxidant genes, *gpx1*$^{+}$ (glutathione peroxidase) and *ctt1*$^{+}$ (catalase), and a phosphatase responsible for dephosphorylating Sty1, *pyp2*$^{+}$ (Wilkinson *et al.*, 1996; Chen *et al.*, 2003). Therefore, Atf1 is involved in the autoregulation of Sty1, through a negative feedback loop involving Pyp2 (Wilkinson *et al.*, 1996).

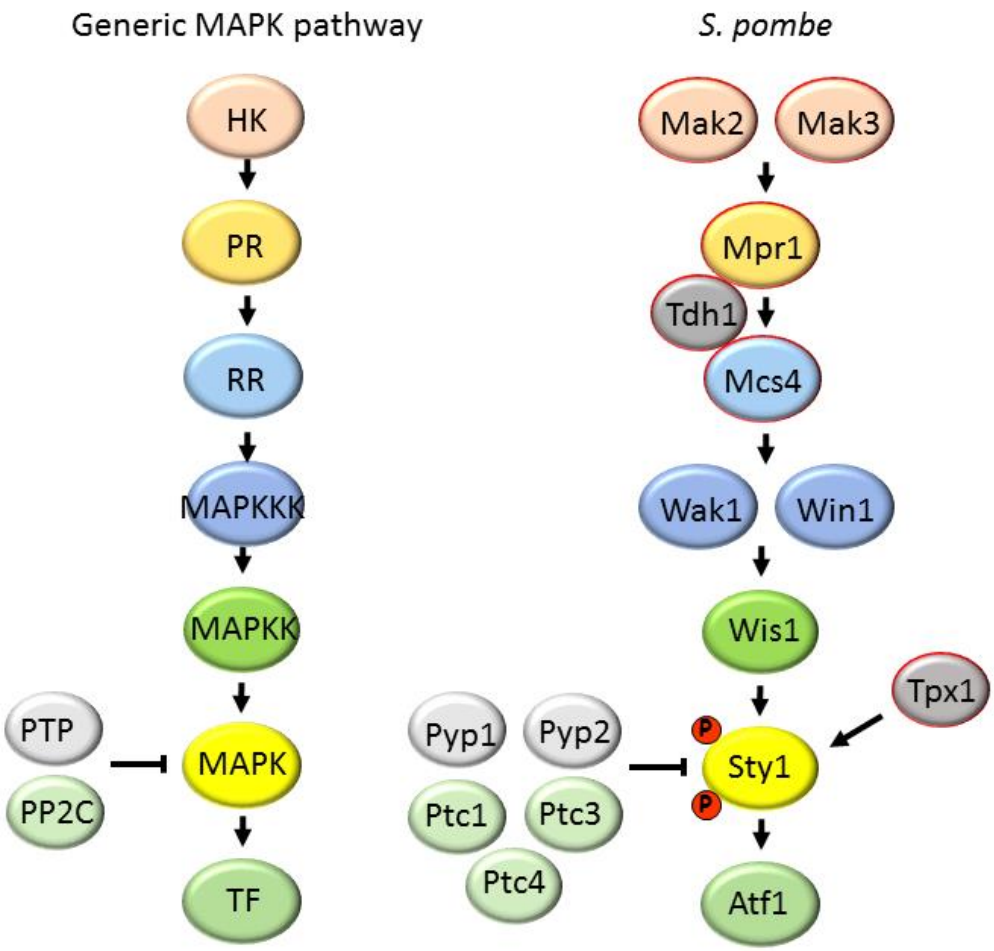

Figure 1.5 The H_2O_2-induced activation of the two-component signalling system and the MAPK pathway in *S. pombe*. Stress signals are transduced through conserved stress-activated protein kinase pathways, such as the Sty1 mitogen activated protein kinase (MAPK) pathway in *S. pombe*, resulting in activation of transcription factors (TF) such as Atf1. Sty1 activation is regulated by phosphorylation of conserved residues by the MAPK kinase (MAPKK) Wis1, which in turn is regulated by the MAPKK kinase (MAPKKK), Wak1 (Wis4) and Win1. Upstream of the MAPK pathway is a two-component signalling system involving two histidine protein kinases (HK), Mak2 and Mak3, a phosphorelay protein (PR) Mpr1, and a response regulator (RR) Mcs4. Sty1 activation in response to H_2O_2 stress is regulated by the single typical 2-Cys Prx, Tpx1, in *S. pombe*. Two protein tyrosine phosphatases (PTP), Pyp1 and Pyp2, and three type 2C serine/threonine phosphatases (PP2C), Ptc1, Ptc3 and Ptc4, dephosphorylate Sty1. The two-component signalling system, Tdh1 and Tpx1 (circled in red) are the H_2O_2 responsive parts of the pathway.

1.6.3.2 Negative regulation of the MAPK pathway, Sty1, in S. pombe

Two protein tyrosine phosphatases (PTP), Pyp1 and Pyp2, dephosphorylate tyrosine 173 of Sty1 (Millar *et al.*, 1992; Millar *et al.*, 1995), whereas three type 2C serine/threonine phosphatases (PP2C phosphatases), Ptc1, Ptc3 and Ptc4, dephosphorylate threonine 171 of Sty1 (Nguyen and Shiozaki, 1999; Di *et al.*, 2012). As activation of Sty1 requires dual phosphorylation of threonine 171 and tyrosine 173, dephosphorylation by any of these phosphatases is sufficient to deactivate Sty1, and attenuate kinase activity.

Pyp1 and Pyp2 regulate Sty1 activity under different conditions; Pyp1 regulates basal Sty1 phosphorylation, whilst Pyp2 regulates Sty1 activity following osmotic stress (Millar *et al.*, 1995; Wilkinson *et al.*, 1996). Pyp1 levels remain constant upon exposure to stress (Chen *et al.*, 2003), however, as a target of Atf1, *pyp2*$^{+}$ mRNA levels are enhanced in response to environmental stress (Wilkinson *et al.*, 1996) (Figure 1.6). Pyp2 expression is therefore regulated in a Sty1/Atf1 dependent manner, forming a negative feedback loop allowing Sty1 kinase activity to be reduced upon stress exposure (Millar *et al.*, 1995; Degols *et al.*, 1996). A Δ*pyp1*Δ*pyp2* is inviable (Millar *et al.*, 1992), suggesting an importance for one of these PTP to be present.

Work to understand the activation of MAPK has focussed on what triggers the phosphorylation of upstream kinases. However, there is evidence that the regulation of dephosphorylation reactions, mediated by PTP, isn't only to allow feedback control of the MAPK activity, but can also be involved in sensing stress stimuli (Nguyen and Shiozaki, 1999).

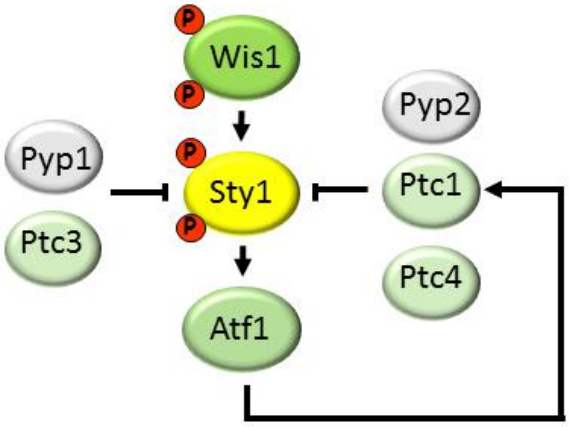

Figure 1.6 Negative regulation of Sty1 activity in *S. pombe*. In *S. pombe*, Sty1 activity is tightly regulated by the MAPKK Wis1, MAPK phosphatases and the 2-Cys Prx, Tpx1. In response to environmental stress, Sty1 becomes phosphorylated on threonine 171 and tyrosine 173 by Wis1. Two protein tyrosine phosphatases (PTP), Pyp1 and Pyp2, dephosphorylate tyrosine 173 in the activation site of Sty1, whereas three type 2C serine/threonine phosphatases (PP2C phosphatases) Ptc1, Ptc3 and Ptc4 dephosphorylate threonine 171 of Sty1. A negative feedback loop exists to reduce Sty1 activity as expression of *pyp2*$^{+}$, *ptc1*$^{+}$ and *ptc4*$^{+}$ is upregulated in a Sty1-dependent manner (Adapted from Holmes, 2013).

1.6.4 Mechanisms of regulation of transcriptional responses

Studies in *S. pombe* have provided some of the first evidence for the role of Prx in stress-induced signal transduction, as discussed in section 1.6.2 and 1.6.3. Tpx1 has been shown to be involved in the regulation of the transcriptional response to H_2O_2 in *S. pombe* via activation of the AP-1 like transcription factor Pap1 and the MAPK Sty1. Two transcription factors, Pap1 and Atf1, are vital for the expression of protective proteins in response to oxidative stress, however depending on the concentration of H_2O_2 the cell is subjected to, either one or both transcription factors are activated to induce different transcriptional responses (Quinn *et al.*, 2002). A third transcriptional activator, Prr1, also plays a role in the oxidative stress response. Oxidation of Pap1 promotes the interaction with Prr1, important for maximal activation of most Pap1 target genes (Calvo *et al.*, 2012). In addition, Prr1 is important in the regulation of Atf1 target genes at higher levels of H_2O_2 (Figure 1.7). Therefore, as expected, deletion of both *atf1*$^+$ and *pap1*$^+$ causes cells to become extremely sensitive to high levels of stress (Quinn *et al.*, 2002). At low (0.2 mM) concentrations of H_2O_2, when the thioredoxin peroxidase activity of Tpx1 is active, both the AP-1 like transcription factor Pap1, and the b-Zip transcription factor Atf1, mediate the stress response to mount an adaptive response (Bozonet *et al.*, 2005; Vivancos *et al.*, 2005). However, after exposure to concentrations of H_2O_2 at which Tpx1 is hyperoxidised (> 1.0 mM), its thioredoxin peroxidase activity is inhibited, preventing Pap1 activation. However, Sty1 can still be activated, resulting in phosphorylation and stabilisation of Atf1 (Lawrence *et al.*, 2007), allowing the transcription of Atf1-dependent genes, such as sulphiredoxin (*srx1*$^+$). Srx1 is able to reduce hyperoxidised Tpx1, reactivating the thioredoxin peroxidase activity of Tpx1, resulting in activation of Pap1 and the transcription of Pap1-dependent genes (Veal *et al.*, 2004; Bozonet *et al.*, 2005; Vivancos *et al.*, 2005). This suggests that although Tpx1 is required for the activation of both Pap1 and Sty1, the thioredoxin peroxidase activity of Tpx1 is dispensable for its role in activating Sty1 (Veal *et al.*, 2004; Bozonet *et al.*, 2005; Vivancos *et al.*, 2005).

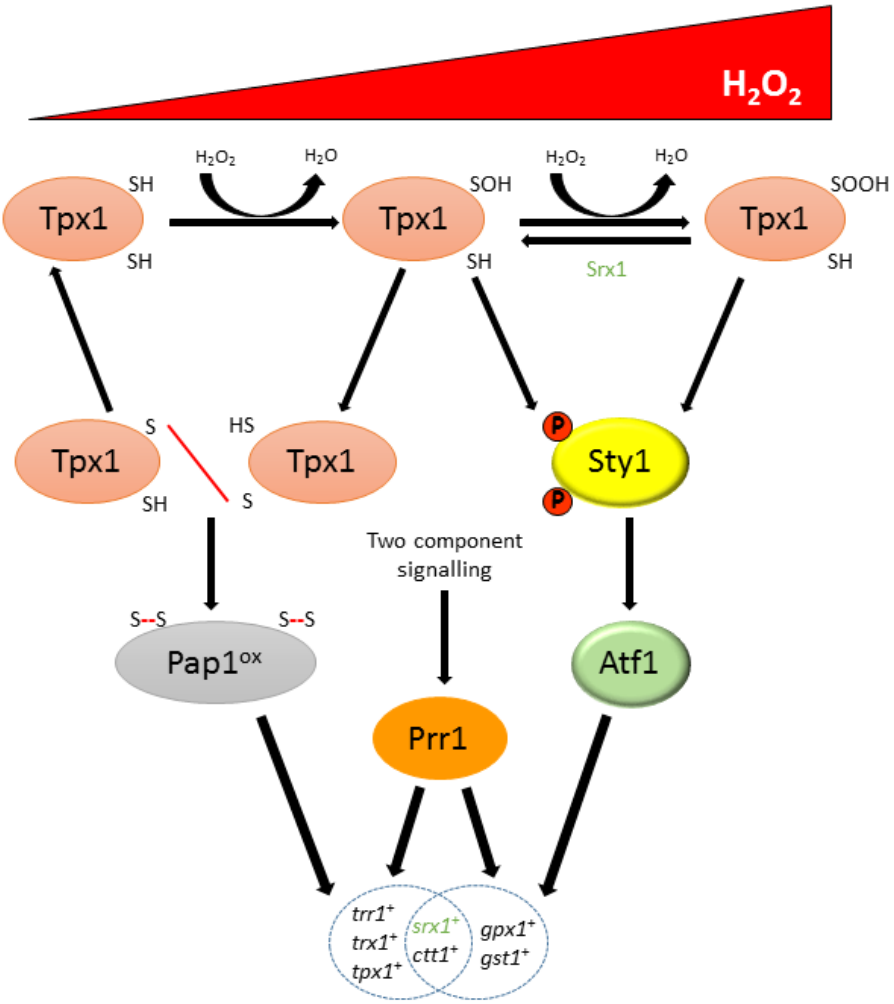

Figure 1.7 Regulation of transcriptional responses in response to different levels of H_2O_2 in *S. pombe*. At low concentrations of H_2O_2, Tpx1 activates the AP-1 like transcription factor Pap1, inducing the expression of Pap1-dependent genes, whilst at higher concentrations of H_2O_2, the Sty1 MAPK and the b-Zip transcription factor Atf1 are increasingly phosphorylated and activated. Oxidation of Pap1 in response to H_2O_2 promotes the interaction with Prr1. Prr1 is regulated via two component signalling, and is required for maximal activation of most Pap1-dependent genes, and is important for the regulation of Atf1 genes at higher H_2O_2 concentrations. When Sty1 is active, Atf1 is phosphorylated, and Atf1-dependent genes are transcribed. Srx1 is able to reduce hyperoxidised Tpx1, restoring its thioredoxin peroxidase activity. At different concentrations of H_2O_2, Atf1, Pap1 and Prr1 regulate the expression of both distinct and overlapping sets of genes, including *trr1*$^+$, *gpx1*$^+$ and *ctt1*$^+$ (Adapted from Veal *et al.*, 2014).

More recently, work from our laboratory has shown that the thioredoxin peroxidase activity of Tpx1 inhibits the Txl1-mediated reduction of oxidised Pap1, and suggests that proteins belonging to the thioredoxin family are responsible for the reduction of oxidised Pap1 (Brown *et al.*, 2013). Taken together, loss of the thioredoxin peroxidase activity of Tpx1 protects Trx1 and Txl1 from oxidation, and prevents Pap1 activation (Day *et al.*, 2012; Brown *et al.*, 2013). This provides evidence for Tpx1 functioning as a key redox-sensing protein, regulating the transcriptional response to H_2O_2, and that the oxidation status of Tpx1 acts as a molecular switch to initiate various signalling pathways. However, the mechanisms by which Prx such as Tpx1 in *S. pombe* sense and respond to increasing levels of H_2O_2 remains unclear.

1.7 Summary and Aims

Exposure of cells to ROS leads to oxidative stress and cellular damage, associated with the initiation and development of many diseases. More recently, positive signalling roles have been identified for low levels of H_2O_2 in the initiation of many biological responses, important for normal health and longevity, but also as an adaptive response to limit the damaging effects of higher levels of ROS. H_2O_2 is able to specifically target oxidation-sensitive signalling proteins, such as Prx. Prx are important in the defence against ROS, to detoxify and reduce peroxides, but have also been shown to have important roles in promoting H_2O_2-induced signal transduction and as molecular chaperones. However, how less reactive proteins become oxidised by H_2O_2 in the presence of highly abundant and more reactive proteins remains unclear. This study aims to identify the molecular mechanisms underlying H_2O_2-sensing and H_2O_2-induced signal transduction in *S. pombe*.

H_2O_2-induced oxidation of susceptible cysteine residues in PTP has been established as an integral part of signal transduction. Based on the H_2O_2-sensitivities of PTP to oxidation, and that activity of the typical 2-Cys Prx, Tpx1, in *S. pombe*, promotes the oxidation of other proteins, we hypothesised that Tpx1 might promote the oxidation of a PTP, Pyp1 or Pyp2, that regulates Sty1 MAPK activity, increasing

activation of Sty1 in response to low levels of H_2O_2. The first objective of this project was to identify whether Tpx1 might promote the H_2O_2-induced activation of Sty1 by regulating Pyp1 or Pyp2 in *S. pombe*.

The glycolytic enzyme GAPDH is important for H_2O_2-induced activation of Sty1. H_2O_2-induced oxidation of the catalytic cysteine inactivates the glycolytic activity of GAPDH, but was proposed to promote its signalling activity. There is evidence that GAPDH oxidation protects cells against ROS by inhibiting glycolysis and allowing increased NADPH production through the pentose phosphate pathway. The second objective of this project was to identify whether H_2O_2-induced GAPDH oxidation is also important for its non-glycolytic signalling functions in *S. pombe*, specifically in promoting the H_2O_2-induced activation of Sty1, and cell survival under oxidative stress conditions.

Alongside their role as an antioxidant, typical 2-Cys Prx have also been shown to act as H_2O_2 sensors to transmit the H_2O_2 signal by promoting the oxidation of less reactive protein-thiols, thus regulating the activity of diverse proteins. Several studies have identified positive roles for Prx in promoting H_2O_2 signal transduction. Indeed, the typical 2-Cys Prx, Tpx1, in *S. pombe*, is needed to promote the H_2O_2-induced activation of the AP-1-like transcription factor Pap1 and the Sty1 MAPK, causing oxidation of their redox-active cysteine residues. This raised the possibility that Tpx1 might have further roles in the regulation of other cytoplasmic proteins, through influencing the redox state of the protein. The third objective of this project was to use a directed and proteomic approach to identify other thiol-containing proteins in *S. pombe* regulated by Tpx1-mediated oxidation following exposure to H_2O_2.

CHAPTER 2

Materials and Methods

2.1 Molecular biology techniques

2.1.1 Polymerase Chain Reaction (PCR)

PCR reactions for gene cloning and to confirm genotypes were performed using the Phusion High-Fidelity PCR System (NEB) in a final volume of 50 µl. Reaction mixes contained 0.1 µg template DNA, 1 x PCR buffer (supplied with enzyme), 200 µM each dNTP (dATP, dCTP, dGTP and dTTP), 100 pmol each oligonucleotide primer (Table 2.1), and 0.5 µl polymerase enzyme. PCR was performed in the thermocycler using the following parameters: 98°C 30 seconds, 35 cycles of 98°C 10 seconds, 52°C 30 seconds, 72°C 1-3 minutes (1 minute per kb), and a final elongation step of 72°C for 10 minutes.

2.1.2 PCR to introduce mutations

Complementary forward and reverse oligonucleotide primers containing the desired mutation were used to introduce the mutation by a two-step overlapping PCR. The first-step PCR generated a megaprimer, containing the desired mutation. The first-step PCR reactions were performed using the Phusion High-Fidelity PCR System (NEB) in a final volume of 50 µl. Reaction mixes contained 0.1 µg template DNA, 1 x PCR buffer (supplied with enzyme), 200 µM each dNTP (dATP, dCTP, dGTP and dTTP), 100 pmol each oligonucleotide primer (Table 2.1), and 0.5 µl polymerase enzyme. PCR was performed in the thermocycler using the following parameters: 98°C 30 seconds, 35 cycles of 98°C 10 seconds, 52°C 30 seconds, 72°C 1-3 minutes (1 minute per kb), and a final elongation step of 72°C for 10 minutes.

Table 2.1 Oligonucleotide primers used in this study. Oligonucleotide primers were supplied by Sigma-Aldrich or Eurofins MWG Operon. Primers containing restriction enzyme sites are underlined and primers used to introduce a mutation are shown in bold.

Primer	Oligonucleotide sequence 5'-3'
*BamH1*GAPDH1C-STOP	CCCAATGGATCCGTTGTCCTTGGCGGCAGTGTA
*BamH1*W/OSTOPPyp1B	TAACGAGGATCCTGTTAAAACCGGGAAATGAACT
*BamH1*W/OSTOPPyp1BShort	TAACGAGGATCCTGTTAAAA
*BamH1*W/OSTOPPyp2B	TAACGAGGATCCAGTCATCAAGGGCTTGGAAGCCTG
*BamH1*W/OSTOPPyp3BLong	TAACGAGGATCCTAACTGAGGAAGAAGAAATTC
*BamH1*W/OSTOPTim40B	TAACGAGGATCCAATTTCCTTTATAACTGACATAGG
GFPcheckB	CCGGCGGCGGTCACGAACTCCAGC
*Nde1*Pyp1C20SF	CCCGACCATATGAATTTTTCAAACGGTTCAAAATCGTCTACTTTTACA ATTGCTCCTTCGGGTTCA**AGT**ATTGCTTTACCTCCTCAG
*Nde1*Pyp1B	AAATTCATATGGGTTTTTTAGATGAATGTTTTGTA
*Nde1*Pyp1F	TATTCGCATATGAATTTTTCAAACGGTTCAAAA
NMTend	GCAGCTTGAATGGGCTTCCC
Pk*Nco1*B	GGAATACCCATGGAATCAAGACC
*Pst1*GAPDH1N	GCGCGAATTCTGCAGATGGCAATTCCTAAGGTTGGTATT
*Pst1*GAPDH1NShort	GCGCGAATTCTGCAGATGGCAAT
*Pst1*NΔ30Pyp1F	TATTCGCTGCAGACGAGTAAGTATGCTGTTCATGCT
*Pst1*Pyp1F	TATTCGCTGCAGATGAATTTTTCAAACGGTTCAAAA
*Pst1*Pyp1FShort	TATTCGCTGCAGATGAATTT
*Pst1*Pyp2F	TATTCGCTGCAGATGCTCCATCTTCTGTCTAAAGAC
*Pst1*Pyp3FLong	TATTCGCTGCAGATGTCTTTTAAAGAAGTATCT
Pyp1checkB	AAAGCATCTGAAAATAATACAAGG
Pyp1checkF	ACTTGTGCTATCCAATATTTGTAT
Pyp1C118SB	AAGCAGGAAC**AGA**AACAAGAATG
Pyp1C222SB	CAGGTAGAGG**AGA**GAAAAAGTTA
Pyp1C441SF	TTGGTCTGAT**TCT**AATTCTCCTG
Pyp1C470SF	ACTATTGTGCAC**TCT**TCTGCCG
Pyp1intcheck	TTTAAGGCCAAATATTCTTAATAC
Pyp1intcheckB	TCTAAAATACCGAAGTCACCAGAA
Pyp1upstreamcheck	TTGGTAAAAATCAAAAATCGTTAG
Pyp2intcheckF	GGTCAACACTCATTTGTTTC
Pyp2intcheck	TTTAAAAGTTTCCTGTATATATAT
Pyp3intcheck	TTAGGAATCATTTAAAGTCGTTTA
*Sph1*Pyp1FNew	TAGGCAGCATGCACTTGATTTCGTTGACGTTTAGTG
*Sph1*Tim40F	TATTCGGCATGCATGTTTGCTAAAAACTTACTTTTC
Tdh1C156SB	AGGGGAGCCAAAGAGTTGGTGGTG
Tdh1intcheck	TCGCTTCTGTATAGATCATTCATC
Tdh1intcheckB	GACAACGTACATGGGGGCGTCCTT
Tim40intcheck	ACATGCAAACTTATATAAACTTAG

In the overlapping PCR, the PCR-amplified megaprimer and an appropriate forward or reverse oligonucleotide primer were used. PCR reactions were performed using the Phusion High-Fidelity PCR System (NEB) in a final volume of 50 µl. Reaction mixes contained 0.1 µg template DNA, 1 x PCR buffer (supplied with enzyme), 200 µM each dNTP (dATP, dCTP, dGTP and dTTP), 100 pmol oligonucleotide primer (Table 2.1), 100 pmol megaprimer, and 0.5 µl polymerase enzyme. PCR was performed in the thermocycler using the following parameters: 98°C 3 minutes, and 10 cycles of 98°C 3 minutes, 40°C 30 seconds, 72°C 2 minutes. Due to the inefficient nature of the megaprimer to further amplify the mutated DNA, 100 pmol another oligonucleotide primer was added to specifically amplify the already amplified, mutated DNA. PCR was performed in the thermocycler using the following parameters: 98°C 3 minutes, 35 cycles of 98°C 10 seconds, 52°C 30 seconds, 72°C 1-3 minutes (1 minute per kb), and a final elongation step of 72°C for 10 minutes.

2.1.3 Agarose gel electrophoresis

1% (w/v) agarose gels were prepared and run in 1 x TAE (40 mM Tris-acetate, 1 mM EDTA [pH8.0]) to separate DNA in PCR products, digested plasmids and digested DNA fragments. Gels were stained with 0.02% ethidium bromide, and excised bands were extracted from the gel using a QIAquick gel extraction kit (QIAGEN). Final DNA concentrations were measured using a Nanodrop spectrophotometer (Labtech).

2.1.4 Oligonucleotide primer sequences

All oligonucleotides were obtained from Sigma-Aldrich, with the exception of Nde1Pyp1C20SF (Eurofins MWG Operon). The sequences are listed in Table 2.1.

2.1.5 DNA sequencing

DNA sequence analysis was performed by GATC BioTech (UK).

2.1.6 Bacterial growth conditions

Escherichia coli were grown in Luria Broth (LB) (2% (w/v) Bacto tryptone, 1% (w/v) Bacto yeast extract, 1% (w/v) NaCl [pH7.2]) media. For the formation of solid media, 2% (w/v) Bacto agar was added. LB media containing 0.1 mg/ml ampicillin (Sigma-Aldrich) was used for the growth of *E. coli* transformed with plasmids carrying the ampicillin resistant gene.

2.1.7 Transformation, propagation and isolation of plasmids

Competent *E. coli* with the genotype *e74-(mcrA-) Δ(mcrCB-hsdSMR-mrr)171 endA1 SupE44 thi-1 gyrA96 relA lac recB recJ shcJ umuC::Tn5 (Kan^r) uvrC[F'proAB lacI^{q}Z Δmis Tn10 (Tet^r)]* were used for the propagation and isolation of plasmids. 100 µl competent cells were incubated with 1-2 µl (5-10 µg) plasmid DNA on ice for 30 minutes, followed by 2 minutes at 42°C to heat shock. To cool cells down, 1 ml liquid LB media was added to cells, before incubation at 37°C for 1 hour. The cells were plated onto LB agar plates containing the appropriate antibiotic and incubated overnight at 37^{o}C. Plasmid DNA was isolated from *E. coli* cells using the GenElute Plasmid Miniprep Kit (Sigma-Aldrich), following the manufacturer's protocol.

2.1.8 Restriction endonuclease digestion, phosphatase treatment and DNA ligation reactions

Restriction enzyme digests were performed using appropriate enzymes (1 µl enzyme) and buffers (5 µl recommended buffer) (Thermo Scientific and Promega) for 2-3 hours at 37°C in a reaction volume of 50 µl. Digested plasmids were then treated with 1 µl alkaline phosphatase and 10 µl 10 x phosphatase buffer for 30 minutes at 37°C to prevent re-ligation, in a reaction volume of 100 µl. The digested plasmid and DNA fragment were purified using a QIAGEN gel purification kit, and ligated together with 1 µl T4 DNA ligase and 2 µl 10 x ligase buffer (Promega) at a 1 plasmid: 5 fragment molar ratio. Ligations were carried out overnight at 15°C in a reaction volume of 20 µl.

2.1.9 Plasmid constructs

The plasmids constructed in this study are listed below:

(1) pRip42Pyp1^{C20S}PkC

The *pyp1*$^{+}$ ORF without the stop codon was amplified by PCR from the plasmid pRip42Pyp1PkC using the oligonucleotide primers *Nde1*Pyp1C20SF, to introduce the desired mutation, and *BamH1*W/OSTOPPyp1B. The PCR product was isolated, digested with *Nde1* and *BamH1* restriction endonucleases, and ligated with pRip42PkC integration vector digested with the same enzymes. To replace the *nmt* promoter in the generated plasmid with the *pyp1* promoter, the *pyp1* promoter was amplified by PCR from CHP429 *S. pombe* genomic DNA using the oligonucleotide primers *Sph1*Pyp1FNew and *Nde1*Pyp1B. The PCR product was isolated, digested with *Sph1* and *Nde1* restriction endonucleases, and ligated with pRip42Pyp1^{C20S}pkC digested with the same enzymes.

(2) pRip42Pyp1^{C118S}PkC, pRip42Pyp1^{C222S}PkC

The *pyp1*$^{+}$ ORF without the stop codon was amplified through a two-step overlapping PCR from the plasmid pRip42Pyp1PkC (Figure 2.1). The first step PCR used the oligonucleotide primers *Pst1*Pyp1F and Pyp1C118SB, or Pyp1C222SB respectively to generate a megaprimer. The PCR-amplified megaprimer, carrying the desired mutation, was subsequently used in the overlapping step with oligonucleotide primers *Pst1*Pyp1FShort and *BamH1*W/OSTOPPyp1B. The PCR product was digested with *Pst1* and *BamH1* restriction endonucleases, and ligated with pRip42PkC (Maundrell *et al.*, 1988) digested with the same enzymes, resulting in the removal of the *nmt* promoter region.

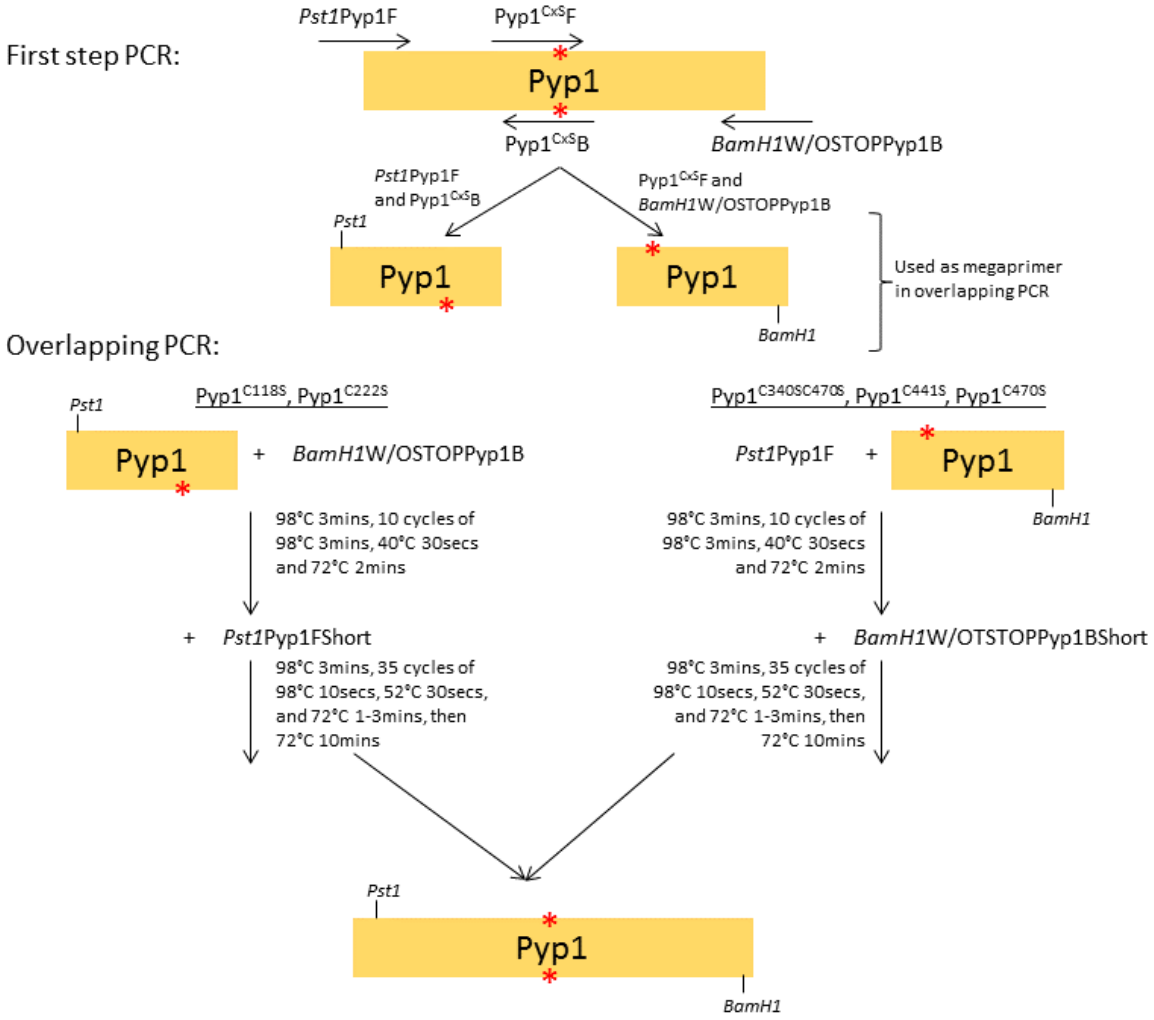

Figure 2.1 Overlapping PCR to generate Pyp1 cysteine mutants, Pyp1^{C118S}, Pyp1^{C222S}, Pyp1^{C340SC470S}, Pyp1^{C441S}, Pyp1^{C470S} and NΔ30Pyp1^{C470S}. A two-step overlapping PCR was employed to amplify the *pyp1*$^{+}$ ORF, using oligonucleotide primers specifically designed for this strategy. The oligonucleotide primers used in the first step and overlapping step of the PCR varied depending on the location of the mutated cysteine residue in the sequence, and the expected size of the PCR-amplified product (see section 2.1.9). The first step of the PCR generated a megaprimer, using either the oligonucleotide primers *Pst1*Pyp1F and Pyp1^{CxS}B, or Pyp1^{CxS}F and *BamH1*W/OSTOPPyp1B, subsequently used in the overlapping PCR step. One of the oligonucleotide primers, Pyp1^{CxS}F or Pyp1^{CxS}B, used in this first step introduced the desired mutation into the megaprimer. In the overlapping PCR, the megaprimer and either *Pst1*Pyp1F or *BamH1*W/OSTOPPyp1B was used to amplify the mutated DNA. Due to the inefficient nature of the megaprimer to further amplify the mutated DNA, another oligonucleotide primer was added after 10 cycles to produce the final amplified mutated DNA. The shortened oligonucleotide primers, *Pst*I Pyp1FShort or *BamHI*W/OSTOPPyp1BShort, were designed to specifically amplify the already amplified mutated DNA, with the cysteine-to-serine substitution, and due to lack of homology to the wild-type version of Pyp1, would prevent amplification of the wild-type copy of DNA. The asterisk (*) indicates the introduced mutation in the DNA.

(3) pRip42Pyp1^{C340SC470S}PkC, pRip42Pyp1^{C441S}PkC, pRip42Pyp1^{C470S}PkC

The *pyp1*$^{+}$ ORF without the stop codon was amplified through a two-step overlapping PCR from the plasmid pRip42Pyp1PkC or pRip42Pyp1^{C340S}PkC (Figure 2.1). The first step PCR used the oligonucleotide primers Pyp1C441SF, or Pyp1C470SF respectively, and *BamH1*W/OSTOPPyp1B to generate a megaprimer. The PCR-amplified megaprimer, carrying the desired mutation, was subsequently used in the overlapping step with oligonucleotide primers *Pst1*Pyp1F and *BamH1*W/OSTOPPyp1BShort. The PCR product was digested with *Pst1* and *BamH1* restriction endonucleases, and ligated with pRip42PkC digested with the same enzymes, resulting in the removal of the *nmt* promoter region.

(4) pRip42NΔ30Pyp1^{C470S}PkC

The *pyp1*$^{+}$ ORF without the stop codon was amplified through a two-step overlapping PCR from NΔ30Pyp1-3PK (NJ1884) *S. pombe* genomic DNA. The first step PCR used the oligonucleotide primers Pyp1C470SF and *BamH1*W/OSTOPPyp1B to generate a megaprimer. The PCR-amplified megaprimer, carrying the desired mutation, was subsequently used in the overlapping step with oligonucleotide primers *Pst1*NΔ30Pyp1F and *BamH1*W/OSTOPPyp1BShort. The PCR product was digested with *Pst1* and *BamH1* restriction endonucleases, and ligated with pRip42PkC digested with the same enzymes, resulting in the removal of the *nmt* promoter region.

(5) pRip42Pyp1PkC

The *pyp1*$^{+}$ ORF without the stop codon was amplified by PCR from the plasmid pRip42Pyp1PkC using the oligonucleotide primers *Pst1*Pyp1F and *BamH1*W/STOPPyp1B. The PCR product was isolated, digested with *Pst1* and *BamH1* restriction endonucleases, and ligated with pRip42PkC digested with the same enzymes, resulting in the removal of the *nmt* promoter region.

(6) pRip42Pyp2PkC

The *pyp2*$^{+}$ ORF without the stop codon was amplified by PCR from CHP429 *S. pombe* genomic DNA using the oligonucleotide primers *Pst1*Pyp2F and *BamH1*W/STOPPyp2B. The PCR product was isolated, digested with *Pst1* and *BamH1* restriction endonucleases, and ligated with pRip42PkC digested with the same enzymes, resulting in the removal of the *nmt* promoter region.

(7) pRip42Pyp3PkC

The *pyp3*$^{+}$ ORF without the stop codon was amplified by PCR from CHP429 *S. pombe* genomic DNA using the oligonucleotide primers *Pst1*Pyp3FLong and *BamH1*W/STOPPyp3BLong. The PCR product was isolated, digested with *Pst1* and *BamH1* restriction endonucleases, and ligated with pRip42PkC digested with the same enzymes, resulting in the removal of the *nmt* promoter region.

(8) pRip42Tdh1^{C156S}PkC

The *tdh1*$^{+}$ ORF without the stop codon was amplified through a two-step overlapping PCR from the plasmid pRip42Tdh1PkC. The first step PCR used the oligonucleotide primers *Pst1*GAPDH1N and Tdh1C156SB to generate a megaprimer. The PCR-amplified megaprimer, carrying the desired mutation, was subsequently used in the overlapping step with oligonucleotide primers *Pst1*GAPDH1NShort and *BamH1*GAPDH1C-STOP. The PCR product was digested with *Pst1* and *BamH1* restriction endonucleases, and ligated with pRip42PkC digested with the same enzymes, resulting in the removal of the *nmt* promoter region.

(9) pRip42Tim40EGFPC

The *tim40*$^{+}$ ORF without the stop codon was amplified by PCR from CHP429 *S. pombe* genomic DNA using the oligonucleotide primers *Sph1*Tim40F and *BamH1*W/STOPTim40B. The PCR product was isolated, digested with *Sph1* and *BamH1* restriction endonucleases, and ligated with pRip42EGFPC digested with the same enzymes, resulting in the removal of the *nmt* promoter region.

(10) Plasmids used in this study

The plasmids used in this study are listed in Table 2.2.

Table 2.2 Plasmids used in this study.

Plasmid	Reference
pRep1	Maundrell *et al.*, 1998
pRep1Tpx1	Veal *et al.*, 2004
pRep41PkC	Maundrell *et al.*, 1998
pRep41FlagTpx1	Veal *et al.*, 2004
pRep41FlagTpx1^{C48}	Veal *et al.*, 2004
pRep41FlagTpx1^{C48SC169S}	E. Veal
pRep41FlagTpx1^{C169S}	Veal *et al.*, 2004
pRep41HM	Maundrell *et al.*, 1998
pRep41Srk1HM	Smith *et al.*, 2002
pRip42PkC	A. Day
pRip42EGFPC	S. Whitehall
pRip42NΔ30Pyp1^{C470S}PkC	This study
pRip42Pyp1PkC	A. Day
pRip42Pyp1^{C20S}PkC	This study
pRip42Pyp1^{C118S}PkC	This study
pRip42Pyp1^{C222S}PkC	This study
pRip42Pyp1^{C340S}PkC	A. Day
pRip42Pyp1^{C340SC470S}PkC	This study
pRip42Pyp1^{C441S}PkC	This study
pRip42Pyp1^{C470S}PkC	This study
pRip42Pyp2PkC	A. Day
pRip42Pyp3PkC	A. Day
pRip42Tdh1PkC	Taylor, 2009
pRip42Tdh1^{C156S}PkC	This study
pRip42Tim40EGFPC	This study

2.2 Growth, maintenance and genetic manipulation of *Schizosaccharomyces pombe*

2.2.1 Strains and growth conditions

The *Schizosaccharomyces pombe* strains used in this study are shown in Table 2.3. Cells were grown at 30°C in either standard rich media (YE5S; 0.5% (w/v) yeast extract, 3% (w/v) glucose and 225 mg/l adenine, histidine, leucine, uracil and lysine) or Edinburgh minimal media (EMM; 3 g/l potassium hydrogen phthalate ($C_8H_5O_4K$), 2.2 g/l di-sodium hydrogen orthophosphate (Na_2HPO_4), 5 g/l ammonium chloride (NH_4Cl_2), 2% (w/v) glucose, 20 ml/l salts (50 x stock [52.5 g/l magnesium chloride ($MgCl_2.6H_2O$), 0.735 mg/l calcium chloride ($CaCl_2.2H_2O$), 50 g/l potassium chloride (KCl) and 2 g/l di-sodium sulphate (Na_2SO_4)]), 1 ml/l vitamins (1000 x stock [1 g/l panthothenic acid, 10 g/l nicotinic acid, 10 g/l *myo*-inositol and 10 mg/l biotin]), 0.1 ml/l minerals (10,000 x stock [5 g/l boric acid, 4 g/l magnesium sulphate ($MnSO_4$), 4 g/l zinc sulphate ($ZnSO_4.7H_2O$), 2 g/l iron chloride ($FeCl_2.6H_2O$), 0.4 g/l molybdic acid , 1 g/l potassium iodide (KI), 0.4 g/l copper sulphate ($CuSO_4.5H_2O$) and 10 g/l citric acid]). EMM was supplemented with appropriate amino acids for selective growth. EMM ½ G (as EMM with NH_4Cl replaced with 1 g/l sodium glutamate) was used for mating and sporulation of strains. For solid media 2% (w/v) bacto-agar was added. *S. pombe* cultures were grown aerobically until mid-log phase (OD_{595} 0.25-0.5), and harvested. Cell numbers were estimated by optical density (OD_{595} 0.5 = $1x10^7$ cells/ml for wild-type cells).

2.2.2 Strain construction and meiosis

2.2.2.1 Genetic mating

Haploid *S. pombe* strains were mated by mixing growing cells of opposite mating types (h^+ and h^-) on EMM ½ G along with a loopful of sterile H_2O. Plates were incubated at 25°C for 3 days until the formation of asci and spores.

Table 2.3 *Schizosaccharomyces pombe* strains used in this study.

Strain	Genotype	Source
972	*h⁺*	Laboratory stock
AD82	*h⁺ ade6-M210 leu1-32 his7-366*	A. Day
CHP428	*h⁺ ade6-M216 leu1-32 ura4-D18 his7-366*	Laboratory stock
CHP429	*h⁻ ade6-M216 leu1-32 ura4-D18 his7-366*	Laboratory stock
EV62	*h⁺ ade6 leu1-32 ura4-D18*	Bioneer Ltd
JR68	*h⁺ ade6 leu1-32 ura4-D18 tpx1::ura4⁺ tpx1+:LEU2*	Day *et al.*, 2012
NT4	*h⁺ ade6-M210 leu1-32 ura4-D18*	N. Jones
ST15	*h⁺ ade6 leu1-32 ura4-D18*	Bioneer Ltd
AD22	*h⁻ ade6-M216 leu1-32 ura4-D18 his7-366 sty1::his7⁺*	Day and Veal, 2010
AD81	*h⁻ ade6-M216 leu1-32 ura4-D18 his7-366 trr1::ura4⁺*	Brown *et al.*, 2013
AD138	*h? ade6 leu1-32 ura4-D18 his7-366 tpx1::ura4⁺ trr1::ura4⁺*	Brown *et al.*, 2013
AD144	*h? ade6-M210 leu1-32 ura4-D18 his7-366 Flag-trx1:ura4⁺ trx1::kanMx4 pyp1-3Pk:kanMX6*	A. Day
EV60	*h⁻ ade6-M216 leu1-32 ura4-D18 his7-366 pyp3::ura4⁺*	E. Veal
JB30	*h⁻ ade6-M216 leu1-32 ura4-D18 his7-366 trx1::kanmx4*	Day *et al.*, 2012
JB120	*h? ade6 leu1-32 ura4-D18 his7-366 trx1::kanmx4 txl1::kanmx4 trr1::ura4⁺*	Brown *et al.*, 2013
JP151	*h⁻ ade6-M216 leu1-32 ura4-D18 his7-366 wis1-12myc:ura4⁺*	J. Quinn
JP203	*h⁻ leu1-32 ura4-D18 srk1(3Pk):ura4⁺*	Smith *et al.*, 2002
JP279	*h⁻ pyp2::kanMX6*	Petersen and Nurse, 2007
JP392	*h⁺ pyp2.13myc_3'UTR(kanMX6)*	Kowalczyk *et al.*, 2013
JP959	*h⁺ pyp2.linker-free.13myc_3'UTR(kanMX6)*	Kowalczyk *et al.*, 2013
JR42	*h⁺ ade6 leu1-32 ura4-D18 his7-366 tpx1::ura4 tpx1^{C169S}:leu2*	Day *et al.*, 2012
NJ102	*h⁺ ade6-M210 leu1-32 ura4-D18 his7-366 pyp1::kanMX6*	N. Jones
NJ209	*h⁺ ade6-210 leu1-32 ura4-D18 his7 sty1::ura4 pyp1-3pk:kan*	N. Jones
NJ197	*h⁺ ade6-M210 leu1-32 ura4-D18 his7-366 pyp1-3Pk:kanMX6*	N. Jones
NJ586	*h⁺ ade6-M210 leu1-32 ura4-D18 his7-366 wis1::ura4 pyp1-3pk*	N. Jones
NJ1088	*h⁺ ade6-M210 leu1-32 ura4-D18 his7-366 wis1DD:12myc:ura pyp1-3PK:kan (1)*	N. Jones
NJ1116	*h⁺ ade6 leu1-32 ura4-D18 his7-366 wis1-12myc:nat pyp1-3pk:kan*	N. Jones
NJ1284	*h⁺ ade6-M210 leu1-32 ura4-D18 his7-366 ptc4::natMX6*	N. Jones
NJ1659	*h⁺ ade6-M210 leu1-32 ura4-D18 his7-366 wis1DD:12myc:ura pyp1-3PK:kan (2)*	N. Jones
NJ1660	*h⁺ ade6-M210 leu1-32 ura4-D18 his7-366 pyp1^{Y337F}-3pk::ura4⁺*	N. Jones
NJ1884	*h⁺ ade6-M210 leu1-32 ura4-D18 his7-366 NΔ30pyp1-3Pk:kanMX6*	Holmes, 2013
NJ1904	*h⁺ ade6-210 leu1 ura4 his7 wis1DD:ura:13myc sty1D::nat pyp1-3pk:kan*	N. Jones
ST1	*h⁻ ade6-M216 leu1-32 ura4-D18 his7-366 tdh1⁺(3PK):ura4⁺*	Taylor, 2009
ST2	*h⁻ ade6-M216 leu1-32 ura4-D18 his7-366 gpd3⁺(3PK):ura4⁺*	Taylor, 2009
ST3	*h⁺ ade6 leu1-32 ura4-D18 tdh1::kan^{mx4}*	Taylor, 2009
ST5	*h⁺ ade6 leu1-32 ura4-D18 gpd3::kan^{mx4}*	Taylor, 2009

TP108-3C	*h⁻ leu1 ura4 pap1::ura4⁺*	Toda *et al.*, 1991
VB1692	*h⁻ ade6-M216 leu1-32 ura4-D18 his7-366* mcs4^{D412N}	Buck *et al.*, 2001
VXOO	*h⁺ ade6 leu1-32 ura4-D18 his7-366 tpx1::ura4⁺*	Veal *et al.*, 2004
HL2	*h⁺ ade6-M210 leu1-32 ura4-D18 pyp1pk::ura4⁺*	This study
HL3	*h⁺ ade6-M210 leu1-32 ura4-D18 pyp1^{C470S}pk::ura4⁺*	This study
HL4	*h⁺ ade6-M210 leu1-32 ura4-D18 pyp1^{C340SC470S}pk::ura4⁺*	This study
HL7	*h⁺ ade6-M210 leu1-32 ura4-D18 pyp1^{C118S}pk::ura4⁺*	This study
HL8	*h⁺ ade6-M210 leu1-32 ura4-D18 pyp1^{C222S}pk::ura4⁺*	This study
HL9	*h⁺ ade6-M210 leu1-32 ura4-D18 pyp1^{C441S}pk::ura4⁺*	This study
HL10	*h⁺ ade6-M210 leu1-32 ura4-D18 his7-366 pyp1::kanMX6 pyp1^{C20S}pk:ura4⁺*	This study
HL11	*h⁺ pyp2::kanMX6*	This study
HL12	*h⁻ pyp2.13myc_3'UTR(kanMX6)*	This study
HL13	*h⁻ leu1-32 mcs4^{D412N} pyp2::kanMX6*	This study
HL14	*h? his7-366 mcs4^{D412N} pyp2.13myc.UTR-kanMX*	This study
HL15	*h⁺ ade6-M210 leu1-32 ura4-D18 his7-366 pyp1^{C340S}-3Pk:kanMX6*	This study
HL16	*h⁺ ade6-M210 leu1-32 ura4-D18 tim40egfp::ura4⁺*	This study
HL17	*h⁺ ade6-M210 leu1-32 ura4-D18 his7-366 tim40egfp::ura4⁺ tpx1::ura4⁺ tpx1^{C169S}:leu2 (1)*	This study
HL18	*h⁺ ade6-M210 leu1-32 ura4-D18 his7-366 tim40egfp::ura4⁺ tpx1::ura4⁺ tpx1^{C169S}:leu2 (2)*	This study
HL19	*h? ade6-M210 leu1-32 ura4-D18 his7-366 pyp1::kanMX pyp3::ura4⁺*	This study
HL20	*h? ade6-M210 leu1-32 ura4-D18 his7-366 NΔ30pyp1-3Pk:kanMX6 pyp3::ura4⁺*	This study
HL21	*h⁺ ade6-M210 leu1-32 ura4-D18 his7-366 pyp1::kanMX6 pyp2.13myc_3'UTR(kanMX6)*	This study
HL23	*h⁻ ade6-M210 leu1-32 ura4-D18 pyp1pk::ura4⁺*	This study
HL24	*h⁻ ade6-M210 leu1-32 ura4-D18 pyp2pk::ura4⁺*	This study
HL25	*h⁻ ade6-M210 leu1-32 ura4-D18 pyp3pk::ura4⁺*	This study
HL26	*h⁺ ade6-M210 leu1-32 ura4-D18 his7-366 pyp2pk::ura4⁺ pyp1::kanMX6 pyp1^{C20S}pk:ura4⁺*	This study
HL27	*h⁺ ade6-M210 leu1-32 ura4-D18 his7-366 pyp1::kanMX6 pyp2pk::ura4⁺*	This study
HL30	*h⁻ ade6-M216 leu1-32 ura4-D18 his7-366 tdh1^{C156S}(3PK):ura4⁺*	This study
HL31	*h⁻ ade6-M216 leu1-32 ura4-D18 his7-366 wis1-12myc:ura4⁺ tdh1⁺(3PK):ura4⁺*	This study
HL32	*h⁻ ade6-M216 leu1-32 ura4-D18 his7-366 wis1-12myc:ura4⁺ tdh1^{C156S}(3PK):ura4⁺*	This study
HL34	*h⁺ ade6-M216 leu1-32 ura4-D18 his7-366 pyp1^{Y160E}pk::ura4⁺*	This study
HL35	*h⁺ ade6-M216 leu1-32 ura4-D18 his7-366 pyp1^{Y160F}pk::ura4⁺*	This study
HL37	*h⁺ ade6-M210 leu1-32 ura4-D18 his7-366 NΔ30pyp1-3Pk:kanMX6 pyp1^{C470S}pk::ura4⁺*	This study
HL38	*h? ade6-M216 leu1-32 ura4-D18 his7-366 tdh1⁺(3PK):ura4⁺ gpd3::kan^{mx4}*	This study
HL39	*h? ade6-M216 leu1-32 ura4-D18 his7-366 tdh1^{C156S}(3PK):ura4⁺ gpd3::kan^{mx4}*	This study

2.2.2.2 Tetrad dissection

Following asci formation, a loopful of mated cells was resuspended in 100 µl H_2O, vortexed and 10 µl resuspension was dropped down a YE5S plate. The plate was dried at 37°C before asci were isolated using a Singer micromanipulator and aligned in grid formation. Asci were dissected following 3-6 hours incubation at 30°C, with each spore being separated by around 3-5 mm in a line of four. Cells were incubated at 30°C until visible colonies formed. Genotypes of the strains were then determined using the appropriate selection plates, PCR and/or Western blotting.

2.2.2.3 Random sporulation

Alternatively, following asci formation, a loopful of mated cells was resuspended in 100 µl 0.5 % (w/v) glucuIyase and incubated overnight at 30°C. 42.5 µl 100% ethanol (EtOH) was added and the mix was incubated at room temperature for 20 minutes to kill vegetative cells. Cells were spread onto EMM agar plates supplemented with the appropriate amino acids and incubated at 30°C until visible colonies formed. Genotypes of the strains were then determined using the appropriate selection plates, PCR and/or Western blotting.

2.2.3 Genomic DNA extraction

DNA was extracted from a scraping of *S. pombe* cells and resuspended in 200 µl DNA breakage buffer (1 mM ethylenediaminetetra acetic acid (EDTA), 100 mM sodium chloride (NaCl), 1% (w/v) sodium dodecyl sulphate (SDS), 2% (v/v) Triton X-100, 10 mM Tris-HCl pH8.0). After the addition of 200 µl phenol:chloroform and 200 µl glass beads (425-600 microns, Sigma-Aldrich), cells were bead beaten for 20 seconds, then pelleted in a microcentrifuge at 13000 rpm for 5 minutes. The supernatant was added to 1/10 volume of 3M sodium acetate [pH5.2] and 2 volumes of 100% ethanol (EtOH). Samples were incubated at -20°C for 30 minutes, followed by centrifugation in a microcentrifuge at 13000 rpm for 15 minutes. The DNA pellet was washed in 70% ethanol (EtOH), centrifuged for a further 5 minutes at 13000 rpm in a microcentrifuge, air-dried for 5 minutes, and resuspended in 100 µl H_2O.

2.2.4 Transformation of *S. pombe*

Plasmid- and PCR-derived DNA was introduced into *S. pombe* cells using the lithium acetate (LiAc) method as described (Moreno *et al.*, 1991). 100 ml exponentially growing cells (OD_{595} 0.5 = $1x10^7$ cells/ml) were pelleted by centrifugation in a microcentrifuge at 2000 rpm for 3 minutes, washed in 20 ml H_2O, resuspended in 500 µl H_2O and pooled into a microfuge tube. Following centrifugation in a microcentrifuge at 7000 rpm for 30 seconds, cells were washed in 1 ml Lithium acetate/Tris-EDTA (1xLiAc/TE) (100 mM LiAc, 0.1 mM EDTA, 10 mM Tris-HCl pH7.5). Cells were pelleted again by centrifugation in a microcentrifuge, and resuspended in 1 ml LiAc/TE. 100 µl cells, 2 µl salmon sperm DNA (10 mg/ml) and up to 10 µl (2 µg) transforming DNA was incubated at room temperature for 10 minutes. 260 µl polyethylene glycol/LiAc/TE (PEG/LiAc/TE) (100 mM LiAc, 1xTE, 50% (w/v) PEG-4000) was added and mixed gently, and the samples were incubated at 30°C for 30-60 minutes with agitation. After the addition of 43 µl dimethyl sulphoxide (DMSO), cells were heat shocked for 5 minutes at 42°C and pelleted by centrifugation in a microcentrifuge at 7000 rpm for 30 seconds. Cells were washed with 1 ml H_2O, pelleted by centrifugation in a microcentrifuge at 7000 rpm for 30 seconds and resuspended in 250 µl H_2O. For auxotrophic selection, cells were plated onto selective media (EMM) agar containing the appropriate amino acids, and incubated at 30°C for 3-5 days until colonies appear.

2.2.5 Chromosomal gene tagging

2.2.5.1 Pyp1^{C20S}Pk

Cells expressing Pyp1^{C20S}, tagged with three C-terminal Pk-epitopes, from their normal chromosomal locus were generated using the non-replicating pRip42PkC integration vector (Figure 2.2). The ORF of *pyp1$^+$* excluding the stop codon and including the introduced C20S mutation was amplified by PCR using specially designed oligonucleotides (Table 2.1). The PCR products were digested with *Nde1* and *BamH1* restriction endonucleases and ligated into pRip42PkC to create pRip42Pyp1^{C20S}PkC. The *pyp1* promoter, including a unique restriction site (*Spe1*) was also amplified by PCR using specially designed

primers. The PCR products were digested with *Sph1* and *Nde1* restriction endonucleases and ligated into pRip42Pyp1^{C20S}PkC. These constructs were linearised by *Spe1* digestion and introduced into Δ*pyp1* (NJ102) cells. Integration results in strains expressing Pk-epitope tagged Pyp1^{C20S} from their normal chromosomal locus. Transformants were screened by growth on EMM medium lacking uracil to select for transformants containing the *ura4*$^{+}$ marker. Integration at the correct chromosomal locus was confirmed by PCR using the oligonucleotide primers Pyp1upstreamcheck and Pyp1intcheckB. Western blotting analysis was used to verify that cells were expressing Pk-epitope tagged Pyp1.

2.2.5.2 Pyp1^{C118S}Pk, Pyp1^{C222S}Pk, Pyp1^{C340SC470S}Pk, Pyp1^{C441S}Pk, Pyp1^{C470S}Pk, NΔ30Pyp1^{C470S}Pk

Cells expressing the Pyp1 cysteine-to-serine mutants, Pyp1^{C118S}, Pyp1^{C222S}, Pyp1^{C340SC470S}, Pyp1^{C441S}, Pyp1^{C470S} and NΔ30Pyp1^{C470S}, tagged with three C-terminal Pk-epitopes, from their normal chromosomal locus were generated using the non-replicating pRip42PkC integration vector (Figure 2.2). The ORF of *pyp1*$^{+}$ excluding the stop codon, including the introduced cysteine-to-serine mutation and a unique restriction site (*SalI*) was amplified by PCR using specially designed oligonucleotides (Table 2.1). The PCR products were digested using *Pst1* and *BamH1* restriction endonucleases and ligated into pRip42PkC to create pRip42Pyp1^{CxS}PkC. These constructs were linearised by *SalI* digestion and introduced into wild-type (NT4) cells, or into NΔ30Pyp1-3PK (NJ1884) cells for construction of NΔ30Pyp1^{C470S}Pk. Integration results in strains expressing Pk-epitope tagged Pyp1 cysteine mutants from their normal chromosomal locus. Transformants were screened by growth on EMM medium lacking uracil to select for transformants containing the *ura4*$^{+}$ marker. Integration at the correct chromosomal locus was confirmed by PCR using the oligonucleotide primers Pyp1intcheck and Pyp1intcheckB. Western blotting analysis was used to verify that cells were expressing Pk-epitope tagged Pyp1.

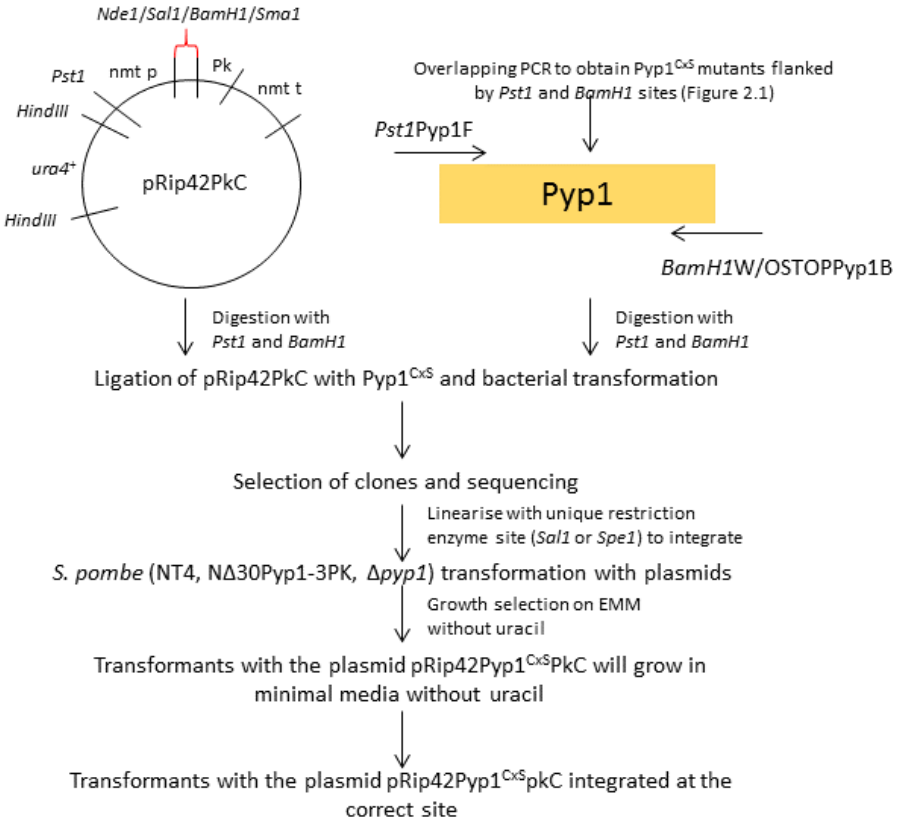

Figure 2.2 Construction of pRip42Pyp1^{CxS}PkC and transformation into *S. pombe*. Overlapping PCR was used to generate Pyp1^{CxS} mutants, and, following double digestion with the restriction enzymes *Pst1* and *BamH1*, was cloned into the plasmid pRip42PkC. The constructed plasmid pRip42Pyp1^{CxS}PkC was transformed into *S. pombe* strains wild-type (NT4) for construction of Pyp1^{C118S}PkC, Pyp1^{C222S}PkC, Pyp1^{C340SC470S}PkC, Pyp1^{C441S}PkC, and Pyp1^{C470S}PkC, NΔ30Pyp1-3PK (NJ1884) for construction of NΔ30Pyp1^{C470S}PkC, or Δ*pyp1* (NJ102) cells for construction of Pyp1^{C20S}PkC. Potential positives were screened through a check PCR to confirm the plasmid had integrated at the correct site. The selectable marker used was *ura4*$^{+}$, and transformants containing the plasmid were maintained in minimal media minus uracil.

2.2.5.3 Pyp1Pk, Pyp2Pk, Pyp3Pk

Cells expressing Pyp1, Pyp2 and Pyp3, tagged with three C-terminal Pk-epitopes, from their normal chromosomal locus were generated using the non-replicating pRip42PkC integration vector. The ORF's of *pyp1*$^{+}$, *pyp2*$^{+}$ and *pyp3*$^{+}$ excluding the stop codon, but including a unique restriction site (*SaI1* for Pyp1, *Kpn21* for Pyp2, and *Bal1* for Pyp3) was amplified by PCR using specially designed oligonucleotides (Table 2.1). The PCR products were digested using *Pst1* and *BamH1* restriction endonucleases and ligated into pRip42PkC to create pRip42Pyp1PkC, pRip42Pyp2PkC and pRip42Pyp3PkC. These constructs were linearised by *SaI1*, *Kpn21* or *Bal1* digestion and introduced into wild-type (NT4) cells. Integration results in strains expressing Pk-epitope tagged Pyp1, Pyp2 and Pyp3 from their normal chromosomal locus. Transformants were screened by growth on EMM medium lacking uracil to select for transformants containing the *ura4*$^{+}$ marker. Integration at the correct chromosomal locus was confirmed by PCR using the oligonucleotide primers Pyp1intcheck and Pyp1intcheckB, Pyp2intcheck and *BamH1*W/OSTOPPyp2B, or Pyp3intcheck and *BamH1*W/OSTOPPyp3BLong. Western blotting analysis was used to verify that cells were expressing Pk-epitope tagged Pyp1, Pyp2 or Pyp3.

2.2.5.4 Tdh1^{C156S}Pk

Cells expressing Tdh1^{C156S}, tagged with three C-terminal Pk-epitopes, from their normal chromosomal locus were generated using the non-replicating pRip42PkC integration vector. The ORF of *tdh1*$^{+}$ excluding the stop codon, including the introduced cysteine-to-serine mutation and a unique restriction site (*SgrA1*) was amplified by PCR using specially designed oligonucleotides (Table 2.1). The PCR products were digested using *Pst1* and *BamH1* restriction endonucleases and ligated into pRip42PkC to create pRip42Tdh1^{C156S}PkC. These constructs were linearised by *SgrA1* digestion and introduced into wild-type (CHP429) cells. Integration results in strains expressing Pk-epitope tagged Tdh1^{C156S} from their normal chromosomal locus. Transformants were screened by growth on EMM medium lacking uracil to select for transformants containing the *ura4*$^{+}$ marker. Integration at the

correct chromosomal locus was confirmed by PCR using the oligonucleotide primers Tdh1intcheck and Tdh1intcheckB. Western blotting analysis was used to verify that cells were expressing Pk-epitope tagged Tdh1.

2.2.5.5 Tim40EGFP

Cells expressing Tim40, tagged with a C-terminal EGFP-protein, from their normal chromosomal locus were generated using the non-replicating pRip42EGFPC integration vector. The ORF of *tim40*$^{+}$ excluding the stop codon, but including a unique restriction site (*Pst1*) was amplified by PCR using specially designed oligonucleotides (Table 2.1). The PCR products were digested using *Sph1* and *BamH1* restriction endonucleases and ligated into pRip42EGFPC to create pRip42Tim40EGFPC. These constructs were linearised by *Pst1* digestion and introduced into wild-type (NT4) cells. Integration results in strains expressing EGFP-protein tagged Tim40 from their normal chromosomal locus. Transformants were screened by growth on EMM medium lacking uracil to select for transformants containing the *ura4*$^{+}$ marker. Integration at the correct chromosomal locus was confirmed by PCR using the oligonucleotide primers Tim40intcheck and GFPcheckB. Western blotting analysis was used to verify that cells were expressing EGFP-epitope tagged Tim40.

2.2.6 Sensitivity tests

2.2.6.1 Spot tests

Cells were grown to mid-log phase (OD_{595} 0.5 = $1x10^7$ cells/ml) and serial 10-fold dilutions were spotted onto solid media containing different reagents of varying concentrations. Plates were incubated at 30°C for 2-4 days, and the growth of each strain was examined. Temperature sensitivity was examined by incubation of plates at 37°C.

2.2.6.2 Liquid survival assay

Cells were grown to mid-log phase before treatment with 25.0 mM H_2O_2. Serial 10-fold dilutions were made and 100 µl of each dilution was spread onto solid media after 0, 30, 60, 90, 120, 150 and 180

minutes. Duplicate samples were plated. Plates were incubated at 30°C for 2-4 days until colonies appeared. Colonies were counted and averaged and the percentage survival calculated.

2.2.6.3 Oxidising reagents used

A range of different oxidising reagents were used in this study, such as hydrogen peroxide (H_2O_2) and *tert*-butyl hydroperoxide (*t*-BOOH), which were both used as peroxides. Fresh 30% (v/v) H_2O_2 was obtained monthly from Sigma-Aldrich and stored at 4°C. *t*-BOOH was also obtained from Sigma-Aldrich and stored at 4°C.

2.2.7 TTC respiration assay

Cells were patched onto YE plates containing 3% glycerol. After four days growth at 30°C, plates were covered with 1.5% bactoagar in 0.067 M phosphate buffer containing 1% 2,3,5-triphenyltetrazolium (TTC). Cells were monitored for up to 3 hours to detect whether the cells turned red, indicative of a functional electron transport chain (Ogur *et al.*, 1957).

2.2.8 Mitochondrial enrichment

S. pombe mitochondria were enriched at The University of Manchester, as described (Chiron *et al.*, 2007). 1 L *S. pombe* cells were grown overnight in YE5S at 30°C to an OD_{595} of 1.0. Cells were harvested by centrifugation at 2000 rpm for 10 minutes at room temperature. Cells were washed in 200 ml H_2O and collected by centrifugation at 2000 rpm, following by washing in 50 ml 10 mM EDTA. Cell pellets were collected and resuspended in a weight per volume ratio of 1:3 ml digestion buffer (1.2 M sorbitol, 10 mM sodium citrate, 0.2 mM EDTA, 0.3% β-mercaptoethanol, pH 5.8) containing 1 mg/ml Zymolase 100T (AMS Biotechnology) and 1 mg/ml lysing enzymes from *Trichoderma harzianum* (Sigma-Aldrich), and incubated at 37°C for 30 minutes. Cells were transferred to ice for five minutes to stop the digestion reaction, and samples were subsequently centrifuged for 15 minutes at 2000 rpm at 4°C. The supernatant was discarded and the pellet was resuspended in 20 ml mitochondrial lysis buffer (0.6 M sorbitol, 10 mM imidazole pH 6.4, 2 mM EDTA, 1 mM PMSF). Protoplasts were broken by 10

strokes of a glass homogenizer, and samples were incubated on ice for 15 minutes before centrifugation at 2500 rpm for 15 minutes at 4°C. The supernatant was transferred to a fresh centrifuge tube and centrifuged at 2500 rpm for 5 minutes at 4°C. This step was repeated to ensure all unbroken cells, cell debris and nuclei were removed. The supernatant was then centrifuged at 12000 rpm for 15 minutes at 4°C in order to collect the unbroken mitochondria. This step was repeated in order to increase the yield. The mitochondrial pellet was resuspended in 30 ml mitochondrial lysis buffer containing 0.2 M KCl and centrifuged at 800 rpm for 2 minutes at 4°C. The supernatant was removed and centrifuged at 12000 rpm for 15 minutes at 4°C to collect the washed mitochondria. The mitochondrial pellet was resuspended in 100 µl lysis buffer and stored at -80°C until further use.

2.3 RNA analysis

2.3.1 RNA extraction

Exponentially growing cells were harvested by centrifugation in a benchtop centrifuge at 3000 rpm for 2 minutes, washed with 1 ml H_2O, and transferred to a ribolyser tube. Following centrifugation in a microcentrifuge at 13000 rpm for 1 minute, pelleted cells were frozen in liquid nitrogen. The cell pellets were resuspended in 200 µl ice-cold RNA extraction buffer (100 mM EDTA, 100 mM NaCl, 50 mM Tris-HCl pH8.0), then 10 µl 10% SDS and 200 µl phenol:chloroform was added. Beads were baked at 160°C for 4 hours. Ice-cold baked glass beads (Biospec products) were added and cells were bead beaten in a Mini Beadbeater-16 (Biospec products, 607EUR) for 30 seconds. 600 µl ice-cold RNA extraction buffer was added, followed by vortexing and centrifugation in a microcentrifuge for 3000 rpm for 15 minutes at 4°C. The aqueous layer was removed and phenol extracted. An equal volume of the supernatant was added to phenol:chloroform in a clean microcentrifuge, and mixed used a vortex. The mixture was separated by centrifugation in a microcentrifuge at 13000 rpm for 1 minute. Again, an equal amount of the supernatant was added to phenol:chloroform in a clean microcentrifuge, and mixed used a vortex. The mixture was separated by centrifugation in a microcentrifuge at 13000 rpm

for 1 minute. The RNA was precipitated by addition of 0.6 volumes isopropanol and incubation overnight at -80°C. The RNA was pelleted by centrifugation in a microcentrifuge at 13000 rpm for 15 minutes, washed with 70% ethanol (EtOH), air-dried and resuspended in 30 µl H_2O by freeze-thaw cycles between 50°C and -80°C. RNA concentrations were determined using a NanoDrop 1000 spectrophotometer (Thermo Scientific).

2.3.2 Northern blotting

15-20 µg RNA was denatured by heating at 50°C for 15 minutes in 12.1 µl RNA denaturing buffer (2.5 µl 40% glyoxal, 8 µl DMSO, 1.5 µl 100 mM sodium phosphate ($NaPO_4$)). The denatured RNA was separated according to size by electrophoresis in a 1.2 % agarose gel (dissolved in 15 mM $NaPO_4$ buffer [pH6.5]) at 4 Volts/cm^2 for 2-3 hours, with buffer recirculation every 30 minutes. RNA was transferred to Genescreen hybridisation membrane (Dupont NEM Life Science Products) by Northern blotting overnight in 25 mM $NaPO_4$ [pH6.5] buffer. Following blotting, RNA was cross-linked to the membrane using a UV Stratalinker 2400 at 1200 J/m^2.

Gene specific probes were produced by PCR amplification of genomic DNA using appropriate oligonucleotide primers. Probes were labelled with 2 µl µCi [α^{32} P]-dCTP (Amersham) using the Promega Prime-a-Gene labelling kit, according to manufacturer's instruction. 100 ng DNA in a final volume of 33 µl was denatured at 100°C for 5 minutes, then put onto ice immediately. Added to this reaction mix was 10 µl 5 x labelling buffer (supplied with Prime-a-Gene labelling kit), 500 µM each Prime-a-Gene dNTP (dATP, dGTP and dTTP), 2 µl BSA, 1 µl DNA polymerase I Large (Klenow) fragment, and 2 µl µCi [α^{32} P]-dCTP (Amersham). Probes were labelled at 37°C for 1 hour. Membranes were pre-hybridised in a minimal volume of hybridisation solution (QuikHyb hybridisation kit [Stratagene]) (~50 µl solution/cm^2) for 20 minutes at 68°C before probing. The labelled probe and salmon sperm DNA (10 mg/ml) were denatured at 100°C for 5 minutes, and added to the hybridisation solution. Hybridisation was performed at 68°C for 1 hour. The membranes were washed twice with 2xSSPE at

60°C for 10 minutes. Probed membranes were then exposed to a phosphoimager screen and analysed using a phosphoimager (Typhoon). Data was quantified using ImageQuant Software.

2.4 Protein analysis

2.4.1 Pombe Lysis Buffer (PLB) protein extraction

Exponentially growing cells were harvested by centrifugation in a benchtop centrifuge at 3000 rpm for 1 minute, and snap frozen in liquid nitrogen. Cell pellets were washed with 1 ml ice-cold pombe lysis buffer (PLB) (150 mM NaCl, 0.5% (v/v) Nonidet P-40 (IGEPAL), 10 mM Imidazole, 50 mM Tris-HCl pH7.5) containing protease inhibitors (0.1% (v/v) p-leupeptin, 0.1% pepstatin A, 1% aprotinin, 1% phenylmethylsulfonyl fluoride (PMSF)). For Sty1 phosphorylation assays, phosphatase inhibitors were added to PLB: (0.2% sodium vanadate (Na_3VO_4), 5% sodium fluoride (NaF)). Pellets were then resuspended in 200 µl PLB. To lyse cells, the cell suspension was added to 1 ml ice-cold glass beads (Biospec products), and cells were bead beaten in a Mini Beadbeater-16 (Biospec products, 607EUR) for two 15 second spins with 1 minute incubation on ice between. An additional 200 µl PLB was added to the beads. The bottom of the ribolyser tube was pierced with a red-hot needle, and placed on top of a microfuge tube to collect the lysate through centrifugation in a benchtop centrifuge at 3000 rpm for 1 minute at 4°C. Insoluble cell debris was pelleted by centrifugation in a microcentrifuge at 13000 rpm for 10 minutes at 4°C, the supernatant was transferred to a fresh microfuge tube, and the samples were frozen at -80°C.

Protein concentration of the clarified cell lysate was measured using the Coomassie blue reagent (Pierce) and absorbance at 595 nm. Equal volumes of protein sample were mixed with 2xSDS loading buffer with β-mercaptoethanol (0.5% (w/v) bromophenol blue, 10% (v/v) SDS, 50% (v/v) glycerol, 10% (v/v) β-mercaptoethanol, 625 mM Tris-HCl pH 6.8), and boiled for 2 minutes at 100°C. Samples were

analysed by reducing or non-reducing SDS-PAGE and Western blotting. The antibodies used in this study are listed in Table 2.4.

2.4.2 Tricholoracetic Acid (TCA) protein extraction

2.4.2.1 Protein oxidation using NEM and AMS

Equal amounts of exponentially growing cells were added to an equal volume of 20% (w/v) trichloroacetic acid (TCA), harvested by centrifugation in a benchtop centrifuge at 3000 rpm for 1 minute, and snap frozen in liquid nitrogen. Cell pellets were resuspended in 200 µl (w/v) 10% TCA. To lyse cells, the cell suspension was added to 750 µl glass beads (Biospec products), and cells were bead beaten in a Mini Beadbeater-16 (Biospec products, 607EUR) for two 15 second spins with 1 minute incubation between. An additional 500 µl 10% TCA was added to the beads. The lysate was collected into a microfuge tube through centrifugation in a benchtop centrifuge at 2000 rpm for 1 minute at 4°C, and the protein pelleted by centrifugation in a microcentrifuge at 13000 rpm for 10 minutes. The pellet was subsequently washed three times with 200 µl acetone, air-dried and resuspended in 20 µl TCA buffer (1% SDS, 1 mM EDTA, 100 mM Tris-HCl pH8.0, supplemented with 25 mM AMS (4-acetamido-4'-maleimidylstilbene-2,2'-disulphonic acid), or 200 mM NEM (*N*-Ethylmaleimide)). AMS- and NEM-treated samples were incubated at 25°C for 30 minutes and 37°C for 5 minutes, and samples were centrifuged at 13000 rpm for 3 minutes. The supernatant was transferred to a fresh microfuge tube and stored at -80°C. Protein concentration of the supernatant was determined using a Pierce BSA protein assay kit (Thermo Scientific).

Equal volumes of protein sample were mixed with 2xSDS loading buffer (0.5% (w/v) bromophenol blue, 10% (v/v) SDS, 50% (v/v) glycerol, 625 mM Tris-HCl pH6.8), and boiled for 2 minutes at 100°C. Samples were analysed by non-reducing SDS-PAGE and Western blotting. The antibodies used in this study are listed in Table 2.4.

2.4.2.2 Protein oxidation using PEG-Maleimide

Equal amounts of exponentially growing cells were added to 20% (w/v) trichloroacetic acid (TCA), harvested by centrifugation in a benchtop centrifuge at 3000 rpm for 1 minute, and snap frozen in liquid nitrogen. Protein was extracted as described in section 2.4.2.1. After washing three times with 200 µl acetone, the pellet was air-dried and resuspended in 20 µl TCA buffer supplemented with PEG-Maleimide (1% SDS, 1 mM EDTA, 25 mM PEG-Maleimide, 100 mM Tris-HCl pH6.7), and incubated at 30°C for 30 minutes. Samples were centrifuged at 13000 rpm for 3 minutes, the protein was precipitated by addition of equal amounts of 20% TCA and incubated on ice for 30 minutes. The protein was re-pelleted by centrifugation at 13000 rpm for 15 minutes at 4°C, washed three times with 200 µl acetone, and re-suspended in 20 µl TCA buffer (1% SDS, 1 mM EDTA, 100 mM Tris-HCl pH6.7). Samples were incubated at 25°C for 30 minutes and 37°C for 5 minutes, and centrifuged at 13000 rpm for 3 minutes. The supernatant was transferred to a fresh microfuge tube and stored at -80°C. Protein concentration of the supernatant was determined using a Pierce BSA protein assay kit (Thermo Scientific). Protein concentration of the supernatant was determined using a Pierce BSA protein assay kit (Thermo Scientific).

Equal volumes of protein sample were mixed with 2xSDS loading buffer (0.5% (w/v) bromophenol blue, 10% (v/v) SDS, 50% (v/v) glycerol, 625 mM Tris-HCl pH6.8), and boiled for 2 minutes at 100°C. Samples were analysed by non-reducing SDS-PAGE and Western blotting. The antibodies used in this study are listed in Table 2.4.

2.4.2.3 Pap1 oxidation

Equal amounts of exponentially growing cells were added to 20% (w/v) trichloroacetic acid (TCA), harvested by centrifugation in a benchtop centrifuge at 3000 rpm for 1 minute, and snap frozen in liquid nitrogen. Protein was extracted as described in section 2.4.2.1. After washing three times with 200 µl acetone, the pellet was air-dried and resuspended in 20 µl IAA (Iodoacetamide) (1% SDS, 75 mM IAA, 100 mM Tris-HCl pH8.0). Samples were incubated at 25°C for 20 minutes, and clarified by

centrifugation at 13000 rpm for 3 minutes. The supernatant was transferred to a fresh microfuge tube and stored at -80°C. Protein concentration of the supernatant was determined using a Pierce BSA protein assay kit (Thermo Scientific). Equal volumes of protein sample were treated with alkaline phosphate (AP) for 60 minutes at 37°C.

Equal volumes of protein sample were mixed with 2xSDS loading buffer (0.5% (w/v) bromophenol blue, 10% (v/v) SDS, 50% (v/v) glycerol, 625 mM Tris-HCl pH6.8), and boiled for 2 minutes at 100°C. Samples were analysed by non-reducing SDS-PAGE and Western blotting. The antibodies used in this study are listed in Table 2.4.

2.4.3 Immunopurification

Exponentially growing cells were harvested and lysates were prepared as in section 2.4.1. After protein lysates were clarified by centrifugation in a microcentrifuge at 13000 rpm for 10 minutes at 4°C, Flag-epitope tagged proteins were purified using anti-Flag (M2) antibody-conjugated agarose (Sigma-Aldrich) by incubation of equal amounts of protein with 10 µl 1:1 M2 agarose slurry (pre-equilibrated in pombe lysis buffer) with gentle agitation for 60 minutes at 4°C. Alternatively, Pk-tagged proteins were purified using anti-Pk (V5) antibody-conjugated agarose (Sigma-Aldrich) by incubation of equal amounts of protein with 10 µl 1:1 Pk agarose slurry (pre-equilibrated in pombe lysis buffer) with gentle agitation for 60 minutes at 4°C. The beads were washed three times with 1 ml ice-cold PLB and resuspended in 10 µl 2xSDS loading buffer (0.5% (w/v) bromophenol blue, 10% (v/v) SDS, 50% (v/v) glycerol, 625 mM Tris-HCl pH6.8), and boiled for 2 minutes at 100°C. Samples were analysed by reducing or non-reducing SDS-PAGE and Western blotting. The antibodies used in this study are listed in Table 2.4.

2.4.4 SDS-PAGE and Western blotting

Equal amounts of protein (6 µg) was resolved on a sodium dodecyl sulfate-polyacrylamide gel electrophoresis (SDS-PAGE) gel. Gel recipes were based on SDS (denaturing) discontinuous buffer

system of Laemmli (Laemmli, 1970). Gels were run at 200V in 1xSDS Running Buffer (19.2 mM glycine, 0.1% SDS, 25 mM Tris-HCl pH 8.0). Separated proteins were transferred to a nitrocellulose transfer membrane in 1xTransfer Buffer (19.2 mM glycine, 20% (v/v) methanol, 25 mM Tris-HCl pH 8.0) at 100V for 2-3 hours. Non-specific binding was reduced by blocking the membrane for 30 minutes at room temperature in 10% (w/v) BSA in 1xTBST (15 mM NaCl, 0.01% (v/v) Tween-20, 1 mM Tris-HCl pH8.0). The membrane was incubated with a primary antibody diluted 1:1000 in TBST containing 5% (w/v) BSA, with gentle agitation at 4°C overnight. When looking at Sty1 phosphorylation, the primary antibody was diluted 1:1000 in TBST containing 5% (w/v) BSA plus phosphatase inhibitors (0.2% sodium vanadate (Na_3VO_4), 5% sodium fluoride (NaF)). The antibodies used in this study are listed in Table 2.4.

The following day the membrane was washed four times with 1xTBST, and then incubated with the relevant secondary antibody (Sigma-Aldrich), conjugated to horseradish peroxidase, diluted 1:2000 in 5% (w/v) BSA in 1xTBST for 1 hour at room temperature. The membrane was again washed four times with 1xTBST. Enhanced chemiluminescence (GE Healthcare) and X-ray film or ImageQuant Software (Typhoon) was used to visualise proteins on the membrane.

Table 2.4 Antibodies used in this study.

Antibody (Species raised in)	Source (Catalog Number)	Dilution
Primary		
Flag (mouse)	Sigma-Aldrich (F3165)	1:1000
GAPDH (rabbit)	Chemicon International (AB2302)	1:1000
GAPDH-SO_3 (rabbit)	Ab Frontier (LF-PA0006)	1:1000
GFP (rabbit)	Thermo Fisher Scientific (A6455)	1:1000
Hog1 (rabbit)	Santa Cruz Biotechnology (sc-9079)	1:1000
Hsp60 (mouse)	From Nic Jones and Caroline Wilkinson, University of Manchester	1:1000
Myc (mouse)	Santa Cruz Biotechnology (C0907)	1:1000
Pap1 (rabbit)	From Nic Jones and Caroline Wilkinson, University of Manchester	1:1000
Pk (mouse)	Sigma-Aldrich (V8012)	1:1000
pp38 (rabbit)	Cell Signalling Technology (9211S)	1:1000
PRDX-2 (#3269) (rabbit)	Day *et al.*, 2012	1:1000
Sty1 (rabbit)	Day and Veal, 2010	1:1000
Tpx1 (rabbit)	Day *et al.*, 2012	1:1000
Secondary		
Anti-rabbit IgG (whole molecule)	Sigma-Aldrich (A6154)	1:2000
Anti-mouse IgG (whole molecule)	Sigma-Aldrich (A4416)	1:2000
Goat anti-mouse	Life Technologies (A11001)	1:200

2.4.5 Mass spectrometry

Mass spectrometry and data analysis was performed by Tobias Dansen at Utrecht University, as described previously (Dansen *et al.*, 2009; Putker *et al.*, 2013).

2.4.5.1 Sample preparation

Large-scale immunopurification was performed on 400 ml exponentially growing cells. Protein samples were prepared as described in section 2.4.3. After the beads were washed three times with 1 ml ice-cold PLB, proteins were eluted from the anti-Flag (M2) antibody-conjugated agarose using 50 µl 100mM Glycine [pH2.0]. The eluate was immediately neutralised with 1/10 1M Tris-HCl pH8.8 and snap frozen in liquid nitrogen for shipping.

2.4.5.2 Protein digestion

At Utrecht University, samples were run on an SDS-PAGE gel under non-reducing conditions. Each lane was cut into 30 pieces and digested with trypsin. The trypsin-digested peptides were ionised and fragmented, and all the fragment ions were recorded. Mass spectrometry was performed as described previously (Putker *et al.*, 2013).

2.4.5.3 Data analysis

Raw data files from the mass spectrometry run were analysed using MaxQuant software (Cox and Mann, 2008; Cox *et al.*, 2011), a software package based on a set of algorithms. Through searching organism specific peptide databases, MaxQuant is able to analyse large-scale mass spectrometry data sets to identify proteins, quantify identified proteins, and provide statistics using the Perseus platform. By inputting the raw data from the mass spectrometry run into MaxQuant, peptides are identified and assembled into protein groups, in which all proteins share the same identified peptides. The outputs from MaxQuant include a peptide score, peptide intensity, and number of unique peptides. The mass and intensity of peptide peaks are detected from the raw data. Peptide and fragment masses are searched for in the *S. pombe* sequence database, which are then scored in a probability-based

approach, to give a peptide score. Peptide hits describe the relative abundance of a protein, where a larger number of peptide hits corresponds to a higher abundant protein. Unique peptides are obtained by removing the redundancy from the peptide hits, indicating the confidence of the protein identification. Unique peptides are peptide sequences common to a protein group, and do not occur in the proteins of other groups. A razor peptide is a peptide assigned to the protein group with the largest number of total peptides identified. Proteins identified with at least two unique peptides were filtered for at least three valid values in one group. The peptide hits are assembled into protein hits, to identify proteins, with each identified peptide contributing to the accuracy of the protein identification. All the individual peptide intensities belonging to a protein group contribute to the intensity. Intensities are based on two algorithms, LFQ (Label Free Quantification) and iBAQ (Intensity Based Absolute Quantification). LFQ intensities are based on the raw intensities and are normalised, allowing relative quantification and comparison between samples. On the other hand, iBAQ intensities are proportional to the molar quantities of the protein, whereby the raw intensities are divided by the number of theoretical peptides. The Perseus tool was used to further analyse the protein group files generated from using the iBAQ and LFQ algorithms. MS/MS count is an indication of whether the quantification is based on enough identified proteins, and refers to the addition of MS/MS events for that specific protein. A standard *t*-test was performed and p-values were plotted against the transformed iBAQ or LFQ logarithm values using the program R. A q-value was also calculated, which is an adjusted p-value using an optimised False Discovery Rate (FDR) approach, to give a posterior error probability (PEP).

2.5. Microscopy

2.5.1 Indirect fluorescence microscopy

8 ml exponentially growing cells were harvested before and after exposure to stress (see individual experiments for details) by the addition of 2 ml freshly prepared 15% formaldehyde solution. This was

prepared by dissolving 6 g paraformaldehyde (PFA) (Sigma) in 20 ml PEM [100 mM piperazine-1, 4-bis (2-ethanesulphonic acid) (PIPES), 1.0 mM EGTA [pH8.0], 1.0 mM $MgSO_4$] to which 120 µl 10 M NaOH was added before incubation in a waterbath at 65°C until PFA had dissolved. Cells were fixed by gentle agitation at 30°C for 20-30 minutes. Cells were pelleted by centrifugation in a benchtop centrifuge at 2000 rpm for 2 minutes, transferred to a microfuge tube and washed three times in 1 ml PEMS (PEM including 1.2 M sorbitol) containing 0.5 mg/ml Zymolase and incubated at 37°C for 70 minutes. Cells were pelleted, resuspended in 1 ml PEMS plus 1% Triton X-100 for 2 minutes at room temperature. Cells were washed three times in PEM and blocked in 1 ml PEMBAL (PEM, 1% (w/v) BSA, 0.1% sodium azide, 0.1 M Lysine) for 30 minutes with gentle agitation at room temperature. Cells were pelleted and resuspended in 200 µl PEMBAL containing 1:1000 dilution of the specific primary antibody and incubated at room temperature overnight with gentle agitation. The antibodies used in this study are listed in Table 2.4.

The following day the cells were washed three times in PEMBAL, resuspended in 200 µl PEMBAL containing 1:200 dilution of the specific Alexa Flour FITC-conjugated secondary antibody (goat anti-mouse or donkey anti-rabbit), and incubated at room temperature for 1 hour with gentle agitation. The cells were washed twice in 1 ml PEMBAL and once in 1 ml PEM before being resuspended in a final volume of 100 µl PEM. 5 µl cells were spread onto poly-L-lysine coated glass microscope slides and allowed to dry. Slides were plunged into ice-cold methanol (MeOH) for 6 minutes, ice-cold acetone for 30 seconds. Once dry, a drop of Vectashield mounting medium containing DAPI (4'-6'-diamidino-2-phenylindole) for nuclear staining was added and a glass cover slip was placed on top and sealed with nail varnish. DAPI and FITC fluorescence was captured by excitation at 450-490 nM and 365 nM wavelengths respectively using a Zeiss Axioscope fluorescence microscope with a 63 x oil immersion objective and Axiovision digital imaging software.

2.5.2 Cell size and morphology of live cells

1 ml exponentially growing cells were pelleted by centrifugation in a microcentrifuge at 13000 rpm for 1 minute and resuspended in 100 µl media. 5 µl cells were spread onto glass microscope slides, covered with a glass cover slip and sealed with nail varnish. Live images of cells were captured using a Zeiss Axioscope fluorescence microscope with a 63 x oil immersion objective and Axiovision digital imaging software.

2.5.3 Cell measurements with the Coulter Counter

4 µl exponentially growing cells were sonicated in 10 ml filter-sterilised CASYton solution. Cell measurements were taken using the CASY Cell Counter + Analyser System, Model TT (Schärfe System).

2.6 Determination of intracellular NADPH/NADP ratios

25 ml exponentially growing cells were pelleted by centrifugation in a benchtop centrifuge at 2500 rpm for 5 minutes, and snap frozen in liquid nitrogen. The pellets were treated with 100 U catalase and resuspended in 200 µl NADP/NADPH Lysis Buffer (Component G, AAT Bioquest Product Number 15264). The cell suspension was added to 1 ml ice-cold glass beads (Biospec products), and cells were bead beaten in a Mini Beadbeater-16 (Biospec products, 607EUR) for two 15 second spins with 1 minute incubation on ice between. An additional 300 µl NADP/NADPH Lysis Buffer was added to the beads. The bottom of the ribolyser tube was pierced with a red-hot needle, and placed on top of a microfuge tube to collect the lysate through centrifugation in a benchtop centrifuge at 3000 rpm for 1 minute at 4°C. Insoluble cell debris was pelleted by centrifugation in a microcentrifuge at 13000 rpm for 10 minutes at 4°C, the supernatant was transferred to a fresh microfuge tube, and the samples were analysed using the Amplite Fluorimetric NADP/NADPH ratio assay kit (AAT Bioquest, California, USA).

25 µl serially diluted NADPH Standards (Prepared from Component C, AAT Bioquest Product Number 15264) and the NADP/NADPH containing test samples were pipetted into wells in a 96 well plate in duplicate. For total NADP and NADPH, NADPH Standards and test samples were treated with 25 µl NADP/NADPH Control Solution (Component F, AAT Bioquest Product Number 15264) for 15 minutes at room temperature, and then another 25 µl NADP/NADPH Control Solution was added, to give a final volume of 75 µl. For NADPH extraction, test samples were treated with 25 µl NADPH Extraction Solution (Component D, AAT Bioquest Product Number 15264) for 15 minutes at room temperature, then NADPH extracts were neutralised by the addition of 25 µl NADP Extraction Solution (Component E, AAT Bioquest Product Number 15264), to give a final volume of 75 µl. For NADP extraction, test samples were treated with 25 µl NADP Extraction Solution (Component E, AAT Bioquest Product Number 15264) for 15 minutes at room temperature, then NADP extracts were neutralised by the addition of 25 µl NADPH Extraction Solution (Component D, AAT Bioquest Product Number 15264), to give a final volume of 75 µl. 75 µl NADP/NADPH Reaction Mixture (Mix of Component A and Component B, AAT Bioquest Product Number 15264) was added to each well of NADPH Standards and NADP/NADPH containing test samples, to give a total NADPH assay volume of 150 µl/well. The reaction was incubated at room temperature for 15 minutes to 2 hours, protected from light. The fluorescence increase was monitored using a fluorescence plate reader at Ex/Em = 540/590 nm, every 30 minutes for 2 hours. Ratios were computed from fluorescence signals at Ex/Em = 540/590 nm. The fluorescence for total NADP and NADPH minus the fluorescence for NADPH can be used to calculate the amount of NADP.

2.7 Determination of GSH/GSSG ratios

40 ml exponentially growing cells were pelleted by centrifugation in a benchtop centrifuge at 2500 rpm for 5 minutes at 4°C. Cell pellets were resuspended in 1 ml cold PO_4/PMSF (20 mM PO_4 [pH7.4], 0.5 mM PMSF), transferred to a microfuge tube and pelleted by centrifugation in a microcentrifuge at

13000 rpm for 30 seconds. The supernatant was removed and the pellet stored at -80°C. Cell pellets were resuspended in 250 µl 8 mM HCl/1.3% SSA and added to 1 ml ice-cold glass beads (Biospec products). Cells were bead beaten for 40 seconds. An additional 100 µl 8 mM HCl/1.3% SSA was added to the beads, and incubated on ice for 15 minutes. The bottom of the ribolyser tube was pierced with a needle, and placed on top of a microfuge tube to collect the lysate through centrifugation in a benchtop centrifuge at 3000 rpm for 1 minute at 4°C. The protein was pelleted by centrifugation in a microcentrifuge at 13000 rpm for 10 minutes at 4°C and the supernatant (total free glutathione) was transferred to a fresh microfuge tube, ready to assay.

To measure total glutathione, 20 µl each sample was pipetted into a well in a 96 well plate in duplicate. The enzymatic reaction was started by quickly adding 40 µl 8.5 U/ml GSSG-reductase. The plate was read at 415 nm every 15 seconds for 2 minutes.

To measure oxidised glutathione, 5 µl 2-vinylpyridine was added to 100 µl each sample and incubated at room temperature for 1 hour, with mixing every 15 minutes. As for total glutathione, 20 µl each sample was pipetted into a well in a 96 well plate in duplicate. The enzymatic reaction was started by quickly adding 40 µl 8.5 U/ml GSSG-reductase. The plate was read at 415 nm every 15 seconds for 2 minutes.

2.8 GAPDH enzyme activity assay

Exponentially growing cells were harvested by centrifugation in a benchtop centrifuge at 3000 rpm for 3 minutes. Cell pellets were treated with 100 U catalase, washed and resuspended in ice-cold lysis buffer (1 mM KPO_4 [pH6.8], 0.1 mM dithiothreitol (DTT), 0.1 mg/ml PMSF). 750 µl ice-cold glass beads (Biospec products) were added to the cell suspension, and cells were bead beaten for two 15 second spins with 1 minute incubation on ice between. The bottom of the ribolyser tube was pierced with a needle, and placed on top of a microfuge tube to collect the lysate through centrifugation in a

benchtop centrifuge at 3000 rpm for 1 minute at 4°C. Insoluble cell debris was pelleted by centrifugation in a microcentrifuge at 13000 rpm for 10 minutes at 4°C, the supernatant was transferred to a fresh microfuge tube, and the samples were frozen at -80°C. Protein concentration of the clarified cell lysate was measured using the Coomassie blue reagent (Pierce) and absorbance at 595 nm. GAPDH enzyme activity was assayed using a spectrophotometer by measuring the formation of NADH at 340 nm following the addition of 10-20 µl cell lysate to 1 ml assay buffer (0.1 M KPO_4 [pH7.4], 10 mM EDTA, 0.1 mM DTT, 4 mM glyceraldehyde-3-phosphate (G3P)). GAPDH activity units are expressed as mmoles of NADH formed/min/mg protein.

2.9 Experimental replication

All experiments were performed at least twice unless otherwise stated.

CHAPTER 3

3. The role of H_2O_2-induced modifications of Pyp1 in regulating the activity of Sty1

3.1 Introduction

The fission yeast *Schizosaccharomyces pombe* contains a single p38/JNK related MAPK pathway, Sty1, mediating vital responses to a variety of stimuli, including H_2O_2. In addition to the role of Prx as antioxidant enzymes, to detoxify H_2O_2 and protect the cell against ROS-induced oxidative damage, there is growing evidence that Prx can promote the H_2O_2-induced activation of p38 MAPK, as discussed in section 1.5.3. For example, the single typical 2-Cys Prx in *S. pombe*, Tpx1 is required for the H_2O_2-induced activation of Sty1 (Veal *et al.*, 2004). Although the thioredoxin peroxidase activity of Tpx1 is not required for the activation of Sty1, the peroxidatic cysteine is required and involved in H_2O_2-induced disulphides between Tpx1 and Sty1 that have been proposed to promote Sty1 activation (Veal *et al.*, 2004). However, overexpressing Tpx1 in a Sty1 mutant in which 5 of the 6 cysteines in Sty1 are substituted to serines ($Sty1^{C13SC35SC153SC158SC242S}$), preventing Tpx1-Sty1 disulphide formation, also boosts H_2O_2-induced Sty1 activation (Day and Veal unpublished data). Nevertheless, overexpression of Tpx1 boosts Sty1 activation in cells expressing a constitutively active mutant form of the Wis1 MAPKK, $Wis1^{DD}$. Importantly, this suggests that Tpx1 can act downstream of the MAPKKK that phosphorylates Wis1 to increase H_2O_2-induced phosphorylation of Sty1, independent of the Tpx1-Sty1 disulphide bond.

H_2O_2-induced oxidation of cysteine thiols in protein tyrosine phosphatases (PTP) has been established as an integral part of signal transduction (For reviews see (Rhee *et al.*, 2000; Rhee *et al.*, 2003)). Based

on the established sensitivities of PTP to oxidation, we wondered whether perhaps Tpx1 might increase H_2O_2-induced Sty1 activation by promoting the oxidation of PTP that regulate Sty1.

Dephosphorylation of tyrosine 173 of Sty1 is catalysed by two PTP, Pyp1 and Pyp2 (Figure 1.6), that utilise catalytic cysteine residues (Millar *et al.*, 1992; Millar *et al.*, 1995). Pyp1 levels remain constant upon exposure to stress (Chen *et al.*, 2003), therefore the constitutive expression of Pyp1 is important to maintain low levels of phosphorylated, active Sty1. However, as a target of Atf1, *pyp2*$^{+}$ mRNA levels are induced in response to environmental stress (Wilkinson *et al.*, 1996) (Figure 1.6), suggesting that Pyp2 is important to restore basal phosphorylation levels of Sty1. Pyp2 expression is regulated in a Sty1/Atf1 dependent manner, forming a negative feedback loop (Millar *et al.*, 1995; Degols *et al.*, 1996). Moreover, Pyp2 has been shown to be subject to post-translational regulation. In response to heat stress, Pyp2 was found to become phosphorylated on two residues, not conserved in Pyp1 (Kowalczyk *et al.*, 2013). Sty1-dependent phosphorylation of the linker region in Pyp2 increased the stability of the protein, which consequently dephosphorylated Sty1 (Kowalczyk *et al.*, 2013).

Interestingly, although Sty1 is activated by heat stress, Wis1 is only weakly activated. Instead, it has been shown that Sty1 becomes activated because Pyp1 is inactivated by heat stress (Nguyen and Shiozaki, 1999). However, no one has investigated whether Pyp1 is regulated by post-translational modifications or whether either Pyp1 or Pyp2 are sensitive to oxidation by H_2O_2. The aim in this chapter was to test the hypothesis that Tpx1 might promote H_2O_2-induced activation of Sty1 by regulating either Pyp1 or Pyp2.

3.2 Results

3.2.1 Pyp1 is required for overexpression of Tpx1 to boost H_2O_2-induced Sty1 activation

To test whether Tpx1 might act to stimulate Sty1 activation by regulating the activity of either Pyp1 or Pyp2, we examined whether either phosphatase was required for overexpression of Tpx1 to increase

H_2O_2-induced phosphorylation of Sty1. As expected, basal levels of Sty1 phosphorylation were increased in mutant Δ*pyp1*, and Sty1 phosphorylation was resistant to further activation in response to H_2O_2 (Figure 3.1A). However, whereas overexpression of Tpx1 was able to boost H_2O_2-induced Sty1 activation in both wild-type (NT4) and mutant Δ*pyp2* cells, overexpressing Tpx1 was unable to stimulate H_2O_2-induced Sty1 activation in a Δ*pyp1* (Figure 3.1A and 3.1B). This showed that Pyp1 was required for increased Tpx1 levels to promote Sty1 activation, consistent with our hypothesis that Tpx1-dependent oxidation of Pyp1 might be important for H_2O_2-induced Sty1 activation.

To further investigate how Pyp1 is regulated by H_2O_2, a strain was constructed expressing Pyp1 from its endogenous locus with a Pk-epitope at its C-terminus (see section 2.2.5.3). The cell length (Figure 3.2A), cell growth (Figure 3.2B), and H_2O_2-induced Sty1 activation (Figure 3.2C and 3.2D) of Pk-epitope tagged wild-type Pyp1 (Pyp1Pk) was compared to untagged wild-type (NT4) and a Δ*pyp1*, confirming that the Pk-epitope tag did not affect the function of Pyp1.

3.2.2 Pyp1 undergoes multiple stress-induced post-translational modifications

First we examined whether, as expected, Pyp1 became oxidised in response to H_2O_2. To examine protein oxidation, samples were treated with AMS, a thiol-binding agent which binds to reduced cysteine residues to increase the protein molecular mass by 0.6 kDa per reduced cysteine. Hence, proteins in which any cysteines are oxidised will bind fewer molecules of AMS, increasing their electrophoretic mobility. Notably, in unstressed cells, in addition to the predominant form of Pyp1Pk, of the expected size, approximately 70 kDa (Figure 3.3A, labelled Unmodified Pyp1Pk), there was an additional form with a slightly slower mobility (Modified Pyp1Pk). However, following exposure of cells to low (0.2 mM and 1.0 mM) concentrations of H_2O_2, levels of the 'Modified Pyp1Pk' form decreased and instead a higher molecular weight form of Pyp1Pk (HMW Pyp1Pk) was detected 30 seconds following H_2O_2 treatment (Figure 3.3A).

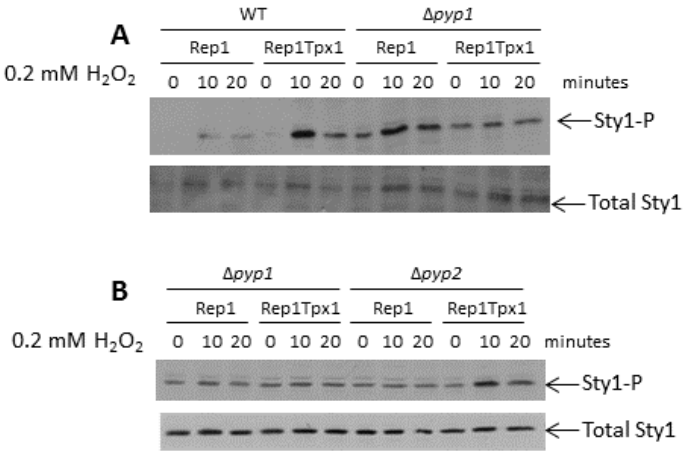

Figure 3.1 The activity of Pyp1, but not Pyp2, is required for overexpression of Tpx1 to boost H_2O_2-induced Sty1 activation. Western blot analysis of levels of phosphorylated Sty1 in *S. pombe* (**A**) wild-type (NT4) and Δ*pyp1* (NJ102), or (**B**) Δ*pyp1* (NJ102) and Δ*pyp2* (JP279) expressing additional Tpx1 from the *S. pombe* expression vector (Rep1Tpx1) or the vector control (Rep1) before and after treatment with 0.2 mM H_2O_2. Anti-pp38 and anti-Sty1 antibodies were used to detect phosphorylated Sty1 and total Sty1 levels, respectively.

A

	WT	Pyp1Pk	Δ*pyp1*
Cell length at division (μm)	7.9 ± 0.9	7.5 ± 0.6	7.0 ± 0.7

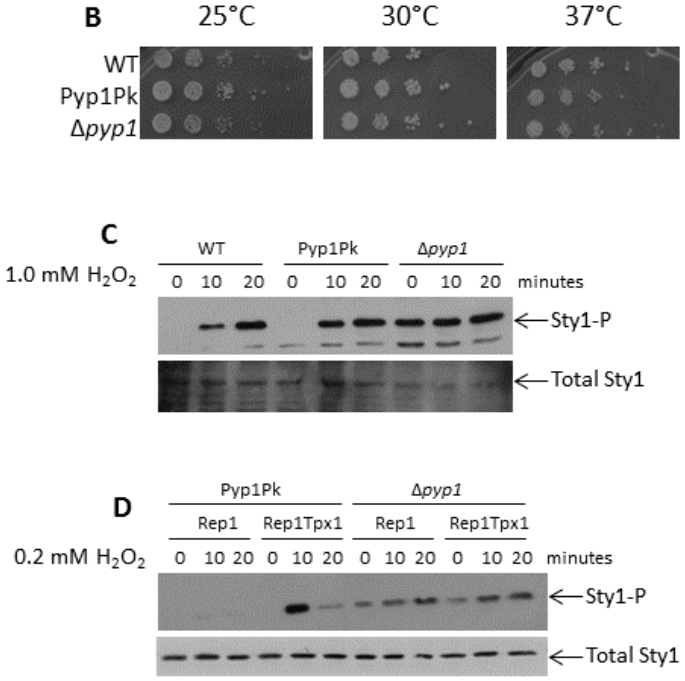

Figure 3.2 The Pk-tagged form of Pyp1 is functional, and does not affect cell growth or H_2O_2-induced Sty1 activation. (**A**) Cell length of wild-type (NT4), Pk-epitope tagged wild-type Pyp1 (Pyp1Pk) (HL2) and Δ*pyp1* (NJ102) dividing cells were measured through analysis by DIC microscopy. (**B**) Serial 10-fold dilutions of wild-type (NT4), Pk-epitope tagged wild-type Pyp1 (Pyp1Pk) (HL2) or Δ*pyp1* (NJ102) were spotted onto YE5S agar plates, and incubated for 3 days at the indicated temperatures. Western blot analysis of levels of phosphorylated Sty1 in (**C**) wild-type (NT4), Pk-epitope tagged wild-type Pyp1 (Pyp1Pk) (HL2) and Δ*pyp1* (NJ102) before and after treatment with 1.0 mM H_2O_2, and (**D**) Pk-epitope tagged wild-type Pyp1 (Pyp1Pk) (HL2) and Δ*pyp1* (NJ102) expressing additional Tpx1 from the *S. pombe* expression vector (Rep1Tpx1) or the vector control (Rep1) before and after treatment with 0.2 mM H_2O_2. Anti-pp38 and anti-Sty1 antibodies were used to detect phosphorylated Sty1 and total Sty1 levels, respectively.

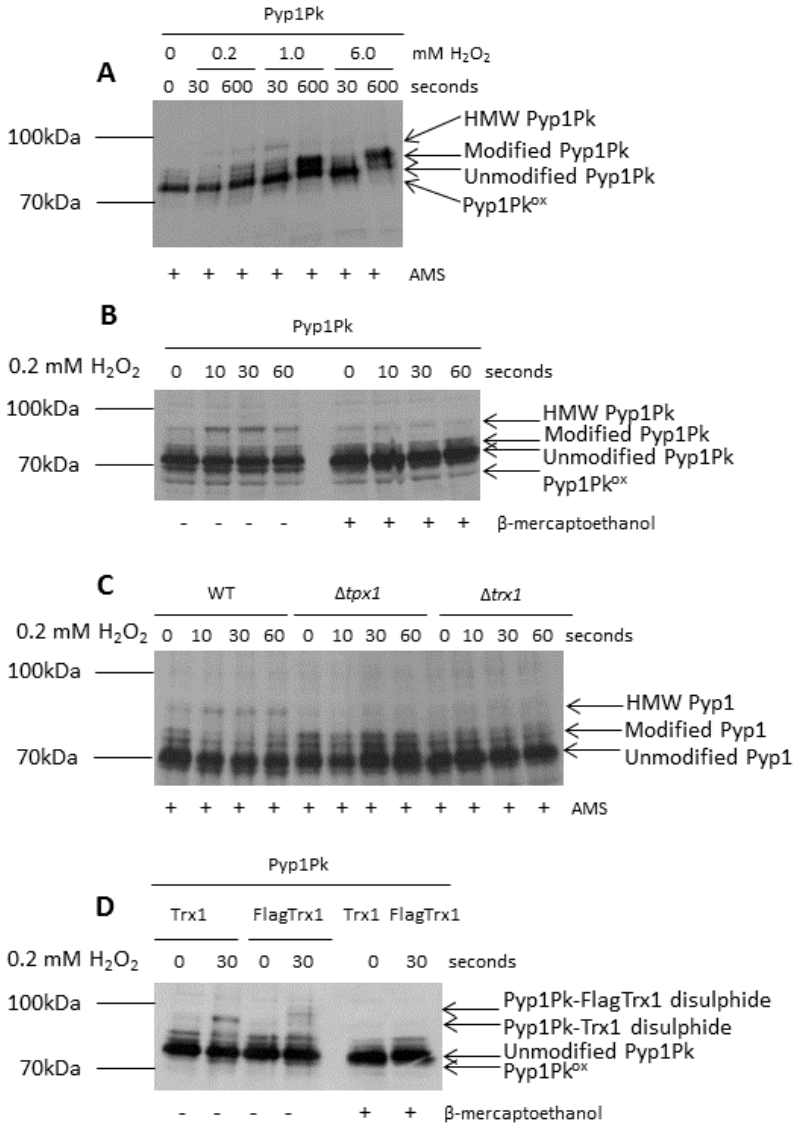

Figure 3.3 Pyp1 undergoes multiple stress-induced post-translational modifications. Western blot analysis of cells expressing (**A**) Pk-epitope tagged wild-type Pyp1 (Pyp1Pk) (NJ197) before and after treatment with 0.2 mM, 1.0 mM and 6.0 mM H_2O_2 for the indicated times, (**B**) Pk-epitope tagged wild-type Pyp1 (Pyp1Pk) (NJ197) before and after treatment with 0.2 mM H_2O_2 for the indicated times, (**C**) wild-type (429), Δ*tpx1* (VXOO) and Δ*trx1* (JB30) before and after treatment with 0.2 mM H_2O_2 for the indicated times, and (**D**) Pk-epitope tagged wild-type Pyp1 (Pyp1Pk), co-expressing untagged Trx1 (NJ197) and Flag-tagged Trx1 (AD144), before and after treatment with 0.2 mM H_2O_2. Anti-Pk antibody was used to detect Pk-tagged Pyp1. Protein samples were treated, as indicated, with the thiol-binding agent AMS, or the reducing agent β-mercaptoethanol, prior to electrophoresis. The different bands are indicated and the molecular weight (MW) markers are shown. (**B**)(**C**)(**D**) These experiments were performed by Dr. A. Day.

In addition, a small proportion of Pyp1 was present in a lower molecular weight form upon H_2O_2 treatment, with an electrophoretic mobility just below the unmodified form of Pyp1, consistent with at least one cysteine becoming oxidised and resistant to AMS ($Pyp1Pk^{ox}$). However, after 600 seconds exposure to low concentrations of H_2O_2, the decrease in 'HMW Pyp1Pk' was accompanied by an increase in the 'Modified Pyp1Pk' form that is also detected under normal conditions. At higher (6.0 mM) concentrations of H_2O_2, the 'HMW Pyp1Pk' form was not detected, and only the 'Modified Pyp1Pk' could be detected 600 seconds following H_2O_2 treatment (Figure 3.3A).

3.2.2.1 Pyp1 forms a H_2O_2-induced disulphide with Trx1 at low levels of H_2O_2

The absence of the higher molecular weight (HMW Pyp1Pk) form of Pyp1, at approximately 85 kDa, from samples treated with β-mercaptoethanol suggests that this represents a reversibly oxidised form (Figure 3.3B). The mobility of the 'HMW Pyp1Pk' form suggested that it might represent a mixed disulphide between Pyp1 and another protein. The failure to detect this band in samples from cells lacking *tpx1*$^+$ or *trx1*$^+$ suggested that it might involve a disulphide between Pyp1 and Tpx1 or Trx1 (Figure 3.3C). In particular, its apparent molecular weight, approximately 12 kDa higher than Pk-epitope tagged Pyp1 (70 kDa) raised the possibility that it might present a disulphide between Trx1 and Pyp1. Consistent with this possibility, the mobility of this form of Pyp1 was slightly increased in cells co-expressing FlagTrx1, compared with cells expressing untagged Trx1 (Figure 3.3D). Taken together, these data suggest that these oxidised forms of Pyp1 are mixed disulphides between Pyp1 and Trx1. Notably, this reversible oxidation of Pyp1 was very rapid and transient in response to H_2O_2, raising the possibility that Trx1 might be involved in the oxidation, rather than the reduction, of Pyp1 at low concentrations of H_2O_2 (Figure 3.3D). These data were consistent with the hypothesis that the Tpx1-dependent oxidation of Pyp1 might be important for H_2O_2-induced Sty1 activation (Figure 3.1A and 3.1B). Moreover, they raised the possibility that Tpx1 might promote the oxidation of Pyp1 by a mechanism involving a rapid H_2O_2-induced disulphide between Pyp1 and Trx1.

In addition, a third modified form of Pyp1 was also observed (Figure 3.3A). This 'Modified Pyp1Pk' form was present both before and after low H_2O_2 stress, suggesting that its formation was inhibited by H_2O_2 but recovered 600 seconds after exposure. Indeed, our data suggested that this post-translational modification was mutually exclusive with formation of the Pyp1-Trx1 disulphide.

To test whether the oxidative modifications of Pyp1 that were observed in response to H_2O_2 also occurred in response to other stresses, Pyp1 was examined in cells exposed to osmotic stress, to allow comparisons between the two stress conditions. The Pyp1-Trx1 mixed disulphide forms 30 seconds after exposure to 1.0 mM H_2O_2, followed by the formation of the 'Modified Pyp1Pk' form at 600 seconds. In contrast, in response to 0.6 M KCl, no Pyp1-Trx1 disulphide was detected, and the 'Modified Pyp1Pk' form was detected earlier, only 30 seconds after exposure to osmotic stress (Figure 3.4). Strikingly, the levels of Pyp1 protein appear to be dramatically reduced following prolonged exposure (600 seconds) to 0.6 M KCl (Figure 3.4). Although, in the absence of a loading control, it is possible that the lower levels of Pyp1 might just reflect lower levels of total protein in these lanes, this suggests that, under these stress conditions, Pyp1 may become less stable, as previously suggested for heat stress where the majority of Pyp1 becomes insoluble following exposure to heat shock (Nguyen and Shiozaki, 1999). Taken together, this indicates that Trx1 is involved in the oxidation of Pyp1 specifically at low concentrations of H_2O_2 (Figure 3.3D), but that other modifications also occur in response to both oxidative and osmotic stress (Figure 3.4).

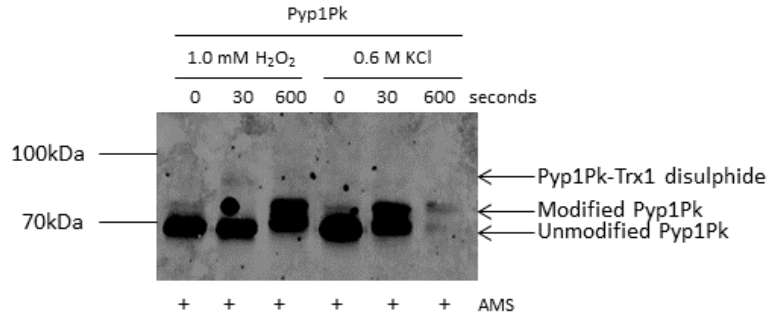

Figure 3.4 Pyp1-Trx1 disulphides form in response to oxidative stress, but not to osmotic stress. Western blot analysis of cells expressing Pk-epitope tagged wild-type Pyp1 (Pyp1Pk) (HL2) before and after treatment for 600 seconds with 1.0 mM H_2O_2 or 0.6 M KCl. All protein samples were treated with the thiol-binding agent AMS. Anti-Pk antibody was used to detect Pk-tagged Pyp1. The different bands are indicated and the molecular weight (MW) markers are shown.

3.2.2.2 Pyp1 undergoes a post-translational modification in response to oxidative and osmotic stress, that is consistent with either hyperoxidation or phosphorylation

Next, we set out to determine the identity of the modification of Pyp1 that takes place in response to both oxidative and osmotic stress. The reduced mobility of this form and its resistance to β-mercaptoethanol (Figure 3.3B) were consistent with it possibly representing hyperoxidation of the catalytic cysteine to sulphinic (Cys-SO_2H) or sulphonic (Cys-SO_3H) forms, which have also been shown to reduce mobility (Lou *et al.*, 2008). Moreover, a form with decreased Pyp1Pk mobility was also observed when samples from cells treated with 1.0 mM H_2O_2 were treated with NEM, despite less NEM-binding being predicted to have a minimal effect on protein mobility (0.125 kDa per reduced cysteine). However, the mobility shift with AMS is greater than with NEM, consistent with this shift being due to hyperoxidation (Figure 3.5). This suggests that the post-translational modification could be hyperoxidation of the catalytic cysteine to a sulphinic or sulphonic residue. We proposed that hyperoxidation would increase AMS-binding as the 'Modified Pyp1Pk' form would bind an extra AMS, or NEM, due to an additional cysteine available for AMS modification, that was perhaps involved in a disulphide bond at earlier time points or lower concentrations of H_2O_2. A third thiol-binding agent, PEG-Maleimide, which adds 5.0 kDa per reduced cysteine residue, was also used to try to improve separation of the protein. However, due to the large molecular weight of Pyp1, the addition of 5.0 kDa per reduced cysteine residue when using PEG-Maleimide, and the different polymerisations of PEG, these bands appear diffuse when run on an SDS-PAGE gel, making the separations difficult to visualise and characterise (Figure 3.5). A newer maleimide reagent, DNA-Maleimide, which comprises a maleimide-conjugated ssDNA (Hara *et al.*, 2013), adding 15.0 kDa per reduced cysteine residue, was also unsuccessfully used to try to improve separation. Hence, although the mobility shift with NEM is smaller than with AMS, consistent with the second modification of Pyp1 possibly representing hyperoxidation, given that it also occurs under osmotic stress conditions (Figure 3.4), it may well reflect a non-oxidative post-translational modification, such as phosphorylation.

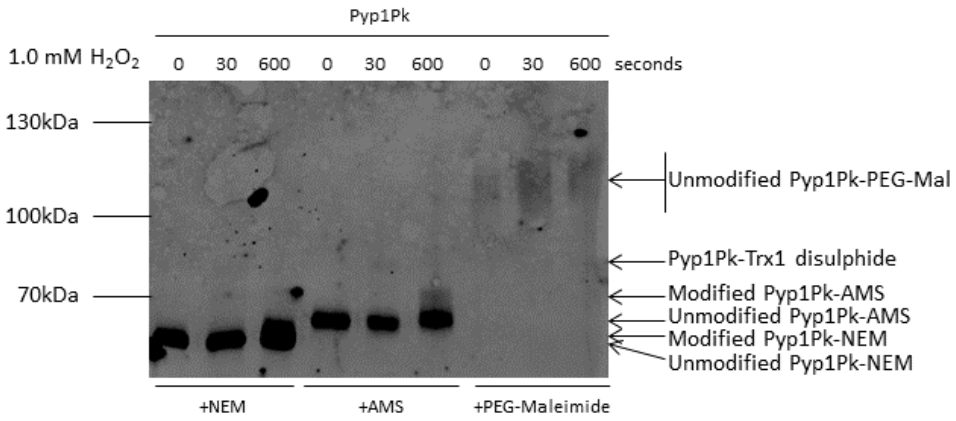

Figure 3.5 The effect of three different thiol-binding agents on mobility of Pyp1. Western blot analysis of cells expressing Pk-epitope tagged wild-type Pyp1 (Pyp1Pk) (HL2) before and after treatment for the indicated times with 1.0 mM H_2O_2. Anti-Pk antibody was used to detect Pk-tagged Pyp1. Protein samples were treated with the thiol-binding agents, NEM, AMS or PEG-Maleimide, as indicated, prior to electrophoretic separation. The different bands are indicated and the molecular weight (MW) markers are shown.

3.2.3 Identification of conserved cysteine residues through sequence alignment

Having identified that Pyp1 is oxidised specifically in response to low levels of H_2O_2 (Figure 3.3A), and also undergoes a second post-translational modification in response to oxidative and osmotic stress (Figure 3.4), the function of these modifications was investigated. The first goal was to identify the cysteine that was involved in forming disulphides with Trx1, and determine whether it was important for the increased activation of Sty1 in cells overexpressing Tpx1.

Alignment of the Pyp1 sequences for four *Schizosaccharomyces* species identified that six of the twelve cysteine residues were conserved (Figure 3.6), increasing the likelihood that these residues might be generally important for the function or regulation of phosphatases. Although cysteine 470 is generally accepted as the catalytic cysteine of Pyp1 (Hannig *et al.*, 1994), sequence similarity between the region around cysteine 340 of Pyp1 and the catalytic cysteine in the dual-specificity phosphatase, Pmp1, that dephosphorylates the MAPK, Pmk1, suggested that cysteine 340 might also have catalytic activity. Therefore, as cysteine 340 and cysteine 470 are both potential catalytic cysteine residues, a double substitution mutant of these two residues was also constructed. In addition to cysteine 340 and cysteine 470, the four other conserved cysteine residues correspond to residues 20, 118, 222 and 441 in Pyp1 in *S. pombe*. Strains were constructed expressing mutant Pyp1, in which the cysteine residue (C) was replaced with serine (S), which cannot become oxidised and form disulphides. Each of the Pyp1 cysteine mutants was expressed with a Pk-epitope at their C-termini (see section 2.2.5.1 and 2.2.5.2), to investigate whether any of these cysteine residues are important for the post-translational modifications of Pyp1, and H_2O_2-induced Sty1 activation.

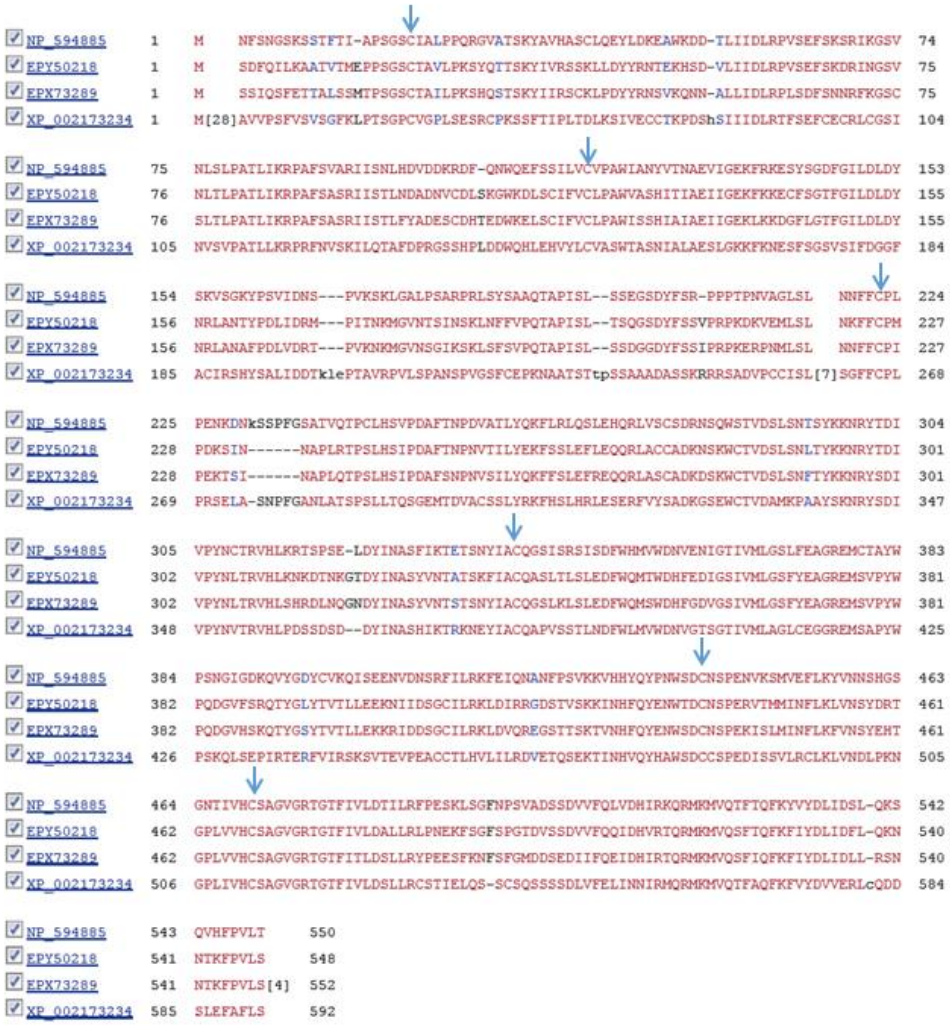

Figure 3.6 Sequence alignment of protein tyrosine phosphatase Pyp1 from *Schizosaccharomyces pombe*, *Schizosaccharomyces cryophilus*, *Schizosaccharomyces octosporus* and *Schizosaccharomyces japonicus*. The amino acid sequence of *S. pombe* (NP_594885.1) Pyp1 and its homologues from *S.cryophilus* (EPY50218.1), *S.octosporus* (EPX73289.1) and *S.japonicus* (XP_002173234.1) were aligned using ClustalX2. Arrows point towards cysteine residues conserved between all four *Schizosaccharomyces* species, corresponding to residues C20, C118, C222, C340, C441, and C470 in Pyp1 from *S. pombe* (From Cobalt). Pyp1 is predicted by PSORT II to be 34.8% mitochondrial, due to a 29 amino acid mitochondrial targeting sequence (MTS) at the N-terminus of Pyp1 (MNFSNGSKSSTFTIAPSGSCIALPPQRG).

3.2.4 The role of two potential catalytic cysteines in Pyp1 in H_2O_2-induced activation of Sty1

3.2.4.1 The catalytic cysteine of Pyp1 is required for H_2O_2-induced activation of Sty1, and for overexpression of Tpx1 to boost H_2O_2-induced Sty1 activation

To test whether either or both cysteine 340 and cysteine 470 were important for Pyp1 activity, the effect of single and double catalytic cysteine mutants on Sty1 phosphorylation was examined. It was found that, similar to wild-type (Pyp1Pk), phosphorylated Sty1 levels were undetectable in Pyp1^{C340S}Pk cells before exposure to H_2O_2, but strongly induced 10 and 20 minutes after exposure to 1.0 mM H_2O_2 (Figure 3.7A). In contrast, Sty1 activation in Pyp1^{C470S}Pk and Pyp1^{C340SC470S}Pk was comparable to that of a Δ*pyp1* (Figure 3.2C and 3.7A), with high basal Sty1 phosphorylation and a lack of induction upon oxidative stress. This indicates that only the accepted catalytic cysteine, cysteine 470, is required for Pyp1 to dephosphorylate and inactivate Sty1. Taken together, this suggests cysteine 470, but not cysteine 340, is required for Pyp1 activity and H_2O_2-induced Sty1 activation.

Having confirmed that the catalytic cysteine of Pyp1, cysteine 470, was important for Pyp1 activity and H_2O_2-induced phosphorylation of the MAPK, Sty1 (Figure 3.7A), it was tested whether this cysteine was also required for the increased H_2O_2-induced Sty1 activation in cells overexpressing Tpx1. Although overexpression of Tpx1 increased H_2O_2-induced Sty1 activation in wild-type (Figure 3.2D), it failed to boost H_2O_2-induced Sty1 activation in either Pyp1^{C470S}Pk or Pyp1^{C340SC470S}Pk (Figure 3.7B), similar to a Δ*pyp1* (Figure 3.2D). This indicates that the increase in H_2O_2-induced Sty1 activation, mediated by Tpx1, is dependent on the catalytic cysteine, cysteine 470, in Pyp1.

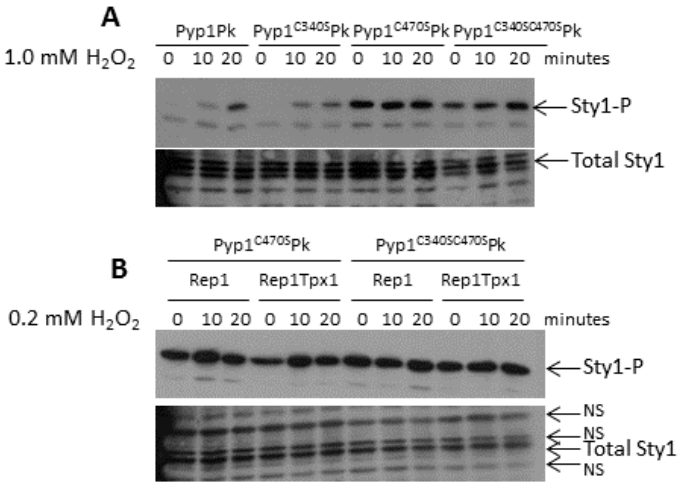

Figure 3.7 The role of two potential catalytic cysteines in Pyp1 in regulating H_2O_2-induced phosphorylation of Sty1. Western blot analysis of levels of phosphorylated Sty1 in cells expressing (**A**) Pk-epitope tagged wild-type Pyp1 (Pyp1Pk) (HL2) or mutant Pyp1^{C340S}Pk (HL15), Pyp1^{C470S}Pk (HL3) and Pyp1^{C340SC470S}Pk (HL4) before and after treatment for the indicated times with 1.0 mM H_2O_2, and (**B**) Pk-epitope tagged Pyp1^{C470S}Pk (HL3) and Pyp1^{C340SC470S}Pk (HL4) cells expressing additional Tpx1 from the *S. pombe* expression vector (Rep1Tpx1) or the vector control (Rep1) before and after treatment for the indicated times with 0.2 mM H_2O_2. Anti-pp38 and anti-Sty1 antibodies were used to detect phosphorylated Sty1 and total Sty1 levels, respectively. The different bands are indicated and the molecular weight (MW) markers are shown. Non-specific (NS) bands are indicated.

3.2.4.2 Putative catalytic cysteines 340 and 470 of Pyp1 are not required for either of the stress-induced post-translational modifications of Pyp1

Having identified that the catalytic cysteine, cysteine 470, of Pyp1 is required for overexpression of Tpx1 to boost H_2O_2-induced Sty1 activation (Figure 3.7B), next we tested our hypothesis that the Tpx1-dependent mixed disulphide between Pyp1 and Trx1 might be important for the regulation of Pyp1.

It seemed plausible that the disulphide between Pyp1 and Trx1 would involve the catalytic cysteine, 470, that is likely to be deprotonated and thus more sensitive to H_2O_2-induced oxidation than other cysteines (see section 1.4.2). However, both the Pyp1-Trx1 mixed disulphide and the 'Modified Pyp1Pk' forms were detected in mutant Pyp1^{C340S}Pk, Pyp1^{C470S}Pk and Pyp1^{C340SC470S}Pk cells after exposure to 1.0 mM H_2O_2 (Figure 3.8A), indicating that neither the putative catalytic cysteine 340, nor the accepted catalytic cysteine 470, is required for either of the post-translational modifications of Pyp1. Intriguingly, in contrast to wild-type cells, the ratio of 'Modified Pyp1Pk' to 'Unmodified Pyp1Pk' did not appear to change following exposure of Pyp1^{C470S}Pk and Pyp1^{C340SC470S}Pk cells to H_2O_2. Importantly, as 'Modified Pyp1Pk' can still form in the catalytic cysteine mutant of Pyp1, this suggests that this modification cannot be hyperoxidation of the catalytic cysteine. Instead, as we will discuss later (see section 3.2.6.1), our data suggest that this modification is phosphorylation.

3.2.4.3 H_2O_2-induced formation of Pyp1^{ox} is dependent on the catalytic cysteine residues of Pyp1

In response to H_2O_2, along with the formation of a transient Pyp1-Trx1 mixed disulphide, a small proportion of Pyp1 was also found to be oxidised upon H_2O_2 treatment, with an increased electrophoretic mobility (Figure 3.3B, labelled Pyp1Pk^{ox}).

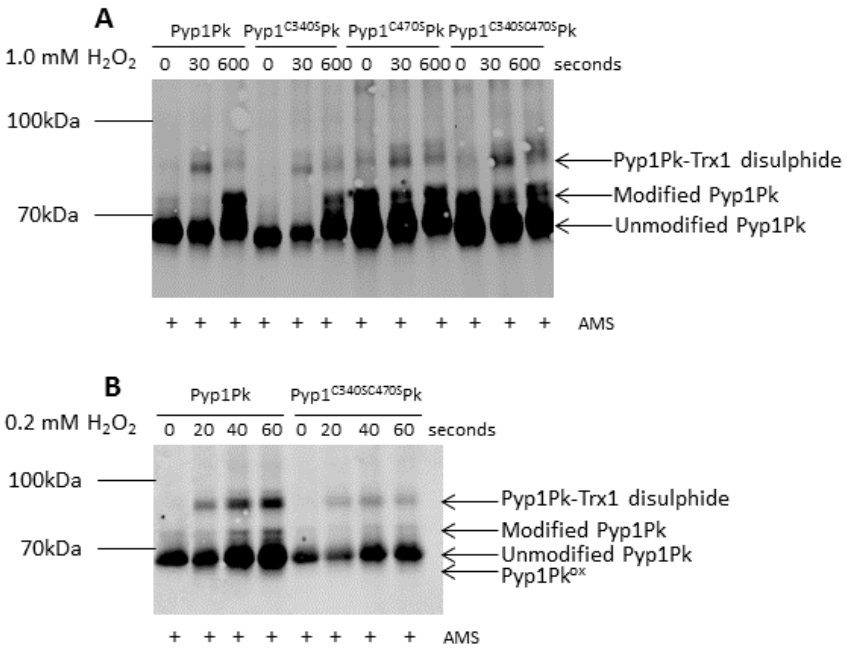

Figure 3.8 The effect of the catalytic cysteine(s) of Pyp1 on post-translational modifications of Pyp1. Western blot analysis of cells expressing (**A**) Pk-epitope tagged wild-type Pyp1 (Pyp1Pk) (HL2) or mutant Pyp1^{C340S}Pk (HL15), Pyp1^{C470S}Pk (HL3) and Pyp1^{C340SC470S}Pk (HL4) before and after treatment for the indicated times with 1.0 mM H_2O_2, and (**B**) Pk-epitope tagged wild-type Pyp1 (Pyp1Pk) (HL2) or mutant Pyp1^{C340SC470S}Pk (HL4) before and after treatment for the indicated times with 0.2 mM H_2O_2. Anti-Pk antibody was used to detect Pk-tagged Pyp1. All protein samples were treated with the thiol-binding agent AMS, prior to electrophoresis. The different bands are indicated and the molecular weight (MW) markers are shown.

To test whether cysteine 340 or cysteine 470 of Pyp1 were required for Pyp1Pk^{ox} formation, the mobility of Pyp1 was examined in cells over a shorter time course following exposure to a lower (0.2 mM) concentration of H_2O_2 in order to maximise the levels of Pyp1-Trx1 mixed disulphide and 'Pyp1Pk^{ox}'. Following treatment with 0.2 mM H_2O_2, a more mobile 'Pyp1Pk^{ox}' form of Pyp1 was detected (Figure 3.3B and 3.8B), consistent with a small proportion of Pyp1 becoming oxidised, and thus binding less AMS. This 'Pyp1Pk^{ox}' form was difficult to separate from the unmodified Pyp1 and attempts to improve this separation using a larger thiol-binding agent DNA-Maleimide were unsuccessful. Although this, and the lower levels of Pyp1^{C340SC470S}Pk protein in this experiment, make it difficult to make a firm conclusion, the absence of this band from samples expressing Pyp1^{C340SC470S}Pk suggests that these cysteines, while dispensable for Pyp1-Trx1 mixed disulphide formation, may be important for this oxidation (Figure 3.8B).

3.2.5 The role of Pyp1-Trx1 disulphides in H_2O_2-induced activation of Sty1

3.2.5.1 Cysteine 222 of Pyp1 is required for the H_2O_2-induced Pyp1-Trx1 disulphide at 1.0 mM H_2O_2, but not at 0.2 mM H_2O_2

As neither the catalytic cysteine, 470, or cysteine 340, were required for H_2O_2-induced Pyp1-Trx1 disulphide formation (Figure 3.8A), next we tested whether other conserved cysteines might be involved. Cysteine residues at position 118, 222 and 441 in the Pyp1 protein sequence are highly conserved between four *Schizosaccharomyces* species (Figure 3.6), therefore the effect of substituting these residues on Sty1 activation and Pyp1 oxidation was investigated.

Firstly, we noted that serine substitution of cysteine 118, 222 or 441 did not affect the stress-induced phosphorylation of Pyp1 (Figure 3.9A). In addition, neither cysteine 118 or cysteine 441 was required for the formation of Pyp1-Trx1 mixed disulphides, as indicated by the presence of the higher molecular weight oxidised form of Pyp1 30 seconds after exposure to 1.0 mM H_2O_2 (Figure 3.9A). In contrast, substitution of cysteine C222 to a serine prevented the formation of the Pyp1-Trx1 disulphide in

response to 1.0 mM H_2O_2. This suggested that cysteine 222 of Pyp1 was important for the formation of H_2O_2-induced mixed disulphides with Trx1.

However, Pyp1-Trx1 disulphides were still detected in Pyp1^{C222S}Pk cells exposed to lower (0.2 mM) concentrations of H_2O_2, although at lower levels than with wild-type Pyp1 (Figure 3.9B). Intriguingly, it was observed that Pyp1-Trx1 disulphides appear to persist for much longer in cells exposed to 0.2 mM H_2O_2 in both wild-type (Pyp1Pk) and mutant Pyp1^{C222S}Pk than in cells exposed to 1.0 mM H_2O_2. Taken together these data suggests that although cysteine 222 is not absolutely required and may not directly participate in Pyp1-Trx1 disulphides, it does affect the kinetics involved in the formation and/or reduction of the disulphide bond between Pyp1 and Trx1 (Figure 3.9B).

3.2.5.2 Substituting cysteine 118, 222 and 441 of Pyp1 does not affect basal or H_2O_2-induced Sty1 phosphorylation

As substituting cysteine 222 of Pyp1 to a serine inhibited H_2O_2-induced formation of mixed disulphides between Pyp1 and Trx1 at 1.0 mM H_2O_2 (Figure 3.9A), and caused a reduction in the levels of Pyp1-Trx1 disulphides at 0.2 mM H_2O_2 (Figure 3.9B), we investigated whether this cysteine was important for H_2O_2-induced Sty1 activation. However, Sty1 activation in cells expressing Pyp1^{C118S}Pk, Pyp1^{C222S}Pk and Pyp1^{C441S}Pk resembles that of wild-type (Pyp1Pk) cells, with similar levels of basal Sty1 phosphorylation and increases upon exposure to 1.0 mM H_2O_2 (Figure 3.10A), although in Pyp1^{C441S}Pk cells there was possibly slightly less Sty1 activation following treatment with H_2O_2 compared to wild-type (Pyp1Pk), Pyp1^{C118S}Pk and Pyp1^{C222S}Pk. Notably the wild-type levels of H_2O_2-induced Sty1 activation in Pyp1^{C222S}Pk cells suggests that the formation of a disulphide between Pyp1 and Trx1 is not important for Pyp1's activity in dephosphorylating Sty1.

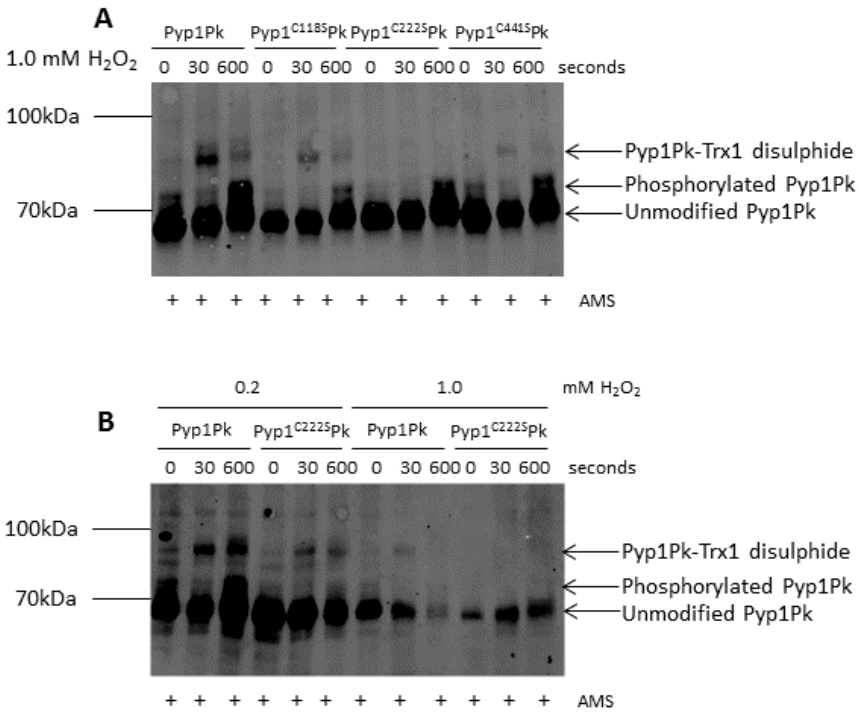

Figure 3.9 Cysteine 222 of Pyp1 is required for the Pyp1-Trx1 disulphide at 1.0 mM H_2O_2, but not at lower (0.2 mM) concentrations of H_2O_2. Western blot analysis of cells expressing (**A**) Pk-epitope tagged wild-type Pyp1 (Pyp1Pk) (HL2) or mutant Pyp1^{C118S}Pk (HL7), Pyp1^{C222S}Pk (HL8) and Pyp1^{C441S}Pk (HL9) before and after treatment with 1.0 mM H_2O_2, and (**B**) Pk-epitope tagged wild-type Pyp1 (Pyp1Pk) (HL2) or mutant Pyp1^{C222S}Pk (HL8) before and after treatment with 0.2 mM or 1.0 mM H_2O_2. Anti-Pk antibody was used to detect Pk-tagged Pyp1. All protein samples were treated with the thiol-binding agent AMS, prior to electrophoresis. The different bands are indicated and the molecular weight (MW) markers are shown.

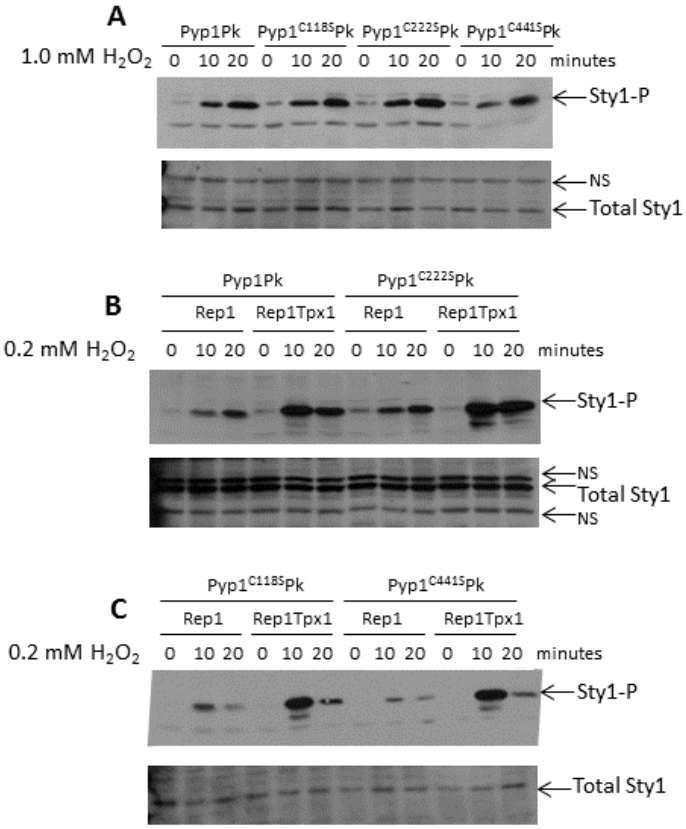

Figure 3.10 The effect of mutant forms of Pyp1 in regulating H_2O_2-induced phosphorylation of Sty1, and on Tpx1 overexpression on Sty1 activation. Western blot analysis of levels of phosphorylated Sty1 in cells expressing (**A**) Pk-epitope tagged wild-type Pyp1 (Pyp1Pk) (HL2) or mutant Pyp1^{C118S}Pk (HL7), Pyp1^{C222S}Pk (HL8) and Pyp1^{C441S}Pk (HL9) before and after treatment with 1.0 mM H_2O_2, (**B**) Pk-epitope tagged wild-type Pyp1 (Pyp1Pk) (HL2) and Pyp1^{C222S}Pk (HL8) cells expressing additional Tpx1 from the *S. pombe* expression vector (Rep1Tpx1) or the vector control (Rep1) before and after treatment with 0.2 mM H_2O_2, and (**C**) Pk-epitope tagged mutant Pyp1^{C118S}Pk (HL7) and Pyp1^{C441S}Pk (HL9) cells expressing additional Tpx1 from the *S. pombe* expression vector (Rep1Tpx1) or the vector control (Rep1) before and after treatment with 0.2 mM H_2O_2. Anti-pp38 and anti-Sty1 antibodies were used to detect phosphorylated Sty1 and total Sty1 levels, respectively. Non-specific (NS) bands are indicated.

3.2.5.3 Overexpression of Tpx1 boosts H_2O_2-induced Sty1 activation in cells expressing Pyp1^{C222S}Pk mutant more than in cells expressing wild-type Pyp1Pk

As the catalytic activity of Pyp1 is required for Tpx1 overexpression to increase H_2O_2-induced Sty1 activation (Figure 3.7B), and Pyp1-Trx1 disulphide formation appears to be Tpx1-dependent (Figure 3.3C), we took advantage of the Pyp1^{C222S}Pk mutant, in which Pyp1-Trx1 disulphide formation was severely impaired, to investigate whether Pyp1-Trx1 disulphide formation was important for overexpression of Tpx1 to stimulate H_2O_2-induced Sty1 phosphorylation.

As previously, overexpression of Tpx1 did not stimulate increased Sty1 activation in Δ*pyp1* cells exposed to 0.2 mM H_2O_2 (Figure 3.1A and 3.1B). Overexpressing Tpx1 in Pyp1^{C118S}Pk and Pyp1^{C441S}Pk cells, mutants which are still able to form the Pyp1-Trx1 mixed disulphide (Figure 3.9A), boosted H_2O_2-induced Sty1 activation similarly to the increase observed in wild-type (Pyp1Pk) cells overexpressing Tpx1 (Figure 3.10B and 3.10C). However, not only did Tpx1 boost Sty1 activation in Pyp1^{C222S}Pk cells, in which Pyp1-Trx1 disulphide formation is inhibited, but it actually stimulated even higher levels of H_2O_2-induced Sty1 phosphorylation than in wild-type (Pyp1Pk) (Figure 3.10B). As Pyp1^{C222S}Pk prevents the formation of the Pyp1-Trx1 mixed disulphide at 1.0 mM H_2O_2 (Figure 3.9A), this suggests that Tpx1 does not boost the H_2O_2-induced activation of Sty1 by promoting Pyp1-Trx1 disulphide formation. Indeed, these data suggest that perhaps Pyp1-Trx1 disulphides actually reduce the sensitivity of Sty1 to Tpx1-driven, H_2O_2-induced increases in its phosphorylation.

3.2.5.4 Effect of overexpression of Tpx1 on post-translational modification of Pyp1Pk or Pyp1^{C222S}Pk

Overexpressing Tpx1 caused a greater elevation in H_2O_2-induced Sty1 phosphorylation in Pyp1^{C222S}Pk cells compared to in wild-type (Pyp1Pk) (Figure 3.10B), but inhibits the formation of the Pyp1-Trx1 disulphide (Figure 3.9A), therefore we investigated the role of Tpx1 on the post-translational modifications of Pyp1 in wild-type and mutant Pyp1^{C222S}Pk.

When we tested whether overexpression of Tpx1 affected the formation of Pyp1-Trx1 or phosphorylation of Pyp1, we observed that the Pyp1-Trx1 disulphide persists for longer in wild-type (Pyp1Pk) cells overexpressing Tpx1; disulphide formation is maximal at 30 seconds in cells containing empty vector (Rep1), whereas in cells overexpressing Tpx1 (Rep1Tpx1) the disulphide was still detected at 600 seconds (Figure 3.11A). However, in the mutant Pyp1^{C222S}Pk, there was a delay in the formation of the disulphide to 600 seconds which was unaffected by overexpression of Tpx1. However, it was noted that, although the levels of phosphorylated Pyp1^{C222S}Pk were unaffected, unmodified Pyp1^{C222S}Pk decreased in cells overexpressing Tpx1 following prolonged exposure (600 seconds) to H_2O_2, and this was associated with the formation of higher molecular weight complexes (Figure 3.11A). Therefore, a longer time course was used to further investigate these potential Tpx1-induced changes in Pyp1.

In wild-type (Pyp1Pk) cells with the empty vector (Rep1) following exposure to 0.2 mM H_2O_2, both the Pyp1-Trx1 disulphide and phosphorylated Pyp1 were detected at 10 and 20 minutes (Figure 3.11B). Similarly, in wild-type (Pyp1Pk) cells overexpressing Tpx1, both modifications were detected at 10 and 20 minutes, however a faint ladder of additional higher molecular weight bands with molecular weight similar to that of Pyp1-Trx1 disulphides appeared at 10 minutes (Figure 3.11B). When exposed to 0.2 mM H_2O_2, Pyp1^{C222S}Pk cells containing the empty vector showed a similar pattern of modifications to wild-type Pyp1Pk. However, strikingly, overexpression of Tpx1 in Pyp1^{C222S}Pk cells caused the formation of higher molecular weight complexes by 10 minutes, and a dramatic reduction in Pyp1 levels by 20 minutes (Figure 3.11B). Although the identity of these additional higher molecular weight forms was not determined, this suggests that overexpressing Tpx1 causes Pyp1 to aggregate or become degraded, by a mechanism that is inhibited by cysteine 222. As cysteine 222 is required for efficient formation of Pyp1-Trx1 disulphides, this suggests these disulphides inhibit Pyp1 turnover.

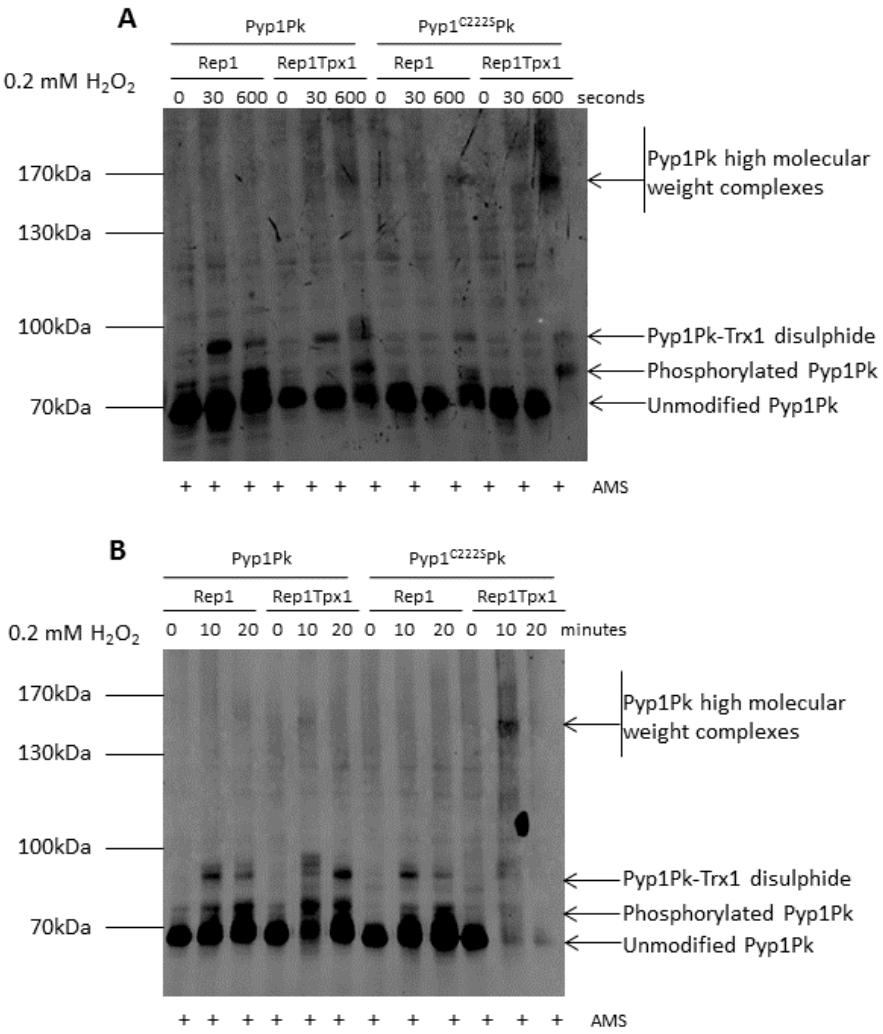

Figure 3.11 The effect of overexpression of Tpx1 on post-translational modification of Pyp1 or Pyp1^{C222S}. (**A**)(**B**) Western blot analysis of cells expressing Pk-epitope tagged wild-type Pyp1 (Pyp1Pk) (HL2) or mutant Pyp1^{C222S}Pk (HL8) expressing additional Tpx1 from the *S. pombe* expression vector (Rep1Tpx1) or the vector control (Rep1) before and after treatment with 0.2 mM H_2O_2 for the indicated times. Anti-Pk antibody was used to detect Pk-tagged Pyp1. All protein samples were treated with the thiol-binding agent AMS, prior to electrophoresis. The different bands are indicated and the molecular weight (MW) markers are shown.

Unfortunately, the absence of a suitable control antibody prevented us confirming that the reduction in Pyp1 protein levels when overexpressing Tpx1, following prolonged exposure to low (0.2 mM) concentrations of H_2O_2, was not due to uneven gel-loading or transfer. Therefore, these data suggest that Tpx1 promotes, and cysteine 222 inhibits, the aggregation and/or turnover of Pyp1 (Figure 3.11B).

3.2.6 The role of phosphorylated Pyp1 in H_2O_2-induced activation of Sty1

3.2.6.1 Pyp1 is phosphorylated in response to oxidative and osmotic stress

To investigate whether 'Modified Pyp1Pk' might be phosphorylation, which would increase molecular mass and reduce mobility, the effect of alkaline phosphatase on mobility was determined. In samples from wild-type (Pyp1Pk) cells treated with 1.0 mM H_2O_2, there is a mobility shift upwards, corresponding to an increase in molecular mass, and a subsequent modification of Pyp1 (Figure 3.12). However, in protein samples treated with alkaline phosphatase, there is a much smaller mobility shift in wild-type (Pyp1Pk) cells upon exposure to H_2O_2, suggesting that Pyp1 is basally phosphorylated, but undergoes further phosphorylation in response to H_2O_2. A similar pattern of mobility shifts following treatment with 1.0 mM H_2O_2 is observed in mutant Pyp1^{C470S}Pk cells compared to wild-type (Pyp1Pk), whereby there is a much smaller mobility shift in protein samples treated with alkaline phosphatase compared to the absence of alkaline phosphatase (Figure 3.12). This suggests that, as in wild-type cells, Pyp1^{C470S}Pk is basally phosphorylated, and that this phosphorylation is not affected by mutation of the catalytic cysteine residue.

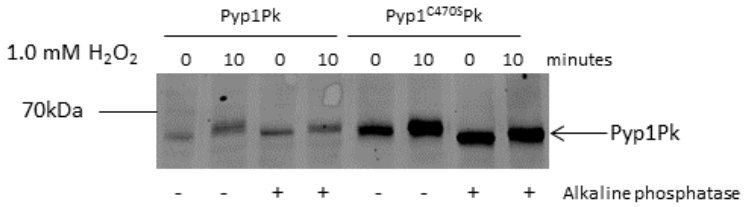

Figure 3.12 Pyp1 is basally phosphorylated, and undergoes further phosphorylation in response to H_2O_2. Western blot analysis of cells expressing Pk-epitope tagged wild-type Pyp1 (Pyp1Pk) (HL2) or mutant Pyp1^{C470S}Pk (HL3) before and after treatment for 10 minutes with 1.0 mM H_2O_2. Anti-Pk antibody was used to detect Pk-tagged Pyp1. Protein samples were treated with alkaline phosphatase, as indicated, prior to electrophoretic separation. The different bands are indicated and the molecular weight (MW) markers are shown.

3.2.6.2 The N-terminus of Pyp1 stabilises the H_2O_2-induced Pyp1-Trx1 disulphide, and is required for Pyp1 phosphorylation

It has been reported that *in vitro* phosphatase activity of Pyp1 is dependent on its N-terminal sequence as well as its catalytic domain (Hannig *et al.*, 1994). It has also been suggested that this region might contain a putative mitochondrial targeting sequence (MTS) (Holmes, 2013). Therefore, we investigated whether the N-terminal 30 amino acids and the single cysteine residue within this region, cysteine 20, were important for post-translational modification of Pyp1, or for Pyp1 function.

First we examined whether either of these mutations affected the post-translational modification of Pyp1. The Pyp1-Trx1 disulphide is a rapid, transient event in wild-type (Pyp1Pk) cells, detected 30 seconds after the addition of 1.0 mM H_2O_2, but not at 600 seconds. Similar to wild-type, both Pyp1^{C20S}Pk and NΔ30Pyp1Pk also formed Pyp1-Trx1 disulphides 30 seconds after exposure to 1.0 mM H_2O_2 (Figure 3.13A). However, these disulphides persisted longer in both mutants than in cells expressing wild-type Pyp1Pk (Figure 3.13B). Based on our previous observations regarding the kinetics of Pyp1-Trx1 disulphide formation and Pyp1 phosphorylation, we predicted that the persistence of the Pyp1-Trx1 disulphide in Pyp1^{C20S}Pk and NΔ30Pyp1Pk cells might block phosphorylation. Indeed, Pyp1-Trx1 disulphides were still detectable in Pyp1^{C20S}Pk and NΔ30Pyp1Pk cells 40 minutes after treatment with 1.0 mM H_2O_2, and no phosphorylated Pyp1^{C20S}Pk and NΔ30Pyp1Pk was detected under any conditions (Figure 3.13B). It was noted that the persistence of the Pyp1-Trx1 disulphide did not seem to protect Pyp1^{C20S}Pk from aggregation or degradation, observed when cells are treated with higher (6.0 mM) concentrations of H_2O_2 (Figure 3.13B).

The phosphorylated form of Pyp1 is absent in a strain lacking the first 30 amino acids at the N-terminus of Pyp1 (Figure 3.13A). To further confirm this post-translational modification is phosphorylation, protein samples from wild-type (Pyp1Pk) and Pyp1^{C470S}Pk, which can form phosphorylated Pyp1 (Figure 3.8A), and NΔ30Pyp1Pk, which cannot form phosphorylated Pyp1, were treated with alkaline phosphatase.

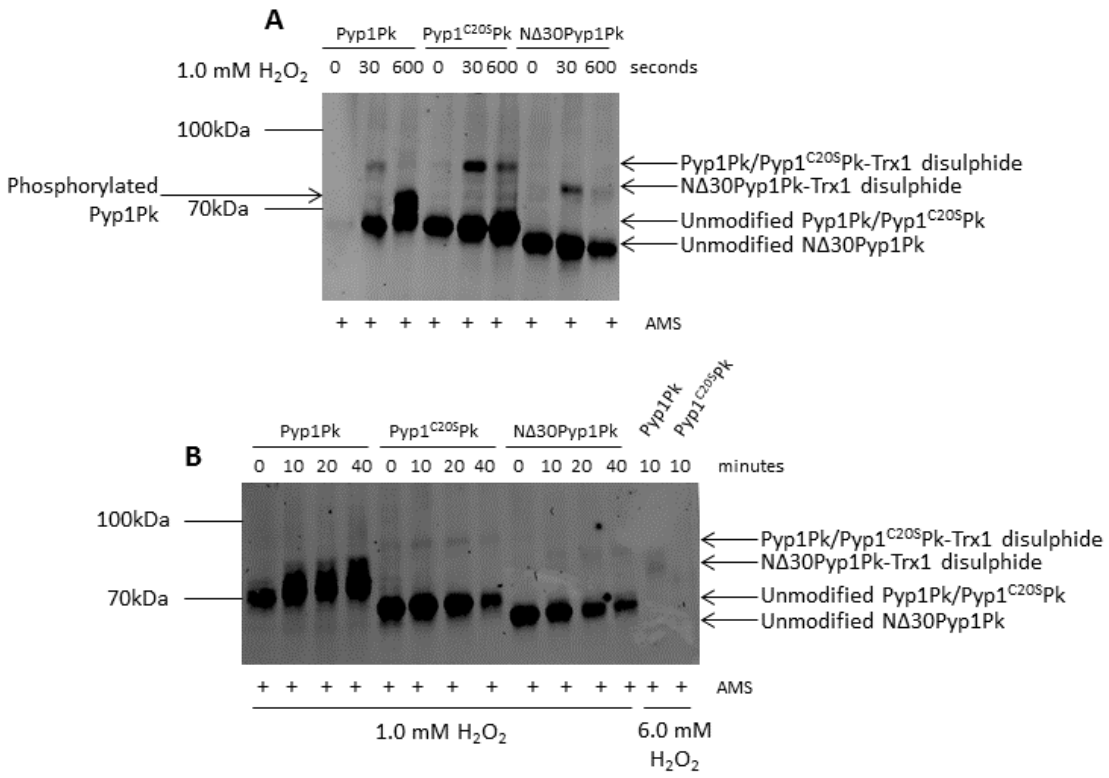

Figure 3.13 The disulphide bond which forms between Pyp1 and Trx1 following exposure to 1.0 mM H_2O_2 persists until 40 minutes in cells lacking cysteine 20. Western blot analysis of cells expressing Pk-epitope tagged wild-type Pyp1 (Pyp1Pk) (HL2) or mutant Pyp1^{C20S}Pk (HL10) and NΔ30Pyp1Pk (NJ1884) before and after treatment with (**A**) 1.0 mM or (**B**) 6.0 mM H_2O_2. Anti-Pk antibody was used to detect Pk-tagged Pyp1. All protein samples were treated with the thiol-binding agent AMS, prior to electrophoresis. The different bands are indicated and the molecular weight (MW) markers are shown.

As previously shown, there is a much smaller shift in protein samples treated with alkaline phosphatase compared to the absence of alkaline phosphatase, in both wild-type (Pyp1Pk) and Pyp1^{C470S}Pk (Figure 3.12), consistent with this shift being due to phosphorylation. However, in Figure 3.14, this mobility shift is less clear in wild-type (Pyp1Pk) and Pyp1^{C470S}Pk, in the presence or absence of alkaline phosphatase. Nevertheless, no mobility shift was detected in NΔ30Pyp1Pk cells following exposure to H_2O_2, either in the presence or absence of alkaline phosphatase (Figure 3.14), confirming that this post-translational modification of Pyp1 is phosphorylation, and indicating that the N-terminus of Pyp1 is required for basal phosphorylation of Pyp1.

3.2.6.3 The N-terminus of Pyp1, including cysteine 20, is important for H_2O_2-induced Sty1 activation

To test whether the N-terminal 30 amino acids or cysteine 20 were important for Pyp1 function, we examined how they affected basal and H_2O_2-induced activation of Sty1. Similar to mutant Δ*pyp1* cells, we found that there was high basal Sty1 activation in Pyp1^{C20S}Pk and NΔ30Pyp1Pk cells compared with wild-type (Pyp1Pk) (Figure 3.15A). This implies that the N-terminus of Pyp1 may be required for dephosphorylating Sty1 under normal conditions, however, unlike a Δ*pyp1*, we did not detect any decrease in the size of these cells. Although, again similar to a Δ*pyp1*, there was little induction upon treatment with 1.0 mM H_2O_2 (Figure 3.15A), there appeared to be some differences between the effects of these mutations and a Δ*pyp1* on the activation of Sty1 by osmotic stress. In wild-type (Pyp1PK) and cells lacking the N-terminal 30 amino acids, levels of Sty1 phosphorylation were increased following 10 minutes exposure to 0.6 M KCl and remained high at 20 minutes, whereas in a Δ*pyp1* and Pyp1^{C20S}Pk, Sty1 was maximally activated by 10 minutes, with levels returning to basal following 20 minutes (Figure 3.15B).

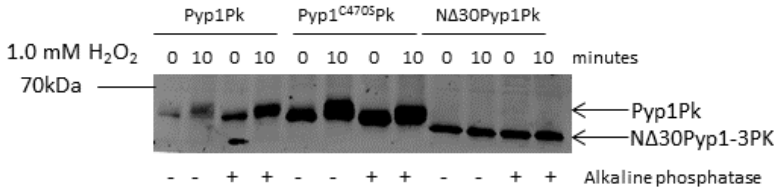

Figure 3.14 Pyp1 becomes phosphorylated in response to oxidative stress, dependent on the N-terminus of Pyp1. Western blot analysis of cells expressing Pk-epitope tagged wild-type Pyp1 (Pyp1Pk) (HL2), or mutant Pyp1^{C470S}Pk (HL3) and NΔ30Pyp1Pk (NJ1884) before and after treatment for 10 minutes with 1.0 mM H_2O_2. Anti-Pk antibody was used to detect Pk-tagged Pyp1. Protein samples were treated with alkaline phosphatase, as indicated, prior to electrophoretic separation. The different bands are indicated and the molecular weight (MW) markers are shown.

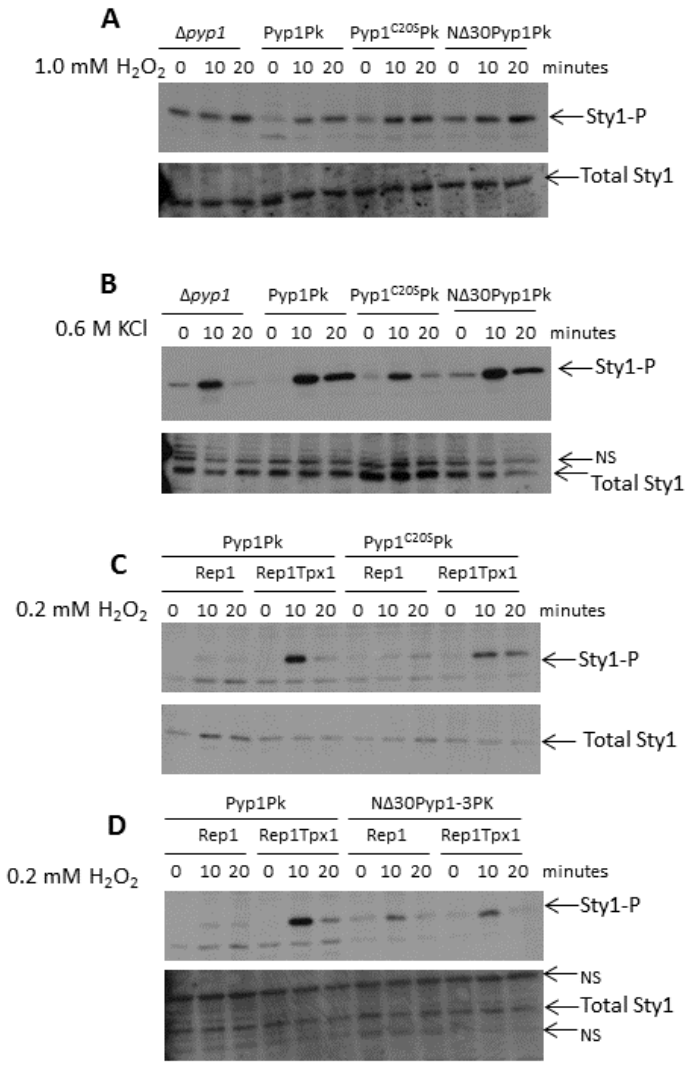

Figure 3.15 The N-terminus of Pyp1, including cysteine 20, is required for activation of Sty1 by H_2O_2, and for overexpression of Tpx1 to boost H_2O_2-induced Sty1 activation. Western blot analysis of levels of phosphorylated Sty1 in *S. pombe* Δ*pyp1* (NJ102) cells, and cells expressing Pk-epitope tagged wild-type Pyp1 (Pyp1Pk) (HL2) or mutant Pyp1^{C20S}pkC (HL10) and NΔ30Pyp1Pk (NJ1884) before and after treatment with (**A**) 1.0 mM H_2O_2 or (**B**) 0.6 M KCl. Western blot analysis of levels of phosphorylated Sty1 in cells expressing (**C**) Pk-epitope tagged wild-type Pyp1 (Pyp1Pk) (HL2) and Pyp1^{C20S}Pk (HL10), and (**D**) Pk-epitope tagged wild-type Pyp1 (Pyp1Pk) (HL2) and NΔ30Pyp1Pk (NJ1884) cells expressing additional Tpx1 from the *S. pombe* expression vector (Rep1Tpx1) or the vector control (Rep1) before and after treatment with 0.2 mM H_2O_2. Anti-pp38 and anti-Sty1 antibodies were used to detect phosphorylated Sty1 and total Sty1 levels, respectively. Non-specific (NS) bands are indicated.

Although Pyp1 is not required for increased Sty1 activation in response to osmotic stress, this result indicates a change in kinetics of Sty1 phosphorylation in response to osmotic stress in a Δ*pyp1*, Pyp1^{C20S}Pk and NΔ30Pyp1Pk, compared with wild-type (Pyp1Pk) (Figure 3.15B).

3.2.6.4 The N-terminus of Pyp1 is required for overexpression of Tpx1 to boost H_2O_2-induced Sty1 activation

As Pyp1^{C20S}Pk and NΔ30Pyp1Pk form stable disulphides with Trx1 but are not phosphorylated (Figure 3.13A), next we tested whether increased levels of Tpx1 still promoted H_2O_2-induced Sty1 activation in cells expressing these mutant forms of Pyp1. Overexpressing Tpx1 caused a much smaller boost in H_2O_2-induced Sty1 activation in Pyp1^{C20S}Pk after exposure to 0.2 mM H_2O_2 (Figure 3.15C), compared to wild-type (Pyp1Pk). In NΔ30Pyp1Pk cells, no increase in H_2O_2-induced Sty1 activation was detected in cells overexpressing Tpx1 compared to empty vector (Rep1) (Figure 3.15D). This suggests that the Tpx1-dependent boost in H_2O_2-induced Sty1 activation might require the N-terminus of Pyp1.

3.2.6.5 Effect of overexpression of Tpx1 on post-translational modification of Pyp1Pk or Pyp1^{C20S}Pk

These experiments identified that mutations in the N-terminus of Pyp1, and the single cysteine residue within this region, cysteine 20, have interesting effects on Pyp1 post-translational modifications and function; (i) preventing Pyp1 phosphorylation (Figure 3.13A), (ii) causing the Pyp1-Trx1 disulphide to persist for longer in response to 1.0 mM H_2O_2 (Figure 3.13B), and (iii) resulting in constitutively high levels of Sty1 phosphorylation (Figure 3.15A) that are barely increased by H_2O_2 and overexpression of Tpx1 (Figure 3.15C and 3.15D). We therefore investigated the role of Tpx1 on the post-translational modifications of Pyp1 in wild-type and mutant Pyp1^{C20S}Pk.

Similar to our observations with Pyp1^{C222S}Pk (Figure 3.11B), overexpression of Tpx1 in Pyp1^{C20S}Pk cells caused a laddering of bands, with the formation of higher molecular weight complexes by 10 minutes, and a dramatic reduction in Pyp1 levels by 20 minutes (Figure 3.16).

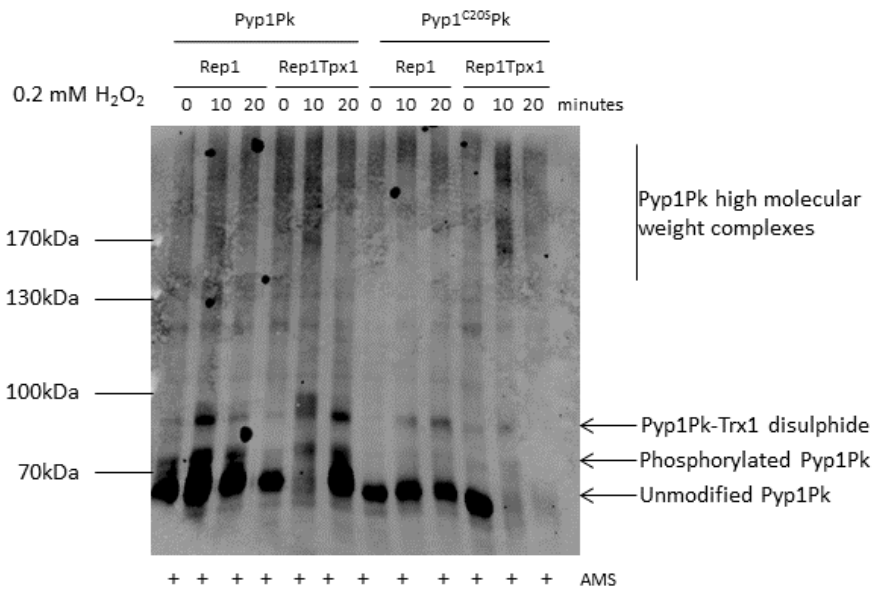

Figure 3.16 The effect of overexpression of Tpx1 on post-translational modification of Pyp1 or Pyp1^{C20S}. Western blot analysis of cells expressing Pk-epitope tagged wild-type Pyp1 (Pyp1Pk) (HL2) or mutant Pyp1^{C20S}pkC (HL10) expressing additional Tpx1 from the *S. pombe* expression vector (Rep1Tpx1) or the vector control (Rep1) before and after treatment with 0.2 mM H_2O_2 for the indicated times. Anti-Pk antibody was used to detect Pk-tagged Pyp1. All protein samples were treated with the thiol-binding agent AMS, prior to electrophoresis. The different bands are indicated and the molecular weight (MW) markers are shown.

The identity of the H_2O_2-induced higher molecular weight complexes is unclear but could be indicative of Pyp1 degradation intermediates, such as ubiquitinated forms, or Pyp1 multimers, suggesting that overexpressing Tpx1 causes Pyp1 to become degraded, by a mechanism that is inhibited by cysteine 20. However, although it appears that the Pyp1 protein levels are reduced when overexpressing Tpx1, following prolonged exposure to low (0.2 mM) concentrations of H_2O_2, this would need confirming through a loading control. Taken together with previous results, this suggests that overexpressing Tpx1 causes Pyp1 to be degraded in response to H_2O_2, and that this degradation is inhibited by two cysteine residues; cysteine 222, which is required for the formation of the Pyp1-Trx1 disulphide, and cysteine 20, which is required for phosphorylation of Pyp1.

3.2.6.6 Effect of the N-terminus of Pyp1 on cell growth and H_2O_2 resistance

In order to investigate whether the 30 amino acids at the N-terminus, or the single cysteine residue within this region, were important for Pyp1 function, cells were grown on control plates and plates containing various stress agents. When cells were grown in standard rich media and incubated at 30°C, no growth differences were observed between Pyp1^{C20S}Pk and NΔ30Pyp1Pk, and wild-type cells (Figure 3.17A). However, when cells were grown in minimal media and incubated at 30°C, NΔ30Pyp1Pk cells exhibited a reduced growth rate (Figure 3.17B), indicating a dominant negative effect of loss of the N-terminal 30 amino acids of Pyp1, specifically on minimal media.

Similar to mutant Δ*pyp1*, Pyp1^{C20S}Pk were more resistant than wild-type (Pyp1Pk) to higher H_2O_2 concentrations, and both Pyp1^{C20S}Pk and NΔ30Pyp1Pk were more resistant than wild-type (Pyp1Pk) to tBOOH (Figure 3.17B). It could be that the increased phosphorylation of Sty1 in a Δ*pyp1* is protective, and therefore, given that Sty1 phosphorylation is increased in Pyp1^{C20S}Pk and NΔ30Pyp1Pk (Figure 3.15A), perhaps it is not surprising that they are also hyper-resistant to high concentrations of H_2O_2. Interestingly, NΔ30Pyp1Pk cells were highly sensitive to $NaAsO_3$, and slow growing under normal growth conditions in minimal media at 30°C (Figure 3.17B).

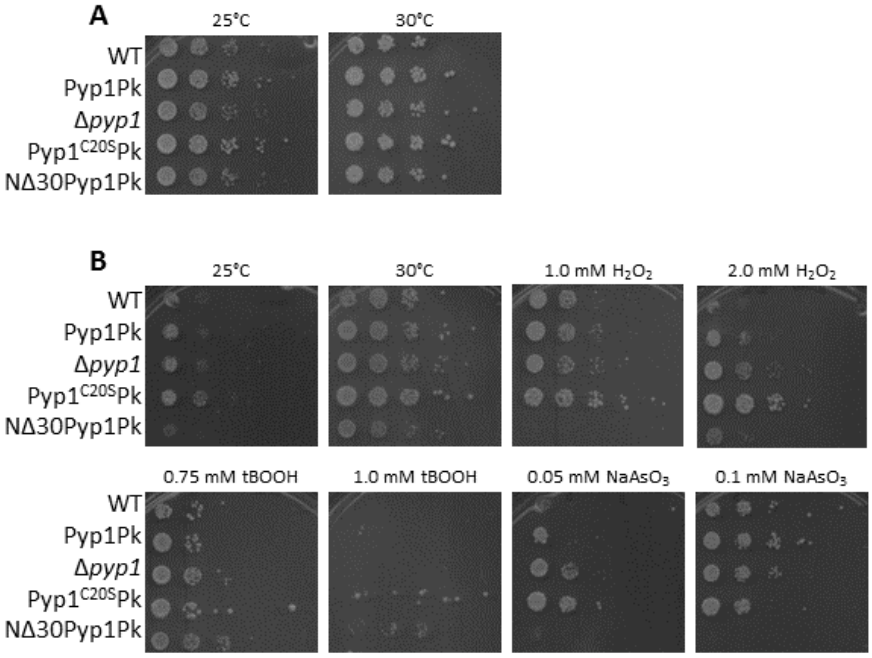

Figure 3.17 The effect of mutations in N terminus of Pyp1 on cell growth and stress resistance. Serial 10-fold dilutions of wild-type (NT4), Pk-epitope tagged wild-type Pyp1 (Pyp1Pk) (HL2), Δ*pyp1* (NJ102), mutant Pyp1^{C20S}Pk (HL10) and NΔ30Pyp1Pk (NJ1884) were spotted onto (**A**) YE5S agar plates for 3 days at 30°C, and (**B**) EMM agar plates containing the indicated stress agents, and incubated for 4-6 days at 30°C, unless otherwise stated.

3.2.6.7 Effect of mutations in Pyp1 that cause hyper-phosphorylation of Sty1 on localisation of Pyp1

Pyp1 has previously been reported to be a cytoplasmic protein (Millar *et al.*, 1995), however Pyp1 is also predicted to encode an N-terminal 29 amino acid MTS. Indeed, although the putative MTS is insufficient to target Pyp1 to the mitochondria (Holmes, 2013), Pyp1 has been shown to be present in both cytoplasmic and mitochondrial cell fractions, with a strong association with mitochondrial membranes (Holmes, 2013). Hence, indirect immunofluorescence using anti-Pk antibodies was used to determine whether any of the post-translational modifications of Pyp1 identified here might influence the intracellular localisation of Pyp1. Wild-type (NT4) cells were used as a control to distinguish specific fluorescence due to Pyp1Pk from any non-specific background fluorescence (Figure 3.18).

Under non-stressed conditions, wild-type Pyp1 (Pyp1Pk) displayed a punctate staining pattern throughout the cytoplasm, which becomes more punctate and excluded from the nucleus following 10 minutes exposure of cells to 1.0 mM H_2O_2 (Figure 3.18). A similar intracellular distribution was observed for Pyp1^{C340SC470S}Pk, which lacks the catalytic cysteine of Pyp1. In contrast, Pyp1^{C20S}Pk and NΔ30Pyp1Pk mutants showed a less punctate, more diffuse distribution throughout the cell under normal conditions and, following treatment with H_2O_2, both mutant proteins became subtly more excluded from the nucleus (Figure 3.18). This indicates that loss of the 30 amino acids at the N-terminus of Pyp1 has some effect on distribution of Pyp1, particularly following exposure to H_2O_2.

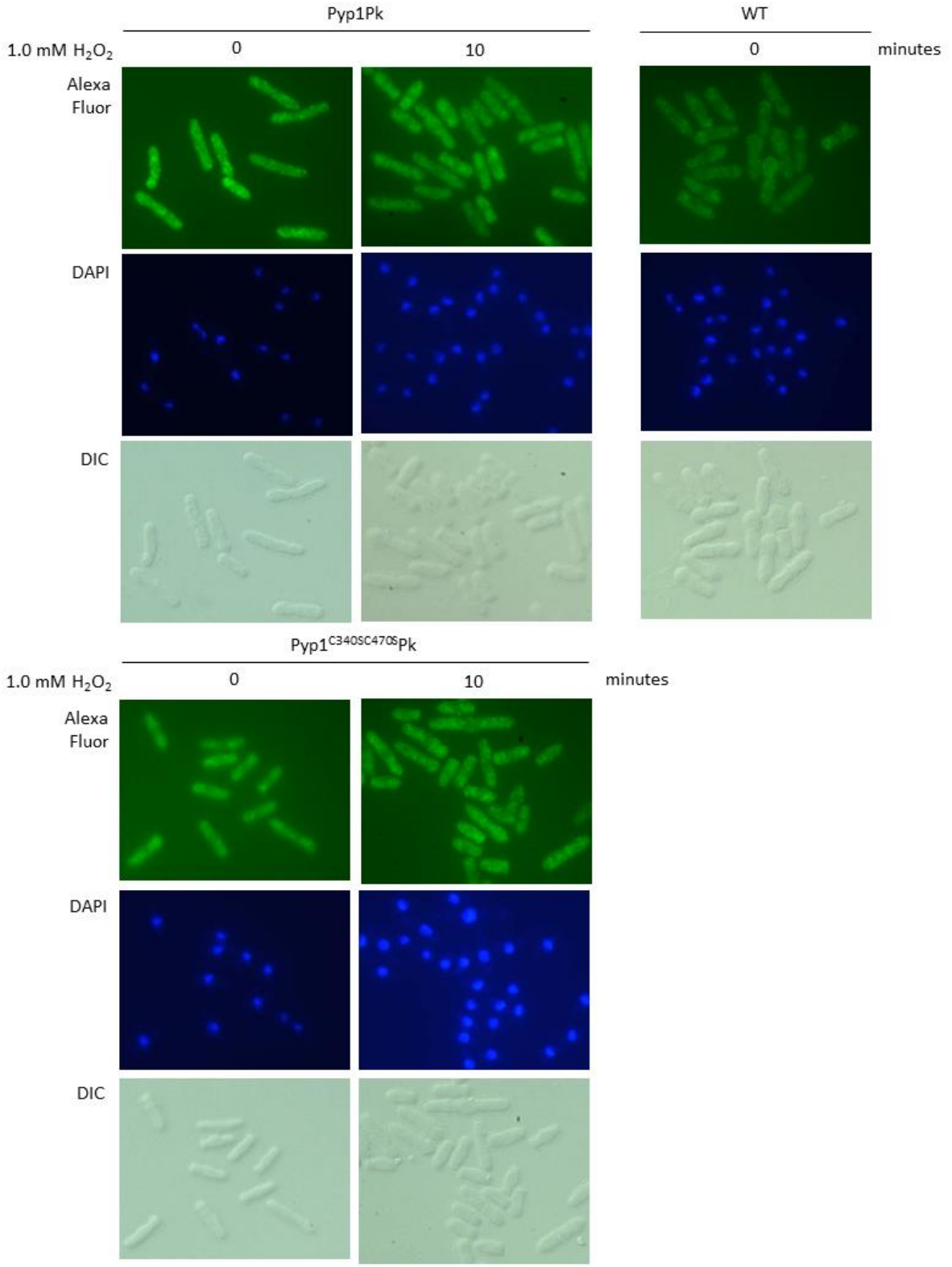
Pyp1Pk
WT
1.0 mM H_2O_2
0
10
0
minutes
Alexa Fluor
DAPI
DIC
$Pyp1^{C340SC470S}Pk$
1.0 mM H_2O_2
0
10
minutes
Alexa Fluor
DAPI
DIC

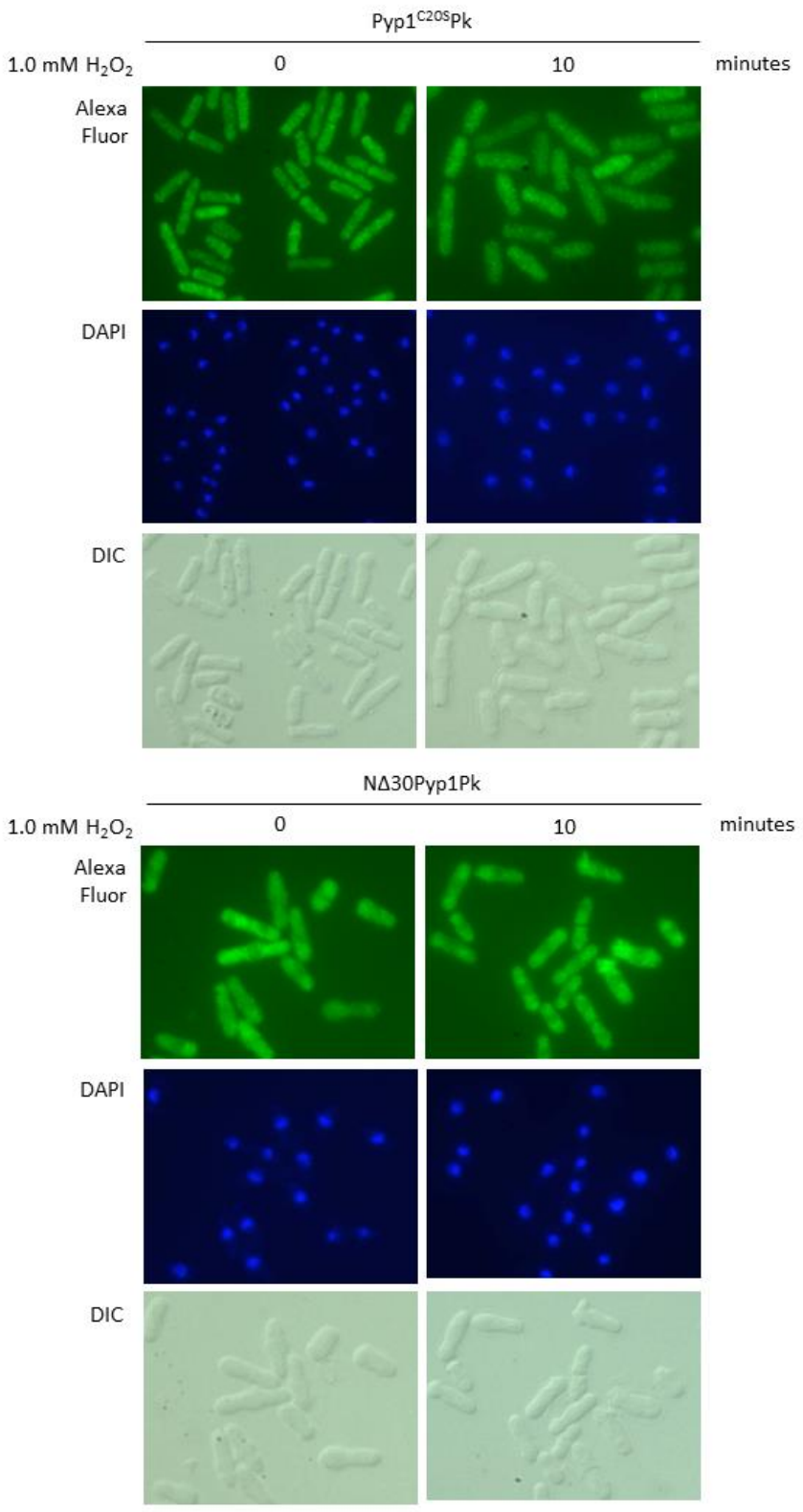

Figure 3.18 Pyp1 becomes excluded from the nucleus after treatment with H_2O_2 in cells lacking the first 30 amino acids at the N-terminus of Pyp1. The cellular distribution of Pk-epitope tagged Pyp1 was examined by indirect immunoflouresence using anti-Pk antibody, in wild-type (NT4), Pk-epitope tagged wild-type Pyp1 (Pyp1Pk) (HL2), mutant $Pyp1^{C340SC470S}$Pk (HL4), $Pyp1^{C20S}$Pk (HL10), and NΔ30Pyp1Pk (NJ1884) cells treated with 1.0 mM H_2O_2 for 0 and 10 minutes. Nuclei were visualised by staining with DAPI.

3.2.6.8 Effect of loss of the N-terminus and catalytic cysteine of Pyp1 on the interaction between Pyp1 and Sty1

The stress-induced phosphorylation of Pyp1, and constitutive phosphorylation of Pyp1 mutants lacking the catalytic cysteine (Figure 3.8A), suggested that Pyp1 might be phosphorylated by Sty1, which is active in both these conditions. Accordingly, it was possible that the lack of phosphorylation of NΔ30Pyp1Pk and Pyp1^{C20S}Pk mutants might reflect reduced interaction with Sty1. Indeed, the N-terminus of Pyp1 is predicted to be a MAPK-binding site (Kowalczyk *et al.*, 2013). Co-immunoprecipitation assays have been used to show weak interactions between phosphatases and their substrates, for example unpublished data from Yujun Di, University of Manchester, has shown an interaction between the MAPK Sty1 and the PP2C phosphatase Ptc4. However, previous work has shown that the interaction between Sty1 and the catalytic cysteine mutant Pyp1^{C470S} is dramatically increased in comparison to the interaction between wild-type Pyp1 and Sty1 (Shiozaki and Russell, 1995). We hypothesised that there would be a reduced interaction between Pyp1 and Sty1 in NΔ30Pyp1Pk compared to wild-type, due to loss of the N-terminus, and therefore loss of the predicted MAPK-binding domain.

Hence we tested whether the N-terminal 30 amino acids of Pyp1 were important for interaction with Sty1 by immunopurifiying Pk-epitope tagged wild-type, catalytically inactive mutant Pyp1^{C470S}Pk, and NΔ30Pyp1Pk, from cells before and following 10 minutes exposure to 1.0 mM H_2O_2. Comparisons of 1% input showed a striking increase in the levels of Pyp1^{C470S}Pk in cell lysate compared with either wild-type or NΔ30Pyp1Pk protein, which were expressed at similar levels (Figure 3.19A). Western blots were also stripped and re-probed with anti-Pk antibodies to confirm that Pk-epitope tagged Pyp1 proteins were effectively immunopurified. As expected, significantly more Sty1 was co-purified with Pyp1^{C470S}Pk than wild-type (Pyp1Pk) (Figure 3.19B) (Shiozaki and Russell, 1995). Indeed, Sty1 was also detected in immunoprecipitates from the untagged control wild-type (NT4), suggesting that a minimal amount of Sty1 was specifically co-purified with wild-type Pyp1. Moreover, slightly more Sty1 was co-

purified with NΔ30Pyp1Pk compared to wild-type (Pyp1Pk) suggesting that rather than disrupting this interaction, the mutant lacking the N-terminal 30 amino acids of Pyp1 might actually have a slightly stronger interaction with Sty1 (Figure 3.19B). However, the non-specific purification of Sty1 with anti-Pk agarose in lysate from the untagged wild-type (NT4) control made it difficult to make a firm conclusion as to whether loss of the N-terminus of Pyp1 affects the interaction between Pyp1 and Sty1, when the interaction with wild-type Pyp1Pk was so weakly detected.

Hence, a strain expressing the catalytically inactive mutant, C470S, was constructed in the NΔ30Pyp1Pk background, creating NΔ30Pyp1^{C470S}Pk, in order to test whether the N-terminus of Pyp1 was required for the strong interaction between Pyp1^{C470S}Pk and Sty1 (Figure 3.19B). Disappointingly, this experiment proved inconclusive in determining how the N-terminus of Pyp1 is involved in the interaction between Pyp1 and Sty1. Despite the immunopurification working well, the presence of a faint band representing Sty1 in the control Δ*sty1* lane of the immunopurifications (Figure 3.20B) meant that it was not possible to determine whether Sty1 co-purifies with Pyp1 that was immunopurified in this experiment. However, we did note that the levels of Pyp1 protein in NΔ30Pyp1^{C470S}Pk were extremely low, much lower than either NΔ30Pyp1Pk or wild-type Pyp1Pk, both in terms of soluble (Figure 3.20A and 3.20B) and total protein levels (Figure 3.20C). Given that there is much more Pyp1 protein in mutant Pyp1^{C470S}Pk compared to wild-type (Pyp1Pk) (Figure 3.19A and 3.19B), this suggests that the increase in Pyp1^{C470S}Pk levels is dependent on the N-terminus of Pyp1. This could indicate that phosphorylation of Pyp1 is important for the increased levels and stability of Pyp1^{C470S}Pk. However, this would require further investigation into the *pyp1*$^{+}$ mRNA and Pyp1 protein levels, to determine if it is the mRNA or protein stability which is being influenced by loss of the N-terminus of Pyp1.

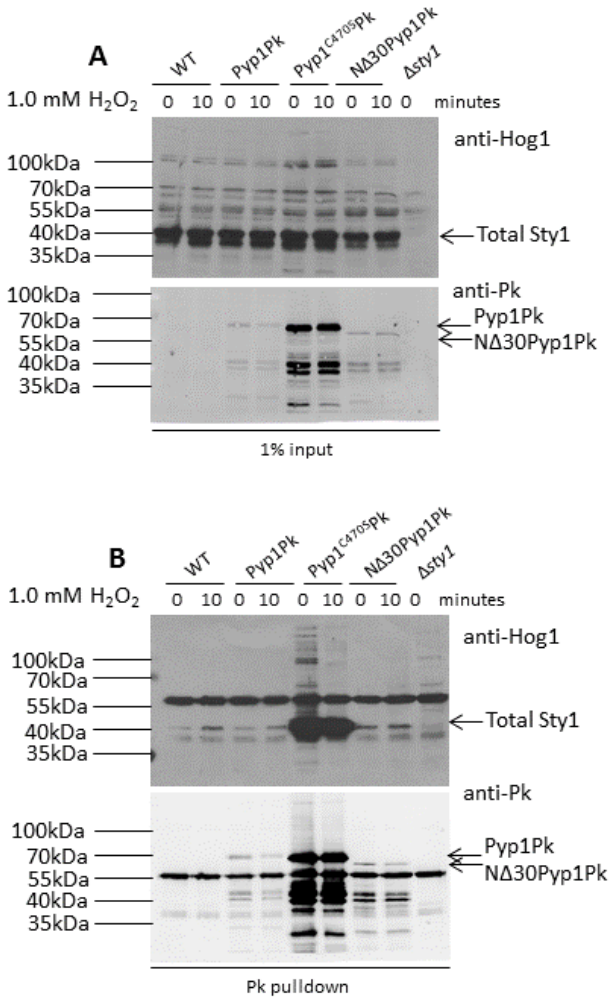

Figure 3.19 The effect of loss of the N-terminus and catalytic cysteine of Pyp1 on *in vivo* interaction with Sty1. Western blot analysis of (**A**) 1% input lysate, or (**B**) proteins immunopurified with anti-Pk conjugated agarose from *S. pombe* wild-type (NT4), Pk-epitope tagged wild-type Pyp1 (Pyp1Pk) (HL2) or mutant Pyp1^{C470S}Pk (HL3) and NΔ30Pyp1Pk (NJ1884), and Δ*sty1* (AD22) cells before and after treatment with 1.0 mM H_2O_2. Anti-Hog1 and anti-Pk antibodies were used to detect total Sty1 and Pk-tagged Pyp1, respectively. The different bands are indicated and the molecular weight (MW) markers are shown.

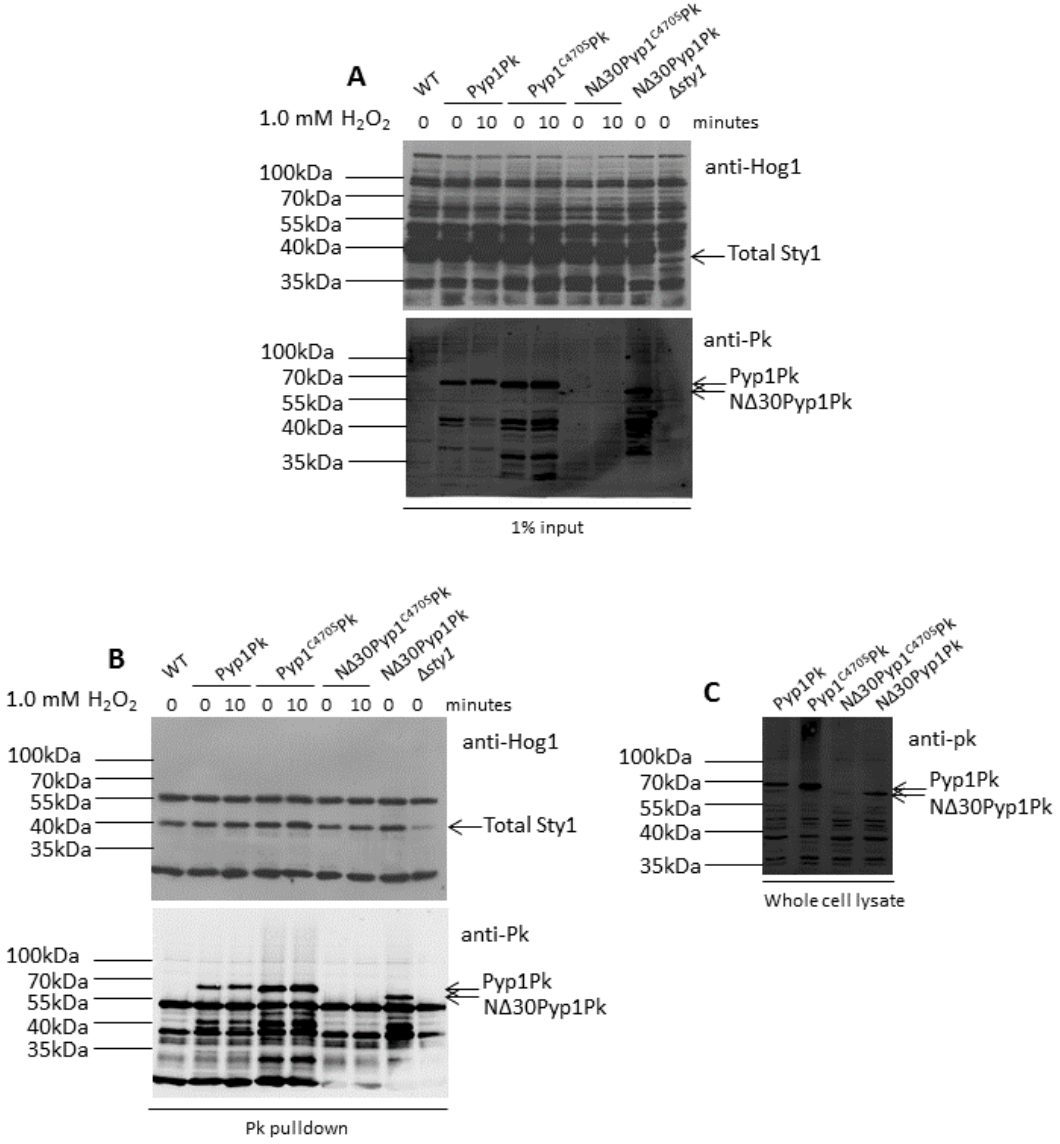

Figure 3.20 The increase in Pyp1^{C470S}Pk protein levels is dependent on the N-terminus of Pyp1. Western blot analysis of (**A**) 1% input lysate, or (**B**) proteins immunopurified with anti-Pk conjugated agarose from *S. pombe* wild-type (NT4), Pk-epitope tagged wild-type Pyp1 (Pyp1Pk) (HL2) or mutant Pyp1^{C470S}Pk (HL3), NΔ30Pyp1^{C470S}Pk (HL36) and NΔ30Pyp1Pk (NJ1884), and Δ*sty1* (AD22) cells before and after treatment with 1.0 mM H_2O_2. Anti-Hog1 and anti-Pk antibodies were used to detect total Sty1 and Pk-tagged Pyp1, respectively. The different bands are indicated and the molecular weight (MW) markers are shown. (**C**) Western blot analysis of Pk-tagged Pyp1 protein in *S. pombe* cells expressing Pk-epitope tagged wild-type Pyp1 (Pyp1Pk) (HL2) or mutant Pyp1^{C470S}Pk (HL3), NΔ30Pyp1^{C470S}Pk (HL36) and NΔ30Pyp1Pk (NJ1884). Anti-Pk antibody was used to detect Pk-tagged Pyp1. The different bands are indicated and the molecular weight (MW) markers are shown.

3.2.7 Pyp1 is phosphorylated on tyrosine 160 by Wis1

3.2.7.1 Pyp1 is phosphorylated by Wis1

Here we have identified that Pyp1 is phosphorylated under normal conditions but that this is increased in response to either oxidative or osmotic stress (Figure 3.4). The dependency of this phosphorylation on the N-terminal 30 amino acids, including cysteine 20, that are important for Pyp1 localisation and function (Figure 3.15A and 3.18), suggested that this phosphorylation might be important for regulating Pyp1 activity. Therefore, to investigate this further we set out to identify the kinase phosphorylating Pyp1, and the residue(s) involved. Interaction data from our collaborators at the University of Manchester (Dawson, Wilkinson and Jones) suggested that Pyp1 interacted with the MAPKK Wis1 (Figure 1.5). As the phosphorylation we observed was increased following stresses which activate Wis1, and hence Sty1, we hypothesised that Pyp1 might be a substrate for either activated Wis1 or Sty1. It is possible that Sty1 phosphorylates Pyp1, as Sty1 has been shown to phosphorylate Pyp2, promoting its stability (Kowalczyk *et al.*, 2013).

To test these possibilities, we examined the phosphorylation of Pyp1Pk strains in different backgrounds. As previously observed, Pyp1 was increasingly phosphorylated 10 minutes following exposure of wild-type cells to 1.0 mM H_2O_2 (Figure 3.21). Although there appears to be a slight reduction in overall Pyp1 protein levels in a Δ*wis1*, the absence of the stress-induced phosphorylated Pyp1 suggested that this phosphorylation was dependent on Wis1 (Figure 3.21). Double substitution of the residues which become phosphorylated on Wis1, serine 469 and threonine 473, to aspartic acid results in a constitutively partially active form of Wis1 and hence, increased phosphorylation of its substrate Sty1 (Shiozaki *et al.*, 1998). The constitutively high levels of phosphorylated Pyp1 in two $Wis1^{DD}$ mutant strains (Figure 3.21), in which Wis1 is partially active and resistant to further activation following stress, is consistent with the possibility that either Wis1 or Sty1 might be responsible for the phosphorylation of Pyp1.

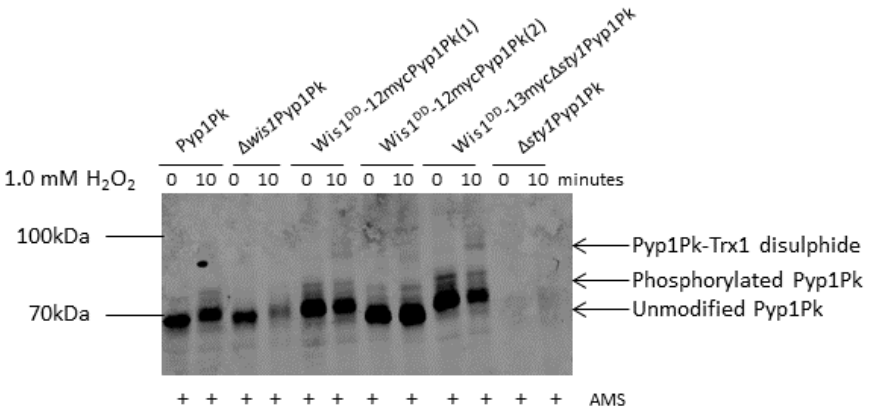

Figure 3.21 The effect of Wis1 and Sty1 on phosphorylation of Pyp1. Western blot analysis of cells expressing Pk-epitope tagged wild-type Pyp1 (Pyp1Pk) (NJ197), or mutant Δ*wis1*Pyp1Pk (NJ586), Wis1^{DD}-12mycPyp1Pk(1) (NJ1088), Wis1^{DD}-12mycPyp1Pk(2) (NJ1659), Wis1^{DD}-13mycΔ*sty1*Pyp1Pk (NJ1904), and Δ*sty1*Pyp1Pk (NJ209) before and after treatment with 1.0 mM H_2O_2. Anti-Pk antibody was used to detect Pk-tagged Pyp1. All protein samples were treated with the thiol-binding agent AMS, prior to electrophoresis. The different bands are indicated and the molecular weight (MW) markers are shown.

Strikingly, Pyp1Pk levels were severely reduced in a Δ*sty1* (Figure 3.21), suggesting that Pyp1 stability or expression is dramatically affected by loss of *sty1*$^{+}$. However, this reduction in Pyp1 levels was rescued in cells co-expressing Wis1^{DD}. Indeed, loss of *sty1*$^{+}$ caused no decrease in the phosphorylation of Pyp1 in a Wis1^{DD} mutant background, suggesting that low levels of Wis1 activity are sufficient for Pyp1 phosphorylation in the absence of Sty1. This suggests that Wis1 is able to phosphorylate Pyp1, independent of Sty1, but that Sty1 may be required for Pyp1 stability in cells where Wis1 is subject to MAPKKK-dependent activation.

3.2.7.2 The role of tyrosine 160 in Pyp1 phosphorylation and H_2O_2-induced Sty1 activation

Mass spectrometric analysis of immunopurified Pyp1 performed by our collaborators at the University of Manchester identified that tyrosine residues 160 and 337 in Pyp1 are phosphorylated. To test whether either tyrosine was important for the stress-induced phosphorylation of Pyp1 we examined the phosphorylation of mutants in which these tyrosine (Y) residues were substituted with phenylalanine (F), to block phosphorylation.

First, we investigated whether tyrosine 337, which is present in the active site of Pyp1, was required for the phosphorylation of Pyp1. A non-phosphorylatable mutant, Pyp1^{Y337F}Pk, supplied by our collaborators at the University of Manchester, was expressed at notably higher levels than an isogenic wild-type control Pyp1Pk, suggesting that this tyrosine does affect Pyp1 expression or protein stability (Figure 3.22). However, formation of the H_2O_2-induced Pyp1-Trx1 disulphide, and the phosphorylated Pyp1 were unaffected (Figure 3.22), indicating that the stress-induced phosphorylation of Pyp1 does not require tyrosine 337.

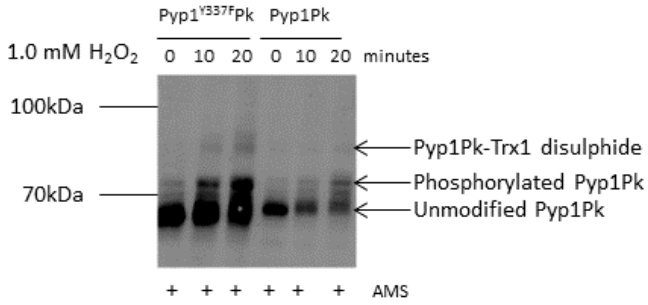

Figure 3.22 The effect of mutation of tyrosine 337 on Pyp1 phosphorylation. Western blot analysis of cells expressing Pk-epitope tagged mutant Pyp1^{Y337F}Pk (NJ1660) or wild-type Pyp1 (Pyp1Pk) (NJ197) before and after treatment with 1.0 mM H_2O_2. Anti-Pk antibody was used to detect Pk-tagged Pyp1. All protein samples were treated with the thiol-binding agent AMS, prior to electrophoresis. The different bands are indicated and the molecular weight (MW) markers are shown.

Next we tested whether tyrosine 160 was important for phosphorylation of Pyp1. Both phosphomimetic (Y160E) and non-phosphorylatable (Y160F) mutants were investigated to determine if they are still able to be phosphorylated. Similar to Pyp1^{Y337F}Pk, it was noted that both Pyp1^{Y160E}Pk and Pyp1^{Y160F}Pk were expressed at higher levels than the isogenic wild-type control Pyp1Pk (Figure 3.23A). In contrast to wild-type (Pyp1Pk) cells, where phosphorylated Pyp1 was detected 10 and 20 minutes following exposure to 1.0 mM H_2O_2, Pyp1^{Y160E}Pk was not phosphorylated (Figure 3.23A). However, Pyp1^{Y160F}Pk was phosphorylated (Figure 3.23A). Together these data suggest that tyrosine 160 is not the residue that is phosphorylated in response to stress, but that phosphorylation of tyrosine 160, here mimicked by Y160E, inhibits stress-induced phosphorylation of residue(s) elsewhere in Pyp1. We also noted increased levels of the H_2O_2-induced Pyp1-Trx1 disulphide in both Pyp1^{Y160E}Pk and Pyp1^{Y160F}Pk mutants (Figure 3.23A). This is reminiscent of our data with NΔ30Pyp1Pk and Pyp1^{C20S}Pk (Figure 3.13A), which also suggested that impaired phosphorylation increased the stability of Pyp1 Trx1 disulphides.

To determine if the effect of Y160E on phosphorylation of Pyp1 affected the function of Pyp1, we examined whether either Pyp1^{Y160E}Pk or Pyp1^{Y160F}Pk mutants affected Sty1 activation before and following treatment with 1.0 mM H_2O_2. In the phosphomimetic mutant, Pyp1^{Y160E}Pk, there was an increase in both basal and stress-induced levels of Sty1 phosphorylation compared to wild-type (Pyp1Pk), suggesting that the function of Pyp1 is impaired by this mutation (Figure 3.23B). In contrast, although there was a low basal level of Sty1 phosphorylation in cells expressing the non-phosphorylatable mutant, Pyp1^{Y160F}Pk, this was not increased in response to H_2O_2 (Figure 3.23B). Intriguingly, this suggests that Pyp1^{Y160F}Pk may be hyperactive towards Sty1, or could be due to the increased Pyp1 levels of this mutant (Figure 3.23A). Sty1 activity is important during normal growth as well as numerous stress conditions. Therefore, as a hyperactive mutant that inhibits Sty1 activation, there is likely to be a strong selection pressure against Pyp1^{Y160F}Pk.

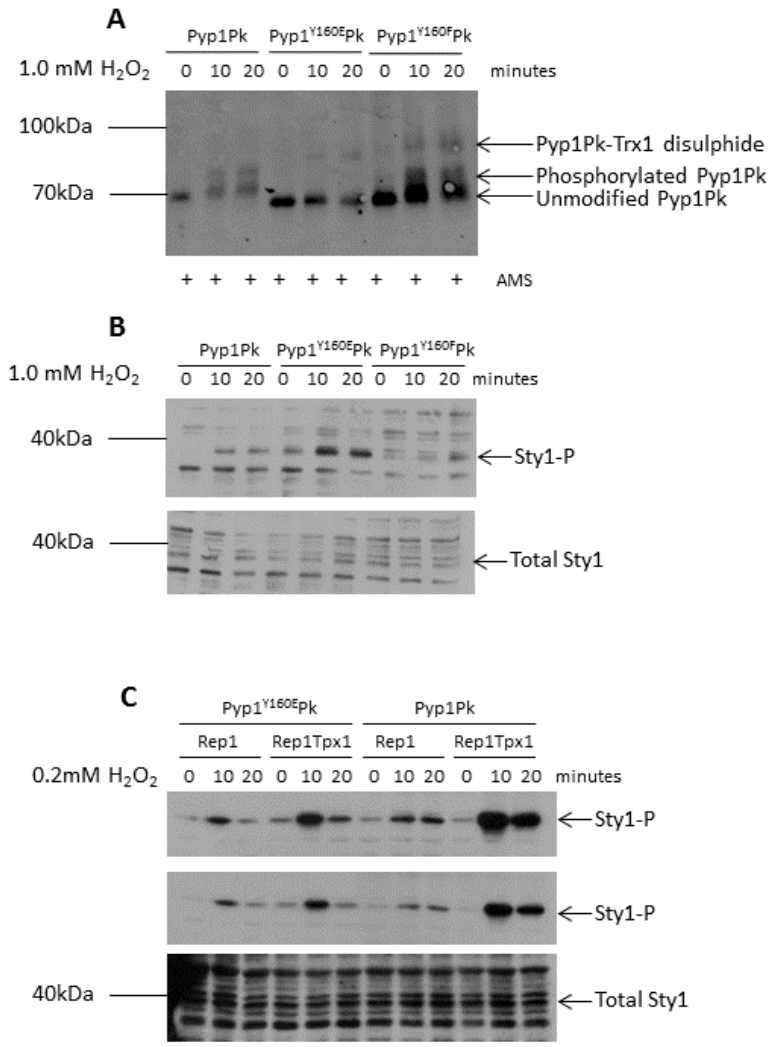

Figure 3.23 Tyrosine 160 of Pyp1 is basally phosphorylated, and the phosphomimetic mutation, Y160E, inhibits stress-induced phosphorylation by Wis1. (**A**) Western blot analysis of cells expressing Pk-epitope tagged wild-type Pyp1 (Pyp1Pk) (NJ197) or mutant Pyp1^{Y160E}Pk (HL34) and Pyp1^{Y160F}Pk (HL35) before and after treatment with 1.0 mM H_2O_2. Anti-Pk antibody was used to detect Pk-tagged Pyp1. All protein samples were treated with the thiol-binding agent AMS, prior to electrophoresis. The different bands are indicated and the molecular weight (MW) markers are shown. Western blot analysis of levels of phosphorylated Sty1 in cells expressing (**B**) Pk-epitope tagged wild-type Pyp1 (Pyp1Pk) (HL2) or mutant Pyp1^{Y160E}Pk (HL34) and Pyp1^{Y160F}Pk (HL35) before and after treatment with 1.0 mM H_2O_2, and (**C**) Pk-epitope tagged wild-type Pyp1 (Pyp1Pk) (HL2) and Pyp1^{Y160E}Pk (HL34) cells expressing additional Tpx1 from the *S. pombe* expression vector (Rep1Tpx1) or the vector control (Rep1) before and after treatment with 0.2 mM H_2O_2. Anti-pp38 and anti-Sty1 antibodies were used to detect phosphorylated Sty1 and total Sty1 levels, respectively.

Indeed, although numerous attempts were made to generate this Pyp1^{Y160F}Pk mutant strain, only one clone, when sequenced, was found to have retained the desired tyrosine-to-phenylalanine substitution. Consequently, cultures of this strain were routinely sequenced following the collection of pellets for experiments. Unfortunately, the Pyp1^{Y160F}Pk was found to revert back to the wild-type sequence on most occasions, making it impossible to study this mutant further.

Overexpressing Tpx1 produced a small increase in H_2O_2-induced levels of Sty1 phosphorylation in Pyp1^{Y160E}Pk compared to empty vector (Rep1), but this was less than the increase associated with overexpressing Tpx1 in wild-type (Pyp1Pk) cells (Figure 3.23C). This suggests that Y160E inhibits Pyp1 phosphorylation but also makes Sty1 more resistant to the effects of Tpx1, possibly by reducing Pyp1 activity (Figure 3.23B).

3.3 Discussion

Here we present data suggesting that Tpx1 promotes Sty1 activation by promoting the oxidation of Pyp1. Although Prx, such as Tpx1, have been shown to transduce H_2O_2 signals directly to H_2O_2-regulated proteins, we did not find any evidence that Tpx1 forms a disulphide with Pyp1. Instead, our data show that Pyp1 forms a H_2O_2-induced disulphide with Trx1 (Figure 3.3D). We have investigated the role of this H_2O_2-induced disulphide with Trx1, and other post-translational modifications of Pyp1, in regulating the activity of Sty1, with the properties of the Pyp1 cysteine mutants summarised in Table 3.1.

Table 3.1 Summary of the properties of Pyp1 cysteine mutants. A tick (✓) indicates the Pyp1 post-translational modification or H_2O_2-induced Sty1 activation can still occur in the Pyp1 cysteine mutant. A cross (X) indicates the Pyp1 post-translational modification or H_2O_2-induced Sty1 activation cannot occur in the Pyp1 cysteine mutant. A tick and a cross (✓X) indicates that overexpressing Tpx1 causes a smaller boost in H_2O_2-induced Sty1 activation in the Pyp1 cysteine mutant compared to wild-type (Pyp1Pk). A double tick (✓✓) indicates that overexpressing Tpx1 causes a greater boost in H_2O_2-induced Sty1 activation in the Pyp1 cysteine mutant compared to wild-type (Pyp1Pk).

Pyp1 cysteine mutant	Pyp1-Trx1 disulphide	Phosphorylated Pyp1	Sty1 activation	Tpx1 boosts Sty1 activation
Pyp1Pk	✓	✓	✓	✓
Pyp1^{C20S}Pk	✓	X	X	✓X
Pyp1^{C118S}Pk	✓	✓	✓	✓
Pyp1^{C222S}Pk	X	✓	✓	✓✓
Pyp1^{C340S}Pk	✓	✓	✓	✓
Pyp1^{C340SC470S}Pk	✓	✓	X	X
Pyp1^{C441S}Pk	✓	✓	✓	✓
Pyp1^{C470S}Pk	✓	✓	X	X
NΔ30Pyp1Pk	✓	X	X	X

The catalytic cysteine of Pyp1, cysteine 470, is required for the H_2O_2-induced activation of Sty1 (Figure 3.7A), and for overexpression of Tpx1 to boost H_2O_2-induced Sty1 activation (Figure 3.7B). However, given the likely sensitivity of the catalytic cysteine to oxidation, we were surprised to find that cysteine 470 is not involved in, or required for, the formation of the H_2O_2-induced Pyp1-Trx1 disulphide (Figure 3.8A). This is in contrast to previous research on PTP1B and PTEN; the catalytic cysteine of PTP1B forms a H_2O_2-induced disulphide with TRX1, detected at 0.2 mM H_2O_2 (Schwertassek *et al.*, 2014), whilst an intramolecular disulphide forms between the cysteine residue at the active site of PTEN and a nearby "backdoor" cysteine, to stabilise oxidised PTEN (Kwon *et al.*, 2004). We have identified that a conserved cysteine residue of Pyp1, cysteine 222, is important for the formation of the Pyp1-Trx1 disulphide (Figure 3.9A), and inhibits Tpx1 overexpression from increasing H_2O_2-induced Sty1 activation (Figure 3.10B). Additionally, although cysteine 222 of Pyp1 was important for the formation of H_2O_2-induced mixed disulphides with Trx1 at 1.0 mM H_2O_2, cysteine 222 was not required at 0.2 mM H_2O_2 (Figure 3.9B). This suggests that at different concentrations of H_2O_2, the disulphide between Pyp1 and Trx1 may involve different cysteine residues of Pyp1, or that the kinetics of disulphide formation are altered by substitution of cysteine 222. Our data suggests that Pyp1-Trx1 disulphide formation is important to maintain, rather than inhibit, Pyp1 activity.

Although the function of Pyp1-Trx1 disulphide formation remains unclear, our data suggest that formation of this disulphide may be important to maintain Pyp1 levels following exposure to H_2O_2. This suggests a possible mechanism by which overexpression of Tpx1 might inhibit Pyp1; one might predict that overexpression of Tpx1 would competitively inhibit Trx1 from forming a disulphide with Pyp1 (Day *et al.*, 2012). However, overexpression of Tpx1 did not cause any obvious change in the levels of Pyp1-Trx1 disulphides, but did result in the formation of high molecular weight (HMW) complexes following prolonged exposure to H_2O_2 (Figure 3.11B). Although the identity of these HMW complexes was not determined, they could be indicative of Pyp1 aggregates or degradation intermediates, for example, ubiquitinated forms or Pyp1 multimers. Previous studies into MAP kinase phosphatases (MKP) has shown that MKP-1 and MKP-5 undergo oxidation-induced oligomerisation,

reflecting inactivity (Kamata *et al.*, 2005). Following treatment with increasing concentrations of H_2O_2, MKP-1 and MKP-5 were present as HMW, β-mercaptoethanol-sensitive forms, suggesting they are MKP-1/-5 mixed disulphides (Kamata *et al.*, 2005). Parallels between the H_2O_2-induced HMW forms of Pyp1 and MKP-1/-5 may indicate that the HMW species observed when overexpressing Tpx1 are likely to represent Pyp1 disulphides. However, treatment of protein samples with β-mercaptoethanol would be needed to help confirm the identity of these HMW forms. Nevertheless, our data suggests that Tpx1 destabilises active Pyp1 and increases Sty1 activation by a mechanism that is inhibited by cysteine 222, which is important for normal levels of Pyp1-Trx1 disulphide formation. This is consistent with Tpx1 acting to inhibit Pyp1 by inhibiting Trx1's function in maintaining Pyp1 levels in cells exposed to low levels of H_2O_2 (Figure 3.11B).

Tpx1 promotes activation of Sty1 in response to low levels of H_2O_2 by regulating the oxidation of Pyp1, involving a rapid, transient H_2O_2-induced disulphide between Pyp1 and Trx1. The Tpx1-dependent boost in H_2O_2-induced Sty1 activation is dependent on the catalytic cysteine, cysteine 470, of Pyp1 (Figure 3.7B). Although formation of the H_2O_2-induced Pyp1-Trx1 disulphide did not require cysteine 470 (Figure 3.8A), formation of a more mobile 'Pyp1Pk^{ox}' form of Pyp1 was detected in wild-type (Pyp1Pk) cells, but absent in Pyp1^{C340SC470S}Pk (Figure 3.8B). This suggests that either of the two potential catalytic cysteine residues, cysteine 340 or cysteine 470, may be important for this oxidation. However, unlike formation of the Pyp1-Trx1 disulphide, formation of 'Pyp1Pk^{ox}' appears to be independent of Tpx1 (Figure 3.3C).

This chapter has provided evidence to suggest that the N-terminus of Pyp1, including a particular cysteine, cysteine 20, are important for Pyp1 phosphorylation (Figure 3.13A) and function (Figure 3.15A), However, both are also important for overexpression of Tpx1 to boost H_2O_2-induced Sty1 activation (Figure 3.15C and 3.15D). Notably, overexpression of Tpx1 causes Pyp1 to aggregate or become degraded in response to H_2O_2, by a mechanism that is inhibited by cysteine 20 (Figure 3.16). As cysteine 20 is required for phosphorylation of Pyp1, this suggests phosphorylation of Pyp1 inhibits

Pyp1 turnover or aggregation. Taken together with the data presented for cysteine 222 (Figure 3.11B), Tpx1 acts to inhibit Pyp1 by stimulating the formation of HMW Pyp1 species. In addition, Pyp1-Trx1 disulphide formation and phosphorylated Pyp1 protects Pyp1 from HMW formation (Figure 3.24). This may represent a mechanism whereby in the absence of phosphorylated Pyp1 in Pyp1^{C20S}Pk and NΔ30Pyp1Pk, Pyp1 is less active, therefore overexpressing Tpx1 has no further effect. We also attempted to investigate the effect of substituting both cysteine 222, required for the H_2O_2-induced Pyp1-Trx1 disulphide (Figure 3.9A), and cysteine 20, important for Pyp1 phosphorylation (Figure 3.13A) on Pyp1 activity and oxidation, however attempts to construct this strain were unsuccessful.

Notably, although Δ*pyp1* mutant cells are small, they double and form colonies at a relatively normal rate in both rich and minimal media. In contrast, NΔ30Pyp1Pk cells exhibited a reduced growth rate specifically on minimal media (Figure 3.17B). The explanation for this apparent dominant negative effect is unclear. It is unlikely that this effect is due to the lack of phosphorylation of NΔ30Pyp1Pk, as Pyp1^{C20S}Pk mutants, which also show impaired phosphorylation, grew normally. Although NΔ30Pyp1Pk is less effective at dephosphorylating Sty1 (Figure 3.15A), perhaps the absence of these N-terminal 30 amino acids means that NΔ30Pyp1Pk dephosphorylates an alternative substrate. Alternatively, minimal media does provide a more aerobic environment for cells to grow compared to standard rich media. Therefore, it is possible that as the N-terminus of Pyp1 is predicted to encode a weak putative MTS, the lack of this potential MTS could be responsible for the different growth rates dependent on the environment.

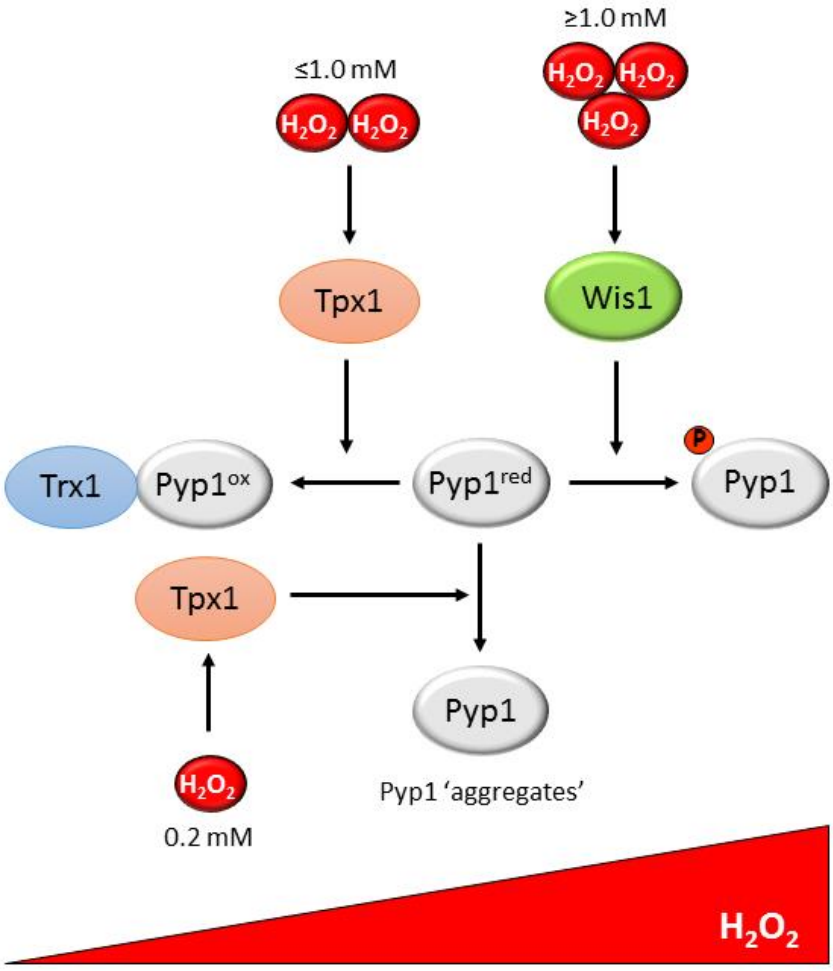

Figure 3.24 Model for the role of Tpx1 in regulating the post-translational modifications and stability of Pyp1. Pyp1 undergoes multiple post-translational modifications. Overexpression of Tpx1 promotes the oxidation of Pyp1 at lower (≤1.0 mM) concentrations of H_2O_2, through formation of disulphides with Trx1. Pyp1 is phosphorylated by the MAPKK Wis1 at higher (≥1.0 mM) concentrations of H_2O_2 and osmotic stress (not shown). Overexpression of Tpx1 stimulates Pyp1 multimerisation/degradation (Pyp1 'aggregates') at low (0.2 mM) concentrations of H_2O_2. It is not clear whether formation of the HMW Pyp1 'aggregates' is reversible, or if these are insoluble and degraded. We propose that reduced Pyp1 is the only form that is susceptible to formation of Pyp1 'aggregates', and that formation of a mixed disulphide with Trx1, or phosphorylation by Wis1, protects Pyp1 from aggregate formation.

Indeed, although it is not apparently required for association with mitochondria (Holmes, 2013), loss of the N-terminal 30 amino acids of Pyp1 does affect the intracellular distribution of Pyp1 (Figure 3.18). However, in the case of both Pyp1^{C20S}Pk and NΔ30Pyp1Pk, distribution was subtly altered compared to wild-type Pyp1Pk, particularly following treatment with H_2O_2 (Figure 3.18). Phosphorylated Sty1 is translocated to the nucleus after stress. Hence, perhaps the phosphorylation of Pyp1 is important for Pyp1 to be co-translocated to, or retained in, the nucleus. It is possible this is due to impaired interaction of these mutants with Sty1, although disappointingly, we were unable to test the effect of these mutations on the interaction between Sty1 and Pyp1. Alternatively, the persistence of Pyp1-Trx1 disulphides in mutant Pyp1^{C20S}Pk and NΔ30Pyp1Pk (Figure 3.13B) could be contributing to the nuclear exclusion. To further investigate this, intracellular localisation of Pyp1 before and following treatment with osmotic stress could be tested, as osmotic stress does not induce formation of Pyp1-Trx1 disulphides, but is able to induce phosphorylation of Pyp1 (Figure 3.4). Although the punctate Pyp1 immunostaining pattern could be attributed to a mitochondrial localisation, which is disrupted in Pyp1^{C20S}Pk and NΔ30Pyp1Pk, to further investigate whether Pyp1 is localised to the mitochondria, and whether mitochondrial localisation is dysregulated in Pyp1^{C20S}Pk and NΔ30Pyp1Pk, co-staining with a mitochondrial stain would need to be conducted. As the MTS is not sufficient for the mitochondrial localisation of Pyp1 (Holmes, 2013), this would suggest that lack of phosphorylated Pyp1 might be affecting intracellular localisation, rather than lack of the MTS.

This study suggests that Pyp1 is phosphorylated by the MAPKK Wis1 (Figure 3.21) in response to both oxidative and osmotic stress (Figure 3.4). Wis1 is activated by the high levels of H_2O_2 and osmotic stress that cause Pyp1 phosphorylation, and has been shown to form a complex with Pyp1, therefore it was quite plausible that Wis1 might phosphorylate Pyp1. Tyrosine 160 and tyrosine 334 of Pyp1 have both been shown to be phosphorylated through mass spectrometric analysis (Dawson, Wilkinson and Jones, University of Manchester). However, neither residue appears to be the site of stress-induced phosphorylation of Pyp1 (Figure 3.22 and 3.23A). However, when phosphorylation of tyrosine 160 is mimicked in Pyp1^{Y160E}Pk, our data suggest that this inhibits stress-induced phosphorylation of

residue(s) elsewhere in Pyp1 (Figure 3.23A). Pyp1 function was impaired in Pyp1^{Y160E}Pk, as judged by increased Sty1 phosphorylation in cells expressing this mutant (Figure 3.23B). Moreover, conversely, Pyp1^{Y160F}Pk was hyperactive towards Sty1 (Figure 3.23B), suggesting that phosphorylation of this tyrosine may be important to allow stable phosphorylation of Sty1. However, the residue in Pyp1 that is phosphorylated by Wis1 remains unknown. MAPKK phosphorylate both the threonine and tyrosine residues in the TXY motif, as exemplified by p38, which becomes phosphorylated at its TGY motif, and Sty1, which becomes phosphorylated by Wis1 on threonine 171 and tyrosine 173, also separated by a glycine residue (Shiozaki and Russell, 1995). Pyp1 contains three TXY motifs, one of which we observed is in the region with most similarity between Sty1 and Pyp1. This TXY motif corresponds to tyrosine 259 of Pyp1, and may represent a consensus site for Wis1-mediated phosphorylation. Therefore, to investigate if tyrosine 259 is a possible site that is phosphorylated by Wis1, and important for the stress-induced phosphorylation of Pyp1, a phenylalanine substitution mutant could be constructed and examined to see if this prevented stress-induced phosphorylation of Pyp1. However, it was noted that neither tyrosine 160 nor tyrosine 334 were present in a TXY motif, which may represent a Wis1 consensus phosphorylation site.

Although *in vitro* interaction/phosphorylation experiments with purified proteins would also be needed to establish that Wis1 directly phosphorylates Pyp1, our data suggesting that Wis1 phosphorylates Pyp1 supports interaction data from collaborators at the University of Manchester, reporting that Wis1 and Pyp1 are potential interactors (Figure 3.21). As the N-terminal 30 amino acids of Pyp1 and cysteine 20 are required for Pyp1 phosphorylation, this may indicate that interactions between Pyp1 and Wis1 are disrupted in Pyp1^{C20S}Pk and NΔ30Pyp1Pk, preventing Wis1 from phosphorylating these mutants. Although interactions between kinase and substrates are likely to be very transient, it is possible that in a partially constitutively active Wis1 mutant (Wis1^{DD}), which promotes the constitutive phosphorylation of Sty1 and Pyp1, the interactions between Pyp1 and Wis1 might be increased.

Based on the data in this chapter, we propose that increased Tpx1 stimulates increased H_2O_2-induced aggregation or degradation of Pyp1 (Figure 3.24) to promote activation of Sty1 in response to low concentrations of H_2O_2 in *S. pombe*. We have also identified that Pyp1 is regulated by multiple post-translational modifications, to regulate the activity of Sty1. However, our analysis of how these modifications affect Sty1 activation, using mutants in Pyp1 or Wis1, is likely to be complicated by the presence of other phosphatases, in particular Pyp2, that also dephosphorylates Sty1 and is essential to prevent lethal hyperactivity of Sty1 in the absence of Pyp1. For instance, it is possible that the levels of Pyp2 may be affected by some of the mutations under study in this chapter. In the next chapter, we have investigated the relationship between Pyp1, Pyp2 and a third related PTP, Pyp3, in the regulation of Sty1.

CHAPTER 4

4. The relationship between related protein tyrosine phosphatases in regulating Sty1

4.1 Introduction

The mitogen activated protein kinase (MAPK), Sty1, in *Schizosaccharomyces pombe* is required for control of mitosis under normal growth conditions, and is also activated in response to a variety of external stresses, activating transcriptional responses which allow homeostasis to be restored (Degols *et al.*, 1996). Increased Sty1 activity leads to accelerated cell division, whilst loss of *sty1*$^{+}$ causes a delayed entry into mitosis. Therefore, regulation of Sty1 activity is important for normal control of cell growth (Millar *et al.*, 1995; Shiozaki and Russell, 1995; Shiozaki *et al.*, 1998). In addition to Pyp1, dephosphorylation of Sty1 is catalysed by Pyp2 (Millar *et al.*, 1992; Millar *et al.*, 1995). TOR (target of rapamycin) signalling, involved in nutrient sensing, is also able to modulate the onset of mitosis through negatively regulating Pyp2, which in turn enhances Sty1 activity, promoting mitotic commitment (Petersen and Nurse, 2007; Hartmuth and Petersen, 2009).

H_2O_2-induced oxidation of cysteine thiols in protein tyrosine phosphatases (PTP) has been established as an integral part of signal transduction (For reviews see (Rhee *et al.*, 2000; Rhee *et al.*, 2003)). Moreover, work in the previous chapter has provided evidence that multiple post-translational modifications regulate Pyp1 in *S. pombe*, consequently regulating the activity of Sty1. However, Pyp2 has also been shown to be subject to both transcriptional and translational regulation. For instance, in response to heat stress, Pyp2 was recently found to become phosphorylated by Sty1 on two residues, serine 234 and threonine 279, in its linker region, not conserved in Pyp1 (Kowalczyk *et al.*, 2013) (Figure 4.1).

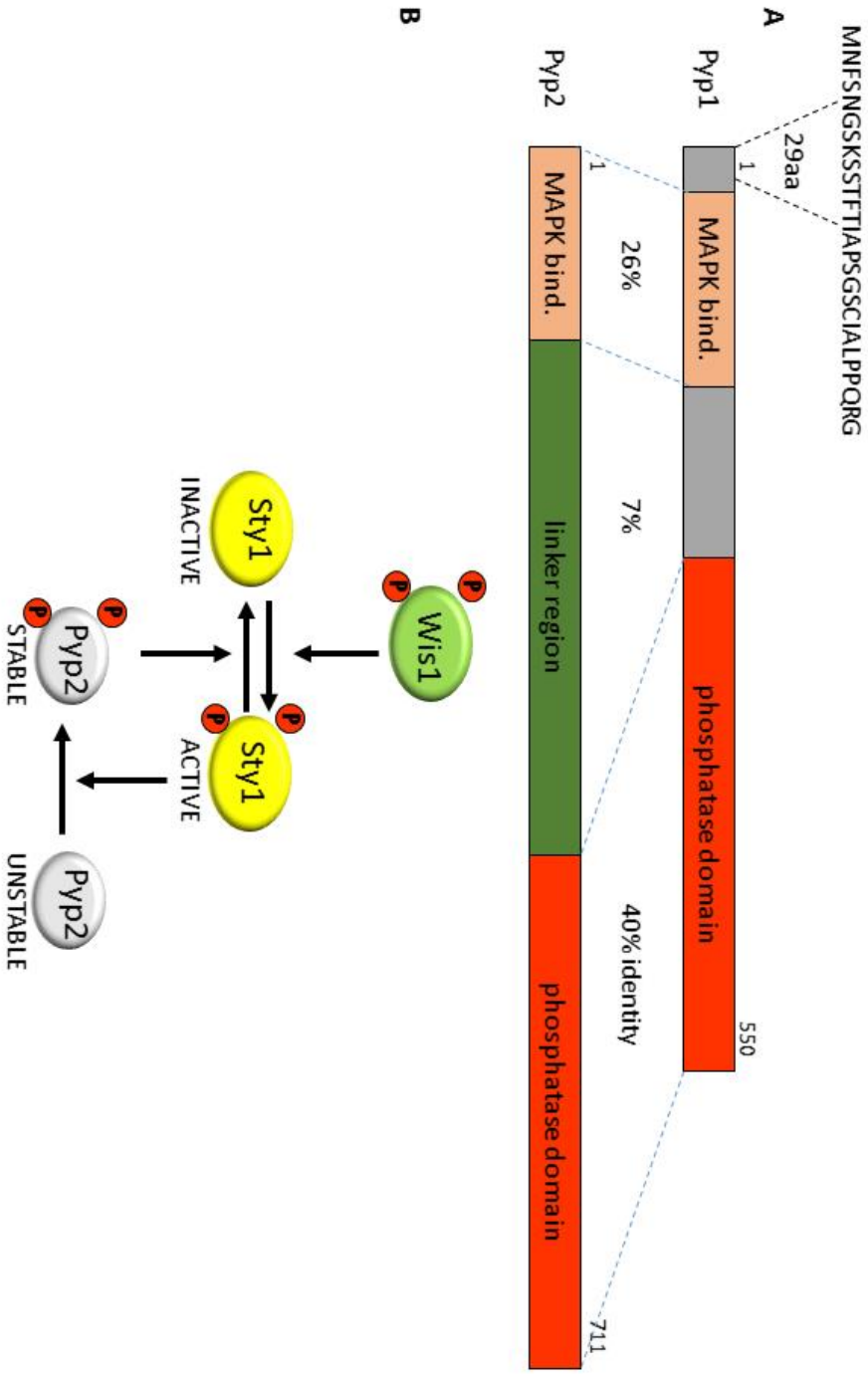

Figure 4.1 Self-regulatory control of Sty1 activity in *S. pombe* through phosphorylation of residues in the linker region of Pyp2. (**A**) A schematic of the Pyp1 and Pyp2 protein structures. A high degree of homology exists between the N-terminal MAPK-binding site and the C-terminal catalytic domains in the protein sequences of Pyp1 and Pyp2. Pyp2 contains an additional region of ~270 amino acids linking the N- and C-termini, which is absent in Pyp1. This Pyp2-specific domain was termed the linker region. Pyp1 is predicted by Mitoprot to encode a 29 amino acid mitochondrial targeting sequence (MTS). (**B**) Increased Sty1 activity, due to increased flow through the MAPK pathway, will promote Pyp2 phosphorylation and protein stability. Pyp2 becomes phosphorylated on serine 234 and threonine 279 in the linker region, which is not conserved in Pyp1, promoting Pyp2 protein stability. Increased Pyp2 will dephosphorylate Sty1, and return its activity back to steady state levels. 'ACTIVE' and 'INACTIVE' refer to the Sty1 MAPK activity. 'STABLE' and 'UNSTABLE' refer to the stability of Pyp2 protein (Adapted from Kowalczyk *et al.*, 2013).

This phosphorylation creates a negative feedback loop to tightly control Sty1 activity, whereby Sty1-dependent phosphorylation of the linker region in Pyp2 increased the stability of Pyp2, thus leading to increased dephosphorylation of Sty1 (Kowalczyk *et al.*, 2013) (Figure 4.1).

Pyp1 and Pyp2 share ~40% identity in their C-terminal catalytic domain, with weak homology in their N-terminal regions (Millar *et al.*, 1992) (Figure 4.1 and 4.2), and share an overlapping function to dephosphorylate Sty1. A third cytosolic PTP, Pyp3, related to human PTP1B and *S. pombe* Pyp1 and Pyp2 (Charbonneau *et al.*, 1989; Ottilie *et al.*, 1991; Millar *et al.*, 1992) is responsible for dephosphorylating and activating the $p34^{cdc2}$ kinase during the cell cycle, inducing mitosis (Millar *et al.*, 1992). This is in opposition to Pyp1 and Pyp2, which function to negatively regulate mitotic entry by dephosphorylating Sty1 that is required for progression from G_2 into mitosis (Millar *et al.*, 1992). Sequence alignment of Pyp3 with Pyp1 and Pyp2 in *S. pombe* reveals that all 3 phosphatases show significant homology in their C-terminal catalytic domains, however Pyp3 is much smaller and does not possess a long N-terminal region (Figure 4.2) Nevertheless, although the only known role for Pyp3 is in promoting mitotic entry, it is possible that there is some additional overlap with the function of Pyp1 and Pyp2 in regulating Sty1.

Protein tyrosine phosphatases all utilise catalytic cysteines and might therefore be predicted to be regulated in response to H_2O_2. Despite their overlapping activities in regulating Sty1, Pyp2 has been shown to be the more tightly regulated phosphatase (Petersen and Nurse, 2007; Hartmuth and Petersen, 2009). In the previous chapter we have established that Pyp1 is also subject to regulation by stress-induced phosphorylation and to regulation by formation of a mixed disulphide with Trx1. We have used specific Pyp1 mutants to investigate the function of these post-translational modifications of Pyp1 in regulating cell growth and stress resistance. However, as hyperactivation of p38 related MAPK can be lethal under normal growth conditions (Millar *et al.*, 1992), both $pyp2^{+}$ and $pyp3^{+}$ gene expression is increased in response to H_2O_2 (Chen *et al.*, 2003).

Figure 4.2 Sequence alignment of protein tyrosine phosphatases Pyp1, Pyp2 and Pyp3 from *Schizosaccharomyces pombe*. The amino acid sequence of *S. pombe* Pyp1 (SPAC26F1.10c), Pyp2 (SPAC19D5.01) and Pyp3 (SPAC11E3.09) were aligned using ClustalO. An asterisk (*) indicates positions which have a single, fully conserved residue. A colon (:) indicates conservation between groups of strongly similar properties. A full stop (.) indicates conservation between groups of weakly similar properties.

We were aware that it was possible that in Pyp1 mutants, where Sty1 activity is increased, there might also be increases in levels of Pyp2 and Pyp3 that could influence the activity of Sty1, and cell division. Therefore, the aim of this chapter was to investigate the relationship between these PTP in control of Sty1 activation, and determine how mutations in Pyp1 affect levels of Pyp2.

4.2 Results

4.2.1 The relative levels of Pyp1, Pyp2 and Pyp3

To allow comparison of the relative levels of the three PTP in *S. pombe*, strains were constructed expressing Pyp1, Pyp2 or Pyp3, with a Pk-epitope tag at their C-termini (see section 2.2.5.3). Pyp2 levels are low in unstressed cells, with Pyp2 expression being enhanced through a Sty1/Atf1 feedback loop in response to most environmental stresses (Wilkinson *et al.*, 1996). Quantitative proteomics analysis identified that, whilst there are 574.47 Pyp1 protein molecules/proliferating cells, both Pyp2 and Pyp3 were undetectable in unstressed conditions (Marguerat *et al.*, 2012). Consistent with this, Pyp2Pk was barely detected under normal growth conditions (Figure 4.3). However, Pyp3Pk was expressed at levels close to those of Pyp1Pk (Figure 4.3).

Previous studies have established that *pyp2*$^{+}$ and *pyp3*$^{+}$ mRNA levels are increased in response to H_2O_2 (Chen *et al.*, 2003). Moreover, Pyp2 protein is stabilised by stress-induced phosphorylation as part of a negative feedback loop to downregulate Sty1 activity (Kowalczyk *et al.*, 2013). We wanted to investigate whether all three PTP were expressed at similar levels under normal growth conditions, and whether the levels of Pyp2 and Pyp3 were induced by H_2O_2 as predicted from transcriptome analysis (Chen *et al.*, 2003) and other studies (Kowalczyk *et al.*, 2013). Therefore, we examined changes in the relative levels of the Pk-tagged Pyp1, Pyp2 and Pyp3 following exposure of cells to 1.0 mM H_2O_2 over a 60 minute time course.

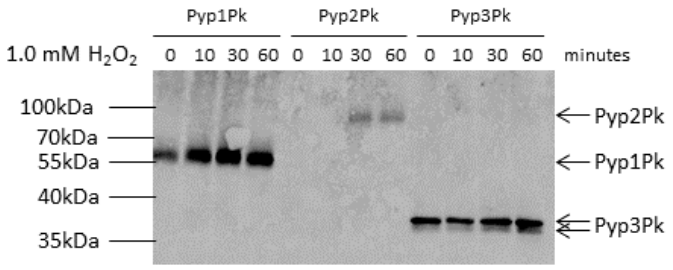

Figure 4.3 The relative levels of the phosphatases, Pyp1Pk, Pyp2Pk and Pyp3Pk. Western blot analysis of cells expressing Pk-epitope tagged wild-type Pyp1 (Pyp1Pk) (HL23), Pyp2 (Pyp2Pk) (HL24), and Pyp3 (Pyp3Pk) (HL25) before and after treatment with 1.0 mM H_2O_2. Anti-Pk antibody was used to detect Pk-tagged Pyp1, Pyp2 and Pyp3. The different bands are indicated and the molecular weight (MW) markers are shown.

There was an increase in total Pyp1Pk protein levels 10 minutes after treatment with 1.0 mM H_2O_2, with Pyp1Pk protein levels remaining fairly constant up to 60 minutes following exposure to H_2O_2 (Figure 4.3). Pyp2Pk was undetectable in unstressed cells and at 10 minutes following treatment with 1.0 mM H_2O_2, however by 30 and 60 minutes, levels of Pyp2Pk protein levels were increased (Figure 4.3). This is in agreement with previous work that has revealed that *pyp2*$^+$ mRNA is induced following stress and that Pyp2 protein becomes stabilised upon treatment with H_2O_2 (Kowalczyk *et al.*, 2013). In contrast, Pyp3Pk was detectable prior to stress, present as two bands, with no increase in the levels of Pyp3Pk protein following exposure to H_2O_2 (Figure 4.3). Although this analysis would need to be repeated with loading controls before any firm conclusions could be made, this suggests that the levels of Pyp1 and Pyp3 are higher than Pyp2 under normal growth conditions, and that all three phosphatases are increased following exposure to H_2O_2.

4.2.2 Pyp2 is less sensitive to H_2O_2-induced inactivation than Pyp1

As Pyp3 shares less homology to Pyp1 and Pyp2 (Figure 4.2), and has not been reported to influence the levels of Sty1 phosphorylation, we focussed our analysis on Pyp2. First we tested whether Pyp2 was oxidised in response to H_2O_2. For this experiment, we utilised myc-epitope tagged Pyp2 strains, which were constructed with the 3'-UTR (3'-untranslated region) of Pyp2 which is important for mRNA stability and translation efficiency. Protein samples were treated with the thiol-binding agent, AMS, to increase the protein molecular mass by 0.6 kDa per reduced cysteine. The absence of a band in untagged wild-type (NT4) control with anti-myc antibodies confirmed that the detected bands represented myc-epitope tagged Pyp2 (Figure 4.4A). When the mobility of myc-epitope tagged wild-type Pyp2 (Pyp2myc) following treatment with AMS was examined, we found no evidence to support the oxidation of Pyp2myc (Figure 4.4A), such as the formation of a Pyp2-Trx1 disulphide bond, or an increase in AMS-resistance. We did observe a slight shift in mobility between 30 and 600 seconds at 0.2 mM and 1.0 mM H_2O_2. However, as this shift was also seen in samples treated with NEM, which has a minimal effect on protein mobility (0.125 kDa per reduced cysteine), this suggests it is not an

oxidation event, and more likely a change in phosphorylation as has been previously reported (Kowalczyk *et al.*, 2013). Although it is possible that differences in detected levels of Pyp2myc may reflect differences in proteins loading, we noted that there was an increase in Pyp2myc levels in response to low (0.2 mM and 1.0 mM) concentrations of H_2O_2, where levels of Pyp2myc increased slightly at 600 seconds, but that at higher (6.0 mM) concentrations of H_2O_2, Pyp2myc protein levels appeared to be reduced (Figure 4.4A).

Pyp2 contains a destabilisation domain which becomes phosphorylated on critical residues, increasing Pyp2 protein stability (Kowalczyk *et al.*, 2013) (Figure 4.1). This 'linker' domain is not present in Pyp1, leading us to propose whether perhaps it protects Pyp2 from oxidation. Hence we examined whether a Pyp2 linker-free (LF) mutant protein, lacking this linker region, was susceptible to oxidation in cells exposed to H_2O_2. As for wild-type Pyp2 (Pyp2myc), there was no evidence to support oxidation of myc-epitope tagged linker-free Pyp2 (Pyp2.LFmyc) following treatment with varying concentrations of H_2O_2 (Figure 4.4B). However, there was no shift in mobility of Pyp2.LFmyc in response to low (0.2 mM and 1.0 mM) concentrations of H_2O_2, with either of the thiol-binding agents, NEM or AMS, consistent with the reduced mobility of wild-type Pyp2 being due to phosphorylation of residues in the linker domain, as previously reported (Kowalczyk *et al.*, 2013). Indeed, as observed previously, there was no increase in Pyp2.LFmyc levels following exposure to low concentrations of H_2O_2, and a more dramatic reduction in Pyp2.LFmyc protein levels after exposure to 6.0 mM H_2O_2.

4.2.3 Pyp2myc protein levels are increased in Mcs4^{D412N} but not in a Δ*pyp1*, however *pyp2*$^{+}$ mRNA levels are not elevated in either of these mutants

A multistep phosphorelay system, involving two histidine kinases, Mak2 and Mak3, a phosphorelay protein Mpr1, and a response regulator Mcs4, regulates activation of the Sty1 MAPK pathway in response to oxidative stress (Nguyen *et al.*, 2000; Buck *et al.*, 2001) (Figure 1.5).

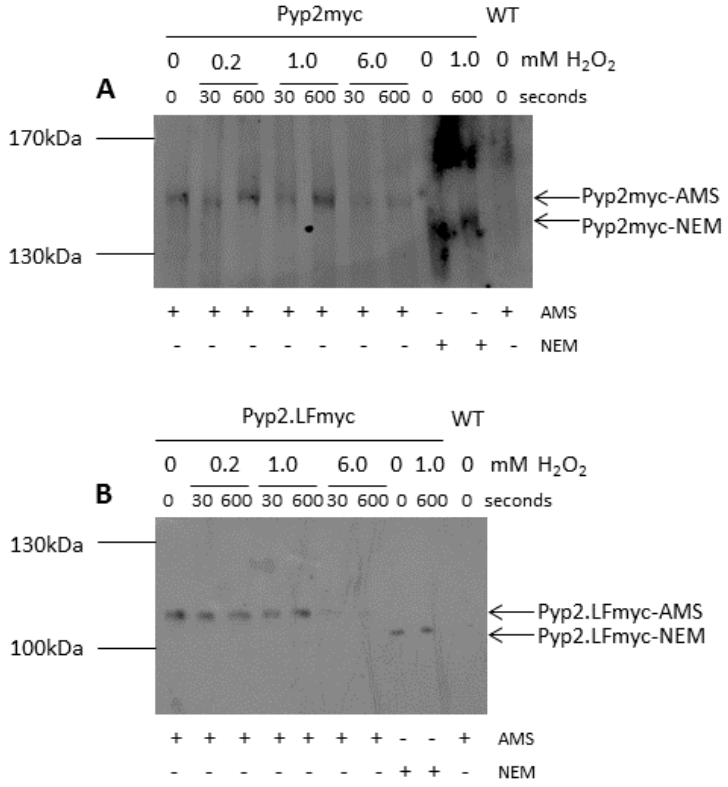

Figure 4.4 The effect of H_2O_2 on the oxidation state of Pyp2myc and Pyp2.LFmyc. Western blot analysis of cells expressing (**A**) myc-epitope tagged wild-type Pyp2 (Pyp2myc) (JP392) or wild-type (NT4) cells, and (**B**) myc-epitope tagged linker-free Pyp2 (Pyp2.LFmyc) (JP959) or wild-type (NT4) cells, before and after treatment with varying concentrations of H_2O_2. Anti-myc antibody was used to detect myc-tagged Pyp2. Proteins were treated with the thiol-binding agents, NEM or AMS, as indicated, prior to electrophoresis. The different bands are indicated and the molecular weight (MW) markers are shown.

Mutation of an aspartic acid residue at position 412 of Mcs4 to a non-phosphorylatable asparagine is predicted to prevent phosphorelay and has been shown to inhibit H_2O_2-induced increases in Sty1 phosphorylation (Buck *et al.*, 2001). Mcs4^{D412N} cells have higher basal Sty1 phosphorylation than wild-type cells, suggesting that the dephosphorylated form of Mcs4 is active (Buck *et al.*, 2001). Accordingly, as Pyp2 expression increases when Sty1 is active, due to both increased transcriptional activation by Atf1 and *pyp2*$^{+}$ mRNA stability, we proposed that Pyp2 levels would be increased in Mcs4^{D412N} cells, and this might be responsible for the lack of H_2O_2-inducibility of Sty1 in Mcs4^{D412N} cells. To support this hypothesis, there was considerably more Pyp2myc in Mcs4^{D412N}Pyp2myc cells compared to wild-type (Pyp2myc) (Figure 4.5A), suggesting that high basal Sty1 activation in Mcs4^{D412N} cells increases the expression of Sty1/Atf1-dependent genes, including *pyp2*$^{+}$.

As Mcs4^{D412N}Pyp2myc cells contained increased Pyp2myc levels compared to the isogenic wild-type (Pyp2myc) (Figure 4.5A), and our data suggested that Pyp2myc might be more resistant to H_2O_2-induced oxidation than Pyp1 (Figure 4.4A), we predicted that loss of Pyp2 might restore H_2O_2-inducible activation of Sty1 to Mcs4^{D412N} cells. To test this hypothesis, we examined Sty1 activation in Mcs4^{D412N}Δ*pyp2* cells. As expected, there was a dramatic increase in the level of phosphorylated Sty1 in wild-type (972) and Δ*pyp2* cells following exposure to 1.0 mM H_2O_2, whereas there was a much smaller increase in Sty1 phosphorylation in Mcs4^{D412N} cells (Figure 4.5B). However, loss of *pyp2*$^{+}$ did not restore Sty1 phosphorylation to Mcs4^{D412N}, suggesting that although Pyp2myc levels are greatly increased in Mcs4^{D412N} cells, these elevated levels are not responsible for the impaired H_2O_2-induced increases in Sty1 phosphorylation in Mcs4^{D412N}. This is consistent with regulation of Mcs4 by two component signalling being important for H_2O_2-induced activation of the MAPKKK Wak1 and Win1, as previously proposed (Nguyen *et al.*, 2000; Buck *et al.*, 2001; Morigasaki *et al.*, 2008).

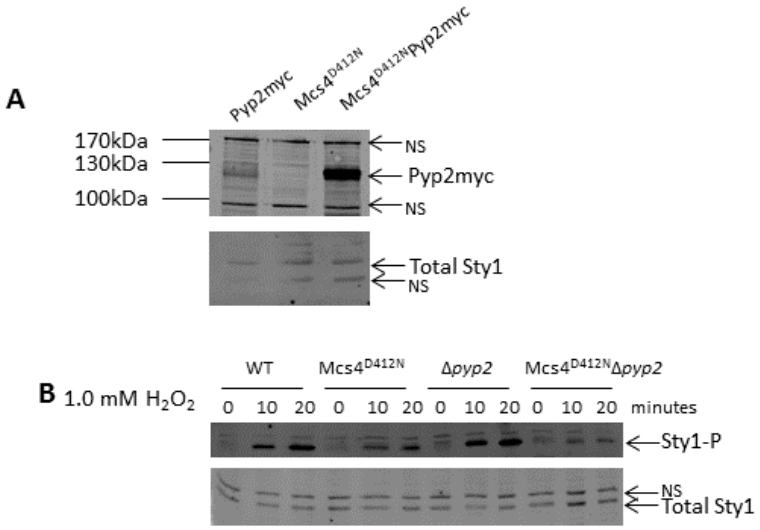

Figure 4.5 Pyp2myc levels are increased in Mcs4^{D412N}, but these high levels of Pyp2 are not responsible for the impaired H_2O_2-inducibilty of Sty1 in an Mcs4^{D412N}. (**A**) Western blot analysis of cells expressing myc-epitope tagged wild-type Pyp2 (Pyp2myc) (JP392), Mcs4^{D412N} (VB1692) and Mcs4^{D412N}Pyp2myc (HL14). Anti-myc and anti-Sty1 antibodies were used to detect myc-tagged Pyp2 and total Sty1 levels, respectively. (**B**) Western blot analysis of levels of phosphorylated Sty1 in wild-type (972), Mcs4^{D412N} (VB1692), Δ*pyp2* (HL11) and Mcs4^{D412N}Δ*pyp2* (HL13) cells before and after treatment with 1.0 mM H_2O_2. Anti-pp38 and anti-Sty1 antibodies were used to detect phosphorylated Sty1 and total Sty1 levels, respectively. The different bands are indicated and the molecular weight (MW) markers are shown. Non-specific (NS) bands are indicated.

Nevertheless, as Sty1 is also hyper-phosphorylated in a Δ*pyp1*, similar to Mcs4^{D412N}, we proposed that Pyp2 levels may also be increased in a Δ*pyp1*, to act as a compensatory mechanism for loss of Pyp1 activity. Indeed, a Δ*pyp1*Δ*pyp2* strain is inviable (Millar *et al.*, 1992), suggesting that Pyp2 is vital to limit Sty1 phosphorylation in the absence of *pyp1*$^{+}$. Hence, we tested whether in Δ*pyp1* mutant cells, in which Sty1 is hyperactive, there might be a compensatory increase in Pyp2 protein levels. However, to our surprise, despite increased basal Sty1 activation in a Δ*pyp1*, there was no increase in the levels of Pyp2myc protein in a Δ*pyp1* mutant strain compared to the isogenic wild-type (Pyp2myc) control strain (Figure 4.6). Indeed, contrary to our prediction and observations with Mcs4^{D412N} (Figure 4.5A), there was actually substantially less Pyp2myc in a Δ*pyp1* mutant than wild-type cells (Figure 4.6, compare lane 2 with lanes 1 and 5).

Next we set out to determine why the levels of Pyp2myc were lower in a Δ*pyp1*. First we examined how loss of Pyp1 affected the levels of *pyp2*$^{+}$ mRNA. The levels of *leu1*$^{+}$ were used as a loading control to allow a fold induction to be normalised relative to wild-type (NT4) cells under normal growth conditions. As expected, there was an increase in *pyp2*$^{+}$ mRNA, and mRNA for a second Atf1-dependent gene, *gpx1*$^{+}$, in wild-type (NT4) cells treated with 1.0 mM H_2O_2, that increases Sty1 phosphorylation, and subsequently Atf1 levels and *pyp2*$^{+}$ and *gpx1*$^{+}$ expression (Figure 4.7). The absence of the induced band in a Δ*pyp2* confirmed that this band represented *pyp2*$^{+}$ mRNA (Figure 4.7). As both Δ*pyp1* and Mcs4^{D412N} mutant cells have elevated basal levels of Sty1 phosphorylation, it would be expected that this would also be reflected in high basal Atf1 activity and hence *pyp2*$^{+}$ gene expression.

Although as expected, the *pyp2myc*$^{+}$ mRNA transcript was larger than *pyp2*$^{+}$ mRNA, given that it also encodes 13 copies of the myc-epitope, the levels of these mRNA were similar in the three wild-type strains (Figure 4.7 and 4.8A); untagged wild-type (NT4), Pk-epitope tagged wild-type Pyp1 (Pyp1Pk), and myc-epitope tagged wild-type Pyp2 (Pyp2myc).

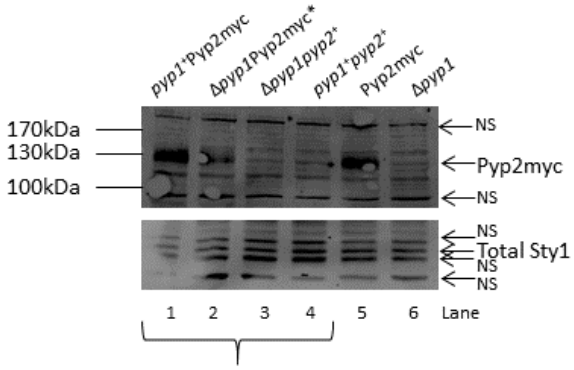

Figure 4.6 Loss of *pyp1*$^{+}$ reduces levels of Pyp2myc. Lanes 1-4 (in the bracket) correspond to the four spores generated by crossing myc-epitope tagged wild-type Pyp2 (Pyp2myc) (HL12) with a Δ*pyp1* (NJ102), to generate a Δ*pyp1*Pyp2myc strain (HL21) (lane 2, indicated by an asterisk (*)). Western blot analysis of cells expressing myc-epitope tagged wild-type Pyp2 (Pyp2myc) (JP392), Δ*pyp1* (NJ102) and Δ*pyp1*Pyp2myc (HL21). Anti-myc and anti-Sty1 antibodies were used to detect myc-tagged Pyp2 and total Sty1 levels, respectively. The different bands are indicated and the molecular weight (MW) markers are shown. Non-specific (NS) bands are indicated.

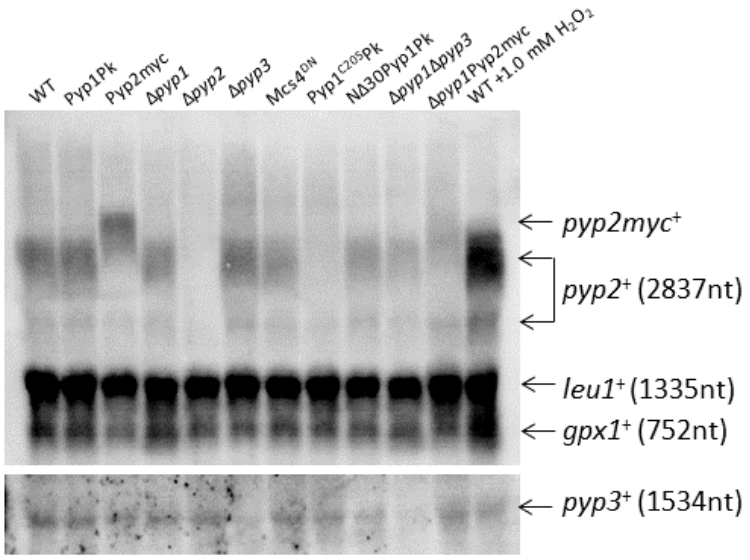

Figure 4.7 The effect of mutations in Mcs4, Pyp1, Pyp2 and Pyp3 on levels of *pyp2*$^+$, *pyp3*$^+$ and *gpx1*$^+$ mRNA. Northern blot analysis of RNA isolated from *S. pombe* wild-type (NT4), Pk-epitope tagged wild-type Pyp1 (Pyp1Pk) (HL2), myc-epitope tagged wild-type Pyp2 (Pyp2myc) (JP392), Δ*pyp1* (NJ102), Δ*pyp2* (JP279), Δ*pyp3* (EV60), Mcs4^{D412N} (VB1692), Pyp1^{C20S}Pk (HL10), NΔ30Pyp1Pk (NJ1884), Δ*pyp1*Δ*pyp3* (HL19), Δ*pyp1*Pyp2myc (HL21), and wild-type (NT4) following treatment with 1.0 mM H_2O_2 for 20 minutes. RNA samples were analysed on the same membrane, using probes specific for *pyp2*$^+$, *pyp3*$^+$, *gpx1*$^+$ and *leu1*$^+$ (loading control) genes. The expected mRNA sizes are shown in brackets.

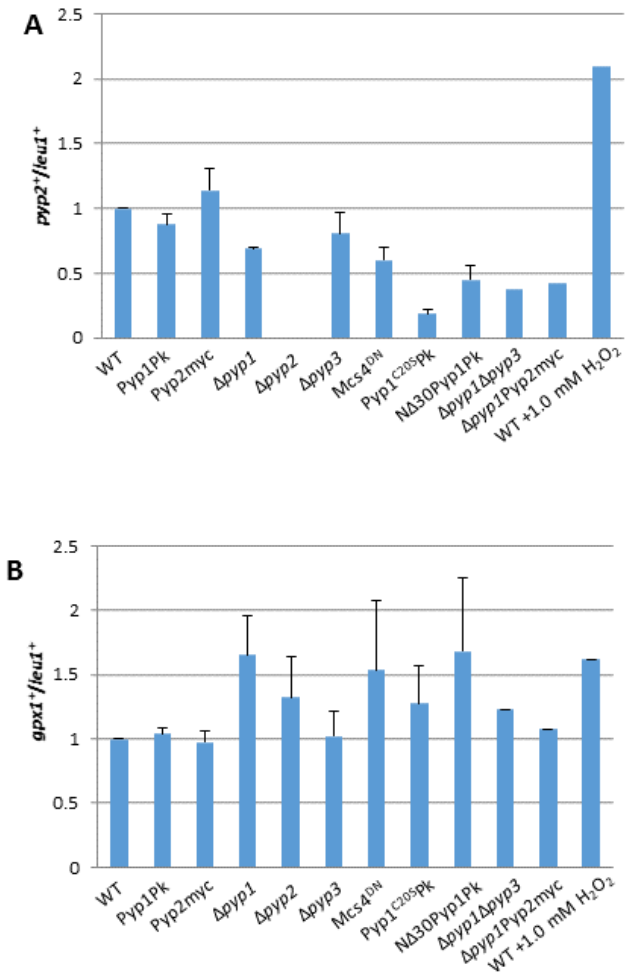

Figure 4.8 Quantification of the effect of mutations in Mcs4, Pyp1, Pyp2 and Pyp3 on levels of *pyp2*$^+$ *and gpx1*$^+$ mRNA. RNA samples were isolated from wild-type (NT4), Pk-epitope tagged wild-type Pyp1 (Pyp1Pk) (HL2), myc-epitope tagged wild-type Pyp2 (Pyp2myc) (JP392), Δ*pyp1* (NJ102), Δ*pyp2* (JP279), Δ*pyp3* (EV60), Mcs4^{D412N} (VB1692), Pyp1^{C20S}Pk (HL10), NΔ30Pyp1Pk (NJ1884), Δ*pyp1*Δ*pyp3* (HL19), Δ*pyp1*Pyp2myc (HL21), and wild-type (NT4) following treatment with 1.0 mM H_2O_2 for 20 minutes. Following Northern blot analysis (Figure 4.7), samples were quantified for *pyp2*$^+$ and *gpx1*$^+$ mRNA levels, relative to the *leu1*$^+$ loading control. Fold induction was calculated relative to the untagged wild-type (NT4) strain, with its ratio set to 1. Error bars indicate the range in values among 2 biological repeats (*n* = 2).

However, we were surprised to find that there was actually a slight reduction in the levels of *pyp2*$^{+}$ mRNA in both a Δ*pyp1* and Mcs4^{D412N} (Figure 4.7 and 4.8A). This suggested that, despite high levels of Sty1 phosphorylation, basal Atf1 activity may not be increased in these strains. In addition, the levels of *pyp2*$^{+}$ mRNA were also examined in myc-epitope tagged wild-type Pyp2 (Pyp2myc) in a Δ*pyp1* background (Δ*pyp1*Pyp2myc). As for a Δ*pyp1*, there was a reduction in the levels of *pyp2*$^{+}$ mRNA in a Δ*pyp1*Pyp2myc (Figure 4.7 and 4.8A). However, the levels of *gpx1*$^{+}$ were increased to a similar extent in both a Δ*pyp1* and Mcs4^{D412N} compared to the three wild-type strains (Figure 4.7 and 4.8B), consistent with high levels of Sty1 phosphorylation, and subsequently Atf1 levels, leading to increased *gpx1*$^{+}$ expression. Notably, this suggests that the increase in Pyp2 protein levels in a Mcs4^{D412N} mutant is not due to increased gene expression and more likely due to increased Sty1-dependent phosphorylation of Pyp2 that increases Pyp2 stability (Kowalczyk *et al.*, 2013). If this is the case, then this would suggest that this mechanism to stabilise Pyp2 may be impaired in the absence of Pyp1. In our previous chapter we showed that, similar to a Δ*pyp1* mutant, Pyp1^{C20S}Pk and NΔ30Pyp1Pk mutant-expressing cells also displayed increased basal Sty1 activation (Figure 3.15A). However, when we examined *pyp2*$^{+}$ mRNA levels in these mutant strains we found that levels of the *pyp2*$^{+}$ mRNA were even lower in both strains, with Pyp1^{C20S}Pk containing only 20% of the level of *pyp2*$^{+}$ mRNA detected in wild-type cells (Figure 4.7 and 4.8A). Similar to a Δ*pyp1*, the levels of *gpx1*$^{+}$ were also increased in Pyp1^{C20S}Pk and NΔ30Pyp1Pk compared to wild-type (Figure 4.7 and 4.8B), suggesting that the effect is specific to *pyp2*$^{+}$ mRNA levels in these mutants, rather than a more general reduction in the expression of Atf1-dependent genes. Surprisingly, this suggests that a single point mutation or complete loss of the N-terminal 30 amino acids of Pyp1, can influence the mRNA levels of a second PTP, Pyp2, more than the complete deletion of Pyp1.

Although *pyp3*$^{+}$ has previously been reported to be induced by H_2O_2 (Chen *et al.*, 2003), we were unable to detect any increase in cells exposed to 1.0 mM H_2O_2 for 60 minutes (Figure 4.3). Moreover, the levels of *pyp3*$^{+}$ mRNA were unchanged in any of the mutants examined, or in response to H_2O_2 (Figure 4.7). This indicates that the absence of either *pyp1*$^{+}$ or *pyp2*$^{+}$ doesn't influence the levels of

pyp3^{+} mRNA, suggesting that the effect of loss of *pyp1*$^{+}$ on *pyp2*$^{+}$ mRNA levels is specific to these phosphatases, and could, in part, be explained due to the overlapping function shared by Pyp1 and Pyp2.

Next we tested genetically any overlap between the functions of Pyp1 and Pyp2 or Pyp3. It has previously been shown that a Δ*pyp1*Δ*pyp2* is inviable (Millar *et al.*, 1992). The unexpected finding that *pyp2*$^{+}$ mRNA and protein levels are not higher in a Δ*pyp1* or in Pyp1^{C20S}Pk and NΔ30Pyp1Pk mutants (Figure 4.7) suggested that any essential function for Pyp2 in a Δ*pyp1* must be supported by basal levels of Pyp2. Hence, we decided to confirm that combined loss of both Pyp1 and Pyp2 was lethal, and also to investigate whether Pyp3 became important in cells lacking *pyp1*$^{+}$. Whilst a Δ*pyp1*Δ*pyp3* was viable, suggesting distinct functions for Pyp1 and Pyp3, our tetrad analysis (not shown) demonstrated that a Δ*pyp1*Δ*pyp2* was inviable, as previously reported (Millar *et al.*, 1992).

Having constructed a Δ*pyp1*Δ*pyp3*, we then examined H_2O_2-induced Sty1 phosphorylation in this strain to determine the effect of loss of *pyp3*$^{+}$ on H_2O_2-induced Sty1 activation. As expected, wild-type (Pyp1Pk) cells show no Sty1 phosphorylation before stress, but in response to oxidative stress, there is an induction by 10 minutes after 1.0 mM H_2O_2, which is maintained at 20 minutes (Figure 4.9). Mutant Δ*pyp3* shows a similar pattern of induction of Sty1 phosphorylation to wild-type, with the kinetics of activation delayed so that maximal Sty1 phosphorylation was detected 20 minutes after H_2O_2 treatment (Figure 4.9). In contrast, both a Δ*pyp1* and a Δ*pyp1*Δ*pyp3* show high basal Sty1 phosphorylation, with no induction upon oxidative stress (Figure 4.9), suggesting that even in the absence of *pyp1*$^{+}$, Pyp3 is not involved in the dephosphorylation of Sty1. This indicates there is no redundancy between Pyp1 and Pyp3 in the regulation of H_2O_2-induced phosphorylation of Sty1. Therefore, as Pyp3 does not appear to have a role in Sty1 activation, we will focus on trying to understand the exciting role of Pyp1 in regulating Pyp2 levels.

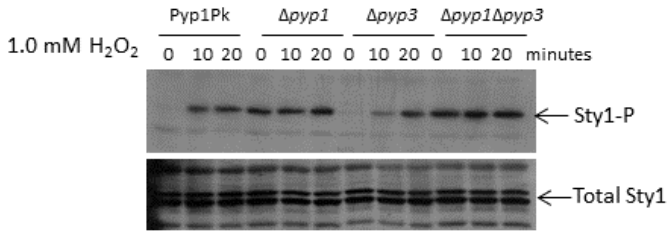

Figure 4.9 Loss of *pyp3*$^{+}$ does not affect H_2O_2-induced Sty1 phosphorylation, even in cells lacking *pyp1*$^{+}$. Western blot analysis of levels of phosphorylated Sty1 in cells expressing Pk-epitope tagged wild-type Pyp1 (Pyp1Pk) (HL2) or Δ*pyp1* (NJ102), Δ*pyp3* (EV60) and Δ*pyp1*Δ*pyp3* (HL19) before and after treatment with 1.0 mM H_2O_2. Anti-pp38 and anti-Sty1 antibodies were used to detect phosphorylated Sty1 and total Sty1 levels, respectively.

The levels of *pyp2*$^{+}$ mRNA were also examined in this double Δ*pyp1*Δ*pyp3* strain. *pyp2*$^{+}$ mRNA levels were similar in Δ*pyp3* mutant to those in wild-type, and there was a similar reduction in the levels of *pyp2*$^{+}$ mRNA in a Δ*pyp1*Δ*pyp3* (Figure 4.7 and 4.8A), suggesting that, even in the absence of *pyp1*$^{+}$, loss of *pyp3*$^{+}$ has no effect on the levels of *pyp2*$^{+}$ mRNA.

4.2.4 There is no detectable Pyp2Pk protein in a Δ*pyp1* or Pyp1^{C20S}Pk

Given the established Sty1-dependent increases in *pyp2*$^{+}$ mRNA levels and Pyp2 protein stability, the lower levels of *pyp2*$^{+}$ mRNA (Figure 4.7 and 4.8A) and Pyp2myc protein (Figure 4.6) in a Δ*pyp1*, where Sty1 phosphorylation is increased, and in which Pyp2 is essential, were unexpected. Pyp2myc contains 13 myc-epitope tags, adding ~1.2 kDa per myc-epitope, whereas Pyp2Pk contains only 3 Pk-epitope tags, each adding ~1.4 kDa. Therefore, the addition of 13 myc-epitope tags is a much greater change to protein molecular weight than the addition of 3 Pk-epitope tags, and, although this strain retains the 3'-UTR of *pyp2*$^{+}$ that is important for *pyp2*$^{+}$ mRNA stability, it was still possible that this epitope tag could be affecting protein levels. Therefore, to test whether the importance of Pyp1 for Pyp2 mRNA and protein levels might involve post-transcriptional mechanisms requiring the 3'-UTR, or be epitope-tag specific, we examined whether loss of *pyp1*$^{+}$ affected the levels of Pk-epitope tagged Pyp2 containing the 3'-UTR from *nmt1*$^{+}$, rather than the *pyp2*$^{+}$ 3'-UTR. Notably, whereas Pyp2Pk levels increased substantially in wild-type cells exposed to 1.0 mM H_2O_2, Pyp2Pk protein levels remained undetectably low in a Δ*pyp1* (Figure 4.10). This suggests that, as well as being required for basal levels of *pyp2*$^{+}$ mRNA (Figure 4.7) and Pyp2myc (Figure 4.6), Pyp1 is also required for H_2O_2-induced increases in Pyp2 protein levels. Moreover, the effect of Pyp1 does not require the 3'-UTR and is therefore likely to be via a transcriptional or post-translational mechanism. As we had found that cysteine 20 in Pyp1 was required for *pyp2*$^{+}$ mRNA levels (Figure 4.7), we tested whether this mutation affected Pyp2Pk protein levels. Although the lack of an appropriate wild-type control (Pyp1PkPyp2Pk) prevents conclusive interpretation of this experiment, the absence of detectable Pyp2Pk from these cells, before or after exposure to H_2O_2 suggests that cysteine 20 is critical for Pyp2 expression.

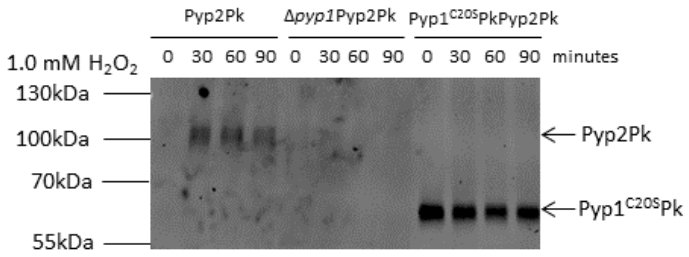

Figure 4.10 Pyp1 activity is required for the H_2O_2-induced increase in Pyp2Pk levels. Western blot analysis of cells expressing Pk-epitope tagged wild-type Pyp2 (Pyp2Pk) (HL24), or mutant Δ*pyp1*Pyp2Pk (HL27) and Pyp1^{C20S}PkPyp2Pk (HL26) before and after treatment with 1.0 mM H_2O_2. Anti-Pk antibody was used to detect Pk-tagged Pyp1. The different bands are indicated and the molecular weight (MW) markers are shown.

Thus, unexpectedly, our data suggest that mutation of a single cysteine in the N-terminus of Pyp1, that is required for stress-induced phosphorylation of Pyp1 (Figure 3.13A), prevents normal expression of Pyp2 or stabilisation of Pyp2 protein in response to H_2O_2.

4.3 Discussion

H_2O_2-induced oxidation of cysteine thiols in PTP has been established as an integral part of signal transduction. Previous studies have demonstrated that Pyp2 is regulated both transcriptionally and translationally (Kowalczyk *et al.*, 2013), and data presented in chapter 3 has provided evidence that multiple post-translational modifications regulate Pyp1 in *S. pombe*. A third PTP, Pyp3, exists, which we have confirmed here doesn't seem to share any overlapping function with Pyp1 and Pyp2 in regulating Sty1 (Figure 4.9). Here we have investigated the relative levels of these three PTP, and how they are affected by loss or mutation of *pyp1*$^+$. Our data suggest that despite the high degree of homology (Figure 4.2) and overlapping functions of Pyp1 and Pyp2, Pyp2 may be less sensitive to H_2O_2-induced oxidation than Pyp1 (Figure 4.4A). More significantly, we have found that, rather than, as expected, increasing Pyp2 levels, loss of *pyp1*$^+$ reduces the levels of Pyp2 (Figure 4.6, 4.7 and 4.8A). Indeed, our data raise the possibility that phosphorylation of Pyp1, which is inhibited by serine substitution of cysteine 20 (Figure 3.13A), may be important for *pyp2*$^+$ transcription.

The activation of MAPK pathways leads to an adaptive response, modulating several aspects of cell physiology essential for cell survival, such as regulating gene expression, translation and cell cycle progression. However, high levels of MAPK activity might be deleterious (Millar *et al.*, 1992), therefore, it is important to maintain low levels of MAPK. Sty1 in *S. pombe* has vital roles in controlling several aspects of normal cellular physiology, such as regulation of the cell cycle (Lopez-Aviles *et al.*, 2005; Lopez-Aviles *et al.*, 2008), and control of mitotic onset and cell size (Petersen and Nurse, 2007) (For a review see (Sanso *et al.*, 2011a)). In addition, Sty1 is important for cell survival following multiple stress conditions, including oxidative stress (Shiozaki and Russell, 1995; Nguyen *et al.*, 2000). Sty1

promotes gene expression, mainly by increasing the levels of the transcription factor Atf1 (Shiozaki and Russell, 1996; Wilkinson *et al.*, 1996). However, additional mechanisms are utilised by Sty1 to regulate gene expression at the post-transcriptional level, interfere with translational machinery, and control cell cycle progression. For example, the phosphorylated form of Sty1 is recruited to the promoters of Atf1-dependent genes (Reiter *et al.*, 2008), enabling transcription initiation through the recruitment of RNA polymerase II and additional factors (Sanso *et al.*, 2011b). Sty1 is also able to regulate gene expression at the post-transcriptional level in response to increased levels of H_2O_2 through control of protein kinases and RNA-binding proteins (RBPs). For example, Sty1 is required to stabilise the mRNA of *atf1*$^+$ (Day and Veal, 2010) and many Atf1-dependent genes, such as *pyp2*$^+$, in response to H_2O_2 (Rodriguez-Gabriel *et al.*, 2003). Sty1 also phosphorylates and stabilises Pyp2 protein (Kowalczyk *et al.*, 2013). These multiple functions in promoting Pyp2 activity form a negative feedback loop and likely reflect the importance that the balance between the phosphorylation and dephosphorylation of Sty1 is tightly regulated. Owing to the multiple roles of MAPK, as exemplified by studies in *S. pombe*, it is evident that maintaining low levels of Sty1 is important for cell viability. Tight control of the amplitude and duration of MAPK-mediated signalling, through negative regulation by phosphatases, also highlights the importance of maintaining low levels of MAPK activity under normal conditions. For instance, the MAPK Pmk1 and Sty1 can be dephosphorylated by Pyp1 and Pyp2, suggesting an overlapping regulation between these two MAPK pathways, with the MAPK activity being tightly controlled and coordinated. This demonstrates a complexity to the MAPK signalling system, whereby cross-talk can occur between different MAPK pathways, to inactivate MAPK activity.

Data presented in chapter 3 suggests that there is a strong selection pressure against mutants which inhibit Sty1 phosphorylation, causing reversion of the desired substitution, as seen with the non-phosphorylatable mutant, Pyp1^{Y160F}Pk (Figure 3.23B). However, other mutants of Pyp1 that inhibit Sty1 activation, such as Pyp1^{C20S}Pk and NΔ30Pyp1Pk (Figure 3.15A), and Mcs4^{D412N} (Buck *et al.*, 2001), were not found to revert back to the wild-type sequence as easily as Pyp1^{Y160F}Pk. Here we present data to suggest that cells have adopted multiple mechanisms to deal with high levels of

phosphorylated Sty1. For instance, in a Δ*pyp1* and Mcs4^{D412N}, which display high basal Sty1 phosphorylation, they have different effects on the levels of Pyp2 protein. Whilst Mcs4^{D412N} cells have increased Pyp2 protein levels (Figure 4.5A), conversely, mutant Δ*pyp1* and Pyp1^{C20S}Pk show no increase in Pyp2 protein levels, and a reduction in *pyp2*$^{+}$ mRNA levels (Figure 4.6, 4.7 and 4.10). This suggests that Δ*pyp1* and Mcs4^{D412N} mutants implement different mechanisms to deal with increased levels of phosphorylated Sty1. It would be interesting to investigate how the other mutations of Pyp1, which also affect levels of phosphorylated Sty1, such as NΔ30Pyp1Pk and Pyp1^{Y160F}Pk, affect the mRNA and protein levels of Pyp2. As the 3'-UTR of *pyp2*$^{+}$ is not required for the Pyp1-dependent regulation of Pyp2 levels, the Pk-epitope tagged Pyp2 strains constructed in this study would provide the appropriate tools to allow these investigations. In addition, our data suggests that Pyp1, or the Wis1-dependent phosphorylation of Pyp1, may be important for *pyp2*$^{+}$ transcription or Pyp2 protein levels. Pyp2Pk protein levels are decreased in both a Δ*pyp1* and Pyp1^{C20S}Pk, mutants which display high basal Sty1 phosphorylation. The absence of nuclear Pyp1 in Pyp1^{C20S}Pk (Figure 3.18) might help explain why this mutant is unable to support the expression of *pyp2*$^{+}$. This could be further tested by investigating whether NΔ30Pyp1Pk, which cannot become phosphorylated, and becomes excluded from the nucleus following treatment with H_2O_2, also contains lower levels of Pyp2 compared to wild-type.

This chapter, together with data presented in chapter 3, has highlighted that the phosphatases, Pyp1 and Pyp2, are regulated differently through post-translational modifications in response to H_2O_2. At least one cysteine residue in Pyp1 can be oxidised following exposure to H_2O_2, dependent on Tpx1. Conversely, we found no evidence to suggest that Pyp2 is sensitive to H_2O_2-induced oxidation. Although we have found that Pyp1 is oxidised in response to low levels of H_2O_2 and mediates the effects of increased Tpx1 on Sty1 activation, oxidation of the catalytic cysteine of GAPDH has also been shown to be important for H_2O_2-induced activation of Sty1 (Morigasaki *et al.*, 2008). Therefore, in the remainder of the thesis we will describe our further investigations into how cysteines in GAPDH and other peroxide-regulated proteins become oxidised, and the involvement of Tpx1 in these oxidation events.

CHAPTER 5

5. The role of GAPDH oxidation in responses to H_2O_2

5.1 Introduction

GAPDH activity is sensitive to inactivation by reversible or irreversible oxidation of the catalytic cysteine following exposure to H_2O_2. H_2O_2-induced oxidation of GAPDH is an important protective response to H_2O_2, as exemplified by studies in mammalian cells and the budding yeast *Saccharomyces cerevisiae* (Brodie and Reed, 1987; Brodie and Reed, 1990; Grant *et al.*, 1999). For example, Tdh3, one GAPDH isoform in *S. cerevisiae*, undergoes reversible S-thiolation of cysteine residue(s), inhibiting its enzyme activity, but also protecting the cysteine from irreversible oxidation to sulphinic or sulphonic derivatives, as activity can be restored by deglutathionylation by glutaredoxins. One way in which GAPDH oxidation has been shown to protect cells against ROS is by inhibiting glycolysis and thus allowing increased NADPH production by the pentose phosphate pathway (PPP) (Ralser *et al.*, 2007). Oxidation of glucose-6-phosphate by the PPP generates NADPH, therefore providing reductive power for the thioredoxin and glutathione systems (Nogae and Johnston, 1990; Pollak *et al.*, 2007). Studies in mammalian cells under oxidative stress have shown enhanced activity of the PPP (Janero *et al.*, 1994; Colussi *et al.*, 2000). In yeast the underlying mechanism is better understood, with oxidation of GAPDH rerouting the carbohydrate flux from glycolysis to the PPP, maintaining the cytoplasmic NADPH/NADP equilibrium to counteract oxidative stress (Ralser *et al.*, 2007). Consistent with this, yeast with low activity of another glycolytic enzyme, TPI (triose-phosphatase isomerase), exhibit similar changes in PPP metabolites and are highly resistant to oxidants, such as diamide (Ralser *et al.*, 2006). Thus, it is now generally accepted that inactivation of GAPDH by H_2O_2-induced oxidation acts as a cellular switch to reroute the metabolic flux, protecting against oxidative stress.

It has been proposed that, although oxidation inactivates GAPDH's glycolytic activity, it also promotes alternative signalling activities. For instance, in fission yeast, GAPDH oxidation has been shown to be important for H_2O_2-induced activation of the p38 related Sty1 MAPK (Morigasaki *et al.*, 2008). Specifically, one of two GAPDH isoforms in *Schizosaccharomyces pombe*, Tdh1, has been shown to form a complex with the MAPKKK Wak1, and the response regulator Mcs4 (Figure 5.1) which is enhanced by transient oxidation of Tdh1 on cysteine 152. Thus, Tdh1 oxidation has been proposed to increase Sty1 phosphorylation by increasing the interaction between Mpr1 and Mcs4. In support of this, substitution of the catalytic cysteine, cysteine 152, with serine (C152S), prevented H_2O_2-induced Tdh1 oxidation and the increased association of Tdh1 with Mcs4, or Mpr1 with Mcs4, and resulted in lower levels of activation of Sty1 in response to H_2O_2 (Morigasaki *et al.*, 2008). This study provided evidence for an essential role for Tdh1 in phosphorelay signalling between the phosphorelay protein and response regulator.

Although an assumption in these studies has been that the sensitivity of GAPDH to oxidation is an inevitable consequence of the essential role of deprotonated cysteines in its catalytic mechanism, a recent study has made the exciting discovery that the glycolytic activity of GAPDH can be separated from the sensitivity of its catalytic cysteine to H_2O_2-induced oxidation (Peralta *et al.*, 2015). Indeed, this work provided strong evidence that the sensitivity of GAPDH to oxidation has evolved specifically to protect cells from oxidative stress. Peralta *et al.*, (2015) established that a second cysteine in the active site of GAPDH, cysteine 156, is important for the H_2O_2-induced oxidation of the catalytic cysteine, cysteine 152, but not for the catalytic activity (Figure 5.2B) (Peralta *et al.*, 2015). A highly conserved proton-shuttling mechanism facilitates the H_2O_2 sensitivity of cysteine 152 but does not affect the reactivity of GAPDH to its glycolytic substrate.

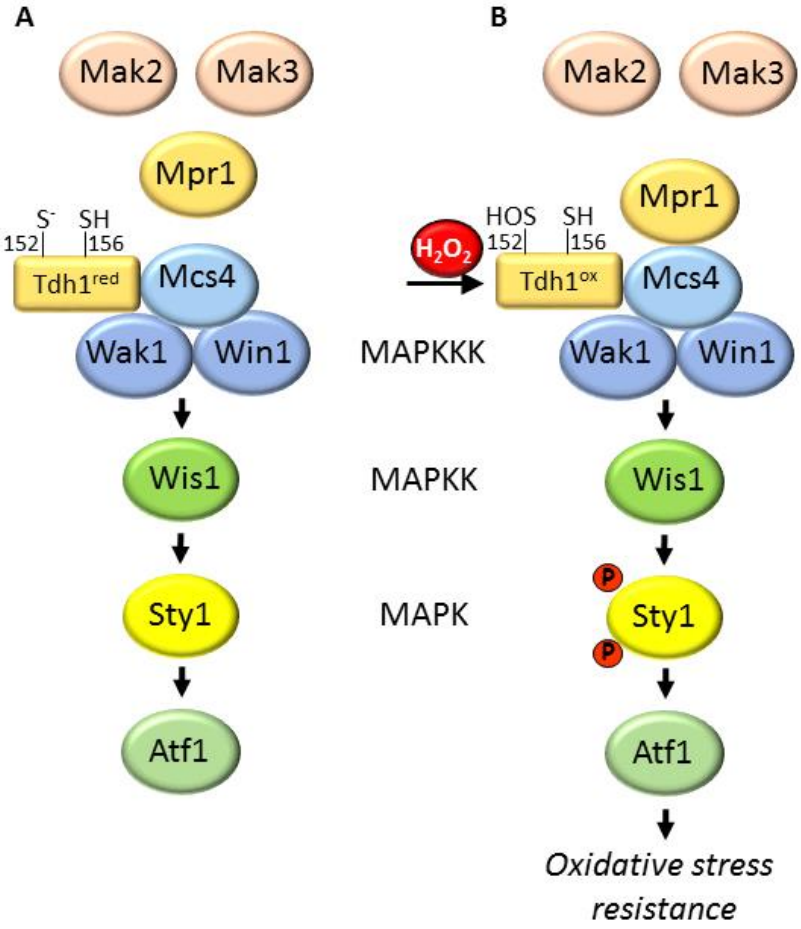

Figure 5.1 The role of Tdh1 in the H_2O_2-induced activation of the Sty1 MAPK pathway in *S. pombe*. (**A**)(**B**) Stress signals are transduced through conserved stress-activated protein kinase pathways. The Sty1 MAPK pathway in *S. pombe* is activated by H_2O_2, resulting in activation of Atf1, and increased antioxidant gene expression and oxidative stress resistance. Sty1 is activated by phosphorylation by the MAPKK Wis1, which is activated by the MAPKKK, Wak1 (Wis4) and Win1. In *S. pombe* a variation of the two-component signalling system found in bacteria, involving two histidine protein kinases, Mak2 and Mak3, a phosphorelay protein Mpr1, and a response regulator Mcs4 is important for the H_2O_2-induced activation of the Sty1 MAPK. (**B**) Upon exposure to H_2O_2, the GAPDH Tdh1 becomes transiently oxidised on cysteine 152, enhancing its interaction with Mcs4. This oxidation is proposed to increase Sty1 phosphorylation by increasing the interaction between Mpr1 and Mcs4.

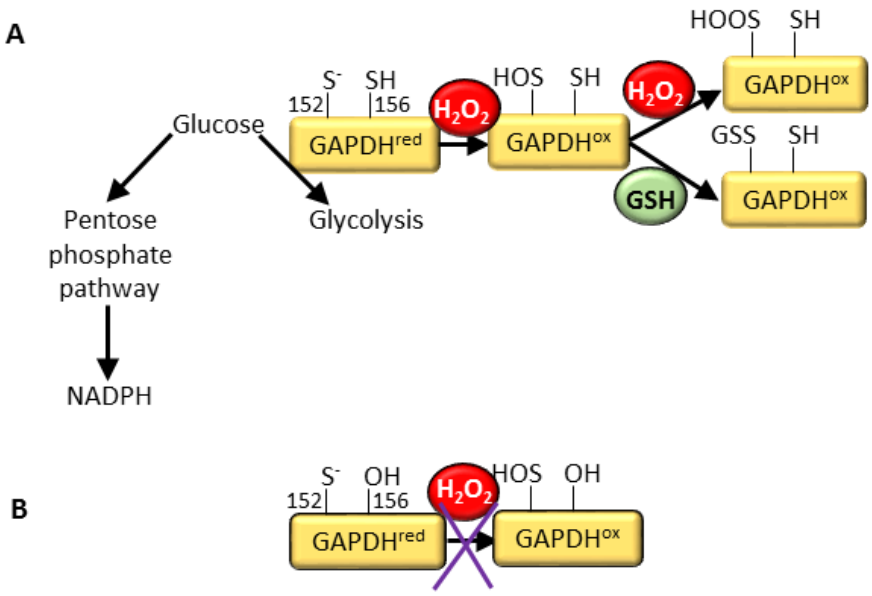

Figure 5.2 H_2O_2 promotes the oxidation of GAPDH, leading to an increase in the generation of NADPH and oxidative stress resistance. (**A**) Under non-stressed conditions, glucose can be used in glycolysis or in the pentose phosphate pathway (PPP) to generate NADPH, which is used in the reduction of thioredoxin (Trx) or glutathione (GSH). Upon exposure to H_2O_2, GAPDH becomes oxidised on cysteine 152 to the sulphenic acid (-SOH). Further oxidation to the sulphinic (-SOOH) and sulphonic (-SOOOH) acid forms can occur at higher H_2O_2. However, in the presence of GSH, S-glutathionylation competes with hyperoxidation. (**B**) In the absence of a second cysteine, cysteine 156, oxidation on cysteine 152 is inhibited (Adapted from Peralta *et al.*, 2015).

By replacing the endogenous yeast GAPDH isoforms with a GAPDH mutant lacking sensitivity to H_2O_2, but which retains full glycolytic activity, Peralta *et al.*, (2015) were able to demonstrate that cysteine 156 was not needed for GAPDH catalytic function, but was required for cysteine 152 to become sulphenylated by reaction with H_2O_2 (Peralta *et al.*, 2015). In the presence of GSH, the sulphenylated form of GAPDH can become glutathionylated, protecting sulphenylated GAPDH against irreversible inactivation by hyperoxidation to sulphinylated and sulphonylated (hyperoxidised) forms. Thus, by impairing the formation of sulphenylated cysteine 152, loss of cysteine 156 prevents the subsequent formation of both reversible and irreversible secondary oxidation products. Structural studies suggest that cysteine 156 is deep in a hydrophobic core, and therefore unlikely to be directly involved in redox reactions. Instead, it was proposed that cysteine 156 influences cysteine 152 indirectly. Consistent with this model, no sulphinylation/sulphonylation or glutathionylation of cysteine 156 was observed, nor a H_2O_2-induced intracellular disulphide bond between the two active site cysteines, cysteine 152 and 156, in cells treated with H_2O_2 (Peralta *et al.*, 2015). Notably, evidence presented by Peralta *et al.*, (2015) suggests that this role of cysteine 156 in facilitating the H_2O_2-induced oxidation of GAPDH is widely conserved. However, previous studies have suggested that substitution of the equivalent cysteine, cysteine 156, with serine (C156S) in *S. pombe* Tdh1 does not affect either H_2O_2-induced Tdh1 oxidation, or Sty1 activation, raising the possibility that this cysteine might not be required for the oxidation of *S. pombe* Tdh1 (Morigasaki *et al.*, 2008).

There are two isoforms of GAPDH in the fission yeast *S. pombe*, Tdh1 and Gpd3. These two GAPDH proteins share a very high degree of homology, with 93% identity, and three conserved cysteine residues (Figure 5.3). The specificity of anti-GAPDH antibodies was tested in protein lysates from wild-type, Δ*gpd3* or Δ*tdh1 S. pombe* cells (Taylor, 2009). The absence of a band in Δ*tdh1* and the presence of a band in Δ*gpd3* suggests that these polyclonal anti-GAPDH antibodies specifically recognises *S. pombe* Tdh1 and not Gpd3, or, more likely, that levels of Tdh1 are much higher than Gpd3. Indeed, this western blot analysis is consistent with quantitative proteomics in suggesting that Tdh1 is the predominant GAPDH enzyme, more than 200-fold more abundant than Gpd3 with an estimated

1017701 Tdh1 molecules per proliferating cell, whereas there are only 4465.64 Gpd3 molecules per proliferating cell (Marguerat *et al.*, 2012). Consistent with this, in cells lacking *tdh1*$^{+}$, GAPDH enzyme activity was severely reduced, whereas loss of *gpd3*$^{+}$ had a negligible effect on cellular GAPDH activity (Taylor, 2009). Together these data suggest that Tdh1 is the major GAPDH enzyme in *S. pombe*, providing more than 90% of cellular GAPDH activity to the cell (Taylor, 2009).

Although previous work has suggested that cysteine 156 is not required for the H_2O_2-induced oxidation of Tdh1, this is at odds with the recent study of Peralta *et al.*, (2015), which provided strong evidence that this active site cysteine is essential to confer H_2O_2-sensitivity on the catalytic cysteine, cysteine 152, of these highly conserved GAPDH enzymes. Hence, the initial aim of this study was to test whether cysteine 156 was important for the *in vivo* H_2O_2-induced oxidation of *S. pombe* Tdh1 and resolve this issue. If, as predicted by Peralta *et al.*, (2015), the role of cysteine 156 in promoting the sensitivity of GAPDH enzymes was found to be conserved in Tdh1, then we planned to use mutants lacking this cysteine to investigate whether the oxidation of GAPDH protects *S. pombe* against oxidative stress. If any protective effect was identified, we next wanted to investigate whether this was due to inhibition of GAPDH activity and an associated increase in NADPH, or due to non-glycolytic functions for oxidised Tdh1, specifically in promoting the H_2O_2-induced activation of the Sty1 MAPK.

5.2 Results

5.2.1 Tdh1 becomes oxidised and its GAPDH activity inhibited following exposure to ≥1.0 mM H_2O_2

Tdh1 is sensitive to oxidation of its catalytic cysteine, cysteine 152, following exposure to H_2O_2, causing reversible inhibition of GAPDH enzyme activity (Morigasaki *et al.*, 2008). Before we could test whether cysteine 156 was required for this H_2O_2-sensitivity, it was important to determine the concentration of H_2O_2 that was required to oxidise and inhibit wild-type Tdh1.

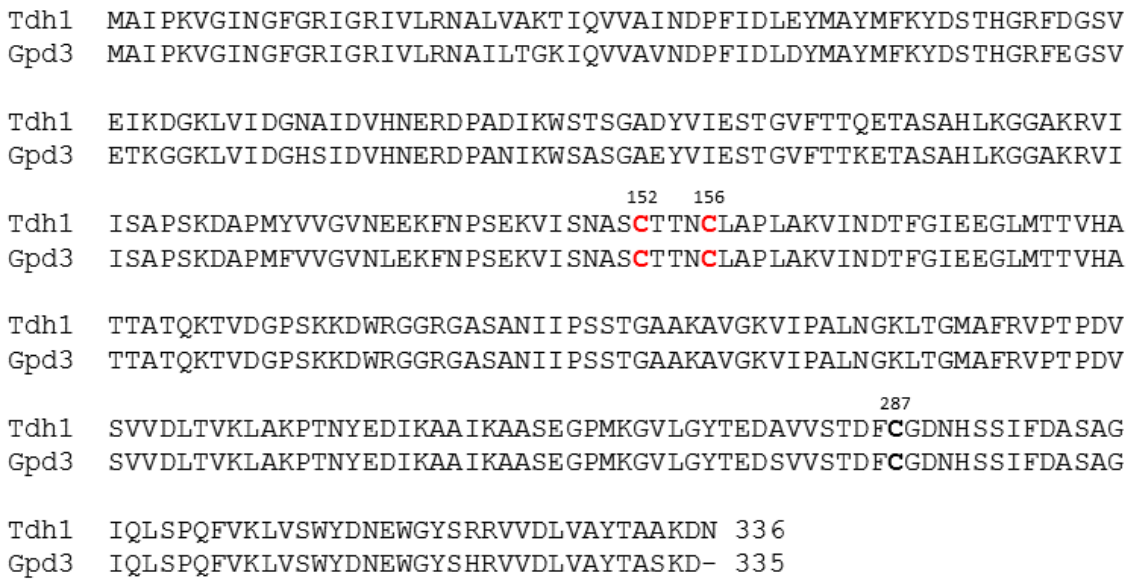

Figure 5.3 *S. pombe* GAPDH isoforms, Tdh1 and Gpd3. Amino acid sequence alignment of the *S. pombe* GAPDH isoforms, Tdh1 and Gpd3. Conserved cysteines are indicated in bold, whilst those in the active site are highlighted in red.

Hence, we examined the oxidation state of endogenous wild-type Tdh1 before and following exposure to different concentrations of H_2O_2 using anti-GAPDH antibodies shown previously to cross-react specifically with *S. pombe* Tdh1 (Taylor, 2009). This analysis revealed that, in untreated cells, GAPDH in wild-type (429) cells was mostly present in the reduced form; as indicated by the AMS-dependent mobility shift, consistent with AMS-modification of each of the three cysteine residues (Figure 5.4A, lanes 1 and 2, labelled $GAPDH^{red}$-3xNEM and $GAPDH^{red}$-3xAMS). There was no detectable difference in the mobility of AMS-treated GAPDH following exposure to low (0.2 mM and 1.0 mM) concentrations of H_2O_2 (Figure 5.4A, lanes 2-6), indicating that GAPDH remains predominantly reduced under these conditions. However, following treatment with 6.0 mM H_2O_2, a more mobile form of GAPDH was detected, consistent with one or two cysteines in GAPDH becoming oxidised, and therefore AMS-resistant (Figure 5.4A, lanes 7 and 8, labelled $GAPDH^{ox}$-AMS). The insensitivity of this form to reduction by β-mercaptoethanol is consistent with irreversible hyperoxidation of the catalytic cysteine to a sulphinic or sulphonic derivative. Following exposure to 6.0 mM H_2O_2, a less mobile form of GAPDH was also detected (Figure 5.4A, lanes 7 and 8), that was sensitive to β-mercaptoethanol (Figure 5.4A, lanes 11 and 12), consistent with this representing glutathionylated GAPDH ($GAPDH^{-SSG}$).

Anti-GAPDH-SO_3 antibodies, specific to the hyperoxidised form of GAPDH, in which the catalytic cysteine is irreversibly oxidised to sulphinic (SO_2) or sulphonic (SO_3) derivatives, were used to confirm that there was no increase in hyperoxidised GAPDH in cells exposed to 0.2 mM H_2O_2. Moreover, although following exposure to 1.0 mM H_2O_2, there was a detectable increase in hyperoxidised GAPDH, levels of hyperoxidised GAPDH were much more substantially increased in cells exposed to 6.0 mM H_2O_2 (Figure 5.4A, lanes 2-8).

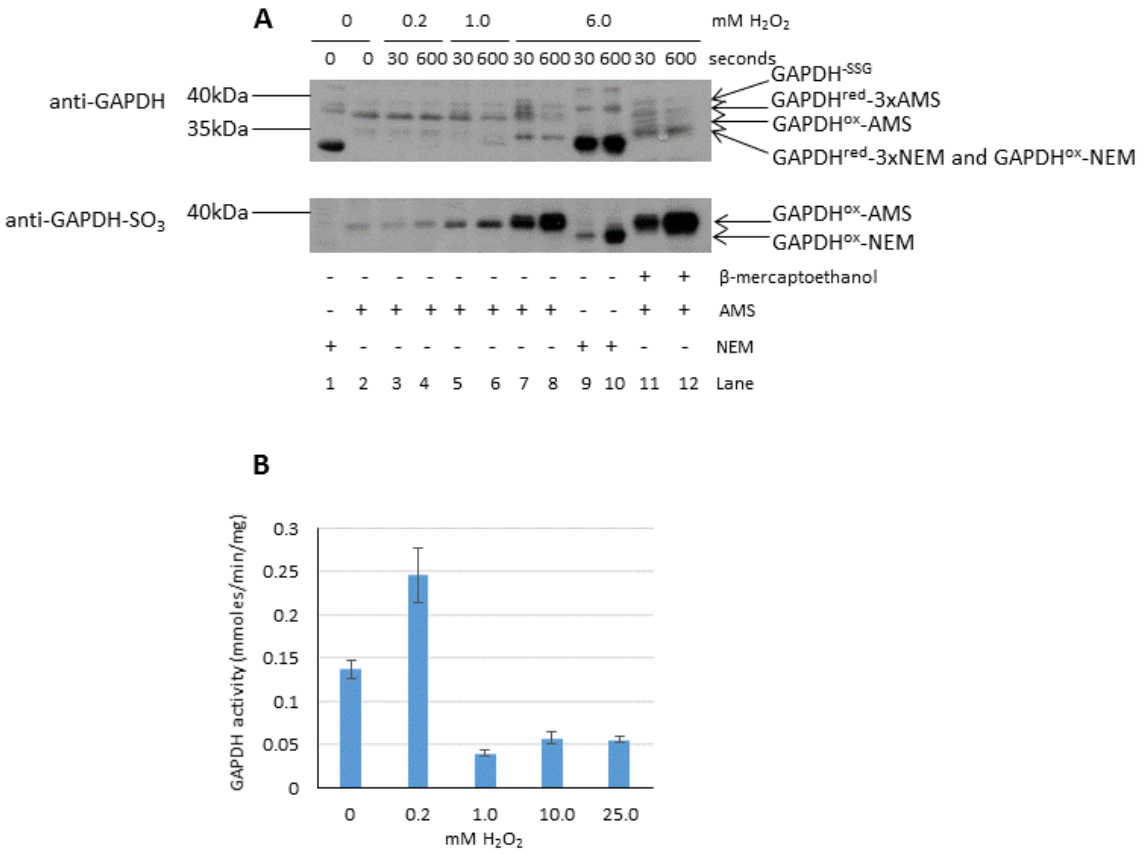

Figure 5.4 GAPDH becomes oxidised and GAPDH activity inhibited following exposure of cells to ≥1.0 mM H_2O_2. (**A**) Western blot analysis of GAPDH oxidation in wild-type (429) *S. pombe* before and after treatment with 0.2, 1.0 and 6.0 mM H_2O_2 for 0, 30 and 600 seconds. Protein samples were treated, as indicated, with the thiol-binding agents, NEM or AMS, and the reducing agent β-mercaptoethanol, prior to electrophoresis. Anti-GAPDH and anti-GAPDH-SO_3 antibodies were used to detect total GAPDH and hyperoxidised GAPDH, respectively. This experiment was performed by Dr. A. Day. (**B**) GAPDH enzyme activity was assayed in wild-type (429) *S. pombe* treated with increasing concentrations of H_2O_2 for 10 minutes. GAPDH activity units are expressed as mmoles of NADH formed/minute/mg protein (Taylor, 2009).

Consistent with the oxidation of Tdh1 in cells exposed to 1.0 and 6.0 mM H_2O_2, cellular GAPDH activity was reduced following exposure to concentrations above 1.0 mM H_2O_2 (Figure 5.4B). Thus, these data reveal that Tdh1 is not sensitive to oxidation following exposure to low (0.2 mM) concentrations of H_2O_2 but becomes oxidised following exposure to higher (≥1.0 mM) concentrations of H_2O_2 (Figure 5.4A). Moreover, oxidation of endogenous Tdh1 was found to correlate with H_2O_2-dependent inhibition of GAPDH activity (Figure 5.4B).

5.2.2 Cysteine 156 is required for H_2O_2-induced oxidation of Tdh1

Having established the concentration of H_2O_2 required to oxidise and inhibit wild-type Tdh1, we set out to test whether cysteine 156, was, as predicted by Peralta *et al*., (2015), important for this H_2O_2-induced oxidation. To investigate this, cells expressing a Tdh1 mutant, in which cysteine 156 was replaced with serine (C156S), with a Pk-epitope tag at the C-terminus were generated (see section 2.2.5.4). Loss of *tdh1*$^+$ results in a severe growth defect (Figure 5.5), presumably due to the reduced GAPDH activity in these cells (Taylor, 2009). Hence, to test whether Tdh1^{C156S}Pk retained Tdh1 functions in cell growth, we set out to compare the growth of Pk-epitope tagged mutant Tdh1^{C156S}Pk with that of untagged wild-type (EV62 and 429), and Pk-epitope tagged wild-type (Gpd3Pk) generated by a previous study (Figure 5.5). Unfortunately, Tdh1Pk and Gpd3Pk strains were mixed up in the Veal lab strain collection, and this problem was only detected when tetrad analysis of potential Tdh1PkΔ*gpd3* mutants, generated late in this study, suggested that the alleles were strongly linked. However, importantly, the growth of cells expressing Gpd3Pk or Tdh1^{C156S}Pk was indistinguishable from cells expressing untagged wild-type Gpd3 or Tdh1, indicating that the Pk-epitope tag and substitution of cysteine 156 in Tdh1 did not affect cell growth (Figure 5.5).

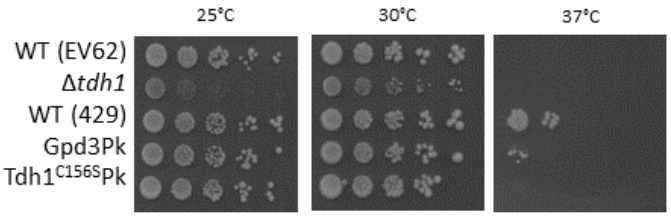

Figure 5.5 The effect of mutations and Pk-epitope tagging of Tdh1 on cell growth. Serial 10-fold dilutions of wild-type (EV62), Δ*tdh1* (ST3), wild-type (429), Pk-epitope tagged wild-type Gpd3 (Gpd3Pk) (ST2) and mutant Tdh1^{C156S}Pk (HL30) were spotted onto YE5S agar plates for 3-5 days at the indicated temperatures.

Next we examined whether cysteine 156 was required for the sensitivity of Tdh1 to H_2O_2-induced oxidation. Proteins were extracted from Pk-epitope tagged wild-type Tdh1 (Tdh1Pk) and mutant Tdh1^{C156S}Pk cells following exposure to 6.0 mM H_2O_2, and protein samples were treated with AMS, either with or without β-mercaptoethanol. Due to the mistake in the strain storage of Tdh1Pk and Gpd3Pk strains, the oxidation of Pk-epitope tagged wild-type Gpd3 (Gpd3Pk) was also examined, enabling us to observe whether both GAPDH isoforms in *S. pombe* are equally sensitive to H_2O_2-induced oxidation. The absence of a band in Δ*tdh1* with both anti-Pk and anti-GAPDH-SO_3 antibodies confirmed that the detected bands represented Tdh1 and sulphinylated (hyperoxidised) Tdh1, respectively (Figure 5.6). Importantly, western blot analysis with anti-Pk antibodies revealed that, similar to endogenous Tdh1 (Figure 5.4A), both wild-type Tdh1 (Tdh1Pk) and Gpd3 (Gpd3Pk) were rapidly oxidised to AMS-resistant forms following treatment with 6.0 mM H_2O_2 (Figure 5.6). In contrast, Tdh1^{C156S}Pk was not detectably oxidised, as the mobility of AMS-treated Tdh1^{C156S}Pk doesn't change following treatment with 6.0 mM H_2O_2 (Figure 5.6). This supports the finding of Peralta *et al*., (2015), that cysteine 156 is required for H_2O_2-induced oxidation of Tdh1. In wild-type Tdh1 (Tdh1Pk) samples following treatment with 6.0 mM H_2O_2, GAPDH was present in approximately equal amounts between two detected bands; proteins were separated for a much shorter time compared to Figure 5.4A, therefore the upper band represents both reduced GAPDH and glutathionylated GAPDH, consistent with it being β-mercaptoethanol-sensitive (Figure 5.6).

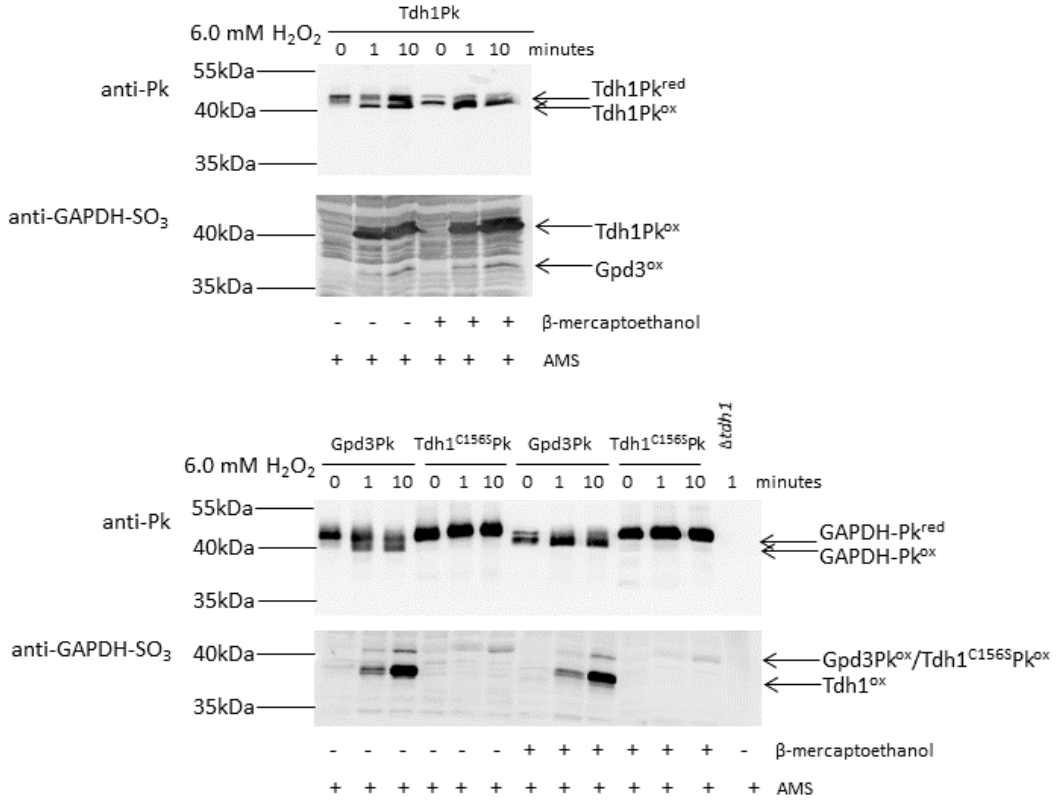

Figure 5.6 The effect of mutations and Pk-epitope tagging of Tdh1 on H_2O_2-induced oxidation of Tdh1. Western blot analysis of cells expressing Pk-epitope tagged wild-type Tdh1 (Tdh1Pk) (ST1), wild-type Gpd3 (Gpd3Pk) (ST2), or mutant Tdh1^{C156S}Pk (HL30) and Δ*tdh1* (ST3) before and after treatment with 6.0 mM H_2O_2 for 0, 1 and 10 minutes. Protein samples were treated, as indicated, with the thiol-binding agent AMS, and the reducing agent β-mercaptoethanol, prior to electrophoresis. Anti-Pk and anti-GAPDH-SO_3 antibodies were used to detect Pk-epitope tagged GAPDH and hyperoxidised GAPDH, respectively.

Anti-GAPDH-SO_3 antibodies, specific for GAPDH enzymes in which the catalytic cysteine, cysteine 152, is sulphinylated or sulphonylated, were used to detect hyperoxidised GAPDH, and to confirm that wild-type oxidised Tdh1 and Tdh1Pk were sulphinylated in cells exposed to 6.0 mM H_2O_2. Importantly, very little GAPDH-SO_3 was detected in cells expressing mutant Tdh1^{C156S}Pk, consistent with the resistance of this protein to oxidation of cysteine 152 (Figure 5.6). However, an intense β-mercaptoethanol-resistant band (just above the 40 kDa protein marker) was detected using anti-GAPDH-SO_3 in wild-type Tdh1 (Tdh1Pk) cells following exposure to 6.0 mM H_2O_2, consistent with this representing hyperoxidised Tdh1Pk (Figure 5.6). A second, less intense band (just below the 40 kDa protein marker), was also observed, whose mobility was consistent with that expected for endogenous Gpd3 (36 kDa). Similarly, two H_2O_2-induced bands were also detected using anti-GAPDH-SO_3 antibodies in wild-type Gpd3 (Gpd3Pk). However, in this case, the lower band (just below the 40 kDa protein marker) with a mobility consistent with endogenous Tdh1 (36 kDa), is the predominant band, whereas the band with a mobility consistent with Gpd3Pk (just above the 40 kDa protein marker) is much fainter (Figure 5.6). The difference in levels of these bands could be attributed to the differences in abundance of the two GAPDH isoforms, with quantitative proteomics suggesting that Tdh1 is 200-fold more abundant than Gpd3 (Marguerat *et al.*, 2012), consistent with the band representing hyperoxidised Tdh1 being much more prominent than the band representing hyperoxidised Gpd3Pk. However, previous work in our lab has shown that Pk-epitope tagged Tdh1 and Gpd3 proteins are expressed at similar levels (Taylor, 2009), suggesting the Pk-epitope tag could be affecting the expression of either Tdh1 or Gpd3. A likely explanation could be that the faint band representing hyperoxidised Gpd3Pk and Tdh1^{C156S}Pk (Figure 5.6) suggests that Gpd3 is resistant to hyperoxidation, similar to Tdh1^{C156S}Pk. Treatment with β-mercaptoethanol causes a mobility shift upwards of oxidised Gpd3Pk, detected using anti-Pk antibodies, raising the possibility that Gpd3 forms an intramolecular disulphide that protects it against hyperoxidation. The presence of Gpd3 in the Pk-epitope tagged strains could be influencing GAPDH oxidation, and could explain the presence of the two forms of oxidised GAPDH detected using anti-

GAPDH-SO_3 antibodies (Figure 5.6). To eliminate the effect of Gpd3, a strain was constructed lacking *gpd3*$^+$ in the wild-type Tdh1Pk or mutant Tdh1^{C156S}Pk background, and GAPDH oxidation examined.

Following treatment with 6.0 mM H_2O_2, wild-type Tdh1 (Tdh1PkΔ*gpd3*) was rapidly oxidised, displaying an increased mobility compared to before stress, suggestive of decreased AMS binding (Figure 5.7A). Importantly, the mobility of Tdh1^{C156S}PkΔ*gpd3* did not change following treatment with 6.0 mM H_2O_2, and no hyperoxidised GAPDH was detected, indicating that cysteine 152 was not oxidised in response to 6.0 mM H_2O_2 in Tdh1^{C156S}PkΔ*gpd3*. These data further support the findings of Peralta *et al*., (2015), that substitution of cysteine 156 to a serine prevents H_2O_2-induced oxidation of Tdh1. Unfortunately, due to an experimental issue, there was no protein in the 1 minute lane for Tdh1^{C156S}PkΔ*gpd3* (Figure 5.7A). Nevertheless, anti-GAPDH-SO_3 antibodies confirmed that Tdh1 becomes hyperoxidised in wild-type (Tdh1PkΔ*gpd3*) cells after treatment with 6.0 mM H_2O_2, whereas Tdh1^{C156S}PkΔ*gpd3* was not hyperoxidised (Figure 5.7A), suggesting that cysteine 156 is required for H_2O_2-induced oxidation of Tdh1. These data provide no evidence that the presence of *gpd3*$^+$ affected the ability of cysteine 156 of Tdh1 to become oxidised.

To determine if cysteine 156 was still required for Tdh1 to become oxidised, even at much higher concentrations of H_2O_2 than 6.0 mM, Tdh1PkΔ*gpd3* and Tdh1^{C156S}PkΔ*gpd3* cells were treated with 25.0 mM H_2O_2. Similar to 6.0 mM H_2O_2, oxidised Tdh1 is detected in wild-type (Tdh1PkΔ*gpd3*) following treatment with 25.0 mM H_2O_2 (Figure 5.7B). However, the presence of a faint band around the same molecular weight of oxidised Tdh1Pk suggests that although there is some irreversible oxidation of cysteine 152 in Tdh1^{C156S}PkΔ*gpd3* at 25.0 mM H_2O_2, this mutant is still much more resistant to H_2O_2-induced oxidation than wild-type (Tdh1PkΔ*gpd3*), even at much higher concentrations of H_2O_2.

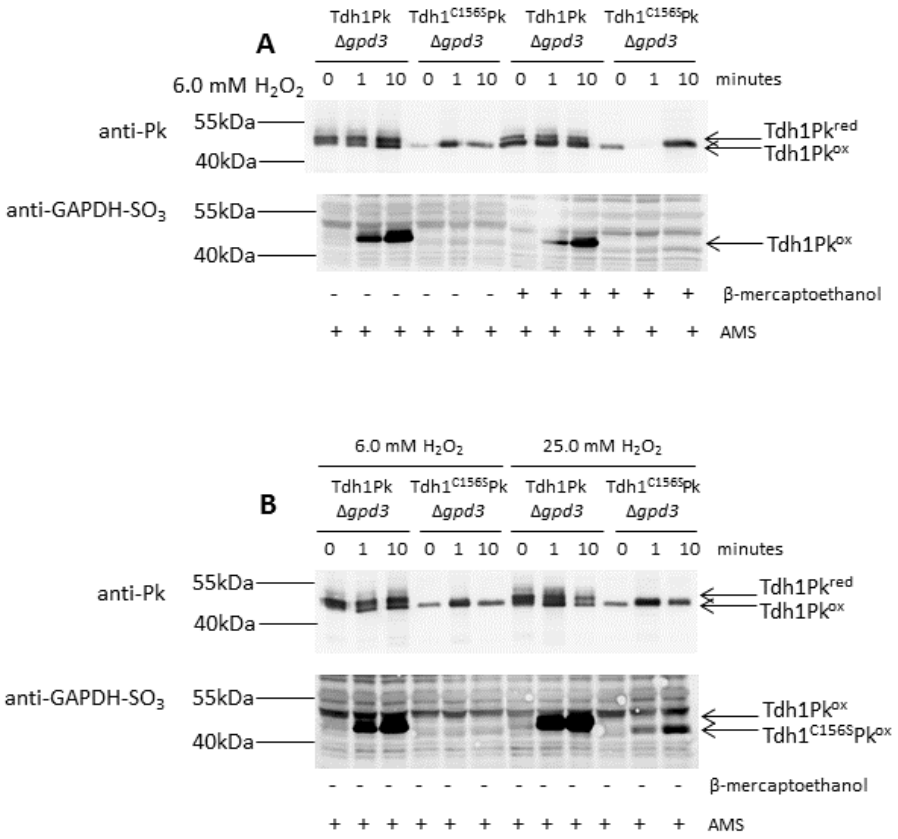

Figure 5.7 Cysteine 156 is required for H_2O_2-induced oxidation of Tdh1, in the absence of *gpd3*$^+$. Western blot analysis of Tdh1PkΔ*gpd3* (HL38) and Tdh1^{C156S}PkΔ*gpd3* (HL39) cells before and after treatment with (**A**) 6.0 mM H_2O_2, or (**B**) 25.0 mM H_2O_2, for 0, 1 and 10 minutes. Protein samples were treated, as indicated, with the thiol-binding agent AMS, and the reducing agent β-mercaptoethanol, prior to electrophoresis. Anti-Pk and anti-GAPDH-SO_3 antibodies were used to detect Pk-epitope tagged GAPDH and hyperoxidised GAPDH, respectively.

5.2.3 The sensitivity of Tdh1 to oxidation is important for the survival of *S. pombe* following exposure to H_2O_2

To investigate whether Tdh1 oxidation was important for oxidative stress resistance, we compared the ability of cells expressing wild-type Tdh1Pk and the H_2O_2-resistant Tdh1^{C156S}Pk mutant to grow in the presence of H_2O_2 (Figure 5.8), or to survive exposure to a lethal dose of H_2O_2 (25.0 mM) (Figure 5.9A). As expected, loss of *tdh1*$^+$ results in a severe growth defect, however there was no difference between the growth of wild-type (Gpd3Pk) and Tdh1^{C156S}Pk cells on plates containing H_2O_2 (Figure 5.8). This suggests that the sensitivity of Tdh1 to oxidation is not important for cells to adapt to chronic oxidative stress conditions. In contrast, cells expressing the oxidation-resistant Tdh1^{C156S}Pk were killed much more rapidly by 25.0 mM H_2O_2 than cells expressing either wild-type Tdh1Pk or Gpd3Pk (Figure 5.9A). For example, after 60 minutes exposure to 25.0 mM H_2O_2, only 22.0% Tdh1^{C156S}Pk cells had survived, whereas Tdh1Pk and Gpd3Pk cells only started to die after 120 minutes exposure to 25.0 mM H_2O_2. This suggested that the sensitivity of Tdh1 to oxidation is important for the survival of *S. pombe* following exposure to potentially toxic levels of H_2O_2.

To eliminate the possibility that the presence of *gpd3*$^+$ might affect cell survival following exposure to H_2O_2, we examined cell survival in Tdh1PkΔ*gpd3* and Tdh1^{C156S}PkΔ*gpd3*. Similarly, the survival of Tdh1^{C156S}PkΔ*gpd3* cells exposed to toxic doses of H_2O_2 was greatly reduced compared with Tdh1PkΔ*gpd3* cells, expressing wild-type Tdh1Pk that is sensitive to oxidation (Figure 5.9B). Only 14.3% Tdh1^{C156S}PkΔ*gpd3* cells survived 60 minutes exposure to 25.0 mM H_2O_2, whereas the viability of Tdh1PkΔ*gpd3* cells only started to drop after 180 minutes (Figure 5.9B). Together these data suggest that the sensitivity of Tdh1 to oxidation is important for the survival of *S. pombe* in response to high levels of H_2O_2.

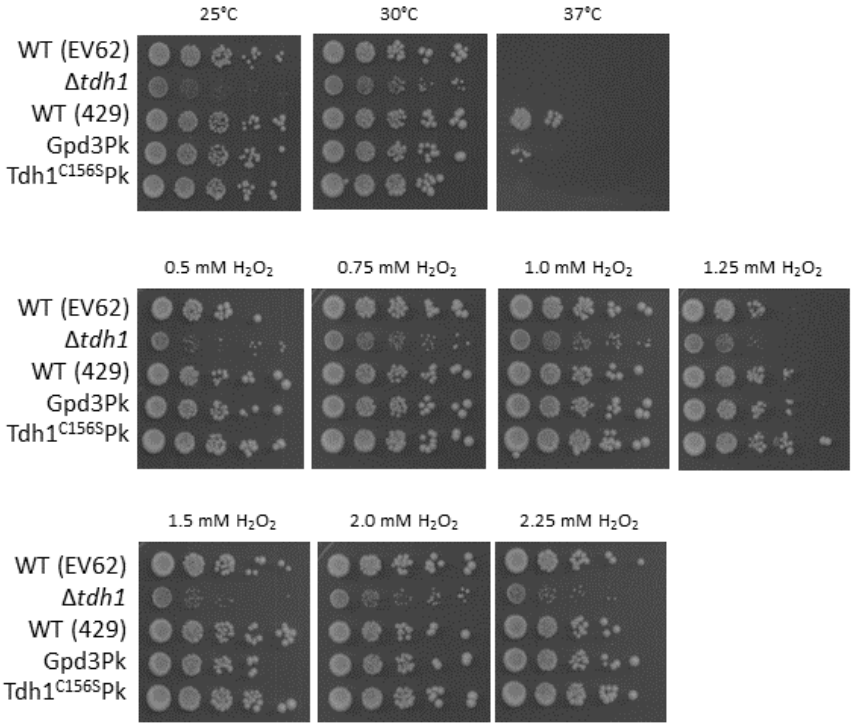

Figure 5.8 The effect of Tdh1 on the growth of cells under different conditions and in response to H_2O_2. Serial 10-fold dilutions of wild-type (EV62), Δ*tdh1* (ST3), wild-type (429), Pk-epitope tagged wild-type Gpd3 (Gpd3Pk) (ST2) and mutant Tdh1^{C156S}Pk (HL30) were spotted onto YE5S agar plates containing the indicated stress agents and incubated for 3-5 days at 30°C, unless otherwise stated.

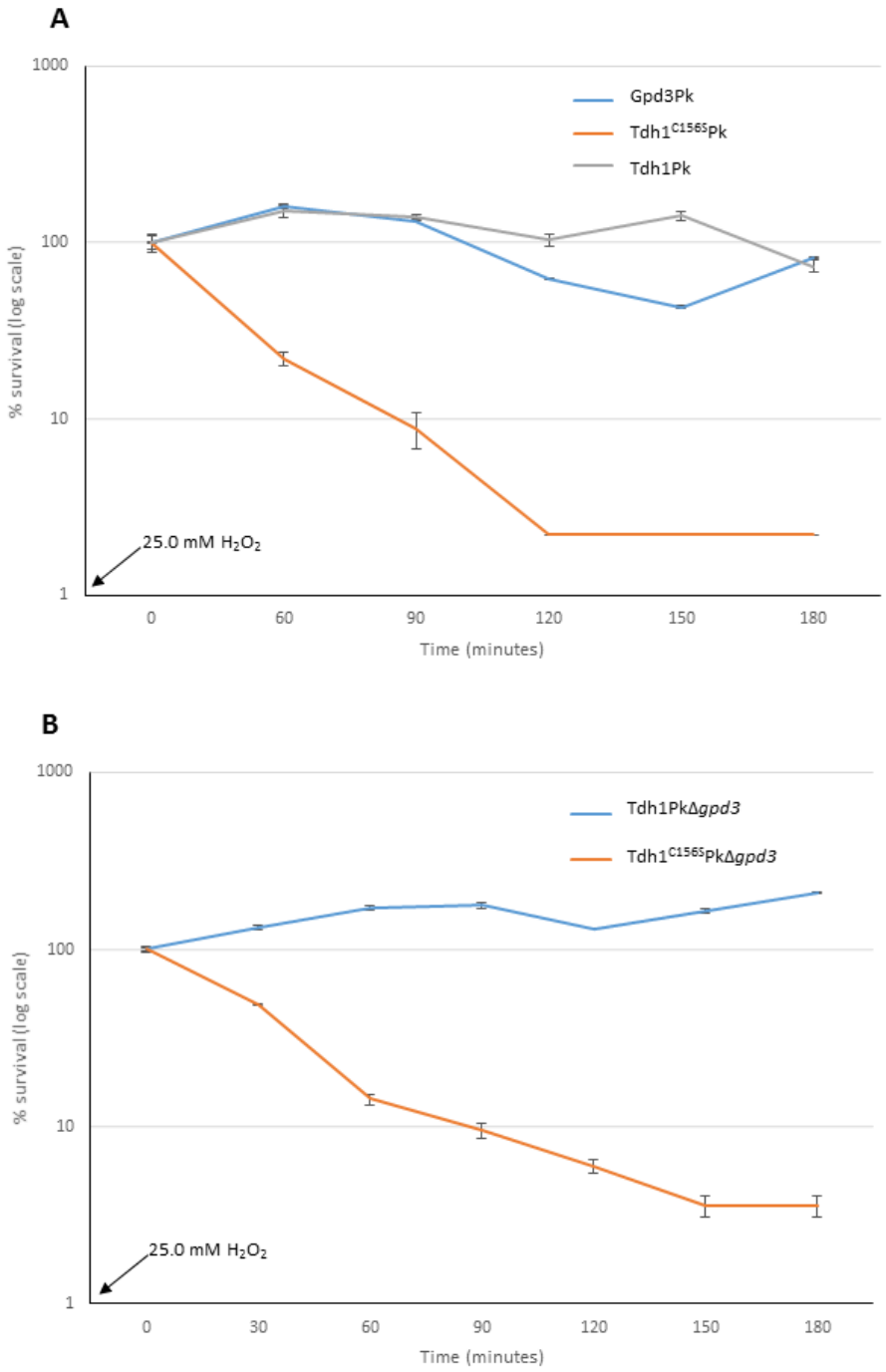

Figure 5.9 The sensitivity of Tdh1 to oxidation is important for the survival of *S. pombe* exposed to 25.0 mM H_2O_2. The viability of (**A**) Pk-epitope tagged wild-type Gpd3 (Gpd3Pk) (ST2), mutant Tdh1^{C156S}Pk (HL30), or wild-type Tdh1 (Tdh1Pk) (ST1), or (**B**) Tdh1PkΔ*gpd3* (HL38) and Tdh1^{C156S}PkΔ*gpd3* (HL39) was assessed (cfu) before and after treatment with 25.0 mM H_2O_2. Error bars indicate the range in values among duplicate plates (*n* = 2). This figure is a representative dataset from duplicate experiments.

5.2.4 The oxidation of Tdh1 is not important for the H_2O_2-induced activation of Sty1

Our data suggest that oxidation of Tdh1 is more important for survival of acute oxidative stress conditions than adaptation to low levels of oxidative stress (Figure 5.8 and 5.9A). Sty1 is important for adaptation to grow in the presence of low levels of H_2O_2 but also survival following exposure to high doses of H_2O_2 (Toone and Jones, 1998; Quinn *et al.*, 2002). Previous studies have shown that oxidation of the catalytic cysteine of Tdh1 is important for H_2O_2-induced Sty1 phosphorylation (Morigasaki *et al.*, 2008). Thus it was possible that the reduced ability of the oxidation resistant Tdh1^{C156S}Pk mutant to survive exposure to high levels of H_2O_2 (Figure 5.9A and 5.9B) might be due to impaired H_2O_2-induced activation of Sty1 in these cells. To test this hypothesis, we examined whether oxidation of Tdh1 affected H_2O_2-induced activation of Sty1 by comparing the H_2O_2-induced activation of Sty1 in cells expressing wild-type and oxidation-resistant forms of Tdh1.

When we compared the levels of Sty1 phosphorylation in Δ*tdh1* and the isogenic wild-type (EV62) over a range of concentrations of H_2O_2 we found that loss of *tdh1*$^+$ did not affect the increase in Sty1 phosphorylation induced by low (0.2 mM and 1.0 mM) concentrations of H_2O_2 (Figure 5.10A), but did reduce the level of phosphorylation of Sty1 induced in response to 6.0 mM H_2O_2 (Figure 5.10B). This was consistent with the idea that oxidation of Tdh1, that only occurs at these higher (6.0 mM) concentrations of H_2O_2, is important for Sty1 activation. However, this is in contrast to a previous study, which showed that Tdh1 was important for H_2O_2 stress signalling to Sty1 in response to lower (0.73 mM) concentrations of H_2O_2 (Morigasaki *et al.*, 2008).

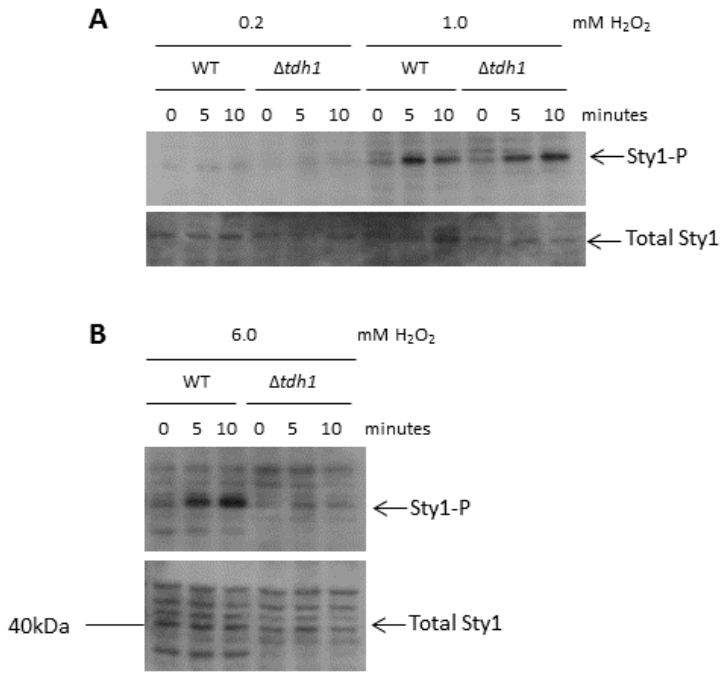

Figure 5.10 Tdh1 is important for H_2O_2-induced activation of Sty1 at 6.0 mM H_2O_2. (**A**)(**B**) Western blot analysis of levels of phosphorylated Sty1 in wild-type (EV62) or Δ*tdh1* (ST3) cells before and after treatment with the indicated concentrations of H_2O_2. Anti-pp38 and anti-Sty1 antibodies were used to detect phosphorylated Sty1 and total Sty1 levels, respectively.

To determine whether oxidation of Tdh1 is needed for the activation of Sty1 in response to H_2O_2, Sty1 phosphorylation was compared in cells expressing Gpd3Pk or the oxidation-insensitive Tdh1^{C156S}Pk mutant. Aside from the high basal Sty1 phosphorylation detected in Tdh1^{C156S}Pk, Sty1 activation in Tdh1^{C156S}Pk was comparable to wild-type (Gpd3Pk), with induction of Sty1 activation upon oxidative stress, with maximal Sty1 phosphorylation detected at 6.0 mM H_2O_2 (Figure 5.11A). Consistent with previous work, this suggests that cysteine 156 is not required for the H_2O_2-induced activation of Sty1. However, as we have shown that cysteine 156 is required for H_2O_2-induced oxidation of Tdh1 (Figure 5.6 and 5.7A), this also suggests that Tdh1 oxidation is not important for H_2O_2-induced Sty1 activation.

To eliminate the possibility that the presence of *gpd3*$^+$ might affect H_2O_2-induced phosphorylation of Sty1, the H_2O_2-induced activation of Sty1 was also compared between Tdh1PkΔ*gpd3* and Tdh1^{C156S}PkΔ*gpd3*. The H_2O_2-induced activation of Sty1 was again similar in cells expressing wild-type (Tdh1PkΔ*gpd3*) and H_2O_2-resistant Tdh1 (Tdh1^{C156S}PkΔ*gpd3*) (Figure 5.11B). In fact, there appeared to be slightly more phosphorylated Sty1 in mutant Tdh1^{C156S}PkΔ*gpd3* compared to Tdh1PkΔ*gpd3* at all concentrations of H_2O_2. This suggests that the sensitivity of Tdh1 to oxidation is not important for H_2O_2-induced Sty1 activation in *S. pombe*.

5.2.5 Substitution of cysteine 156 of Tdh1 reduces the catalytic activity of GAPDH

Having established that the hypersensitivity of cells expressing H_2O_2-resistant Tdh1^{C156S}Pk to acutely toxic doses of H_2O_2 does not reflect impaired activation of the Sty1 MAPK, we tested whether it might be because, in Tdh1^{C156S}Pk cells, GAPDH activity remains high after exposure to H_2O_2, preventing the rerouting of carbon to the PPP to generate NADPH. Consistent with Peralta *et al*., (2015), who showed that mutating the equivalent cysteine had no effect on the GAPDH activity of yeast and human GAPDH enzymes, our analysis indicated that Tdh1^{C156S}Pk was able to complement the growth defect of Δ*tdh1* mutant cells (Figure 5.8). Nevertheless, it was important to test whether substitution of cysteine 156 in Tdh1 affected GAPDH activity in *S. pombe*. GAPDH enzyme activity was determined in wild-type (EV62), Δ*tdh1*, Pk-epitope tagged wild-type (Gpd3Pk) and mutant Tdh1^{C156S}Pk cells.

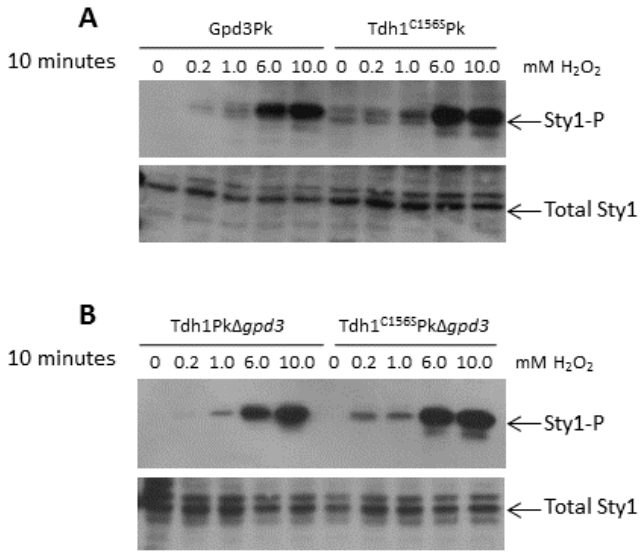

Figure 5.11 The oxidation of Tdh1 is not important for the H_2O_2-induced activation of Sty1. Western blot analysis of levels of phosphorylated Sty1 following 10 minute exposure of (**A**) Pk-epitope tagged wild-type Gpd3 (Gpd3Pk) (ST2) or mutant Tdh1^{C156S}Pk (HL30), or (**B**) Tdh1PkΔ*gpd3* (HL38) and Tdh1^{C156S}PkΔ*gpd3* (HL39) at the indicated concentrations of H_2O_2. Anti-pp38 and anti-Sty1 antibodies were used to detect phosphorylated Sty1 and total Sty1 levels, respectively.

Consistent with previous work from our laboratory (Taylor, 2009), loss of *tdh1*$^{+}$ caused a dramatic reduction in GAPDH enzyme activity compared to wild-type (EV62), indicating Tdh1 is the major contributor to cellular GAPDH activity (Figure 5.12). Intriguingly, Pk-epitope tagged wild-type (Gpd3Pk) cells had a slightly reduced GAPDH activity compared to untagged wild-type (EV62), in three biological repeats. This suggests that either the Pk-epitope tag or the associated restoration of uracil metabolism by the associated *ura4*$^{+}$ marker may affect GAPDH activity. Moreover, cells expressing Tdh1^{C156S}Pk had reduced GAPDH activity compared with those expressing wild-type Gpd3Pk, in three biological repeats (Figure 5.12). This raises the possibility that, in contrast to previous studies of GAPDH, cysteine 156 may be required for both the catalytic and peroxidatic activities associated with cysteine 152 of *S. pombe* Tdh1 (Peralta *et al.*, 2015). However, it is difficult to make firm conclusions without measuring GAPDH activity in the correct wild-type Tdh1Pk control. Additionally, it was possible that Gpd3Pk is expressed at higher levels than untagged Gpd3, which could explain why Gpd3Pk cells have higher GAPDH activity than Tdh1^{C156S}Pk (Figure 5.12).

As H_2O_2-induced oxidation of Tdh1 inhibits GAPDH activity, we expected that GAPDH activity would be resistant to H_2O_2-induced inactivation in cells expressing mutant Tdh1^{C156S}Pk. Hence, we tested the impact of H_2O_2 on GAPDH enzyme activity in cells expressing Pk-epitope tagged wild-type (Gpd3Pk) and Tdh1^{C156S}Pk *S. pombe* using 6.0 mM H_2O_2, that causes oxidation of Gpd3Pk and Tdh1 but not mutant Tdh1^{C156S}Pk (Figure 5.6). As expected, given the oxidation of Gpd3Pk and Tdh1 under these conditions, following 10 minutes exposure of wild-type (Gpd3Pk) cells to 6.0 mM H_2O_2, cellular GADPH activity decreased by 36.3% (Figure 5.13A). Notably, mutagenesis of cysteine 156 in Tdh1 caused a much greater reduction in GAPDH enzyme activity compared to wild-type (Gpd3Pk) in non-stressed conditions (Figure 5.13A), than observed in Figure 5.12, indicating there is some unexplained variation between experiments. Nevertheless, GAPDH activity was consistently reduced in Tdh1^{C156S}Pk in each of the three independent biological repeats conducted. Surprisingly, although Tdh1^{C156S}Pk was resistant to oxidation of its catalytic cysteine (Figure 5.6), we found there was a further reduction in GAPDH activity in cells expressing Tdh1^{C156S}Pk following exposure to 6.0 mM H_2O_2 (Figure 5.13A).

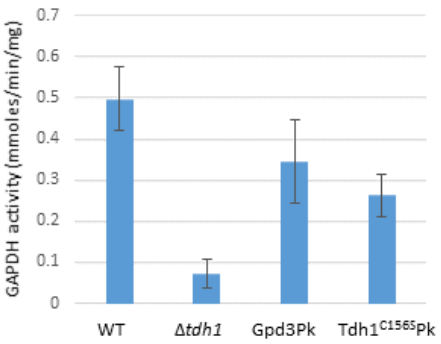

Figure 5.12 The effect of mutations and Pk-epitope tagging on cellular GAPDH activity. GAPDH activity was assayed in wild-type (EV62), Δ*tdh1* (ST3), Pk-epitope tagged wild-type Gpd3 (Gpd3Pk) (ST2) or mutant Tdh1^{C156S}Pk (HL30) cells. GAPDH activity is expressed as mmoles of NADH formed/minute/mg protein. Mean values are shown. Error bars indicate the range in values among 3 biological repeats (*n* = 3), each with two technical repeats.

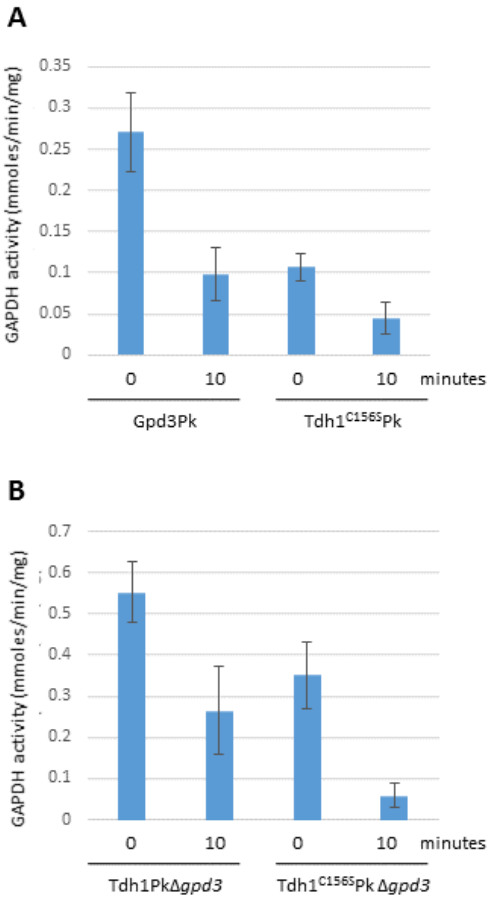

Figure 5.13 Substitution of cysteine 156 of Tdh1 reduces the glycolytic activity of GAPDH. GAPDH activity was assayed in (**A**) Pk-epitope tagged wild-type Gpd3 (Gpd3Pk) (ST2) or mutant Tdh1^{C156S}Pk (HL30), or (**B**) Tdh1PkΔ*gpd3* (HL38) and Tdh1^{C156S}PkΔ*gpd3* (HL39) cells before and after 10 minute exposure to 6.0 mM H_2O_2. GAPDH activity is expressed as mmoles of NADH formed/minute/mg protein. Mean values are shown. Error bars indicate the range in values among 3 biological repeats (*n* = 3).

Although it has previously been shown that loss of *gpd3*$^{+}$ has a negligible effect on GAPDH catalytic activity (Taylor, 2009), it remained possible that the presence of *gpd3*$^{+}$ in the Pk-epitope tagged wild-type and oxidation-insensitive mutant could be influencing GAPDH catalytic activity in these strains. For instance, it was possible that Gpd3 could be upregulated in the Tdh1^{C156S}Pk. Therefore, to eliminate this possibility and be sure that the only enzyme contributing to GAPDH activity is either wild-type or H_2O_2-resistant Tdh1, we re-examined the effect of cysteine 156 on GAPDH activity in the Δ*gpd3* mutant background. Similar to our observations in *gpd3*$^{+}$ cells, following exposure of Tdh1PkΔ*gpd3* to 6.0 mM H_2O_2, GAPDH activity was reduced by 47.9% (Figure 5.13B), consistent with Tdh1 becoming oxidised and inactivated. GAPDH activity was reduced in Tdh1^{C156S}PkΔ*gpd3* cells compared to Tdh1PkΔ*gpd3*, again suggesting that cysteine 156 is required for GAPDH activity. In addition, despite the insensitivity of this mutant to H_2O_2-induced oxidation, there was a further reduction of 16.7% in GAPDH activity following treatment with 6.0 mM H_2O_2 (Figure 5.13B).

As Tdh1^{C156S}PkΔ*gpd3* cells still exhibit reduced GAPDH activity compared to Tdh1PkΔ*gpd3*, this suggests that the potentially elevated levels of Gpd3Pk compared to untagged Gpd3 in Tdh1^{C156S}Pk is not the only explanation for the differences in GAPDH activity observed between strains in Figure 5.13A. Taken together, these experiments suggest that substitution of cysteine 156 in Tdh1 reduces the catalytic activity of Tdh1 prior to stress, and that following treatment with high (6.0 mM) concentrations of H_2O_2, Tdh1^{C156S}Pk can become further inactivated, by a mechanism that apparently does not involve oxidation of the catalytic cysteine. This is in contrast to previous studies, as it suggests that cysteine 156 of *S. pombe* Tdh1 is required for both the catalytic and peroxidatic activities of Tdh1. It also reveals that H_2O_2 can inhibit GAPDH activity by mechanisms that apparently do not involve oxidation of the catalytic cysteine.

5.2.6 Total levels of NADPH are reduced in Tdh1^{C156S}Pk compared to wild-type (Tdh1Pk)

A previous study has shown that inactivation of GAPDH results in an increased cellular NADPH/NADP ratio, causing the reroute of carbohydrates from glycolysis to the PPP (Ralser *et al.*, 2007). Loss of the

majority of the GAPDH activity in a Δ*tdh1* (Figure 5.12) may have the same effect on PPP metabolites as inactivation by oxidation, redirecting metabolic flux and thus increasing the reduction of NADP. We predicted that a Δ*tdh1* mutant would have much lower GAPDH activity, accompanied by an increase in the ratio of NADPH/NADP. To test this hypothesis, intracellular levels of NADPH and the NADPH/NADP ratio were assayed for wild-type (EV62) and a Δ*tdh1*. Intriguingly, levels of total NADPH+NADP, and the individual levels of NADPH and NADP, were all reduced compared with wild-type (EV62), suggesting that, in general, there is less NADP in mutant Δ*tdh1* than in wild-type cells (Figure 5.14). Nevertheless, there still appeared to be a slight increase in the NADPH/NADP ratio in Δ*tdh1* cells compared with wild-type, although this difference is small and the error bars overlap, indicating this was not statistically significant (Figure 5.14).

Data presented here indicates that mutant Tdh1^{C156S}Pk in *S. pombe* is resistant to H_2O_2-induced oxidation (Figure 5.6), but, surprisingly, exhibits reduced glycolytic activity (Figure 5.13A). As inactivation of GAPDH leads to an increase in NADPH/NADP ratio (Ralser *et al.*, 2007), levels of NADPH and NADP were investigated in the oxidation-resistant Tdh1 mutant. The effect of H_2O_2 on NADPH levels was assayed as GAPDH activity becomes oxidised and inactivated following exposure to ≥1.0 mM H_2O_2 in wild-type cells (Figure 5.4A and 5.4B). A striking reduction in total levels of NADPH+NADP was observed in Tdh1^{C156S}Pk compared to wild-type (Gpd3Pk), both before and after treatment with 6.0 mM H_2O_2 (Figure 5.15). Unexpectedly, this data raised the possibility that cysteine 156 of Tdh1 is required for maintenance of intracellular levels of both reduced and oxidised NADP. As total levels of NADPH+NADP, and therefore the individual levels of NADPH and NADP, are reduced in Tdh1^{C156S}Pk compared to wild-type (Gpd3Pk), the corresponding NADPH/NADP ratio is similar between wild-type and the oxidation-resistant Tdh1 mutant, and doesn't change much upon H_2O_2 treatment (Figure 5.15).

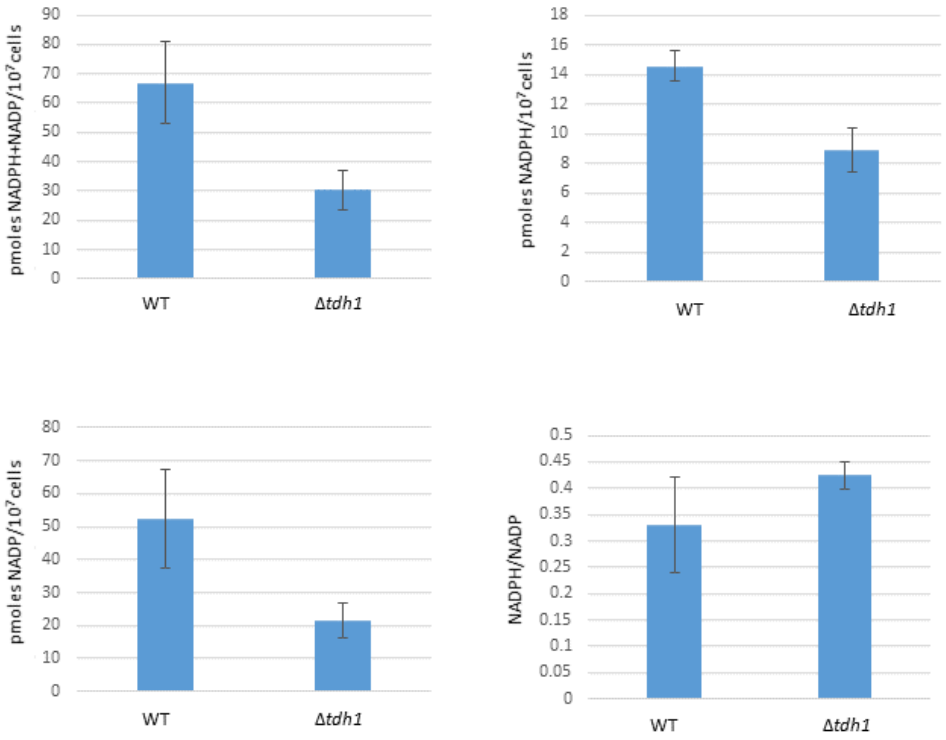

Figure 5.14 Loss of *tdh1*$^+$ reduces the total levels of NADPH and NADP. Intracellular levels of total NADPH+NADP, NADPH, NADP, and the NADPH/NADP ratio were assayed in wild-type (EV62) and Δ*tdh1* (ST3). Intracellular levels of total NADPH+NADP, NADPH and NADP are expressed as pmoles of total NADPH+NADP, NADPH or NADH/10^7cells. Mean values are shown. Error bars indicate the range in values among 3 biological repeats (*n* = 3), each with two technical repeats.

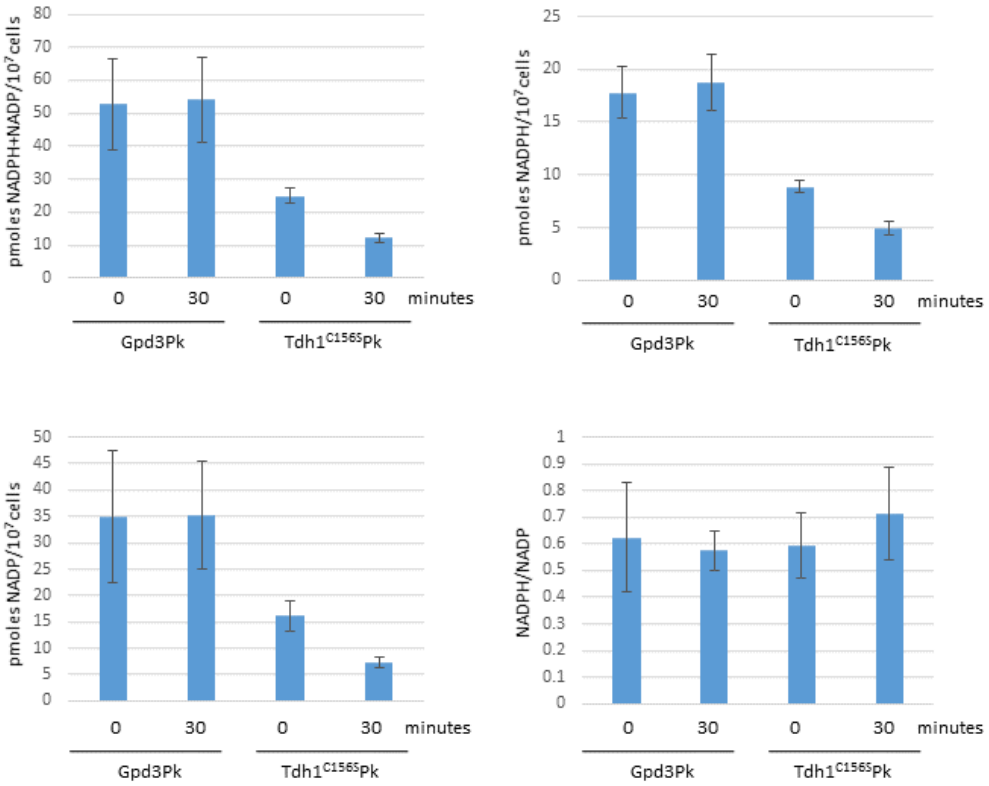

Figure 5.15 The effect of H_2O_2 treatment on levels of reduced and oxidised NADP in wild-type and Tdh1^{C156S}Pk. Intracellular levels of total NADPH+NADP, NADPH, NADP, and the NADPH/NADP ratio were assayed in Pk-epitope tagged wild-type Gpd3 (Gpd3Pk) (ST2) or mutant Tdh1^{C156S}Pk (HL30) before and after exposure to 6.0 mM H_2O_2 for the indicated times. Intracellular levels of total NADPH+NADP, NADPH and NADP are expressed as pmoles of total NADPH+NADP, NADPH or NADH/10^7cells. Mean values are shown. Error bars indicate the range in values among 3 biological repeats (*n* = 3), each with two technical repeats.

To eliminate the possibility that some of the differences in total NADPH levels and ratios were not due to Gpd3Pk or untagged Gpd3, we next examined intracellular levels of NADPH in Tdh1Pk*Δgpd3* and Tdh1^{C156S}Pk*Δgpd3* cells. In contrast to experiments in which Gpd3Pk or Gpd3 was present, where substantial differences were observed between Gpd3Pk cells expressing wild-type Tdh1 and Tdh1^{C156S}Pk containing Gpd3, total NADPH+NADP levels and the individual levels of NADPH and NADP were only very slightly reduced in Tdh1^{C156S}Pk*Δgpd3* compared to Tdh1Pk*Δgpd3* (Figure 5.16). This suggests that altered activity of Gpd3 may account for some of the differences in NADPH levels observed in Figure 5.15. However, following exposure to 6.0 mM H_2O_2, the total and individual levels of NADPH and NADP in Tdh1^{C156S}Pk*Δgpd3* were reduced compared to Tdh1Pk*Δgpd3* (Figure 5.16). These data have detected a remarkable and unexpected reduction in the levels of total NADPH+NADP, due to mutation of cysteine 156 of Tdh1. However, despite the differences in these levels, the NADPH/NADP ratios are similar in cells expressing either Tdh1Pk or the Tdh1^{C156S}Pk mutant, either in the presence or absence of *gpd3*$^{+}$, and don't change following treatment with H_2O_2 (Figure 5.15 and 5.16). This suggests that the ability of Tdh1 to become oxidised does not affect the intracellular NADPH/NADP ratio, but that it is important following treatment with H_2O_2, to prevent a reduction in total levels of NADPH/NADP.

5.2.7 Total glutathione levels are similar in wild-type and a Δ*tpx1*

Similar to Tdh1 (Figure 5.10B), the 2-Cys Prx, Tpx1, is also important for activation of Sty1 at 6.0 mM H_2O_2 but, like Tdh1, the peroxide-reacting cysteine in Tpx1 is hyperoxidised to sulphinic (SO_2) and sulphonic (SO_3) acid derivatives at these concentrations (Bozonet *et al.*, 2005). Intriguingly, unpublished work from our laboratory has suggested that Tpx1 is required for the hyperoxidation and inactivation of Tdh1, as anti-GAPDH-SO_3 antibodies did not detect any increase in hyperoxidised GAPDH in Δ*tpx1* mutant cells (Day and Veal unpublished work).

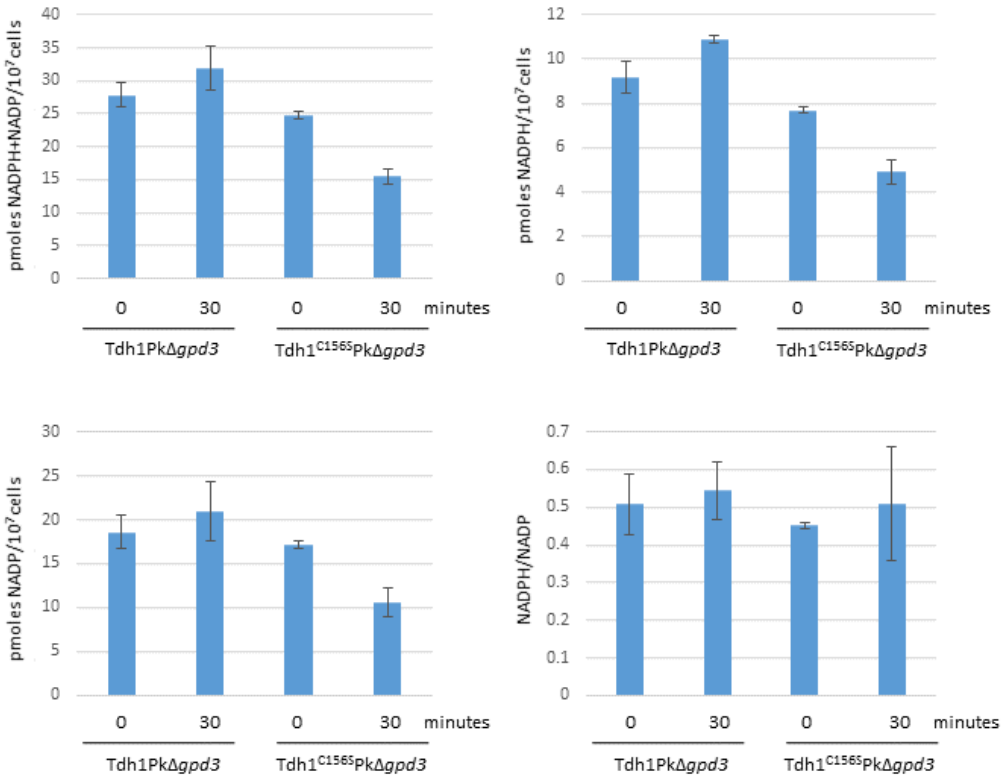

Figure 5.16 The effect of H_2O_2 treatment on levels of reduced and oxidised NADP in cells where Tdh1 and Tdh1^{C156S}Pk are the only GAPDH. Intracellular levels of total NADPH+NADP, NADPH, NADP, and the NADPH/NADP ratio were assayed in Tdh1PkΔ*gpd3* (HL38) and Tdh1^{C156S}PkΔ*gpd3* (HL39) before and after exposure to 6.0 mM H_2O_2 for the indicated times. Intracellular levels of total NADPH+NADP, NADPH and NADP are expressed as pmoles of total NADPH+NADP, NADPH or NADH/10^7cells. Mean values are shown. Error bars indicate the range in values among 3 biological repeats (*n* = 3).

When we investigated this further, using AMS to separate oxidised and reduced forms of GAPDH, that were then detected with anti-GAPDH or anti-GAPDH-SO_3 antibodies, we confirmed this observation that, in contrast to wild-type, there was no detectable increase in hyperoxidised GAPDH in Δ*tpx1* cells exposed to 6.0 mM H_2O_2 (Figure 5.17A, labelled $GAPDH^{ox2}$). However, western blot analysis showed that GAPDH was still oxidised in Δ*tpx1* mutant cells (Figure 5.17A, labelled $GAPDH^{ox}$), but that other forms, with mobilities and β-mercaptoethanol-sensitivity consistent with them involving reversible disulphides with glutathione ($GAPDH^{-SSG}$) or other cysteines in Tdh1, predominated instead (Figure 5.17A and 5.17B).

Anti-GAPDH-SO_3 antibodies detect hyperoxidised GAPDH, and confirmed that GAPDH cannot become hyperoxidised in Δ*tpx1* cells exposed to 6.0 mM H_2O_2 (Figure 5.17A). This indicates that, although Tdh1 is still oxidised in a Δ*tpx1* exposed to 6.0 mM H_2O_2, it cannot be hyperoxidised, indicating that Tpx1 promotes the hyperoxidation of Tdh1. Based on this, it suggests that oxidation to the sulphenylated (SO) form may be more readily stabilised, by the rapid formation of a β-mercaptoethanol-sensitive, reversibly oxidised form in a Δ*tpx1* mutant.

One possible mechanism by which Tdh1 is protected from hyperoxidation of the sulphenylated form, to the sulphinylated and sulphonylated forms, in a Δ*tpx1* in *S. pombe* would be if Tdh1 was more rapidly glutathionylated, potentially due to increased levels of glutathione. Indeed, previous work has shown that loss of the 2-Cys Prx, PRDX-2, in the nematode worm *Caenorhabditis elegans*, caused these animals to contain approximately twice as much total glutathione (GSH) compared to wild-type (Olahova *et al.*, 2008). Taken together, this led us to hypothesise that a Δ*tpx1* might contain increased levels of total glutathione.

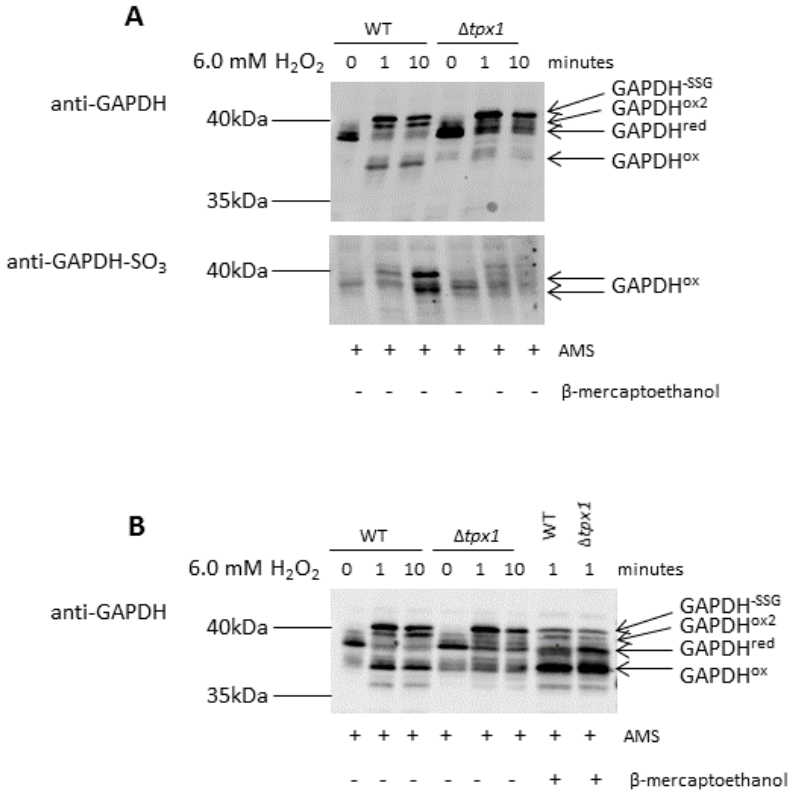

Figure 5.17 The effect of Tpx1 on H_2O_2-induced Tdh1 oxidation. (**A**)(**B**) Western blot analysis of wild-type (NT4) or mutant Δ*tpx1* (VXOO) cells before and after treatment with 6.0 mM H_2O_2. Protein samples were treated, as indicated, with the thiol-binding agent AMS, and the reducing agent β-mercaptoethanol, prior to electrophoresis. Anti-GAPDH and anti-GAPDH-SO_3 antibodies were used to detect total GAPDH and hyperoxidised GAPDH, respectively.

The levels of total glutathione were determined in cells lacking *tpx1*$^+$ compared to wild-type (NT4). The glutathione assay was used to detect both total and oxidised (GSSG) forms of glutathione, allowing levels of reduced (GSH) glutathione to be calculated from these values. The ratio of reduced to oxidised glutathione (GSH/GSSG) was then calculated, with this ratio acting as an indicator of cellular health. However, levels of intracellular GSSG in unstressed cells are extremely low, and therefore prone to high error, therefore measurements of GSSG and ratios of GSH/GSSG were likely to be less accurate. However, we found that the total intracellular glutathione levels were similar in wild-type (NT4) and Δ*tpx1* cells (Figure 5.18), detected in millimolar concentrations (~3.0 mM). This suggests that there are other reasons why Tdh1 is protected against irreversible oxidation in a Δ*tpx1*.

5.2.8 The effect of Tdh1 on H_2O_2-induced Tpx1 oxidation

Both Tdh1 (Figure 5.10B) and Tpx1 are required for normal levels of Sty1 activation in response to 6.0 mM H_2O_2. In addition, Tpx1 is required for the hyperoxidation of Tdh1 (Figure 5.17A), however the effect of loss of *tdh1*$^+$ on the oxidation of Tpx1 has not been investigated. The bands labelled Tpx1 monomeric forms represent both reduced and hyperoxidised (Tpx1-$SO_{2/3}$) forms of Tpx1 (Figure 5.19). The increase in the Tpx1 monomeric forms in Δ*tdh1* at 1, 5 and 10 minutes following treatment with 0.2 mM H_2O_2 suggests that there may be more formation of Tpx1-$SO_{2/3}$ at 0.2 mM H_2O_2 than normally observed in wild-type (EV62) (Figure 5.19). In addition, the doublet detected in Δ*tdh1* mutant would be consistent with an increase in hyperoxidised Tpx1-$SO_{2/3}$, which would be expected to have a slightly increased mobility, due to binding one rather than two AMS molecules. This suggests that lack of *tdh1*$^+$ may be affecting Tpx1 oxidation by promoting hyperoxidation to Tpx1-$SO_{2/3}$, however, probing with anti-Prx-SO_3 antibodies, which specifically detect hyperoxidised Prx, would be needed to confirm this.

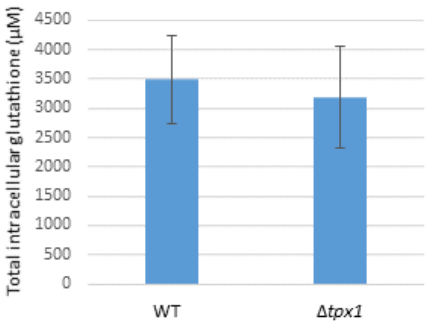

Figure 5.18 Wild-type (NT4) and Δ*tpx1* cells contain similar levels of glutathione. Intracellular levels of total glutathione (µM) were assayed in wild-type (NT4) or mutant Δ*tpx1* (VXOO) cells. Error bars indicate the range in values among 4 biological repeats (*n* = 4), each with two technical repeats.

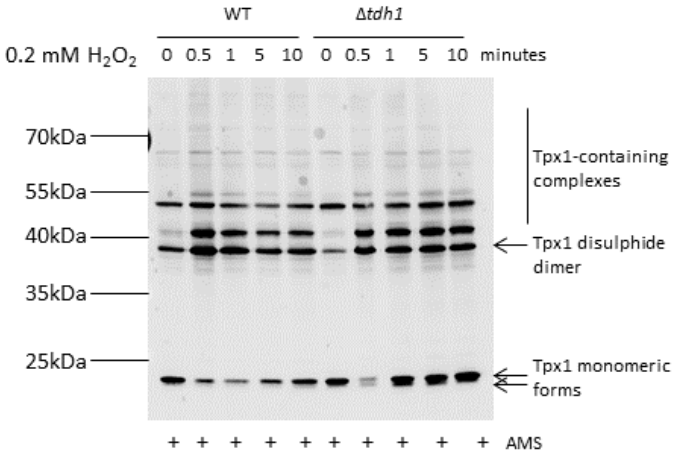

Figure 5.19 The effect of Tdh1 on H_2O_2-induced Tpx1 oxidation. Western blot analysis of wild-type (EV62) or Δ*tdh1* (ST3) cells before and after treatment with 0.2 mM H_2O_2. Anti-3269 antibody was used to detect Tpx1. The different bands are indicated and the molecular weight (MW) markers are shown.

5.3 Discussion

GAPDH functions as a glycolytic enzyme, but has also been shown to be a multifunctional protein with many other activities in signal transduction (For reviews see (Sirover, 2011; Hildebrandt *et al.*, 2015)). GAPDH contain catalytic cysteine residues that are susceptible to oxidation by H_2O_2, which can act as an important protective response to H_2O_2, increasing NADPH production by the PPP (Figure 5.2A). Based on the work of Peralta *et al*., (2015), we generated a Tdh1 mutant that is predicted to be resistant to H_2O_2-induced oxidation. Data presented here suggests that cysteine 156 of Tdh1 is required for the H_2O_2-induced oxidation of Tdh1 (Figure 5.6 and 5.7A), and that the sensitivity of Tdh1 to oxidation is important for the survival of *S. pombe* following exposure to potentially toxic levels of H_2O_2 (Figure 5.9A and 5.9B). In addition, the oxidation of Tdh1 is not important for H_2O_2-induced Sty1 activation (Figure 5.11A and 5.11B). However, in contrast to previous studies, here we present data that suggests that cysteine 156 of *S. pombe* Tdh1 is required for both the glycolytic (Figure 5.13A and 5.13B) and peroxidatic activities of Tdh1.

Consistent with previous studies, this chapter has provided evidence that GAPDH becomes oxidised and inactivated following exposure of cells to H_2O_2, whereby H_2O_2-induced oxidation of endogenous Tdh1 correlates with H_2O_2-dependent inactivation of GAPDH activity at concentrations ≥1.0 mM H_2O_2 (Figure 5.4A and 5.4B). H_2O_2-induced oxidation of GAPDH is an important protective response to H_2O_2. Importantly, here we have shown that the oxidation of a GAPDH Tdh1 is important for survival under acute stress conditions (Figure 5.9A and 5.9B). However, the fact that GAPDH is only oxidised at such high concentrations of H_2O_2 has implications for its responses, and suggests that oxidation of GAPDH is a signalling event that only occurs when cells are exposed to doses of H_2O_2 they are unable to cope with, i.e. an acute survival response. This is consistent with previous findings in *S. cerevisiae*, which found that only high, cell death-inducing concentrations of H_2O_2 caused oxidation and inactivation of GAPDH, and that GAPDH activity is largely unresponsive to low or moderate regulatory levels of H_2O_2 (Cyrne *et al.*, 2010).

The catalytic cysteine, cysteine 152, of GAPDH is intrinsically more sensitive to oxidation than most cytosolic cysteine residues, and can become sulphenylated, sulphinylated and sulphonylated in response to H_2O_2 (Peralta *et al.*, 2015). The sulphenylated form of GAPDH can become glutathionylated, protecting GAPDH against irreversible hyperoxidation. Glutathionylation of cysteine thiols has emerged as a potential mechanism in the regulation of a variety of regulatory and signalling proteins, contributing to the regulation of signalling pathways (For a review see (Dalle-Donne *et al.*, 2007)). Here we present findings that suggest that Tpx1 is required for the hyperoxidation of Tdh1 (Figure 5.17A and 5.17B). In response to H_2O_2, GAPDH can become oxidised in both wild-type (NT4) and a Δ*tpx1*, however whilst there was no detectable increase in hyperoxidised GAPDH in a Δ*tpx1* mutant, other forms were present, indicative of glutathionylated GAPDH (Figure 5.17A). This indicates that Tpx1 is required for the irreversible oxidation and inactivation of Tdh1 by hyperoxidation of its catalytic cysteine. The regulation of GAPDH by glutathionylation results in inhibition of its glycolytic activity (Little and O'Brien, 1969), but protects GAPDH from irreversible hyperoxidation through further exposure to H_2O_2. Interestingly, despite the more rapid glutathionylation of Tdh1 in a Δ*tpx1* mutant compared to wild-type, the total intracellular glutathione levels were similar in wild-type (NT4) and Δ*tpx1* cells (Figure 5.18), suggesting that there are other reasons why Tdh1 is protected against irreversible oxidation in a Δ*tpx1*. This could suggest that in *S. pombe* cells lacking *tpx1*$^+$, it is favourable for GAPDH to become glutathionylated, which can be readily reduced via disulphide exchange reactions using the thioredoxin system and glutaredoxins, rather than for GAPDH to become hyperoxidised and inactivated. Behind Prx, GAPDH are the most reactive proteins in the cytosol, owing to their high abundance and specific H_2O_2 sensitivity (Winterbourn and Hampton, 2008). Initially, Prx maintain low levels of H_2O_2, leading to a reduction in NADPH levels due to the Prx catalytic mechanism. However, once H_2O_2 concentrations increase, GAPDH can become sulphenylated and subsequently glutathionylated. Glutathionylation of GAPDH keeps GAPDH inactive until NADPH levels are restored to steady-state levels, to allow the reductive reactivation of GAPDH. In the absence of Prx, GAPDH may act as a first line of defence to keep H_2O_2 levels low, therefore the formation of reversible

glutathionylated GAPDH, rather than irreversible hyperoxidised GAPDH, would be favourable. Consistent with this idea, glutathionylated but not hyperoxidised GAPDH is detected in the absence of the 2-Cys Prx, *tpx1*$^{+}$, in *S. pombe* (Figure 5.17A).

Unfortunately, Pk-epitope tagged wild-type strains (Tdh1Pk and Gpd3Pk) were mixed up in the Veal lab strain collection, and this problem was only detected late on in the project. However, this allowed us to investigate the sensitivities of the two GAPDH isoforms in *S. pombe*, Tdh1 and Gpd3, to H_2O_2-induced oxidation. Both wild-type Tdh1 (Tdh1Pk) and Gpd3 (Gpd3Pk) were rapidly oxidised to AMS-resistant forms following treatment with 6.0 mM H_2O_2 (Figure 5.6). Anti-GAPDH-SO_3 antibodies were used to detect hyperoxidised GAPDH in Tdh1Pk and Gpd3Pk; whilst hyperoxidised Tdh1Pk was detected as the prominent band in wild-type Tdh1 (Tdh1Pk) cells, with a faint band representing hyperoxidised endogenous Gpd3, on the other hand, hyperoxidised endogenous Tdh1 was the prominent band in wild-type Gpd3 (Gpd3Pk) cells, with hyperoxidised Gpd3Pk being a much fainter band (Figure 5.6). Intriguingly, this suggests that Gpd3 is resistant to hyperoxidation, similar to Tdh1^{C156S}Pk, but may instead be more readily reversibly oxidised. To eliminate the effect of Gpd3, we constructed Tdh1Pk and Tdh1^{C156S}Pk strains also lacking *gpd3*$^{+}$, therefore Tdh1Pk and Tdh1^{C156S}Pk were the only GAPDH present in these cells. However, as these strains were only constructed late on during the project, some experiments involving Tdh1PkΔ*gpd3* and Tdh1^{C156S}PkΔ*gpd3* would need repeating before final conclusions can be drawn; NADPH levels and GAPDH activity were measured in three independent biological repeats, however the H_2O_2-induced oxidation of Tdh1 and the H_2O_2-induced phosphorylation of Sty1 were only examined once.

We show that cysteine 156 in the active site of Tdh1 is important for the H_2O_2-induced oxidation of Tdh1 (Figure 5.6 and 5.7A), but that this oxidation is not important for the H_2O_2-induced activation of Sty1 in *S. pombe* (Figure 5.11A and 5.11B). As the predominant GAPDH isoform in *S. pombe*, Tdh1, is important in the activation of Sty1 specifically in response to high (6.0 mM) levels of H_2O_2 (Figure 5.10B), this may represent a way to modify Sty1 activity according to the intensity of the stimulus, and

to increase antioxidant expression. However, although the oxidation of Tdh1 is not important for the H_2O_2-induced activation of Sty1, our data suggests that Tdh1 is only required for activation of Sty1 at concentrations when Tdh1 is oxidised, implying that the activation of Sty1 in response to H_2O_2 is unlikely to involve only reduced Tdh1 (Figure 5.20). Hence, it remains unclear the role of Tdh1 oxidation in protecting cells against acute oxidative stress.

Our observation that cysteine 156 of Tdh1 is important for the H_2O_2-induced oxidation of Tdh1 (Figure 5.6 and 5.7A) is consistent with the findings of Peralta *et al.*, (2015), who determined that cysteine 156 was required for the oxidation of cysteine 152. Molecular dynamics (MD) simulations of human GAPDH confirmed that the distance between cysteine 152 and cysteine 156 was stably maintained at ~9 Å, and showed that cysteine 156 was not accessible for H_2O_2 (Peralta *et al.*, 2015). In addition, mass spectrometry identified sulphonylated and glutathionylated cysteine 152, but there was no evidence of these H_2O_2-induced oxidative modifications of cysteine 156 (Peralta *et al.*, 2015). These findings suggested that cysteine 156 influences cysteine 152 indirectly. However, this is in contrast to previous studies which have suggested that substitution of cysteine 156 with serine (C156S) in *S. pombe* Tdh1 does not affect H_2O_2-induced Tdh1 oxidation (Morigasaki *et al.*, 2008). However, the detection of cysteine oxidation of Tdh1 in the study by Morigasaki *et al.*, (2008) was conducted using a biotin-switch method, which swaps an oxidative modification for a stable and easily detectable biotin-tag. This assay is based on the assumption that only an oxidatively modified cysteine residue will become biotinylated. Therefore, false positive signals can occur if non-oxidised thiols are not blocked with an appropriate agent, such as IAA or NEM. This could help explain the differences in susceptibility to H_2O_2-induced oxidation of Tdh1^{C156S}Pk between this study and the work of Morigasaki *et al.*, (2008).

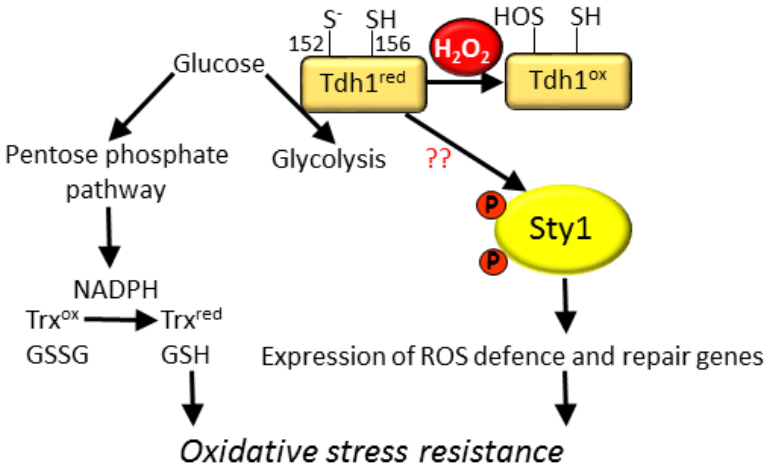

Figure 5.20 Model for the role of GAPDH in responses to H_2O_2. Under non-stressed conditions, glucose can be used in glycolysis or in the pentose phosphate pathway (PPP) to generate NADPH. Upon exposure to H_2O_2, GAPDH becomes oxidised on cysteine 152 to the sulphenic acid (-SOH). In *S. pombe*, although the oxidation of Tdh1 is not important for the H_2O_2-induced activation of the Sty1 MAPK (??), our data suggests that Tdh1 is only required for activation of Sty1 at concentrations when Tdh1 is oxidised. It remains unclear how oxidation of Tdh1 protects cells against acute oxidative stress.

In contrast to the findings of Peralta *et al.*, (2015), this study has revealed that substitution of cysteine 156 of Tdh1 reduces the glycolytic activity of GAPDH both before and following treatment with 6.0 mM H_2O_2 (Figure 5.13A and 5.13B). In this study, initial rates of GAPDH enzyme activity were determined using a spectrophotometer by measuring the formation of NADH at 340 nm for one minute. However, in the study by Peralta *et al.*, (2015), initial rates were measured during the first 5-15 minutes using an automated plate reader. This could help explain the differences observed in the GAPDH activity in mutant Tdh1^{C156S}Pk between the two studies. Despite the unexplained variation between experiments investigating GAPDH activity, mutagenesis of cysteine 156 caused a reduction in cellular GAPDH activity compared to both wild-type strains (Gpd3Pk and Tdh1PkΔ*gpd3*), in each of three independent biological repeats conducted. This suggests that cysteine 156 of *S. pombe* Tdh1 is required for both the glycolytic and peroxidatic activities of Tdh1. In addition, despite Tdh1^{C156S}Pk being resistant to H_2O_2-induced oxidation, the activity of Tdh1^{C156S}Pk can become further inactivated (Figure 5.13A and 5.13B). This may indicate that an additional mechanism may have evolved to inhibit Tdh1 that doesn't require cysteine 156, or oxidation of the catalytic cysteine, cysteine 152, following treatment with H_2O_2.

Whilst the total intracellular levels of NADPH+NADP remain fairly constant in both wild-type strains (Gpd3Pk and Tdh1PkΔ*gpd3*) upon exposure to H_2O_2, these levels are reduced in mutant Tdh1^{C156S}Pk following treatment with 6.0 mM H_2O_2 (Figure 5.15 and 5.16). In addition, we observed a difference in the total NADPH+NADP levels in mutant Tdh1^{C156S}Pk in the presence or absence of the minor *S. pombe* GAPDH isoform, *gpd3*$^{+}$, before treatment with H_2O_2 (Figure 5.15 and 5.16). Taking this result, together with the fact that the activity of Tdh1^{C156S}Pk becomes further H_2O_2-induced inactivated (Figure 5.13A and 5.13B), this indicates that the ability of Tdh1 to become oxidised affects intracellular redox homeostasis, and regulates the total intracellular levels of NADPH+NADP, only following treatment with H_2O_2. These data have detected a novel and unexpected finding that intracellular levels of reduced and oxidised NADP are reduced, due to mutation of cysteine 156 of Tdh1. This was unpredicted based on previous work into GAPDH inactivation on cellular NADPH/NADP ratio, and

cannot be rationalised in terms of changes in PPP metabolites. Instead, this could imply that another process, such as NAD kinase, which phosphorylates NAD to NADP, is leading to loss of NADP, affected by substitution of cysteine 156 to a serine, and in response to H_2O_2. As levels of NADP are lower in Tdh1^{C156S}Pk compared to wild-type (Figure 5.15 and 5.16), this could suggest that the activity of NAD kinase might be reduced in this mutant, and interestingly that cysteine 156 of Tdh1 might be regulating NAD kinase. There are three NAD kinase genes in *S. pombe* (SPAC1B1.02c, SPAC3H5.11 and SPCC24B10.02c), therefore investigations into their mRNA or protein levels could be conducted to determine if they were reduced in mutant Tdh1^{C156S}Pk. Alternatively, overexpression of one of the NAD kinase genes in a Tdh1^{C156S}Pk could be investigated to observe if this restores oxidative stress resistance. Finally, the levels of NAD could be compared between wild-type and mutant Tdh1^{C156S}Pk, which we would predict would be reduced in Tdh1^{C156S}Pk.

In addition to the role of Tpx1 in promoting the oxidation of Tdh1 at high concentrations of H_2O_2 (Figure 5.17A), unpublished work from our laboratory has shown that both Tpx1 and Tdh1 are required for the H_2O_2-induced activation and phosphorylation of the MAPKK Wis1 at high levels of H_2O_2. The use of phos-tag gels, which allow greater separation of phosphorylated and non-phosphorylated proteins, showed a mobility shift consistent with an increase in the phosphorylation of Wis1 in response to high (6.0 mM) concentrations of H_2O_2 and to an osmotic stress of 0.6 M KCl, but not to low (0.2 and 1.0 mM) concentrations of H_2O_2 (Day and Veal unpublished data). However, Wis1 does not become phosphorylated in response to 6.0 mM H_2O_2, in the absence of either *tpx1*$^+$ or *tdh1*$^+$ (Day and Veal unpublished data). This is consistent with the idea that Tpx1 is acting through Tdh1 to promote the activation of Sty1 by high concentrations of H_2O_2, and that increased Wis1 phosphorylation might only be important for H_2O_2-induced phosphorylation of Sty1 at high levels of H_2O_2. In addition, as both Tpx1 and Tdh1 are required for the H_2O_2-induced phosphorylation of Wis1 at high levels of H_2O_2, this suggests that Tpx1 may act as a 'scaffold' to bring the components of the Sty1 MAPK pathway together. This study has suggested that the ability of Tdh1 to become oxidised is

not important for the H_2O_2-induced activation of Sty1 (Figure 4.20), however whether oxidation of Tdh1 is important for H_2O_2-induced phosphorylation of Wis1 could be investigated.

In summary, the results described in this chapter highlight that cysteine 156 of Tdh1 is required for H_2O_2-induced oxidation of Tdh1 in *S. pombe*, and in the survival of *S. pombe* following exposure to potentially toxic levels of H_2O_2, however the ability of Tdh1 to become oxidised is not important for H_2O_2-induced activation of the MAPK Sty1. Therefore, it remains unclear the reason that oxidation of Tdh1 protects cells against acute oxidative stress, as it is not by the activation of Sty1. In addition, our data has highlighted that Tpx1 is required for the hyperoxidation of Tdh1, and for the oxidation of Pyp1 (Chapter 3), therefore it is possible that Tpx1 might be involved in the H_2O_2-induced oxidation of other cytoplasmic proteins. In the next chapter, we have examined the role of Tpx1 in the oxidation of other *S. pombe* proteins.

CHAPTER 6

6. The role of Tpx1 in promoting the oxidation of Pap1 and other *S. pombe* proteins

6.1 Introduction

Alongside their roles in removing peroxides, Prx have also been shown to act as H_2O_2 sensors, transmitting the H_2O_2 signal by promoting the oxidation of less reactive protein-thiols. For example, Tpx1 has been suggested to transmit redox signals to the AP-1 like transcription factor Pap1, and the MAPK Sty1, causing oxidation of specific cysteine residues. However, although Tpx1 is required for the oxidation of Pap1 (Bozonet *et al.*, 2005; Vivancos *et al.*, 2005), Pyp1 (Chapter 3) and Tdh1 (Chapter 5), our data suggest that the role of Tpx1 in oxidation of these proteins does not necessarily involve direct disulphides between Tpx1 and the protein that is oxidised. For example, it is clear that, although in $Tpx1^{C169S}$ cells, where the resolving cysteine is substituted to a serine, Pap1 is still able to form H_2O_2-induced disulphide complexes, Pap1 is still exported from the nucleus and inactive (Vivancos *et al.*, 2005; Brown *et al.*, 2013). This is because the thioredoxin peroxidase activity of Tpx1, requiring both peroxidatic and resolving cysteines, is important for Pap1 activation in order to inhibit the thioredoxin-like protein (Txl1)-mediated reduction of oxidised Pap1. Indeed, in cells lacking thioredoxin reductase (Trr1), in which Txl1 is completely oxidised and Trx1 partially oxidised, Pap1 is constitutively nuclear and oxidised (Vivancos *et al.*, 2004; Brown *et al.*, 2013), consistent with proteins belonging to the thioredoxin family being responsible for the reduction of oxidised Pap1. Nevertheless, in the absence of both Trx1 and Txl1, despite Pap1 being nuclear, the majority of Pap1 is insoluble and resistant to H_2O_2-induced oxidation (Brown *et al.*, 2013). This indicates an additional role for Trx1 and Txl1 in

activation of Pap1 that cannot be simply explained in terms of them participating in the reduction of active, oxidised Pap1.

Recent work has provided evidence for the targeting of redox active proteins, such as Prx and Trx, into the mitochondrial intermembrane space (IMS) of *Saccharomyces cerevisiae* (Vogtle *et al.*, 2012). These include the thioredoxin peroxidase Gpx3, thioredoxin Trx1, and thioredoxin reductase Trr1 (Vogtle *et al.*, 2012). The presence of these proteins in the IMS could reflect a need to remove ROS generated by Erv1 during oxidative folding of IMS proteins (see section 1.5.2). However, as Gpx3 is required for the H_2O_2-induced oxidation and activation of Yap1 (Delaunay *et al.*, 2002; Veal *et al.*, 2003), this also raises the possibility that Gpx3 might be directly involved in the oxidative folding of IMS proteins, perhaps in a similar way to that suggested for PrxIV in the endoplasmic reticulum (ER) (see section 1.5.1). Consistent with this possibility, in *Schizosaccharomyces pombe*, some Tpx1 has also been shown to be co-purified with mitochondria (Di *et al.*, 2012). The mitochondrial IMS promotes the oxidation of cysteine residues and the formation of disulphide bonds, similar to the ER and the bacterial periplasm (see section 1.5.1). However, unlike the reducing environment of the cytosol, disulphide bonds are able to form in the IMS, in the presence of Trx (Herrmann and Riemer, 2010; Riemer *et al.*, 2011). Indeed, redox measurements of the mitochondrial IMS suggested that the IMS environment was more oxidising compared to both the cytosol and mitochondrial matrix, supporting the folding of IMS imported proteins (Hu *et al.*, 2008; Riemer *et al.*, 2009). Tim40 is the essential inner mitochondrial membrane oxidoreductase, which functions to introduce disulphide bonds into target proteins, including small Tim proteins and other twin CX_9C proteins, to facilitate their import into the mitochondria and subsequent folding. Once precursor proteins have crossed the outer mitochondrial membrane, they form transient disulphide bonds with the oxidised form of Tim40. These disulphide bonds become transferred to the precursor protein through a disulphide relay, resulting in oxidation of the precursor protein, and a reduced form of Tim40, which is oxidised by Erv1, a sulphydryl oxidase in the IMS. Formation of disulphide bonds in IMS proteins is often crucial for the function of mitochondrial proteins (Allen *et al.*, 2005; Mesecke *et al.*, 2005). However, oxidised precursor proteins

cannot be imported into the mitochondria. Indeed, only reduced precursor proteins are competent for import into the mitochondria (Lu *et al.*, 2004; Tokatlidis, 2005; Morgan and Lu, 2008). The cytosolic thioredoxin system has been shown to be required to keep small Tim proteins in a reduced, import-competent form in the cytosol, facilitating their mitochondrial import. Importantly, the thioredoxin system is required to specifically facilitate the import of redox-sensitive IMS proteins, but not of other mitochondrial target proteins (Durigon *et al.*, 2012).

The unexpected detection of Gpx3 in the IMS (Vogtle *et al.*, 2012), together with work showing that some Sty1, which is H_2O_2-activated, is imported into mitochondria (Di *et al.*, 2012), and that Trx1 and Txl1 have an unidentified role in Pap1 activation (Brown *et al.*, 2013), all led us to the hypothesis that under normal growth conditions, Pap1 might be associated with the mitochondria, and that this mitochondrial association might be important for H_2O_2-induced oxidation of Pap1. We considered that perhaps Tim40 might participate in the oxidation of Pap1, forming a disulphide bond with Pap1 to initiate Pap1 oxidation leading to the nuclear accumulation of active, oxidised Pap1. This could potentially explain our discovery that, in a mutant lacking Trx1 and Txl1, Pap1, like other proteins oxidised in the IMS, is insoluble and resistant to oxidation (Durigon *et al.*, 2012; Brown *et al.*, 2013).

Although Tpx1 is required for the oxidation of Pap1, Sty1, Pyp1 and Tdh1, no Tpx1-Pyp1 or Tpx1-Tdh1 disulphide has been consistently identified, and there is little evidence that Tpx1-Pap1 disulphides are involved in Pap1 oxidation (Bozonet *et al.*, 2005; Vivancos *et al.*, 2005; Brown *et al.*, 2013; Calvo *et al.*, 2013) (Chapter 3; Chapter 5). Nevertheless, Prx, including Tpx1, have been shown to form H_2O_2-induced disulphide bonds with several redox-regulated proteins (Veal *et al.*, 2004; Sobotta *et al.*, 2015). Thus, it has been proposed that Prx-mediated redox relays may be involved in the redox regulation of multiple proteins (Sobotta *et al.*, 2015; Winterbourn and Hampton, 2015). To test this possibility in *S. pombe*, here we have examined whether Tpx1 might be directly involved in the H_2O_2-induced oxidation of other cytoplasmic proteins, in addition to Sty1. Through a directed and proteomic approach, this study aimed to explore the role of the peroxidatic cysteine of Tpx1 in the activation of

Pap1 and in the oxidation of other *S. pombe* proteins. Potentially, the identification of other proteins that form H_2O_2-induced disulphides with Tpx1 could also identify new H_2O_2-regulated proteins that mediate the physiological effects of H_2O_2.

6.2 Results

6.2.1 Pap1, the single AP-1 like transcription factor in *S. pombe*, can be detected in the mitochondrial fraction in wild-type and Δ*trx1* cells

First, to test our hypothesis that Pap1 might become oxidised at mitochondria we examined whether any Pap1 was co-purified with mitochondria. Strikingly, a substantial amount of Pap1 was found to be associated with the mitochondria rather than the cytosol of wild-type cells (Figure 6.1A, 6.1B and 6.1C). To test whether this mitochondrial association might be important for H_2O_2-induced oxidation of Pap1, we began by determining how loss of thioredoxin or thioredoxin reductase influenced Pap1's distribution between cytosol and mitochondria. Recent findings have shown that the thioredoxin system is required to keep mitochondrial precursor proteins in a reduced, import-competent state, therefore loss of thioredoxin family proteins would permit oxidation of proteins in the cytosol, preventing their association with the mitochondria, and therefore preventing their import. Consistent with this, Trx1 and Txl1 have been shown to have semi-redundant functions in maintaining Pap1 in a soluble form that is sensitive to H_2O_2-induced oxidation. Previous studies have suggested that Pap1 must be present in a soluble form to become oxidised, therefore in the absence of Trx1 and Txl1, Pap1 would be unable to associate with the mitochondria. Therefore, the role of thioredoxin family proteins, in particular Trx1 and Txl1, on Pap1 localisation was investigated.

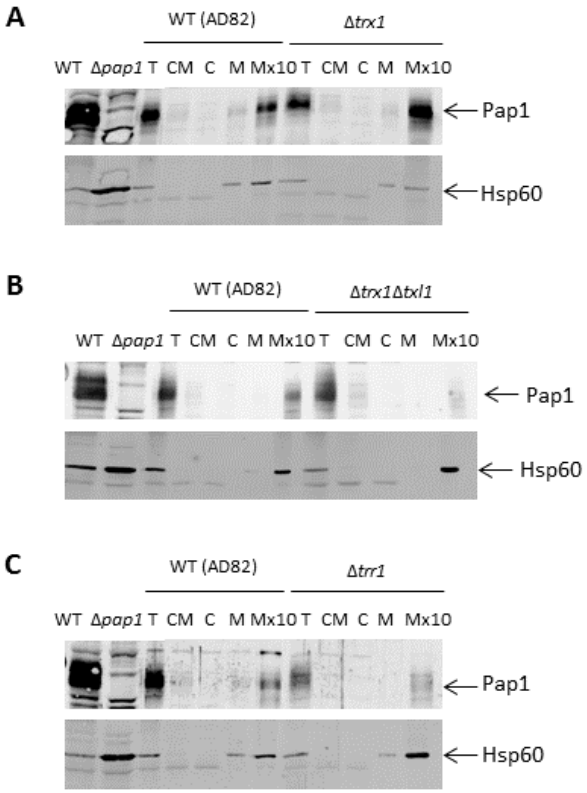

Figure 6.1 Pap1 can be detected in the mitochondrial fraction in wild-type *S. pombe* cells. Mitochondrial enrichment was performed on wild-type (AD82) and (**A**) Δ*trx1* (JB30), (**B**) Δ*trx1*Δ*txl1* (JB120), and (**C**) Δ*trr1* (AD81) cells, and fractions were analysed by western blotting of equivalent cell volumes. Protein was also extracted from wild-type (NT4) and Δ*pap1* (TP108-3C) cells, which were also analysed by western blotting. Anti-Pap1 and anti-Hsp60 antibodies were used to detect Pap1 and the mitochondrial protein Hsp60, respectively. Probing with anti-Hsp60 acts as a control for the mitochondrial fractions, and to confirm mitochondrial enrichment has been successful. T=total, CM=cytoplasmic and mitochondrial, C=cytoplasmic, M=mitochondrial, and Mx10=10x enriched mitochondrial.

Consistent with our hypothesis that Pap1 might become oxidised at the mitochondria, Pap1 was detected in the mitochondrial fraction of wild-type cells. Moreover, at least as much Pap1 was detected in the mitochondrial fraction of Δ*trx1* cells compared to wild-type (Figure 6.1A), consistent with Pap1 still becoming oxidised in these cells following treatment with H_2O_2 (Brown *et al.*, 2013). However, there was notably less Pap1 in the mitochondria of Δ*trx1*Δ*txl1* cells compared to wild-type (Figure 6.1B). This is consistent with Trx1 and Txl1 being required to maintain Pap1 in a form that can be associated with the mitochondria. However, it was also possible that the lack of mitochondrially associated Pap1 could be because Pap1 is constitutively nuclear in a Δ*trx1*Δ*txl1* (Brown *et al.*, 2013). However, Pap1 is also constitutively nuclear in a Δ*trr1* (Vivancos *et al.*, 2004; Brown *et al.*, 2013), and only slightly less Pap1 was detected in the mitochondrial fraction of this mutant compared to wild-type cells (Figure 6.1C). These data fit with our hypothesis that the mitochondrial localisation of reduced Pap1 may be required for Pap1 to become oxidised, in response to H_2O_2, before it accumulates in the nucleus. It is worth noting that antibodies against an established non-mitochondrial protein should also be used to confirm that cytosolic proteins aren't generally co-purified with our mitochondrial fractions. Nevertheless, Hsp60 was used as a mitochondrial marker to confirm mitochondrial enrichment had been successful. Intriguingly, there appears to be more total Hsp60 in a Δ*pap1* compared to wild-type (Figure 6.1A, 6.1B and 6.1C), suggesting loss of *pap1*$^+$ may increase the expression of this mitochondrial chaperone.

6.2.2 Tim40 is not involved in the direct oxidation of Pap1

Although we did not establish which sub-organellular compartment contained Pap1, the IMS oxidoreductase, Tim40, has been shown to be essential in yeast and mammalian cells to introduce disulphide bonds into target IMS proteins, hence we considered whether Tim40 might be involved in Pap1 oxidation. Although a high-throughput study has found that the single orthologous Tim40-encoding gene is essential in *S. pombe* (Kim *et al.*, 2010), the function of the encoded protein has not been previously studied. To test whether *S. pombe* Tim40 might be involved in the oxidation of Pap1,

a strain was constructed expressing Tim40 with an EGFP-protein tag at its C-terminus, from its endogenous locus (see section 2.2.5.5). Importantly, studies have shown that the fusion of GFP to the C-terminus of *Arabidopsis thaliana* Mia40/Tim40 does not affect the targeting or localisation of Mia40 to the mitochondria (Carrie *et al.*, 2010). Nevertheless, it was possible that this EGFP-protein tag might affect Tim40 localisation or function in *S. pombe*, so we first examined where it was localised and whether it supported the essential functions of Tim40. Wild-type (NT4) cells were used as a control to distinguish the fluorescent signal produced by the Tim40EGFP fusion protein from any background fluorescence. Although the mitochondrial localisation was not confirmed by co-staining with a mitochondrial stain or mitochondrial marker, nevertheless, examination of cells expressing Tim40EGFP fusion protein revealed a distinct punctate pattern, excluded from the nucleus, consistent with Tim40EGFP localising to the mitochondria (Figure 6.2). Indeed, a similar pattern was observed when the expression of a Tim40YFP fusion protein was examined in a genome-wide study of the localisation of *S. pombe* proteins. Although it was possible that the EGFP-protein tag affected the localisation of Tim40, these data were consistent with the expected pattern if Tim40EGFP was correctly localised to the mitochondrial IMS. Importantly, the general cell morphology observed in the overlay between GFP and DAPI looks the same between the untagged wild-type (NT4) and the Tim40EGFP fusion protein, suggesting that the EGFP-protein tag has no obvious effect on cell growth and morphology. Consistent with this, when cells were grown in liquid culture to prepare samples for western blotting there was no difference between the growth rate of Tim40EGFP-expessing cells and wild-type cells.

To investigate whether Tim40 participated in the oxidation of Pap1 at the IMS, we tested whether any high molecular weight (HMW) oxidised forms of Pap1 that are detected in cells expressing $Tpx1^{C169S}$ (Vivancos *et al.*, 2005; Brown *et al.*, 2013) represent mixed disulphides with Tim40. First we examined Tim40EGFP fusion protein by western blotting using anti-GFP antibodies.

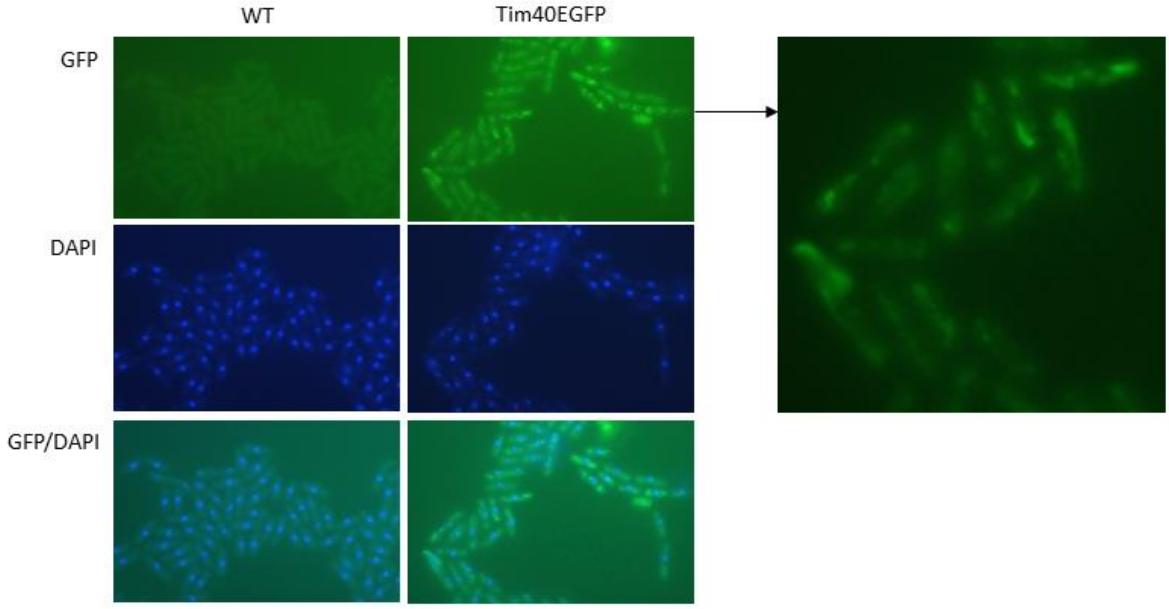

Figure 6.2 Tim40EGFP displays a distinct punctate pattern, consistent with localisation to the mitochondria. Visualisation of GFP in live cells expressing EGFP-protein tagged wild-type Tim40 (Tim40EGFP) (HL16) in comparison with wild-type (NT4). Nuclei were visualised by staining with DAPI.

Tim40EGFP is present as several HMW forms, which don't change upon H_2O_2 treatment, and are resistant to β-mercaptoethanol (Figure 6.3 and 6.4B), indicating these post-translational modifications of Tim40EGFP don't represent disulphide bonds. Tim40 has a protein molecular mass of 35 kDa, with the EGFP-protein tag adding a further 20 kDa. In addition, protein samples were treated with the thiol-binding agent, AMS, which adds 0.6 kDa per reduced cysteine residue. Tim40 contains eight cysteine residues, therefore in the fully reduced state, the protein molecular mass of Tim40EGFP would be approximately 60 kDa. Upon treatment with H_2O_2, there are no shifts in protein mobility compared to before H_2O_2, suggesting that Tim40EGFP isn't becoming oxidised in response to H_2O_2.

Next we compared the mobility of Pap1 complexes formed in $Tpx1^{C169S}$-expressing cells with those in cells co-expressing Tim40EGFP. In $Tpx1^{C169S}$-expressing cells, Pap1 cannot form intramolecular disulphide bonds in response to H_2O_2, however the presence of $Tpx1^{C169S}$ leads to the formation of multiple, less mobile forms of Pap1 that are sensitive to β-mercaptoethanol, suggestive of mixed disulphide complexes with other proteins (Vivancos *et al.*, 2005). If Tim40 was involved in a mixed disulphide bond with Pap1, we would expect to see a mobility shift of one or several of these HMW Pap1 disulphide complexes, consistent with the addition of the EGFP fusion protein (20 kDa).

To examine the redox state of Pap1, protein samples were treated with IAA to alkylate free thiol groups present on reduced cysteine residues, increasing the protein molecular mass by 0.19 kDa per reduced cysteine. In unstressed wild-type cells, Pap1 is present predominantly in a reduced state, detected by two bands (Figure 6.4A). Following exposure to 0.2 mM H_2O_2, Pap1 becomes reversibly oxidised on several cysteine residues in wild-type cells, causing the protein to migrate faster, consistent with oxidised, active forms of Pap1 (Bozonet *et al.*, 2005). However, in $Tpx1^{C169S}$-expressing cells, Pap1 cannot become oxidised through formation of an intramolecular disulphide bond, but instead forms HMW complexes in response to H_2O_2 (Vivancos *et al.*, 2005). As expected, HMW complexes containing Pap1 were detected in cells expressing $Tpx1^{C169S}$, and these increased following H_2O_2 treatment (Figure 6.4A).

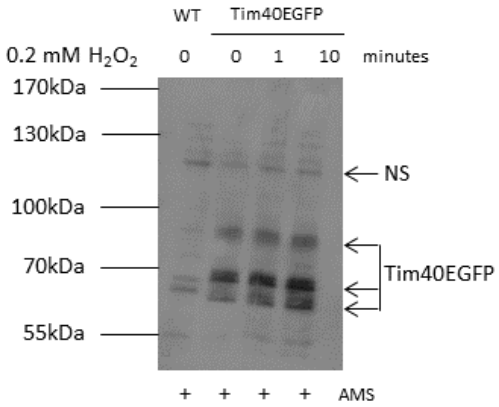

Figure 6.3 Analysis of Tim40EGFP by western blotting. Western blot analysis of Tim40EGFP fusion protein in wild-type (NT4) and EGFP-protein tagged wild-type Tim40 (Tim40EGFP) (HL16) cells. All protein samples were treated with the thiol-binding agent AMS, prior to electrophoresis. Anti-GFP antibody was used to detect EGFP-protein tagged Tim40. The different bands are indicated and the molecular weight (MW) markers are shown. Non-specific (NS) bands are indicated.

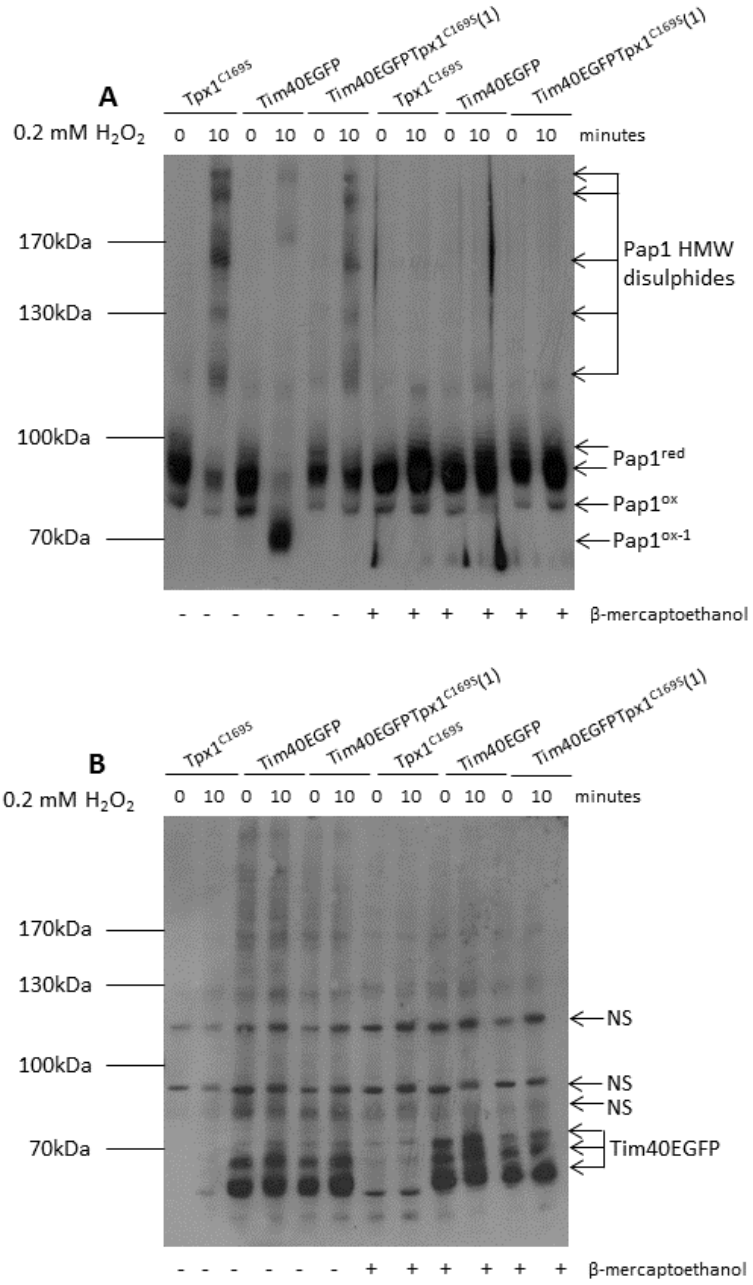

Figure 6.4 The oxidation of Pap1 and Tim40EGFP in cells expressing wild-type Tpx1 or Tpx1^{C169S} before and following treatment with H_2O_2. Western blot analysis of (**A**) Pap1 and (**B**) Tim40EGFP fusion protein in cells expressing mutant Tpx1^{C169S} (JR42), EGFP-protein tagged wild-type Tim40 (Tim40EGFP) (HL16), and mutant Tim40EGFPTpx1^{C169S} (HL17) before and after treatment with 0.2 mM H_2O_2 for 10 minutes. All protein samples were treated with the alkylating agent IAA, and the reducing agent β-mercaptoethanol, as indicated, prior to electrophoresis. (**A**) Anti-Pap1 and (**B**) anti-GFP antibodies were used to detect Pap1, and EGFP-protein tagged Tim40, respectively. The different bands are indicated and the molecular weight (MW) markers are shown. Non-specific (NS) bands are indicated.

The Pap1 HMW complexes were sensitive to treatment with the reducing agent β-mercaptoethanol (Figure 6.4A), confirming these complexes were mixed disulphide bonds between Pap1 and other unidentified proteins.

Importantly, in cells expressing the Tim40EGFP fusion protein, Pap1 was predominantly reduced in unstressed conditions, however following exposure to 0.2 mM H_2O_2, the majority of Pap1 becomes oxidised, as observed in wild-type cells. This oxidised form of Pap1, which is sensitive to β-mercaptoethanol, and detected only when the resolving cysteine of Tpx1 is present, was termed $Pap1^{ox\text{-}1}$ (Figure 6.4A). In $Tpx1^{C169S}$-expressing cells, Pap1 becomes oxidised to HMW disulphide-bonded forms (Figure 6.4A) (Vivancos *et al.*, 2005; Brown *et al.*, 2013). These forms were also observed in $Tpx1^{C169S}$-expressing cells co-expressing Tim40EGFP (Figure 6.4A). If Tim40 was involved in any of these HMW Pap1 disulphides then a mobility shift would be expected, consistent with the additional molecular weight of the EGFP-protein tag (20 kDa) in the Tim40EGFP fusion protein, between the HMW complexes in $Tpx1^{C169S}$-expressing cells expressing wild-type Tim40 or Tim40EGFP. However, there was no difference in mobility of any of the HMW Pap1 disulphide complexes between cells expressing $Tpx1^{C169S}$ and cells co-expressing Tim40EGFP. This suggests that Tim40 is not directly involved in the oxidation of Pap1, through the formation of mixed disulphide bonds between Tim40 and Pap1 (Figure 6.4A). As mentioned previously, there is pattern of bands representing several Tim40EGFP modifications, which don't change upon treatment with H_2O_2, and are resistant to β-mercaptoethanol (Figure 6.3 and 6.4B). The same pattern of bands can also be seen in cells co-expressing $Tpx1^{C169S}$ and Tim40EGFP, indicating these forms of Tim40EGFP don't require the resolving cysteine of Tpx1 to be present (Figure 6.4B).

To provide better resolution of bands, Pap1 oxidation and the detection of Tim40EGFP fusion proteins were repeated using an SDS-PAGE gel with fewer wells. Although, as expected, there was none of the active oxidised form of Pap1 detected following H_2O_2 treatment of $Tpx1^{C169S}$-expressing cells expressing endogenous Tim40, or in two clones of cells co-expressing Tim40EGFP ((1) and (2)), the

pattern of H_2O_2-induced HMW Pap1 complexes was similar in all three strains (Figure 6.5A). In unstressed conditions, the majority of Pap1 is present as two bands, indicative of the reduced state. However, following exposure to 0.2 mM H_2O_2, Pap1 forms HMW complexes in cells expressing Tpx1^{C169S} (Figure 6.5A). Although the majority of these Pap1 HMW complexes did not show a mobility shift between Tpx1^{C169S}-expressing cells and cells co-expressing Tpx1^{C169S} and Tim40EGFP, one of the Pap1 HMW bands (Figure 6.5A, labelled #) did exhibit a slight shift upwards in cells co-expressing Tpx1^{C169S} and Tim40EGFP (Figure 6.5A, labelled *). This suggests that Tim40 may be involved in the oxidation of Pap1. To further investigate this potential Tim40-Pap1 disulphide bond, proteins could be separated on a lower percentage SDS-PAGE gel to improve separation of these very high molecular weight forms. However, although Figure 6.5A suggests the possibility that Tim40 and Pap1 could form disulphides, the Pap1 HMW disulphide complexes in Figure 6.4A showed no difference in mobility between cells expressing Tpx1^{C169S} and cells co-expressing Tim40EGFP. Hence, these results were inconclusive.

Although multiple Tim40EGFP forms were detected with a range of mobilities, both before and following treatment with H_2O_2 (Figure 6.5B), interestingly, a band at approximately 100 kDa was detected in cells expressing wild-type Tpx1, but was not detected in cells co-expressing Tpx1^{C169S} (Figure 6.5B). Given that many of the Tim40EGFP bands are resistant to β-mercaptoethanol (Figure 6.4B), treatment with β-mercaptoethanol would first be needed to confirm that this 100 kDa form represented an oxidised form of Tim40EGFP. However, assuming that this is the case, then its absence from cells expressing Tpx1^{C169S} does suggest that Tpx1 might be involved in the function of Tim40 in the import of mitochondrial proteins by the Tim40 pathway. For example, it is possible that this band could even represent a mixed disulphide with Tpx1-Tpx1 disulphides, which would not be formed by Tpx1 lacking the resolving cysteine (Tpx1^{C169S}).

Intriguingly, this suggests additional proteins might be oxidised by mechanisms that require the resolving cysteine of Tpx1. This led us to investigate the oxidation of other *S. pombe* proteins by Tpx1.

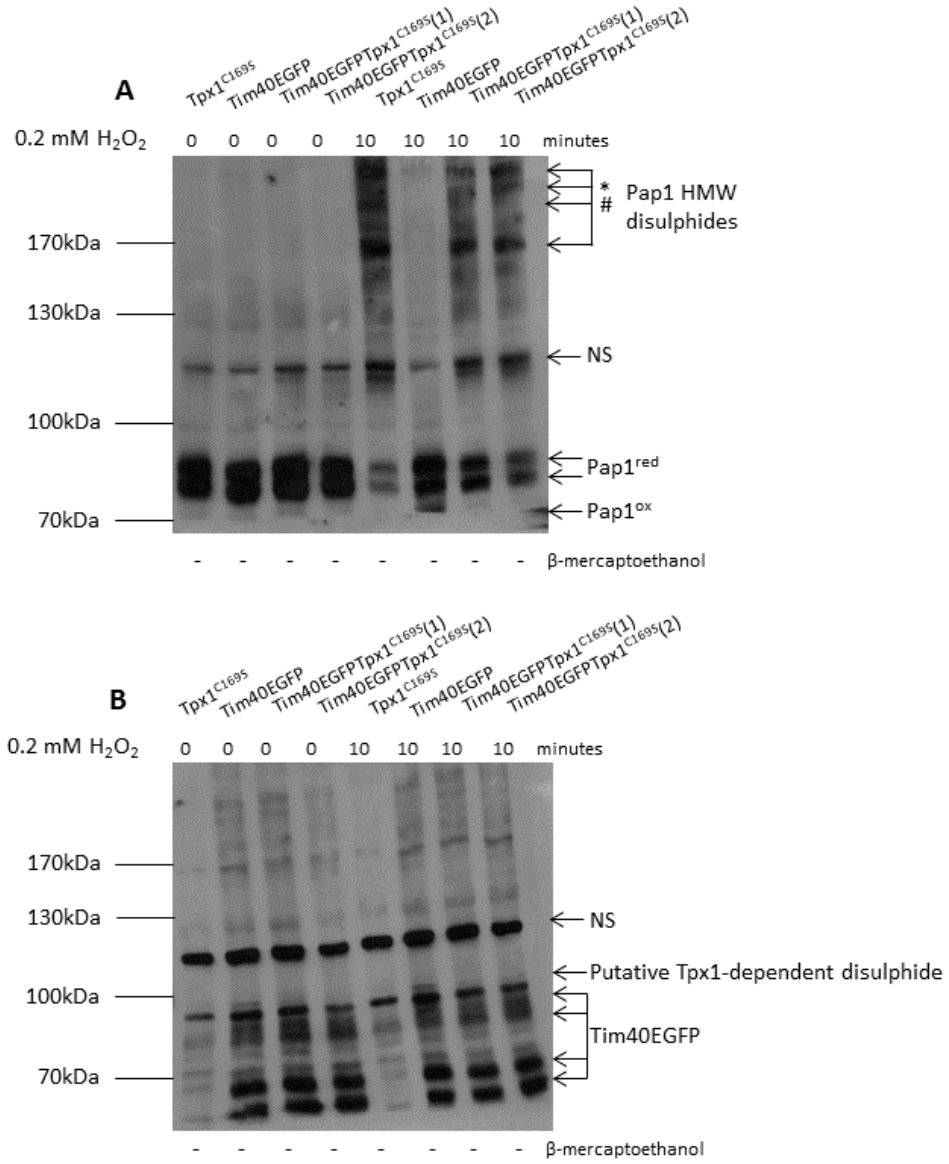

Figure 6.5 The effect of H_2O_2 on oxidation of Pap1 and Tim40EGFP in cells expressing wild-type Tpx1 or Tpx1^{C169S}. Western blot analysis of (**A**) Pap1 and (**B**) Tim40EGFP fusion protein in cells expressing mutant Tpx1^{C169S} (JR42), EGFP-protein tagged wild-type Tim40 (Tim40EGFP) (HL16), mutant Tim40EGFPTpx1^{C169S}(1) (HL17), and Tim40EGFPTpx1^{C169S}(2) (HL18) before and after treatment with 0.2 mM H_2O_2 for 10 minutes. All protein samples were treated with the alkylating agent IAA, prior to electrophoresis. (**A**) Anti-Pap1 and (**B**) anti-GFP antibodies were used to detect Pap1, and EGFP-protein tagged Tim40, respectively. The different bands are indicated and the molecular weight (MW) markers are shown. Non-specific (NS) bands are indicated. The hash (#) indicates a Pap1 HMW disulphide which appears to have a mobility shift upwards to the band indicated by an asterisk (*).

6.2.3 Large-scale immunopurification of cysteine mutants of Tpx1 demonstrates Tpx1 interacts with a number of proteins

The ability of Prx to function as an H_2O_2 sensor, to oxidise redox-regulated signalling proteins directly has been previously demonstrated in *S. cerevisiae* (Delaunay *et al.*, 2002; Okazaki *et al.*, 2005), and also suggested to occur in *S. pombe* (Veal *et al.*, 2004; Bozonet *et al.*, 2005; Calvo *et al.*, 2013), with some evidence provided in this chapter for a potential Tpx1-Tim40 disulphide bond (Figure 6.5B). Therefore, we combined a trapping mutant strategy, whereby mutation of the resolving cysteine of Tpx1 allows trapping of its targets, and analysis of complexes involving wild-type Tpx1, to identify further proteins forming mixed disulphide bonds with Tpx1, using large-scale immunopurification and mass spectrometry.

When the resolving cysteine of Tpx1, cysteine 169, is replaced with a serine (C169S), the disulphide bond between Tpx1 and the unidentified target protein forms a stable intermediate, as only the peroxidatic cysteine of Tpx1 is present. Using the peroxidatic cysteine mutant ($Tpx1^{C48S}$) and the Tpx1 mutant lacking both the resolving and peroxidatic cysteine residues ($Tpx1^{C48SC169S}$/$Tpx1^{2CS}$) as controls allowed us to identify interacting proteins dependent on the presence of the peroxidatic cysteine residue, rather than just due to non-covalent interactions with Tpx1. Flag-epitope tagged Tpx1, $Tpx1^{C48S}$, $Tpx1^{C48SC169S}$ and $Tpx1^{C169S}$ transformed into Δ*tpx1* cells were immunopurified from cells treated with 0.2 mM and 1.0 mM H_2O_2 for 10 minutes to investigate the effect of H_2O_2 concentration and mutant forms of Tpx1 on potential Tpx1-interacting proteins. The large-scale immunopurification (see section 2.4.5.1) and mass spectrometry analysis was performed three times.

Large-scale immunopurification of *S. pombe* cells was performed on FlagTpx1-containing complexes to identify Tpx1-interacting proteins. The resolving cysteine mutant, $FlagTpx1^{C169S}$, was utilised as the disulphide bond between Tpx1 and the target protein is more stable, and therefore more easily identified. Use of $FlagTpx1^{C169S}$ ensures that the mixed disulphide complexes contain Tpx1 and other proteins, and don't represent oligomeric forms of Tpx1. When analysing mass spectrometry data for

Tpx1 interactors, proteins enriched in cells expressing FlagTpx1^{C169S}, and the wild-type FlagTpx1, but not mutant FlagTpx1^{C48S} or FlagTpx1^{C48SC169S}, under oxidative stress conditions were identified as potential candidate target proteins. This allowed the identification of proteins that interact with Tpx1, dependent on the presence of the peroxidatic cysteine of Tpx1. Different H_2O_2 concentrations were compared as we predicted that treatment with 0.2 mM H_2O_2 would generate more disulphides with wild-type Tpx1 than 1.0 mM, because thioredoxin will be more oxidised and inhibited at the lower concentration (Day *et al.*, 2012).

Comparisons of a 1% input of the cell lysate used in the immunopurification and 1/40th of the immunopurified proteins analysed by non-reducing SDS-PAGE and western blotting with anti-Flag antibodies confirmed that the immunopurification, using anti-Flag antibody-conjugated agarose, had worked effectively (Figure 6.6A and 6.6B). The predominant bands detected in the input were enriched in the Flag pulldown in all FlagTpx1-containing strains, with the faint higher molecular weight bands in the input also enriched in the Flag pulldown in FlagTpx1 and FlagTpx1^{C169S}. This suggests that immunopurification using anti-Flag antibody-conjugated agarose has enriched both Flag-tagged wild-type and mutant Tpx1 proteins. A band the size of a FlagTpx1 monomer was detected in all FlagTpx1-containing strains, with FlagTpx1 dimers and FlagTpx1-containing complexes detected only in FlagTpx1 and FlagTpx1^{C169S} expressing cells (Figure 6.6A and 6.6B). Based on the direct comparison between the input and 1/40th of the immunoprecipitates, it is estimated that at least 80% of the Flag-epitope tagged Tpx1/Tpx1 mutant protein was immunopurified. Treatment with the reducing agent β-mercaptoethanol demonstrated that these forms of Tpx1 were sensitive to β-mercaptoethanol, indicative of disulphide bonds between Tpx1 and unidentified proteins (Taylor, 2009).

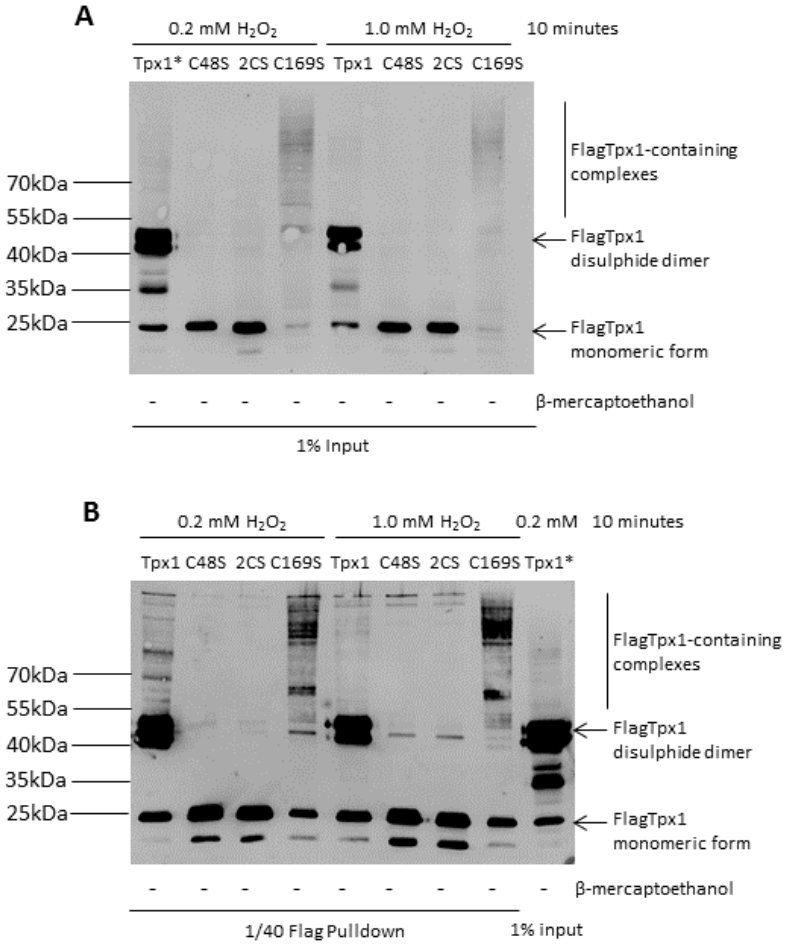

Figure 6.6 Analysis of protein lysate and immunopurified Flag-tagged wild-type and Tpx1 cysteine mutants. Western blot analysis of (**A**) 1% input lysate, or (**B**) proteins immunopurified with anti-Flag conjugated agarose from Δ*tpx1* (VXOO) cells containing the *S. pombe* expression vector Rep41FlagTpx1 (Tpx1), Rep41FlagTpx1^{C48S} (C48S), Rep41FlagTpx1^{C48SC169S} (2CS), and Rep41FlagTpx1^{C169S} (C169S) before and after treatment with 0.2 mM or 1.0 mM H_2O_2 for 10 minutes. Remainder of IPs were analysed by mass spectrometry (Tobias Dansen, Utrecht University). (**A**)(**B**) Anti-Flag antibodies were used to detect Flag-epitope tagged proteins. The asterisk (*) indicates the 1% input sample of Δ*tpx1* (VXOO) cells containing the *S. pombe* expression vector Rep41FlagTpx1 (Tpx1) run alongside the Flag pulldown samples.

As expected, the wild-type FlagTpx1 was found to form more FlagTpx1-containing complexes at 0.2 mM H_2O_2 than at 1.0 mM (Figure 6.6B). This is because, as well as reducing the amount of Tpx1 available to form protein disulphides, hyperoxidation of Tpx1 to thioredoxin-resistant sulphinylated forms in cells exposed to 1.0 mM H_2O_2, means that more thioredoxin is available to reduce Tpx1-protein disulphides (Day *et al.*, 2012).

6.2.4 Mass spectrometry analysis

The immunopurified proteins were separated by non-reducing SDS-PAGE, with each lane excised into 30 pieces and digested with trypsin. To identify the proteins, the excised bands were subjected to mass spectrometry, and matches were searched for in the *S. pombe* database. Mass spectrometry and computational analysis was carried out by Tobias Dansen at Utrecht University.

The raw data obtained was analysed with MaxQuant software, providing information for each immunopurified protein based on peptide score, peptide intensity, and number of unique peptides (see section 2.4.5.3). The score indicates a probability based on the peptide and fragment masses, where a higher score indicates a higher probability that the peptide masses have been correctly assembled into protein hits to identify the protein. Intensities are based on two algorithms, LFQ (Label Free Quantification) and iBAQ (Intensity Based Absolute Quantification). LFQ intensities allow relative protein quantification, however iBAQ algorithms can be used as an estimate of absolute protein abundance within a sample. The LFQ algorithm was used to compare multiple conditions, for instance comparing different H_2O_2 concentrations and different mutant forms of Tpx1 on potential Tpx1-interacting proteins. In most cases, proteins were represented by the number generated by taking the $\log_2$ of the LFQ algorithm, however proteins which were not detected in the analysis of a particular immunopurification were given the arbitrary number 10. The iBAQ algorithm was used to provide an estimate of absolute protein abundance as an intensity. Unique peptides are common to all peptides of a protein group, and do not occur in the proteins of other groups. Therefore, the higher the number of unique peptides identified, the more confident we can be that the peptide hits have been correctly

identified into protein hits. Proteins that were specifically detected in FlagTpx1^{C169S} pulldowns, with a high score, high intensity, and high number of unique peptides were considered as potential candidates for cysteine-dependent interactors of Tpx1 (Appendix 1 and 2).

Once the raw data files from the mass spectrometry run had been analysed by MaxQuant, with peptide hits grouped into proteins, protein hits that were most likely to represent true interactors of Tpx1 were considered, based on: (1) the protein was enriched in cells expressing the Tpx1 resolving cysteine mutant, based on the LFQ algorithm, (2) the protein had a high score, (3) the protein had a high intensity, represented by the iBAQ algorithm, and (4) there was a high number of unique peptides identified (Table 6.1 and 6.2). For example, Srk1 was enriched in FlagTpx1^{C169S} cells at 0.2 mM and 1.0 mM H_2O_2, with a fold increase compared to mutant FlagTpx1^{C48S} or FlagTpx1^{C48SC169S} of 3.0, has a score of 237.14, and was identified with 22 unique peptides (Table 6.1 and 6.2).

Treatment with different concentrations of H_2O_2 didn't affect the interactions detected in the FlagTpx1^{C169S} immunopurifications, as every protein, with the exception of two, co-purified at both 0.2 mM and 1.0 mM H_2O_2, with similar log_2 values generated by the LFQ algorithm (Appendix 1). The two proteins, SPBC2D10.11c and Brr2, co-purified at 1.0 mM H_2O_2, but not at 0.2 mM (Appendix 1). However, FlagTpx1 immunopurifications formed more disulphide complexes at 1.0 mM H_2O_2 compared to 0.2 mM, with 13 proteins being detected at 1.0 mM and not 0.2 mM H_2O_2, but only 6 proteins at 0.2 mM and not 1.0 mM H_2O_2 (Appendix 1).

6.2.5 Bioinformatic analysis of identified Tpx1-interacting proteins

Having obtained the processed data from the mass spectrometry analysis, only 34 proteins were co-purified with mutant FlagTpx1^{C169S}, but not with FlagTpx1^{C48S} or FlagTpx1^{C48SC169S}, at 0.2 mM and 1.0 mM H_2O_2, with 8 of these also being enriched in wild-type FlagTpx1 (Table 6.1). As this is a fairly small data set of proteins, it is difficult to draw many conclusions in terms of characteristics and phenotypes shared by these hits.

Table 6.1 Proteins enriched in Tpx1 immunoprecipitation dependent on the peroxidatic cysteine residue of Tpx1. Results of the mass spectrometry analysis to identify potential $Tpx1^{C169S}$-interacting proteins are shown. Proteins that are specifically enriched in the data sets of mutant $FlagTpx1^{C169S}$, but not in either $FlagTpx1^{C48S}$ or $FlagTpx1^{C48SC169S}$, at 0.2 mM H_2O_2 are listed in descending score (probability of identification). The asterisk (*) indicates the proteins also enriched in the data sets of wild-type FlagTpx1. Protein names for the genes identified were obtained from UniProtKB. The raw mass spectrometric data was analysed with Maxquant software to give each protein a score and intensity based on the iBAQ alogrithm. Unique peptides for each protein are shown. Protein abundance in proliferating cells is shown as copy number/cell (Marguerat *et al.*, 2012).

Gene name	Protein	Score	Intensity ($x10^8$)	Unique peptides	Protein abundance (copy number/cell)
Rpn12	26S proteasome regulatory subunit rpn12	323.31	8.5	8	27427.67
Kap123	Probable importin subunit beta-4	316.08	6.15	16	20408.63
Pka1	cAMP-dependent protein kinase catalytic subunit	310.83	4.4	6	1805.1
Not1	General negative regulator of transcription subunit 1	262.22	4.06	23	3791.25
Sal3	Importin subunit beta-3	238.82	12.3	17	10272.12
Srk1*	Serine/threonine-protein kinase srk1	237.14	4.93	22	3804.1
SPAC5H10.10	Putative NADPH dehydrogenase C5H10.10	228.89	6.89	7	14485.51
Mug58*	Uncharacterized kinase mug58	198.8	1.48	7	5040.57
Pho8	Alkaline phosphatase	183.82	11.7	13	5236.58
Vac8	Vacuolar protein 8	140.79	3.29	11	7198.14
Cao1*	Copper amine oxidase 1	140.58	3.55	15	2262.91
Brr2*	Pre-mRNA-splicing factor brr2	135.18	5.21	16	3424.64
Gid7*	Uncharacterized WD repeat-containing protein C343.04c	104.96	0.35	7	2235.77
SPBC12C2.03c*	Uncharacterized FAD-binding protein C12C2.03c	101.4	5.66	15	14438.9
Met6	Homoserine O-acetyltransferase	87.143	1.31	11	14402.48
Msh2	DNA mismatch repair protein msh2	72.387	0.79	7	1881.87
SPCC569.03	UPF0612 protein C569.003	58.636	0.71	12	NA
Isp6	Sexual differentiation process putative subtilase-type proteinase isp6	52.024	9.7	7	15550.03
Hal4	Serine/threonine-protein kinase hal4	37.574	0.35	7	7431
Mef1*	Elongation factor G, mitochondrial	37.562	1.34	6	5594.72

Hhp1*	Casein kinase I homolog hhp1	37.488	2.42	12	14271.58
Sec63	Translocation protein sec63	37.241	2.47	6	7325.97
SPBC9B6.11c	Probable RNA exonuclease C9B6.11c	31.641	1.26	7	8962.33
Cpd1	tRNA (adenine(58)-N(1))-methyltransferase catalytic subunit trm61	27.738	1.09	8	6794.04
Ret2	Coatomer subunit delta	20.135	1.09	6	10763.43
Egt1	Meiotically up-regulated gene 158 protein	19.788	0.98	11	NA
Gal10	Bifunctional protein gal10;UDP-glucose 4-epimerase;Aldose 1-epimerase	18.791	0.36	10	125.8
Mak1	Peroxide stress-activated histidine kinase mak1	16.68	0.23	12	373.5
Mcm7	DNA replication licensing factor mcm7	13.904	1.1	8	3436.12
Ubr11	E3 ubiquitin-protein ligase ubr11	13.569	1.85	9	3033.73
Mkh1	MAP kinase kinase kinase mkh1	13.029	0.30	8	237.4
Ppt1*	Serine/threonine-protein phosphatase T	11.801	2.28	7	2698.7
Gcd10	tRNA (adenine(58)-N(1))-methyltransferase non-catalytic subunit trm6	10.642	0.53	6	4938.44
Mug161	CWF19-like protein mug161	9.4323	0.20	7	5417.67

Table 6.2 Fold increase for proteins identified in FlagTpx1^{C169S}, but not the mutants FlagTpx1^{C48S} or FlagTpx1^{C48SC169S}. Fold increase was calculated by dividing the intensity of the protein in FlagTpx1^{C169S} by the intensity of the protein in mutants FlagTpx1^{C48S} or FlagTpx1^{C48SC169S}. Most proteins were represented by the number generated by taking the $\log_2$ of the LFQ algorithm, however proteins which were not detected in the analysis were given the arbitrary number 10 (see Appendix 1). When there are two fold increases, these proteins had an intensity in the run of one of the mutants FlagTpx1^{C48S} or FlagTpx1^{C48SC169S} but not the other. The askterisk (*) indicates the proteins enriched in the data sets of wild-type FlagTpx1, as well as mutant FlagTpx1^{C169S}, at 0.2 mM H_2O_2.

Gene name	Fold increase (FlagTpx1^{C169S}/FlagTpx1$^{C48S/C48SC169S}$)	
	0.2 mM H_2O_2	1.0 mM H_2O_2
Rpn12	2.366	2.331
Kap123	1.042 (Tpx1^{C48S}) 2.554 (Tpx1^{C48SC169S})	2.554
Pka1	2.605	2.624
Not1	2.533	2.604
Sal3	2.541	2.473
Srk1*	2.963	3.017
SPAC5H10.10	2.559	2.622
Mug58*	2.665	2.686 (Tpx1^{C48S}) 1.139 (Tpx1^{C48SC169S})
Pho8	1.003 (Tpx1^{C48S}) 2.346 (Tpx1^{C48SC169S})	2.412
Vac8	2.568	2.615
Cao1*	2.786	2.788
Brr2*	1	2.553
Gid7*	1.166 (Tpx1^{C48S}) 2.655 (Tpx1^{C48SC169S})	2.578
SPBC12C2.03c*	2.460	2.532 (Tpx1^{C48S}) 1.059 (Tpx1^{C48SC169S})
Met6	2.878	2.827
Msh2	2.338	2.438
SPCC569.03	2.940	2.733
Isp6	2.440	2.385
Hal4	2.637	2.503
Mef1*	2.426	2.479
Hhp1*	2.927	2.769
Sec63	2.493	2.494
SPBC9B6.11c	2.465	2.455
Cpd1	2.587	2.539
Ret2	2.458	2.330
Egt1	2.478	2.593
Gal10	2.691	2.668
Mak1	2.565	2.566
Mcm7	2.405	2.455
Ubr11	2.485	2.541
Mkh1	2.560	2.581
Ppt1*	1.059 (Tpx1^{C48S}) 2.624 (Tpx1^{C48SC169S})	2.559
Gcd10	2.415	2.332
Mug161	2.365	2.322

It is worth noting that despite Sty1 having been shown to form a disulphide bond with Tpx1 (Veal *et al.*, 2004), Sty1 was not detected amongst the immunopurified FlagTpx1^{C169S}-containing complexes. In addition, previous work from our laboratory has detected a disulphide bond between Tpx1^{C169} and the MAPKK Wis1 (Veal unpublished data), which is also absent in the immunopurifications, suggesting this approach is not comprehensive in identifying Tpx1 interacting proteins, and may be limited to the most abundant Tpx1 containing complexes.

To identify orthologues in *Homo sapiens* and any common protein families, the 34 proteins enriched in FlagTpx1 and FlagTpx1^{C169S} were inputted into the online tool PANTHER (protein analysis through evolutionary relationships). PANTHER can classify proteins and their genes using sophisticated bioinformatics into a general family, based on groups of evolutionary related proteins, with further classification into a more specific protein class (Mi *et al.*, 2016). Notably, the majority of these proteins (71%, 24 proteins) has a human orthologue (Table 6.3). These proteins include representatives from many different protein families, including non-receptor serine/threonine protein kinases (Hal4, Hhp1, Srk1) and importin betas (Kap123, Sal3) (Table 6.3). In addition, four of the 34 genes are essential genes (Brr2, Mef1, Not1, Ret2), whereby gene deletion leads to an inviable vegetative cell population under normal laboratory growth conditions. The phenotypes associated with some of the respective genes indicate a role in oxidative stress resistance. For example, cells lacking Cpd1, Met6, Pka1 or Ppt1 are sensitive to H_2O_2. Some proteins are encoded by genes that are upregulated in response to exposure to H_2O_2, including Isp6, Pka1 and Srk1 (Chen *et al.*, 2003). In addition, some proteins showed a significant change in protein abundance following exposure to H_2O_2, including Brr2, Mug158, Sal3 and Srk1 (Lackner *et al.*, 2012). As some of these proteins have previously been linked with responses to H_2O_2, this gives an indicator that these proteins may be affected by H_2O_2, and therefore potentially regulated by Tpx1-mediated, H_2O_2-induced oxidation of redox-sensitive cysteine residues.

Table 6.3 Orthologues, PANTHER family and protein class. The list of proteins in Table 6.1 were inputted into PANTHER, giving the orthologues in *Homo sapiens*, and the PANTHER family and protein class the protein belongs to. A dash (-) indicates there is no orthologue in *Homo sapiens*, or PANTHER classification. The askterisk (*) indicates the proteins enriched in the data sets of wild-type FlagTpx1, as well as mutant FlagTpx1^{C169S}, but not in either FlagTpx1^{C48S} or FlagTpx1^{C48SC169S}, at 0.2 mM H_2O_2.

Gene name	Orthologues in *Homo sapiens*	PANTHER Family	PANTHER Protein Class
Rpn12	PSMD8	26S proteasome non-ATPase regulatory subunit 8	Enzyme modulator
Kap123	IPO4	Importin beta	Transporter Transfer/carrier protein
Pka1	PRKX PRKACG PRKACA PRKACB	Cyclic nucleotide-dependent protein kinase	-
Not1	CNOT1	CCR4-Not transcription complex	Transcription factor
Sal3	IPO5 RANBP6	Importin beta	Transporter Transfer/carrier protein G-protein modulator
Srk1*	-	Serine/threonine protein kinase	Non-receptor serine/threonine protein kinase
SPAC5H10.10	-	NADH oxidoreductase-related	Oxidoreductase
Mug58*	-	Uridine kinase	Glycosyltransferase Nucleotide kinase
Pho8	ALPI ALPL ALPP ALPPL2	Alkaline phosphatase	Phosphatase
Vac8	-	Beta catenin-related armadillo repeat-containing	Storage protein Signalling molecular Cytoskeletal protein Cell junction protein Cell adhesion molecule
Cao1*	AOC1 AOC2 AOC3	Copper amine oxidase	-
Brr2*	SNRNP200	-	-
Gid7*	WDR26	-	-
SPBC12C2.03c*	MTRR	Flavodoxin-related	-
Met6	-	Family not named	-
Msh2	MSH2	DNA mismatch repair MutS related proteins	DNA binding protein
SPCC569.03	-	Leucine-rich protein	-
Isp6	PCSK9	Proprotein convertase subtilisin/kexin	Serine protease
Hal4	-	Serine/threonine protein kinase	Non-receptor serine/threonine protein kinase

Mef1*	GFM1	Translation factor	Translation elongation factor Translation initiation factor Hydrolase G-protein
Hhp1*	CSNK1D CSNK1E	Casein kinase-related	Non-receptor serine/threonine protein kinase
Sec63	SEC63	Family not named	Chaperone
SPBC9B6.11c	PDE12	Carbon catabolite repressor protein 4	Exoribonuclease Nuclease
Cpd1	TRMT61A	Uncharacterised methyltransferase	Methyltransferase
Ret2	ARCN1	Coatomer subunit delta	Vesicle coat protein
Egt1	-	Alpha-ketoglutarate-dependent sulphonate dioxygenase	Oxidoreductase
Gal10	GALE	NAD dependent epimerase/dehydratase	Oxidoreductase Dehydratase Epimerase/racemase
Mak1	-	Two-component sensor histidine kinase	Protein kinase Transcription factor Esterase
Mcm7	MCM7	DNA replication licensing factor	DNA helicase Helicase Hydrolase
Ubr11	UBR1 UBR2	Ubiquitin ligase E3 alpha-related	-
Mkh1	-	-	-
Ppt1*	COQ2	Serine/threonine protein phosphatase	Protein phosphatase Calcium-binding protein
Gcd10	TRMT6	Translation initiation factor eIF3-related	Translation initiation factor
Mug161	CWF19L1	-	-

6.2.6 Validation and characterisation of the Tpx1-Srk1 interaction

With any high-throughput approach there will likely be false positives, so it was important to test whether we could confirm interactions with a directed approach. Based on the criteria listed in section 6.2.4, Srk1 was selected as a suitable candidate protein for further investigation. Firstly, Srk1 was enriched in FlagTpx1^{C169S} cells compared to FlagTpx1^{C48S} and FlagTpx1^{C48SC169S} cells (Table 6.1) and had the highest fold increase of all the protein hits from the mass spectrometry analysis (Table 6.2). Secondly, Srk1 had the sixth highest score, of 237.14, indicative of a high probability that the peptide masses have been accurately grouped to identify the protein. Srk1 also had quite a high intensity, indicating a high abundance of Srk1 within the sample. Additionally, Srk1 was identified with 22 unique peptides, with only Not1 having more unique peptides with 23. This suggests a high confidence in the protein identification, as there are a large number of unique peptides only present in this protein group. Furthermore, as Srk1 is a fairly lowly abundant protein in proliferating cells, with 3804.1 protein copy number/cell (Marguerat *et al.*, 2012) (Table 6.1), this also suggested that Srk1 was less likely to be non-specifically co-purified with Tpx1. Importantly, although it was detected at much lower levels than in FlagTpx1^{C169S} immunoprecipitates (Appendix 1, compare the $\log_2$ of the LFQ algorithm), Srk1 was also enriched in FlagTpx1 cells at 1.0 mM H_2O_2. Taken together, this suggests Srk1 is one of the top potential candidates for interacting with Tpx1. Therefore, we set out to validate the interaction between Tpx1 and Srk1.

Srk1 (Sty1-regulated kinase 1) encodes a putative serine/threonine kinase, related to the mammalian calmodulin-dependent kinases and MAPK-activated protein kinases (MAPKAP kinases), which becomes upregulated in response to multiple stresses. Previous studies have demonstrated that Srk1 is a substrate of the Sty1 MAPK in *S. pombe*, and forms a stable complex with the unphosphorylated and phosphorylated forms of Sty1 (Smith *et al.*, 2002). Srk1 undergoes Sty1-dependent phosphorylation, and upon stress, Sty1-dependent translocation of Srk1 from the cytoplasm to the nucleus. Sequence alignment of Srk1 with other MAPKAP kinases, *S. pombe* Cmk2, *S. cerevisiae* Rck2,

and mammalian MAPKAP kinase 2 (Figure 6.7) reveals that Cmk2 shares 39% amino acid sequence identity with Srk1, and Rck2 shares 32% with Srk1 (Dahlkvist *et al.*, 1995). The main region of homology is located at the C-terminus of MAPKAP kinase 2, however there is an extra un-conserved sequence present in Srk1 and Cmk2, but not MAPKAP kinase 2 (Figure 6.7). Srk1 contains five cysteine residues in its protein sequence, four of which are conserved in Cmk2, and three of which are conserved between Srk1, Cmk2 and Rck2. In addition, two of the five cysteines of Srk1 are conserved in mammalian MAPKAP kinase 2, located in the most highly conserved region of the four proteins (Figure 6.7). Sequence comparison of Srk1, Rck2, a substrate for the Hog1 MAPK in *S. cerevisiae*, (Bilsland-Marchesan *et al.*, 2000; Teige *et al.*, 2001), and MAPKAP kinase 2, which is phosphorylated by the mammalian p38 MAPK, revealed a conserved MAPK-binding motif at the C-terminus (Teige *et al.*, 2001).

6.2.6.1 Tpx1 interacts with Srk1 at low concentrations of H_2O_2

The enrichment of Srk1 in immunopurified Tpx1 is dependent on the peroxidatic cysteine, suggesting that Srk1 may form disulphides with Tpx1. Hence, we examined whether we could detect Tpx1-Srk1 disulphides by a directed *in vivo* approach. First we examined the oxidation of Srk1 in cells expressing Pk-tagged Srk1 from the endogenous locus (Smith *et al.*, 2002). Western blotting to detect Pk-epitope tagged Srk1 demonstrates that a very small amount of Srk1 protein becomes oxidised in response to low (0.2 mM) concentrations of H_2O_2 (Figure 6.8A), but not at 1.0 mM H_2O_2 (Figure 6.8B). The vast majority of Srk1 protein wasn't oxidised, as observed by the lack of a mobility shift after treatment with H_2O_2. However, a very faint band approximately 21 kDa less mobile than the main form of Srk1 can be detected after exposure to 0.2 mM H_2O_2. This faint band has a molecular weight consistent with a mixed disulphide bond between Tpx1 and Srk1, which is present at 0.2 mM H_2O_2 (Figure 6.8A), but not at 1.0 mM H_2O_2 (Figure 6.8B). There were also faint higher molecular weight forms of Srk1 detected at approximately 115 kDa and 130 kDa at 0.2 mM H_2O_2, but not at 1.0 mM H_2O_2, which are sensitive to treatment with β-mercaptoethanol.

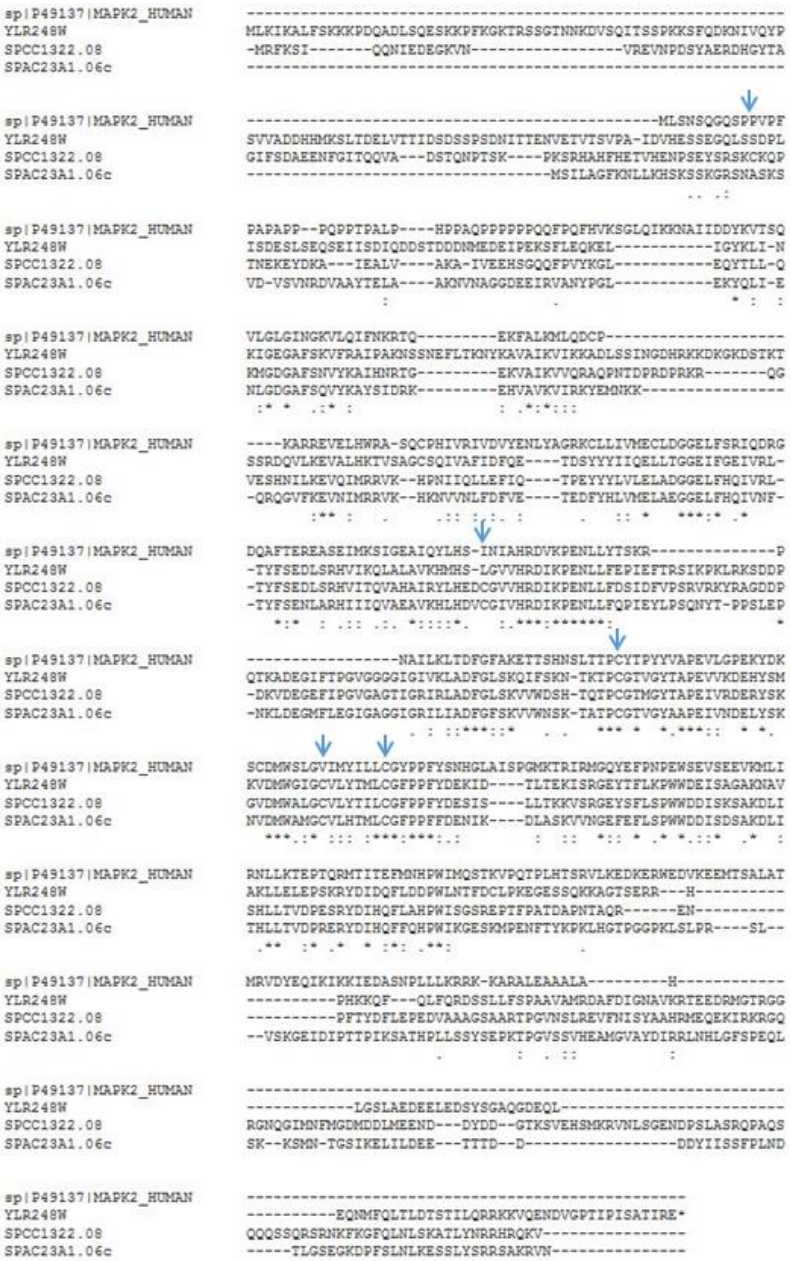

Figure 6.7 Sequence alignment of *Schizosaccharomyces pombe* Srk1 with other MAPK-activated protein kinases. The amino acid sequence of mammalian MAPKAP kinase 2 (sp|P49137|MAPK2_HUMAN), *S. cerevisiae* Rck2 (YLR248W), *S. pombe* Srk1 (SPCC1322.08), *S. pombe* Cmk2 (SPAC23A1.06c) were aligned using ClustalO. Amino acid sequence comparison revealed that the greatest degree of amino acid sequence identity of Srk1 was shared with *S. pombe* Cmk2 (39%), and *S. cerevisiae* Rck2 (32%) (Dahlkvist *et al.*, 1995). An asterisk (*) indicates positions which have a single, fully conserved residue. A colon (:) indicates conservation between groups of strongly similar properties. A full stop (.) indicates conservation between groups of weakly similar properties. Arrows point towards the five cysteine residues in *S. pombe* Srk1, corresponding to residues C85, C251, C324, C351 and C358.

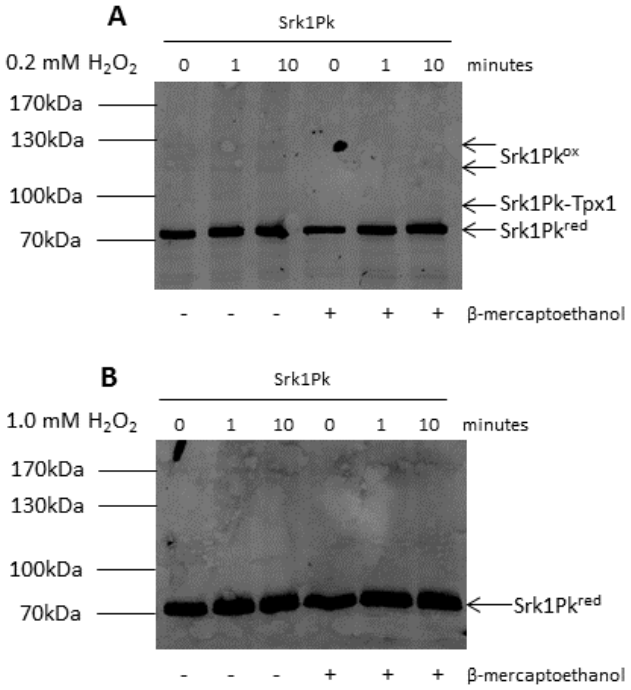

Figure 6.8 Srk1 transiently forms disulphides with Tpx1 in response to low (0.2 mM) concentrations of H_2O_2. Western blot analysis of cells expressing Pk-epitope tagged wild-type Srk1 (Srk1Pk) (JP203) before and after treatment with (**A**) 0.2 mM or (**B**) 1.0 mM H_2O_2. Protein samples were treated with the reducing agent β-mercaptoethanol, as indicated, prior to electrophoresis. Anti-Pk antibody was used to detect Pk-tagged Srk1. The different bands are indicated and the molecular weight (MW) markers are shown.

The reduced mobility of the higher molecular weight, H_2O_2-induced, β-mercaptoethanol-sensitive forms of Srk1 (Figure 6.8A) indicates that a small proportion of Srk1 becomes oxidised at low concentrations of H_2O_2, potentially indicative of Srk1 oligomers or a disulphide bond between endogenous Tpx1 and Srk1.

As the amount of Srk1 that was found to be oxidised in cells expressing endogenous levels of Tpx1 was so small, to investigate these oxidised forms further we ectopically overexpressed Tpx1 or Tpx1^{C169S} in Srk1Pk-expressing cells. Consistent with the previous analysis, immunoblot analysis of cells expressing wild-type Tpx1 revealed that Srk1 was reduced under normal growth conditions but that following exposure to H_2O_2, multiple lower mobility bands were detected (Figure 6.9A and 6.9B). The sensitivity of these forms to β-mercaptoethanol (Figure 6.9B) indicated that they likely represented disulphide-linked complexes (DLC). In cells expressing Tpx1^{C169S} the mobility of these DLC was higher than in cells expressing Tpx1, raising the possibility that complexes may normally involve disulphides between Srk1 and Tpx1-Tpx1 disulphide dimers. Moreover, in Tpx1^{C169S}-expressing cells, complexes were detected under non-stressed conditions, consistent with the idea that in the absence of the resolving cysteine, these oxidised complexes will be more stable.

To establish whether any of these oxidised Srk1 DLC contained Tpx1, we compared the mobilities of complexes formed in Srk1Pk cells containing either wild-type Tpx1 or the mutant Tpx1^{C169S}, both with and without the Flag-epitope tag (wild-type FlagTpx1 and mutant FlagTpx1^{C169S}). The reduced mobility of DLC formed in cells expressing Flag-epitope tagged versions of both wild-type and Tpx1^{C169S} mutant is consistent with a mobility shift due to the Flag-epitope, providing evidence of direct protein disulphides forming between Tpx1 and Srk1. Importantly. the sensitivity of these higher molecular weight bands to β-mercaptoethanol confirms that all shifted bands are due to the formation of disulphide bonds in Srk1 (Figure 6.9B).

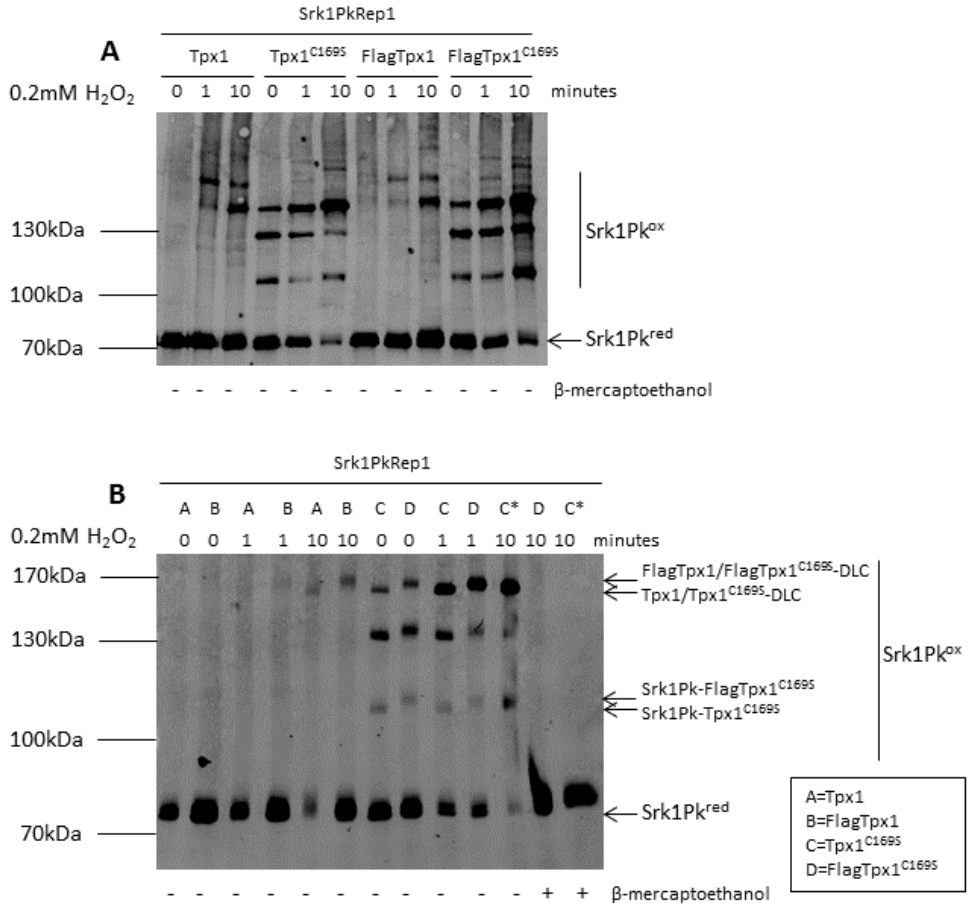

Figure 6.9 Overexpressing the trapping mutant, Tpx1^{C169S}, promotes the H_2O_2-induced oxidation of Srk1. (**A**)(**B**) Western blot analysis of cells expressing Pk-epitope tagged wild-type Srk1 (Srk1Pk) (JP203) containing the *S. pombe* expression vector Rep1Tpx1 (Tpx1) (A), Rep1FlagTpx1 (FlagTpx1) (B), Rep1Tpx1^{C169S} (Tpx1^{C169S}) (C), and Rep1FlagTpx1^{C169S} (FlagTpx1^{C169S}) (D) before and after treatment with 0.2 mM H_2O_2. Protein samples were treated with the reducing agent β-mercaptoethanol, as indicated, prior to electrophoresis. Anti-Pk antibody was used to detect Pk-tagged Srk1. The different bands are indicated (DLC, disulphide-linked conjugates), and the molecular weight (MW) markers are shown. The asterisk (*) indicates the Srk1PkRep1Tpx1FlagTpx1^{C169S} (C) sample with and without the reducing agent β-mercaptoethanol.

Although the mobility shifts were not the expected combined Srk1-Tpx1 molecular weight, collaborators at Utrecht University have also observed that disulphide-dependent complexes involving human PRDX can cause a greater mobility shift depending on which cysteine residue is involved (Dansen unpublished observations). Potentially, the three high intensity shifted bands in the Tpx1^{C169S} could represent DLC involving multiple cysteines in Srk1. Importantly, the decreased mobility of oxidised forms of Srk1 in cells expressing Flag epitope-tagged forms of Tpx1, suggests that these oxidised forms of Srk1 involve disulphides between Srk1 and Tpx1.

6.2.6.2 Overexpressing Srk1 increases cell length in a Δtpx1

Srk1 has been shown to regulate the onset of mitosis by inhibiting the Cdc25 phosphatase and entry into mitosis (Lopez-Aviles *et al.*, 2005). Accordingly, cells overexpressing Srk1 are longer than wild-type cells when they enter mitosis (Smith *et al.*, 2002; Lopez-Aviles *et al.*, 2005). Conversely, cells lacking *srk1*$^{+}$ have a shortened G_2 phase and enter mitosis prematurely due to loss of the Srk1-mediated phosphorylation of Cdc25. To investigate whether Tpx1-dependent oxidative modifications of Srk1 might be important for the G_2 delay associated with increased Srk1 expression, we tested whether overexpressing Srk1 also increased the length of Δ*tpx1* cells.

As expected, overexpressing Srk1 (Rep41HMSrk1) in wild-type (NT4) cells compared to the empty expression vector (Rep41HM) caused an elongated cell morphology (Figure 6.10A), indicative of a G_2 delay (Smith *et al.*, 2002). Overexpression of Srk1 also increased the length at which Δ*tpx1* cells divide, however to a much lesser extent than wild-type (NT4) (Figure 6.10A and 6.10B). This indicates that formation of disulphides between Tpx1 and Srk1 might be important in order for Srk1 to phosphorylate Cdc25 and promote mitotic delay. Consistent with an important role for Tpx1-Srk1 disulphides in Srk1 function, Δ*tpx1* cells were slightly but significantly (T test: $p=7.8x10^{-8}$) shorter at division than wild-type (Figure 6.10C), as has been previously reported for a Δ*srk1* mutant (Lopez-Aviles *et al.*, 2005).

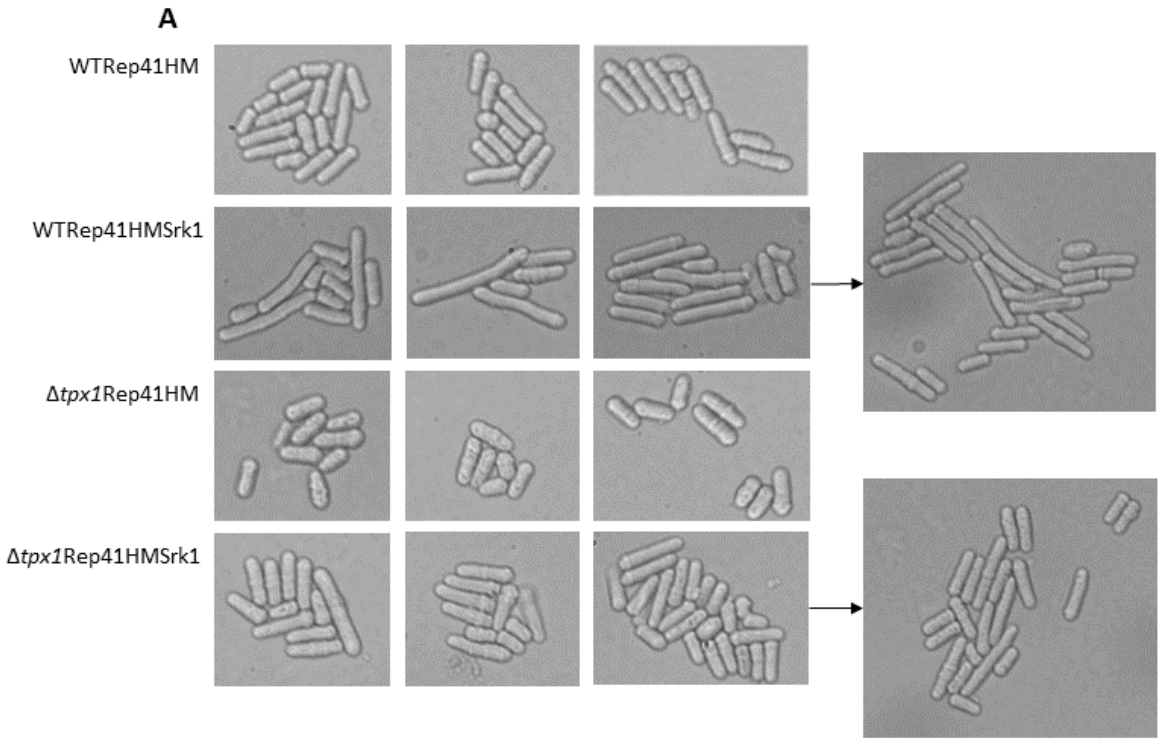

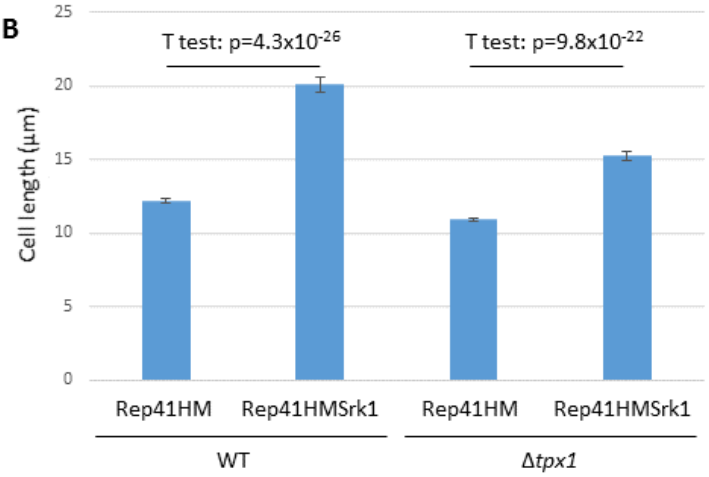

C

Plasmid	Rep41HM		Rep41HMSrk1	
Strain	WT	Δ*tpx1*	WT	Δ*tpx1*
Cell length at division (µm)	12.2 ± 1.5	10.9 ± 1.5	20.1 ± 4.3	15.2 ± 2.9

Figure 6.10 Overexpressing Srk1 increases cell length in wild-type, and to a lesser extent in a Δ*tpx1*. (**A**)(**B**)(**C**) Cell size was measured in wild-type (NT4) and Δ*tpx1* (VXOO) cells containing the *S. pombe* expression vector Rep41HM and Rep41HMSrk1. Cells were grown to mid-log in minimal media and photographed using a Zeiss Axioscope fluorescence microscope. Cell length was calculated in pixels and converted to µm. Mean values are shown. Error bars indicate the range in values among 84 cells (*n* = 84).

6.3 Discussion

This chapter has provided evidence to demonstrate that Pap1 is localised to the mitochondria in wild-type *S. pombe* (Figure 6.1A, 6.1B and 6.1C). Consistent with our hypothesis that the mitochondrial association of Pap1 might be important for H_2O_2-induced oxidation of Pap1, Pap1 was barely detected in the mitochondria isolated from Δ*trx1*Δ*txl1* (Figure 6.1B), where Pap1 is insoluble and resistant to H_2O_2-induced oxidation (Brown *et al.*, 2013). Moreover, previous studies have also shown that, although the vast majority of Tpx1 is present in the cytoplasm both before and after exposure to H_2O_2, a small amount of Tpx1 is present in the mitochondria following H_2O_2 treatment (Di *et al.*, 2012). However, further work is required to confirm the detection of Tpx1 in isolated mitochondria, along with Tim40 and Pap1.

Hsp60 was used as a mitochondrial marker. Intriguingly, there was more total Hsp60 in a Δ*pap1* compared to wild-type (Figure 6.1A, 6.1B and 6.1C), suggesting that loss of $pap1^+$ may increase the expression of this mitochondrial chaperone. In other systems, most notably *C. elegans*, mitochondrial defects lead to increased expression of Hsp60. Therefore, the increased levels of Hsp60 in a Δ*pap1* mutant could be indicative that Pap1 is important for mitochondrial function.

Nevertheless, it remains unclear whether the association of Pap1 with the mitochondria is important for Pap1 function. One could envisage that it might be beneficial to locate an H_2O_2-activated transcription factor close to the major site of ROS-generation. Sub-organellular fractionation of mitochondria is required before we can determine how closely Pap1 is associated with mitochondria and whether it is targeted to a particular compartment. However, we speculated that perhaps the IMS oxidoreductase, Tim40, which introduces disulphide bonds into target IMS proteins, was involved in the oxidation of Pap1. If this was the case, then this would also require a mechanism for exporting the oxidised Pap1 back into the cytoplasm where it could be translocated to the nucleus and activate transcription. Notably, previous studies have shown that in mutants in which Pap1 is constitutively nuclear, Pap1 cannot be oxidised. This implies that the oxidation must take place prior to nuclear

import. Nevertheless, further analysis will be required to determine whether only mitochondrial-associated Pap1 can be oxidised.

Tim40EGFP is modified in a β-mercaptoethanol-resistant way, both before and after H_2O_2 treatment (Figure 6.4A and 6.4B). Therefore, the higher molecular weight bands of Tim40EGFP do not represent disulphide bonded forms of Tim40EGFP, but due to the increase in protein molecular weight, could be due to Tim40 forming complexes with other proteins. Interestingly, in Tim40EGFP-expressing cells, a band at approximately 100 kDa can be detected both before and after H_2O_2 stress (Figure 6.5B). Although Tim40 was not detected in our mass spectrometry analysis of proteins that are co-purified with Tpx1, we have speculated that this band represents a mixed disulphide, possibly between Tim40 and Tpx1 disulphides, however treatment with β-mercaptoethanol would be needed to confirm this. Furthermore, this band cannot be detected in cells co-expressing $Tpx1^{C169S}$ and Tim40EGFP (Figure 6.5B), suggesting that the resolving cysteine of Tpx1 is required. As the resolving cysteine of Tpx1 is required, this suggests that this band is more likely to represent a Tim40-Tpx1-Tpx1 disulphide, but this would need confirming. In order to determine whether a Tim40-Tpx1-Tpx1 disulphide existed, the mobility of Tpx1 complexes present in cells expressing Tim40EGFP could be examined to assess whether one of the Tpx1-Tpx1 disulphides has a mobility shift consistent with the molecular weight of the Tim40EGFP fusion protein. However, as Tpx1 forms multiple complexes (Figure 6.6B) with many proteins (Table 6.1), this might be difficult to identify. Instead, Flag-epitope tagged and untagged Tpx1 could be ectopically expressed in Tim40EGFP-expressing cells and we could examine if there was a shift in the mobility of this Tim40 complex. However, it is possible that an N-terminal Flag-epitope tag may reduce the mitochondrial association of Tpx1 (Di *et al.*, 2012) and inhibit this interaction.

In order to identify which cysteine residue in Tim40 is oxidised, it would be necessary to create serine substitution mutants of Tim40, and examine the effect on potential Tim40-Tpx1 or Tim40-Tpx1-Tpx1 disulphides. Tim40 contains eight cysteine residues, however as the CPC motif is easily accessible and most likely to form a transient disulphide bond with its substrate (Grumbt *et al.*, 2007), mutation of

one or both of these cysteine residues would provide a good foundation for identifying any cysteine residue of Tim40 involved in the interactions with Tpx1.

The potential Tpx1-Tim40 disulphide bond (Figure 6.5B) highlighted the possibility that Tpx1 could form disulphides with other oxidised proteins, in addition to those previously detected (Veal *et al.*, 2004). Therefore, large-scale immunopurification of FlagTpx1-containing complexes and mass spectrometry analysis was utilised to identify proteins which potentially form mixed disulphides with Tpx1. Interestingly, some of the higher molecular weight bands representing FlagTpx1-containing complexes are different between wild-type FlagTpx1 and mutant FlagTpx1^{C169S} (Figure 6.6B), possibly reflecting that Tpx1-Tpx1 disulphides may form complexes with target proteins, as has been proposed for Pap1 (Calvo *et al.*, 2013). Importantly, this means comparisons of wild-type FlagTpx1 and mutant FlagTpx1^{C48S} pulldowns may also be important to identify proteins that are H_2O_2- and/or Tpx1-regulated *in vivo* in order to eliminate any FlagTpx1^{C169S} disulphides that may have formed as a result of proximity to the highly reactive sulphenylated peroxidatic cysteine of Tpx1^{C169S}.

A fairly small set of proteins (34 proteins) were co-purified with mutant FlagTpx1^{C169S}, but not with FlagTpx1^{C48S} or FlagTpx1^{C48SC169S}, at 0.2 mM H_2O_2 (Table 6.1). It is worth noting that Sty1, Pap1, Trx1 and Txl1, which have all previously been shown to form disulphide bonds with Tpx1, are absent amongst the immunopurified FlagTpx1^{C169S}-containing complexes. This suggests the list of proteins is not comprehensive in identifying Tpx1-interacting proteins. These proteins include representatives with many different functions, including protein kinases and importin betas (Table 6.3), of which several have been previously linked with responses to H_2O_2. Notably, 71% of these proteins has a human orthologue.

Based on certain selection criteria (see section 6.2.4), Srk1 was selected as a strong candidate for a Tpx1-regulated protein. Srk1 has previously been linked with oxidative stress responses; the expression of *srk1*$^{+}$ has been shown to be strongly induced in response to H_2O_2, and Srk1 is phosphorylated by active Sty1 in response to H_2O_2 and other stresses (Smith *et al.*, 2002; Chen *et al.*,

2003). Given that previous work from our lab has detected disulphide bonds between Tpx1^{C169} and the MAPKK Wis1 (Veal unpublished data), and Tpx1^{C169} and Sty1 (Veal *et al.*, 2004), it was intriguing that Srk1 should also be found to form disulphides with Tpx1^{C169S}, as all three kinases are in the same signalling cascade (Figure 1.5), raising the possibility that Tpx1 may be acting as a 'scaffold'. It is worth noting that, despite a high degree of homology and four out of the five cysteine residues in Srk1 being conserved in Cmk2 (Figure 6.7), Cmk2 was not detected in the FlagTpx1 immunopurification. Srk1 protein is more abundant than Cmk2 (3804.1 and 2428.18 protein copy number/cell, respectively) (Marguerat *et al.*, 2012), so perhaps this might explain why it was not detected, however there are a few proteins less abundant than Cmk2 which have been enriched in the FlagTpx1 pulldowns (Table 6.1). Intriguingly this suggests that the interaction between Tpx1 and Srk1 may be specific. Western blotting analysis confirmed that Tpx1 interacts with Srk1, through a direct disulphide bond at low (0.2 mM) concentrations of H_2O_2 (Figure 6.8A, 6.9A and 6.9B). The three high intensity disulphide-linked conjugates (DLC) that are detected in the Tpx1^{C169S} mutant and shift upwards in FlagTpx1^{C169S}-expressing cells could either represent different oxidised forms of Srk1 involved in Tpx1-Srk1 complexes or complexes containing different numbers of Tpx1 molecules (Figure 6.9B). The formation of a disulphide bond between the typical 2-Cys Prx in *S. pombe*, Tpx1, and Srk1, could reflect the previously reported involvement of Prx in disulphide formation with their targets (Jarvis *et al.*, 2012). Prdx1 functions as a signal peroxidase in mammalian cells, forming a mixed disulphide bond between Prdx1 and the MAPKKK ASK1 in response to H_2O_2 that is involved in promoting ASK1 dimerisation and kinase activity (Jarvis *et al.*, 2012) (Figure 1.2A). Similarly, Prx2 forms a transient H_2O_2-induced disulphide with STAT3 that is involved in STAT3 oxidation (Sobotta *et al.*, 2015). Therefore, it could be postulated that the regulation of Srk1 by Tpx1 is also mediated through the H_2O_2-induced Tpx1-Srk1 disulphide bond. To investigate which cysteine residue of Srk1 is involved in the disulphide bond with Tpx1, serine substitution mutants of the four conserved cysteine residues in Srk1 and Cmk2 could be constructed, and the presence or absence of the high molecular weight bands of Srk1 observed.

Srk1 provides a molecular link between the Sty1 MAPK pathway and the G_2-M transition (Lopez-Aviles *et al.*, 2005). Srk1 becomes phosphorylated and activated by Sty1 in response to H_2O_2, inducing the dissociation of Sty1 and Srk1, and inhibiting cell cycle progression and mitotic entry through the translocation of Cdc25 from the nucleus to the cytoplasm. Sty1-mediated phosphorylation of Srk1 causes Srk1 protein to become unstable, promoting its degradation by the proteasome (Lopez-Aviles *et al.*, 2008). It would be interesting to test whether the Tpx1-Srk1 mixed disulphide affects the phosphorylation of Srk1, the proteasome-mediated degradation of Srk1, or Srk1 function in the phosphorylation of Cdc25 and inhibition of mitosis. For instance, formation of an H_2O_2-induced disulphide bond with Tpx1 may stabilise Srk1, preventing its degradation. In addition, serine substitution mutants of Srk1 could be examined to determine whether these mutants can increase cell length.

Having validated the interaction between Tpx1 and Srk1 with a directed approach, it would be important to test other potential interactions generated from the mass spectrometry analysis (Table 6.1). For example, two importin betas, Kap123 and Sal3, were found to be enriched in FlagTpx1^{C169S} pulldowns (Table 6.1). Importin betas are a specific type of karyopherin, which transport proteins into the nucleus through a nuclear pore, by binding to specific nuclear localisation sequences (NLS). Recent work into the mammalian Forkhead Box O (FOXO) family of transcription factors, which regulate a wide variety of target genes involved in several cellular processes, has identified several functional disulphide bonds between two members of the FOXO family, FOXO3 and FOXO4, and Prx (Putker, 2014). Interestingly, several importins and importin betas were also identified as forming disulphides with FOXO3 or FOXO4. In addition, FOXO4 forms a disulphide with the nuclear import receptor transportin-1, required for the nuclear localisation of FOXO4 (Putker *et al.*, 2013). This could suggest that disulphides are generally involved in nuclear import, which could be further tested by examining whether Tpx1 is important for the import of the substrates of Kap123 and Sal3. Along with the selection criteria (see section 6.2.4) used to select Srk1 as a strong candidate for a Tpx1-interacting

protein, the number of conserved cysteine residues in other potential candidate proteins could be investigated, in order to determine which proteins to select for future study.

Taken together, the results described in this chapter highlight the potential disulphide bond between Tpx1 and Tim40, and indicates that Tpx1 also interacts with Srk1 via a disulphide bond, although only small amounts of total cellular Srk1 are involved in the disulphide bonded complex with Tpx1. The exact role for the Tpx1-Srk1 interaction in the oxidative stress response has not yet been elucidated, however it has been shown that the role of Srk1 in mitotic delay does involve its interaction with Tpx1. This proteomic approach has also provided a novel list of proteins regulated by Tpx1, many of which would be of great interest to investigate further.

CHAPTER 7

7. Discussion

The research outlined in this thesis has provided novel insights into the complex relationship between peroxiredoxins (Prx) and the thioredoxin (Trx) system in the regulation of mitogen activated protein kinase (MAPK) signalling pathways in *Schizosaccharomyces pombe*. The wider impact of these insights regarding the biological role of Prx is discussed below.

7.1 Does a role in mitochondrial function underlie any of the roles of Tpx1 in growth and H_2O_2 signalling?

As discussed in chapter 6, we have found some evidence that one of the H_2O_2-activated signalling proteins that is regulation by Tpx1 and thioredoxin, Pap1, is associated with mitochondria. Together with reports of other Prx, Trx and signalling proteins, such as Sty1, in the mitochondria, this suggested that perhaps Prx may play a role in mitochondrial function. In support of this, Tpx1 has previously been found to be essential for growth under aerobic conditions (Jara *et al.*, 2007). While this has been proposed to be because Tpx1 is important for preventing damage by removing peroxides that are generated as unwanted by-products of respiration, it is also possible that this reflects a role for Prx in mitochondrial function. Indeed, unpublished work has shown that loss of the 2-Cys Prx, PRDX-2, in *Caenorhabditis elegans* leads to defective mitochondria (Olahova and Veal unpublished data). To test whether Tpx1 is required for mitochondrial function in *S. pombe*, we examined electron transport chain (ETC) activity using 2,3,5-triphenyltetrazolium (TTC), which is reduced by succinate dehydrogenase (complex II), generating a red pigment (Ogur *et al.*, 1957). Δ*ptc4* and Δ*sty1* cells were used as controls as Δ*ptc4* cells, lacking a mitochondrial phosphatase involved in regulation of

mitochondrial Sty1, have previously been shown to have reduced colouration, indicative of a mitochondrial defect (Di *et al.*, 2012), whereas Δ*sty1* cells show increased respiration in the presence of TTC, as they are darker in colour compared to wild-type (Holmes, 2013). The red colouration of wild-type (AD82) cells indicates that the dehydrogenase enzymes of the ETC have reduced TPH (white) to TPF (red). A lighter colour indicates lower activity of these dehydrogenase enzymes, resulting in less TPH reduced to TPF. Although this is a qualitative assay, the paler colour of Δ*tpx1* cells suggests impaired reduction of TPH, indicating that Tpx1 may be required for ETC activity.

Notably, Δ*pap1* cells contained higher levels of Hsp60 than wild-type (Figure 6.1A, 6.1B and 6.1C). Hsp60 is a mitochondrial chaperone that is induced in response to mitochondrial damage in animals. Hence it was possible that the elevated levels of Hsp60 in a Δ*pap1* compared to wild-type reflected a mitochondrial defect. However, Δ*pap1* cells were a darker red colour compared to wild-type cells (Figure 7.1), suggesting that, if anything, the dehydrogenase enzymes of the ETC are more active in Δ*pap1* than wild-type cells.

Some of Tpx1's functions require its thioredoxin peroxidase activity, for example Pap1 activation, which can be rescued by loss of *trr1*$^{+}$, whereas the peroxidatic cysteine is sufficient to promote Sty1 activation (Veal *et al.*, 2004). Hence, to test whether the thioredoxin peroxidase activity of Tpx1 was important for mitochondrial respiration, the TTC assay was also used to compare the resolving cysteine mutant, Tpx1^{C169S}, with the isogenic wild-type (JR68). Interestingly, both wild-type (JR68) and Tpx1^{C169S} cells appear to show decreased respiration in the presence of TTC, as they are lighter in colour than the wild-type (AD82) cells (Figure 7.1). Surprisingly, this indicates that wild-type (JR68) cells have reduced ETC activity. In contrast to AD82, these cells are *leu*$^{+}$, and contain Tpx1 that has the 3'-UTR from the *nmt1*$^{+}$ gene. Thus, it is possible that the altered auxotrophy or regulation of Tpx1 in this strain are responsible for its lower ETC activity. Unfortunately, this makes it difficult to make any conclusion from the analysis of the Tpx1^{C169S} mutant as to whether the thioredoxin peroxidase activity of Tpx1 is important for ETC activity.

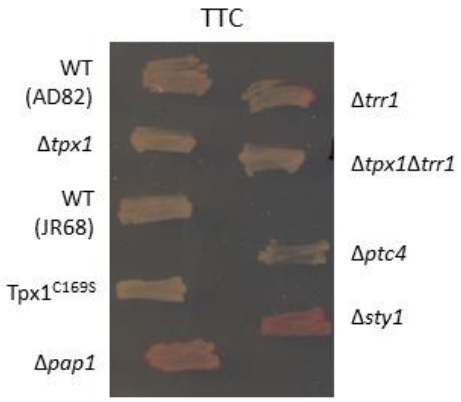

Figure 7.1 Effect of Tpx1, Pap1, Sty1 and Trr1 on mitochondrial respiration. 1% TTC was poured onto YE plates containing 3% glycerol, on which wild-type (AD82), Δ*tpx1* (VXOO), wild-type (JR68), Tpx1^{C169S} (JR42), Δ*pap1* (TP108-3C), Δ*trr1* (AD81), Δ*tpx1*Δ*trr1* (AD138), Δ*ptc4* (NJ1284) and Δ*sty1* (AD22) cells had been growing for four days. In this assay, a red colouration of the yeast cells indicates that TTC has been reduced by dehydrogenase enzymes of the ETC, and therefore the ETC is functional. Δ*ptc4* and Δ*sty1* cells were used as controls.

As an alternative approach to answer this question, we tested whether loss of *trr1*$^{+}$ was able to restore normal ETC activity to a Δ*tpx1*. We hypothesised that if the inability to regulate or oxidise thioredoxin is responsible for the mitochondrial defect of a Δ*tpx1*, then, like Pap1 activation, loss of *trr1*$^{+}$ might rescue this defect. Interestingly, both Δ*trr1* and Δ*tpx1*Δ*trr1* cells appear a lighter colour than wild-type (AD82) cells (Figure 7.1), however the Δ*trr1* cells are turning red on the edge of the colonies, suggesting that the ETC is partially functional in cells lacking *trr1*$^{+}$. On the other hand, Δ*tpx1*Δ*trr1* cells show a similar reduced colouration to Δ*tpx1* cells (Figure 7.1), indicating that loss of *trr1*$^{+}$ doesn't rescue the mitochondrial defect of a Δ*tpx1*. Therefore, consistent with the active ETC in a Δ*pap1* (Figure 7.1), the mitochondrial defect of a Δ*tpx1* cannot be due to the inability to oxidise Trx1 or Txl1 and Pap1. This suggests it is more likely to be through another role. Given the possible Tpx1-dependent form of Tim40 detected in chapter 6 (Figure 6.5B), this represents a possible alternative mechanism. The TTC assay doesn't appear to be a particular sensitive assay, and provides qualitative rather than quantitative data. To further assess the role of Tpx1 in cellular respiration and mitochondrial activity, oxygen consumption, which occurs at cytochrome *c* oxidase (complex IV), could be measured as a direct readout of ETC activity, to gain more quantitative data regarding rates of respiration in Δ*tpx1* and Tpx1^{C169S} cells compared to wild-type.

Recent work has shown that the thioredoxin peroxidase, Gpx3, in *S. cerevisiae*, resides in the mitochondrial IMS (Vogtle *et al.*, 2012). In addition, although the majority of Tpx1 is present in the cytoplasm, a small amount of Tpx1 is present in the mitochondria following H_2O_2 treatment (Di *et al.*, 2012). Intriguingly, in contrast to other eukaryotes, there is apparently no mitochondrially targeted 2-Cys Prx in *S. pombe*. Indeed, work from our laboratory has shown that expression of a mitochondrially targeted Prx, *C. elegans* PRDX-3, in *S. pombe* was toxic (Taylor, 2009). Of the five Prx in *S. cerevisiae*, the single 1-Cys Prx is localised to the mitochondria, where it has a specific protective role towards peroxides produced during respiration at the mitochondria (Pedrajas *et al.*, 2000). It is therefore possible that some Tpx1 may be present in the mitochondria, contributing to mitochondrial function, and having a similar protective function. Therefore, in the absence of *tpx1*$^{+}$, cells display reduced

respiration in the presence of TTC compared to wild-type (Figure 7.1), and have mitochondrial defects. In chapter 6, a band potentially representing a disulphide bond between Tim40 and Tpx1, both before and after treatment with H_2O_2, which requires the resolving cysteine of Tpx1, was detected (Figure 6.5B). This suggests that Tpx1 is important for the import of mitochondrial proteins by the Tim40 pathway, and could help explain why Δ*tpx1* cells display a mitochondrial defect.

7.2 Models of H_2O_2 sensing and signalling

There is now evidence that Prx can promote H_2O_2 signalling through different mechanisms, which are not mutually exclusive; (i) H_2O_2 can directly oxidise a Prx, which is then able to transmit the oxidation state to a signalling protein, such as a phosphatase or a transcription factor, through a disulphide relay, and (ii) by modulating the redox state of Trx, whereby H_2O_2 can oxidise a Prx, which is reduced by Trx, allowing the oxidised Trx to relay the oxidation to the signalling protein (For a review see (Netto and Antunes, 2016)).

Here this study has provided new examples of how cysteines in peroxide-regulated proteins are oxidised, and the role of the single typical 2-Cys Prx, Tpx1, in *S. pombe* in mediating H_2O_2 signalling. It will be discussed whether these roles of Tpx1 fit with the suggested mechanisms of Prx in promoting H_2O_2 signalling, or whether data from this study suggests that there are alternative mechanisms involving Tpx1, directly or indirectly, in the oxidation of H_2O_2-sensitive proteins. As described in chapter 3, the protein tyrosine phosphatase (PTP), Pyp1, forms a disulphide bond with Trx1 in *S. pombe*, dependent on Tpx1 (Figure 3.3C and 3.3D). This indicates that Tpx1 promotes the oxidation of Pyp1, however, unlike mechanism (i), Tpx1 does not participate directly in the oxidation of Pyp1. The presence of the Pyp1-Trx1 disulphides inhibits the Tpx1-mediated H_2O_2-induced degradation of Pyp1 (Figure 3.11B), suggesting that formation of this disulphide may be important to maintain Pyp1 levels following exposure to H_2O_2. In addition, the Pyp1-Trx1 disulphide may be important to prevent further H_2O_2-induced oxidations that are promoted by Tpx1. In most cases, the reaction of H_2O_2 with a

signalling protein is too slow to outcompete the reaction of H_2O_2 with a Prx, however GAPDH contain cysteine thiols which are able to react quicker with H_2O_2 than cysteine residues present in most signalling proteins. Chapter 5 identified that Tpx1 promotes the hyperoxidation of Tdh1 (Figure 5.17A and 5.17B). Unpublished work from our laboratory suggests that hyperoxidation of Tdh1 is also important for the activation of the Wis1 MAPKK, and that Tpx1 is required for both H_2O_2-induced modifications (Day and Veal unpublished data). The role for Tpx1 in the oxidation of Tdh1 remains unclear, and does not fit with either mechanism (i) or (ii) described above. However, as both Tpx1 and Tdh1 are required for the H_2O_2-induced phosphorylation of Wis1 at high levels of H_2O_2, this suggests that Tpx1 may act as a 'scaffold' to bring the components of the Sty1 pathway together (Figure 1.5). Finally, in chapter 6, through a directed and proteomic approach, this study identified and verified Srk1 as an interactor of Tpx1 at low (0.2 mM) concentrations of H_2O_2 (Figure 6.8A, 6.9A and 6.9B). The altered mobility of the higher molecular weight bands observed in cells expressing $Tpx1^{C169S}$ compared with wild type Tpx1, or Flag-epitope tagged compared with untagged Tpx1 or $Tpx1^{C169S}$, confirmed that Tpx1 is directly involved in Srk1 oxidation (Figure 5.9A). Furthermore, the sensitivity of the higher molecular weight bands to β-mercaptoethanol confirmed that the shifted bands are due to the formation of disulphide bonds in Srk1 (Figure 5.9B). However, the exact role of Tpx1 in oxidising Tim40 and Srk1 has not yet been elucidated and remains an outstanding question. For instance, does Tpx1 participate in a direct 'redox-transducing' role to oxidise Tim40 and/or Srk1, or does Tpx1 inhibit Trx1 from reducing the Tpx1-Tim40 or Tpx1-Srk1 mixed disulphide bonds?

7.3 Final summary and future perspectives

This study aimed to increase the understanding of the complex relationship between Prx and Trx in redox-signalling activities and in the regulation of MAPK signalling pathways in *S. pombe*. Prx have been shown to be important in H_2O_2 signalling, as exemplified by Tpx1 in *S. pombe*, which acts as a H_2O_2 sensor in the activation of both Pap1 and Sty1 (Veal *et al.*, 2004; Bozonet *et al.*, 2005). This raised

the possibility that Tpx1 may regulate the redox state of cysteine thiols in other proteins, transducing H_2O_2 signals through H_2O_2-induced oxidation. Indeed, this study has provided evidence that Tpx1 can regulate the oxidation state of multiple proteins, including Pyp1 (Chapter 3), Tdh1 (Chapter 5), and Srk1 (Chapter 6).

Previous work from our laboratory, incorporating computational modelling and experimental approaches, predicted a bi-phasic response to increased levels of extracellular H_2O_2, where hyperoxidation of Prx only occurred once the H_2O_2-removing activities were saturated (Tomalin *et al.*, 2016). This study has provided examples of the oxidation of proteins by different mechanisms at low and high levels of H_2O_2, to regulate the Sty1 MAPK pathway. Whilst the oxidation of Pyp1 occurred at low (0.2 mM and 1.0 mM) concentrations of H_2O_2 (Figure 3.3A), Tdh1 oxidation was only detected at higher (6.0 mM) concentrations of H_2O_2 (Figure 5.4A), both dependent on Tpx1. However, the fact that Tdh1 is only oxidised at these high concentrations of H_2O_2 suggests that GAPDH oxidation is a signalling event that only occurs when cells are exposed to doses of H_2O_2 they are unable to cope with. This highlights the idea that cells might use Prx in different mechanisms depending on whether the H_2O_2 signal is one they can adapt to, or one that is likely to lead to the generation of other, more toxic ROS, whereby damage limitation is required to allow cell survival.

S. pombe is a great system to investigate the kinetics of oxidation using a modelling approach due to the reduced gene redundancy, ease of genetic manipulation and presence of single components, such as the single typical 2-Cys Prx, Tpx1. In addition, the availability of global quantification of the *S. pombe* proteome allows an estimation of the copy number per cell for proteins. Therefore, modelling approaches to provide quantitative data and kinetic parameters are likely to be extremely useful for identifying key features in the complex network regulating MAPK activity in response to changing redox conditions.

Appendices

Appendix 1 The log_2 of the LFQ algorithm for proteins detected in the analysis of each immunopurification. Mass spectrometry analysis of proteins immunopurified with anti-Flag conjugated agarose from Δ*tpx1* (VXOO) cells containing the *S. pombe* expression vector Rep41FlagTpx1 (Tpx1), Rep41FlagTpx1^{C48S} (C48S), Rep41FlagTpx1^{C48SC169S} (2CS), and Rep41FlagTpx1^{C169S} (C169S) treated with 0.2 mM or 1.0 mM H_2O_2 for 10 minutes. Proteins are represented by the number generated by taking the log_2 of the LFQ algorithm, however proteins which were not detected were given the arbitrary number 10.

Gene name	C48S 1.0 mM	C48S 0.2 mM	C169S 1.0 mM	C169S 0.2 mM	2CS 1.0 mM	2CS 0.2 mM	Tpx1 1.0 mM	Tpx1 0.2 mM
mss116	25.13649	10	25.3693	24.65234	10	10	10	10
SPAC11E3.14	24.15228	10	24.91561	24.79208	10	24.00744	10	10
ubr11	10	10	25.40837	24.84781	10	10	10	10
SPAC17A5.13	23.74427	10	25.24096	24.97049	10	10	24.02876	24.97845
slt1	25.69198	10	24.39467	24.35023	10	10	10	10
ptr1	25.08493	10	26.2596	24.1277	10	10	10	10
SPAC19G12.05	24.25364	10	25.26109	24.70425	10	24.15445	25.67428	24.45764
hal4	10	10	25.03002	26.36873	10	10	10	10
SPAC6F6.11c	24.7686	10	25.51081	24.73505	10	10	10	10
cpd1	10	10	25.38643	25.87375	10	10	10	10
cao2	25.11275	10	25.46815	26.40261	10	10	10	24.50773
SPBC16A3.08c	24.93202	10	25.02808	26.50569	10	26.44182	27.70279	27.36545
syj1	24.3765	10	24.60738	24.4062	10	10	10	10
vac8	10	10	26.15165	25.67726	10	10	10	10
ppt1	10	10	25.59172	26.24178	10	24.78017	25.12345	24.44278
pre10	26.33897	10	25.04922	25.35632	10	10	10	10
pmr1	24.66644	10	24.15383	24.72567	10	10	10	10
met6	10	10	28.27013	28.78028	10	10	10	10
kap123	10	10	25.54301	25.79198	10	24.75348	10	10

SPBC14F5.13c	10	10	24.12242	23.45889	10	23.3806	10	10
SPCC1672.11c	23.2839	10	23.32306	24.00273	10	10	10	10
scw1	22.79432	10	23.64306	26.6147	10	22.72844	10	10
sal3	10	10	24.72874	25.41096	10	10	10	10
ret2	10	10	23.3009	24.57957	10	10	10	10
msh2	10	10	24.37729	23.38271	10	10	10	10
sec231	24.85315	10	25.38555	24.25904	10	25.61661	26.56024	10
mcm7	10	10	24.5501	24.05341	10	10	10	10
SPCC1620.06c	24.39198	10	24.48204	25.94905	10	25.12384	10	25.89472
srk1	10	10	29.62718	30.17677	10	10	24.06316	10
mug158	10	10	25.93195	24.77891	10	10	10	10
nog1	10	10	25.80329	25.3318	10	24.12305	25.07782	10
sec232	24.93261	10	25.1991	26.29058	10	24.98425	26.10189	10
nsa1	23.94101	10	23.47098	23.26513	10	10	10	10
leu1	10	10	22.72307	25.09623	10	23.93832	23.09302	24.54304
ccr1	25.02141	10	25.51141	24.96596	10	10	10	10
hhp1	10	10	27.69445	29.26787	10	10	25.34496	10
pka1	10	10	26.23934	26.05246	10	10	10	10
isp6	10	10	23.85167	24.39885	10	10	10	10
SPAC4A8.14	24.68817	10	25.96647	27.01861	10	24.40347	10	10
rpn12	10	10	23.31341	23.66438	10	10	10	10
SPBC2D10.11c	10	10	23.25338	10	10	10	10	10
not1	10	10	26.04366	25.33091	10	10	10	10
hmt1	24.53392	10	24.33047	25.7751	10	25.07721	25.0757	25.55622
ptc3	24.96133	10	25.83193	26.95172	10	25.68862	25.45275	25.75842

mlo3	24.3534	10	23.90251	24.49644	10	10	10	24.87544
SPAC5H10.10	10	10	26.2188	25.58964	10	10	10	10
SPBC12C2.03c	23.91816	10	25.32083	24.59673	10	10	29.80186	27.05858
pim1	10	10	24.65168	24.76734	10	23.81519	10	10
Uncharacterised peptidase C22G7.01c	26.98587	10	28.98174	28.47456	10	10	25.7434	10
ubp5	10	10	25.68126	25.2116	10	24.23608	10	23.45839
cys2	24.21623	10	25.66359	25.00727	10	10	24.50857	25.06188
mkh1	10	10	25.8098	25.60261	10	10	10	10
mug161	10	10	23.2177	23.65371	10	10	10	10
vid27	24.49589	10	23.88762	23.77435	10	23.51881	10	10
trr1	25.56851	10	24.48904	24.74139	10	10	10	10
SPAPB8E5.07c	25.00744	10	25.50773	24.45331	10	10	10	10
gde1	23.01667	10	25.5198	24.46806	10	10	10	10
gal10	10	10	26.68231	26.90896	10	10	10	10
gcd10	10	10	23.32045	24.15252	10	10	10	10
sec63	10	10	24.94033	24.92814	10	10	10	10
ubp2	24.32787	10	24.53908	25.15839	10	24.13391	10	24.3221
cao1	10	10	27.87988	27.85911	10	10	23.48873	10
get3	24.38502	10	26.44271	24.98237	10	10	25.21286	10
mak1	10	10	25.65559	25.64952	10	10	10	10
nop58	10	10	25.60261	26.89758	10	26.78569	26.59847	10
sec72	10	10	24.81064	23.42777	10	23.46936	10	10
spe1	24.18896	10	26.21438	26.7313	10	24.21104	25.46728	24.65141
SPAC890.06	24.4036	10	26.3041	25.515	10	22.99094	10	23.56813
SPAC732.02c	10	10	22.7403	24.6049	10	25.61894	25.90855	24.25796

mef1	10	10	24.78531	24.26119	10	10	24.66335	10
brr2	10	10	25.52686	10	10	10	10	10
SPAC343.04c	10	10	25.77914	26.54648	10	22.771	24.12715	10
dus3	10	10	24.60405	23.6621	10	23.55004	23.0946	10
SPAC15E1.04	26.21801	10	25.21886	25.78925	10	25.91604	26.21089	25.71209
mug58	23.57635	10	26.86065	26.65048	10	10	25.02039	10
SPBC9B6.11c	10	10	24.55239	24.64752	10	10	10	10
SPCC569.03	10	10	27.32834	29.40143	10	10	10	10

Appendix 2 Outputs from MaxQuant analysis of raw data files from the mass spectrometry run. The outputs from MaxQuant for each protein include a peptide score, peptide intensity, and number of unique peptides, as described in section 2.4.5.3.

Gene name	Q-value	Score	Intensity	MS/MS count	Peptides	Razor + unique peptides	Unique peptides
mss116	0	70.727	2.83E+08	45	10	10	10
SPAC11E3.14	0	55.462	2.5E+08	62	9	9	9
ubr11	0	13.569	1.85E+08	25	9	9	9
SPAC17A5.13	0	12.441	2.09E+08	26	6	6	6
slt1	0	97.968	2.34E+08	46	8	8	8
ptr1	0	105.64	3.1E+08	64	14	14	14
SPAC19G12.05	0	106.81	1.23E+08	23	6	6	6
hal4	0	37.574	34857000	16	7	7	7
SPAC6F6.11c	0	50.033	4.04E+08	27	27	6	6
cpd1	0	27.738	1.09E+08	38	8	8	8
cao2	0	71.756	3.56E+08	71	15	15	15
SPBC16A3.08c	0	323.31	3.53E+09	105	14	14	14
syj1	0	24.662	1.7E+08	39	8	8	8
vac8	0	140.79	3.29E+08	57	11	11	11
ppt1	0	11.801	2.28E+08	30	7	7	7
pre10	0	107.26	3.35E+08	45	6	6	6
pmr1	0	166.09	4.33E+08	68	12	12	12
met6	0	87.143	1.31E+08	38	11	11	11
kap123	0	316.08	6.15E+08	96	16	16	16
SPBC14F5.13c	0	183.82	1.17E+09	124	13	13	13
SPCC1672.11c	0	248.48	2.41E+08	44	8	8	8
scw1	0	21.285	31179000	22	10	10	10
sal3	0	238.82	1.23E+09	97	17	17	17
ret2	0	20.135	1.09E+08	34	6	6	6
msh2	0	72.387	78721000	28	7	7	7
sec231	0	323.31	3.08E+09	148	18	18	17
mcm7	0	13.904	1.1E+08	25	8	8	8
SPCC1620.06c	0	38.808	3.33E+08	30	6	6	6
srk1	0	237.14	4.93E+08	92	22	22	22
mug158	0	19.788	97856000	28	11	11	11
nog1	0	241.27	2.35E+08	62	11	11	11
sec232	0	323.31	8.92E+08	80	16	15	15
nsa1	0	14.121	47852000	23	6	6	6
leu1	0	20.545	59772000	32	6	6	6
ccr1	0	52.55	5.77E+08	47	9	9	9
hhp1	0	37.488	2.42E+08	34	12	12	12
pka1	0	310.83	4.4E+08	39	6	6	6
isp6	0	52.024	9.7E+08	40	7	7	7
SPAC4A8.14	0	132.74	2.81E+08	37	7	7	7
rpn12	0	323.31	8.5E+08	74	8	8	8
SPBC2D10.11c	0	63.285	1.74E+08	44	7	7	7
not1	0	262.22	4.06E+08	92	23	23	23
hmt1	0	184.75	7.53E+08	64	10	10	10
ptc3	0	22.149	5.72E+08	53	8	8	8

mlo3	0	186.01	7.08E+08	75	12	12	12
SPAC5H10.10	0	228.89	6.89E+08	55	7	7	7
SPBC12C2.03c	0	101.4	5.66E+08	73	15	15	15
pim1	0	35.377	1.6E+08	38	12	12	12
Uncharacterised peptidase C22G7.01c	0	78.593	3.48E+08	47	11	11	11
ubp5	0	73.245	2.59E+08	47	12	12	12
cys2	0	132.86	4.95E+08	81	11	11	11
mkh1	0	13.029	29673000	17	8	8	8
mug161	0	9.4323	19635000	10	7	7	7
vid27	0	27.565	1.43E+08	26	7	7	7
trr1	0	176.13	4.63E+08	62	7	7	7
SPAPB8E5.07c	0	12.629	3.03E+08	23	6	6	6
gde1	0	86.57	3.85E+08	52	13	13	13
gal10	0	18.791	36062000	21	10	10	10
gcd10	0	10.642	52857000	21	6	6	6
sec63	0	37.241	2.47E+08	35	6	6	6
ubp2	0	197.09	5.31E+08	107	21	21	21
cao1	0	140.58	3.55E+08	88	15	15	15
get3	0	96.786	3.17E+08	35	6	6	6
mak1	0	16.68	23448000	16	12	12	12
nop58	0	134.77	9.31E+08	56	9	9	9
sec72	0	115.78	1.22E+08	50	11	11	11
spe1	0	44.766	3.32E+08	52	7	7	7
SPAC890.06	0	126.1	7.06E+08	129	19	19	19
SPAC732.02c	0	87.055	5.09E+08	62	10	10	10
mef1	0	37.562	1.34E+08	34	6	6	6
brr2	0	135.18	5.21E+08	47	16	16	16
SPAC343.04c	0	104.96	35058000	12	7	7	7
dus3	0	32.747	1.01E+08	30	6	6	6
SPAC15E1.04	0	323.31	6.18E+08	41	7	7	7
mug58	0	198.8	1.48E+08	35	7	7	7
SPBC9B6.11c	0	31.641	1.26E+08	43	7	7	7
SPCC569.03	0	58.636	71063000	34	14	14	12

References

Allen, S., Balabanidou, V., Sideris, D.P., Lisowsky, T. and Tokatlidis, K. (2005) 'Erv1 mediates the Mia40-dependent protein import pathway and provides a functional link to the respiratory chain by shuttling electrons to cytochrome c', *J Mol Biol*, 353(5), pp. 937-44.

Aslund, F. and Beckwith, J. (1999) 'Bridge over troubled waters: sensing stress by disulfide bond formation', *Cell*, 96(6), pp. 751-3.

Avery, A.M. and Avery, S.V. (2001) 'Saccharomyces cerevisiae expresses three phospholipid hydroperoxide glutathione peroxidases', *J Biol Chem*, 276(36), pp. 33730-5.

Banci, L., Bertini, I., Cefaro, C., Ciofi-Baffoni, S., Gallo, A., Martinelli, M., Sideris, D.P., Katrakili, N. and Tokatlidis, K. (2009) 'MIA40 is an oxidoreductase that catalyzes oxidative protein folding in mitochondria', *Nat Struct Mol Biol*, 16(2), pp. 198-206.

Barrett, W.C., DeGnore, J.P., Konig, S., Fales, H.M., Keng, Y.F., Zhang, Z.Y., Yim, M.B. and Chock, P.B. (1999) 'Regulation of PTP1B via glutathionylation of the active site cysteine 215', *Biochemistry*, 38(20), pp. 6699-705.

Bauer, M.F., Rothbauer, U., Muhlenbein, N., Smith, R.J., Gerbitz, K., Neupert, W., Brunner, M. and Hofmann, S. (1999) 'The mitochondrial TIM22 preprotein translocase is highly conserved throughout the eukaryotic kingdom', *FEBS Lett*, 464(1-2), pp. 41-7.

Berlett, B.S. and Stadtman, E.R. (1997) 'Protein oxidation in aging, disease, and oxidative stress', *J Biol Chem*, 272(33), pp. 20313-6.

Bihlmaier, K., Mesecke, N., Terziyska, N., Bien, M., Hell, K. and Herrmann, J.M. (2007) 'The disulfide relay system of mitochondria is connected to the respiratory chain', *J Cell Biol*, 179(3), pp. 389-95.

Bilsland-Marchesan, E., Arino, J., Saito, H., Sunnerhagen, P. and Posas, F. (2000) 'Rck2 kinase is a substrate for the osmotic stress-activated mitogen-activated protein kinase Hog1', *Mol Cell Biol*, 20(11), pp. 3887-95.

Biswas, S., Chida, A.S. and Rahman, I. (2006) 'Redox modifications of protein-thiols: emerging roles in cell signaling', *Biochem Pharmacol*, 71(5), pp. 551-64.

Biteau, B., Labarre, J. and Toledano, M.B. (2003) 'ATP-dependent reduction of cysteine-sulphinic acid by S. cerevisiae sulphiredoxin', *Nature*, 425(6961), pp. 980-4.

Boileau, C., Eme, L., Brochier-Armanet, C., Janicki, A., Zhang, C.C. and Latifi, A. (2011) 'A eukaryotic-like sulfiredoxin involved in oxidative stress responses and in the reduction of the sulfinic form of 2-Cys peroxiredoxin in the cyanobacterium Anabaena PCC 7120', *New Phytol*, 191(4), pp. 1108-18.

Bokov, A., Chaudhuri, A. and Richardson, A. (2004) 'The role of oxidative damage and stress in aging', *Mech Ageing Dev*, 125(10-11), pp. 811-26.

Bozonet, S.M. (2006) *Role of peroxiredoxins in the stress response of Schizosaccharomyces pombe*. Newcastle University.

Bozonet, S.M., Findlay, V.J., Day, A.M., Cameron, J., Veal, E.A. and Morgan, B.A. (2005) 'Oxidation of a eukaryotic 2-Cys peroxiredoxin is a molecular switch controlling the transcriptional response to increasing levels of hydrogen peroxide', *J Biol Chem*, 280(24), pp. 23319-27.

Brodie, A.E. and Reed, D.J. (1987) 'Reversible oxidation of glyceraldehyde 3-phosphate dehydrogenase thiols in human lung carcinoma cells by hydrogen peroxide', *Biochem Biophys Res Commun*, 148(1), pp. 120-5.

Brodie, A.E. and Reed, D.J. (1990) 'Cellular recovery of glyceraldehyde-3-phosphate dehydrogenase activity and thiol status after exposure to hydroperoxides', *Arch Biochem Biophys*, 276(1), pp. 212-8.

Brown, J.D., Day, A.M., Taylor, S.R., Tomalin, L.E., Morgan, B.A. and Veal, E.A. (2013) 'A peroxiredoxin promotes H2O2 signaling and oxidative stress resistance by oxidizing a thioredoxin family protein', *Cell Rep*, 5(5), pp. 1425-35.

Buck, V., Quinn, J., Soto Pino, T., Martin, H., Saldanha, J., Makino, K., Morgan, B.A. and Millar, J.B. (2001) 'Peroxide sensors for the fission yeast stress-activated mitogen-activated protein kinase pathway', *Mol Biol Cell*, 12(2), pp. 407-19.

Budanov, A.V., Sablina, A.A., Feinstein, E., Koonin, E.V. and Chumakov, P.M. (2004) 'Regeneration of peroxiredoxins by p53-regulated sestrins, homologs of bacterial AhpD', *Science*, 304(5670), pp. 596-600.
Cabiscol, E., Piulats, E., Echave, P., Herrero, E. and Ros, J. (2000) 'Oxidative stress promotes specific protein damage in Saccharomyces cerevisiae', *J Biol Chem*, 275(35), pp. 27393-8.
Calvo, I.A., Ayte, J. and Hidalgo, E. (2013) 'Reversible thiol oxidation in the H2O2-dependent activation of the transcription factor Pap1', *J Cell Sci*, 126(Pt 10), pp. 2279-84.
Calvo, I.A., Garcia, P., Ayte, J. and Hidalgo, E. (2012) 'The transcription factors Pap1 and Prr1 collaborate to activate antioxidant, but not drug tolerance, genes in response to H2O2', *Nucleic Acids Res*, 40(11), pp. 4816-24.
Cao, J., Schulte, J., Knight, A., Leslie, N.R., Zagozdzon, A., Bronson, R., Manevich, Y., Beeson, C. and Neumann, C.A. (2009) 'Prdx1 inhibits tumorigenesis via regulating PTEN/AKT activity', *Embo j*, 28(10), pp. 1505-17.
Carrie, C., Giraud, E., Duncan, O., Xu, L., Wang, Y., Huang, S., Clifton, R., Murcha, M., Filipovska, A., Rackham, O., Vrielink, A. and Whelan, J. (2010) 'Conserved and novel functions for Arabidopsis thaliana MIA40 in assembly of proteins in mitochondria and peroxisomes', *J Biol Chem*, 285(46), pp. 36138-48.
Castillo, E.A., Ayte, J., Chiva, C., Moldon, A., Carrascal, M., Abian, J., Jones, N. and Hidalgo, E. (2002) 'Diethylmaleate activates the transcription factor Pap1 by covalent modification of critical cysteine residues', *Mol Microbiol*, 45(1), pp. 243-54.
Chacinska, A., Pfannschmidt, S., Wiedemann, N., Kozjak, V., Sanjuan Szklarz, L.K., Schulze-Specking, A., Truscott, K.N., Guiard, B., Meisinger, C. and Pfanner, N. (2004) 'Essential role of Mia40 in import and assembly of mitochondrial intermembrane space proteins', *Embo j*, 23(19), pp. 3735-46.
Charbonneau, H., Tonks, N.K., Kumar, S., Diltz, C.D., Harrylock, M., Cool, D.E., Krebs, E.G., Fischer, E.H. and Walsh, K.A. (1989) 'Human placenta protein-tyrosine-phosphatase: amino acid sequence and relationship to a family of receptor-like proteins', *Proc Natl Acad Sci U S A*, 86(14), pp. 5252-6.
Chaudiere, J. and Ferrari-Iliou, R. (1999) 'Intracellular antioxidants: from chemical to biochemical mechanisms', *Food Chem Toxicol*, 37(9-10), pp. 949-62.
Chen, C.Y., Willard, D. and Rudolph, J. (2009) 'Redox regulation of SH2-domain-containing protein tyrosine phosphatases by two backdoor cysteines', *Biochemistry*, 48(6), pp. 1399-409.
Chen, D., Toone, W.M., Mata, J., Lyne, R., Burns, G., Kivinen, K., Brazma, A., Jones, N. and Bahler, J. (2003) 'Global transcriptional responses of fission yeast to environmental stress', *Mol Biol Cell*, 14(1), pp. 214-29.
Chen, D., Wilkinson, C.R., Watt, S., Penkett, C.J., Toone, W.M., Jones, N. and Bahler, J. (2008) 'Multiple pathways differentially regulate global oxidative stress responses in fission yeast', *Mol Biol Cell*, 19(1), pp. 308-17.
Chiron, S., Gaisne, M., Guillou, E., Belenguer, P., Clark-Walker, G.D. and Bonnefoy, N. (2007) 'Studying mitochondria in an attractive model: Schizosaccharomyces pombe', *Methods Mol Biol*, 372, pp. 91-105.
Cho, S.H., Lee, C.H., Ahn, Y., Kim, H., Kim, H., Ahn, C.Y., Yang, K.S. and Lee, S.R. (2004) 'Redox regulation of PTEN and protein tyrosine phosphatases in H(2)O(2) mediated cell signaling', *FEBS Lett*, 560(1-3), pp. 7-13.
Choi, M.H., Lee, I.K., Kim, G.W., Kim, B.U., Han, Y.H., Yu, D.Y., Park, H.S., Kim, K.Y., Lee, J.S., Choi, C., Bae, Y.S., Lee, B.I., Rhee, S.G. and Kang, S.W. (2005) 'Regulation of PDGF signalling and vascular remodelling by peroxiredoxin II', *Nature*, 435(7040), pp. 347-53.
Claiborne, A., Yeh, J.I., Mallett, T.C., Luba, J., Crane, E.J., 3rd, Charrier, V. and Parsonage, D. (1999) 'Protein-sulfenic acids: diverse roles for an unlikely player in enzyme catalysis and redox regulation', *Biochemistry*, 38(47), pp. 15407-16.
Collinson, E.J. and Grant, C.M. (2003) 'Role of yeast glutaredoxins as glutathione S-transferases', *J Biol Chem*, 278(25), pp. 22492-7.

Collinson, E.J., Wheeler, G.L., Garrido, E.O., Avery, A.M., Avery, S.V. and Grant, C.M. (2002) 'The yeast glutaredoxins are active as glutathione peroxidases', *J Biol Chem*, 277(19), pp. 16712-7.
Colussi, C., Albertini, M.C., Coppola, S., Rovidati, S., Galli, F. and Ghibelli, L. (2000) 'H2O2-induced block of glycolysis as an active ADP-ribosylation reaction protecting cells from apoptosis', *Faseb j*, 14(14), pp. 2266-76.
Conway, J.P. and Kinter, M. (2006) 'Dual role of peroxiredoxin I in macrophage-derived foam cells', *J Biol Chem*, 281(38), pp. 27991-8001.
Cooke, M.S., Mistry, N., Ahmad, J., Waller, H., Langford, L., Bevan, R.J., Evans, M.D., Jones, G.D., Herbert, K.E., Griffiths, H.R. and Lunec, J. (2003) 'Deoxycytidine glyoxal: lesion induction and evidence of repair following vitamin C supplementation in vivo', *Free Radic Biol Med*, 34(2), pp. 218-25.
Cox, J. and Mann, M. (2008) 'MaxQuant enables high peptide identification rates, individualized p.p.b.-range mass accuracies and proteome-wide protein quantification', *Nat Biotechnol*, 26(12), pp. 1367-72.
Cox, J., Neuhauser, N., Michalski, A., Scheltema, R.A., Olsen, J.V. and Mann, M. (2011) 'Andromeda: a peptide search engine integrated into the MaxQuant environment', *J Proteome Res*, 10(4), pp. 1794-805.
Cyrne, L., Antunes, F., Sousa-Lopes, A., Diaz-Berrio, J. and Marinho, H.S. (2010) 'Glyceraldehyde-3-phosphate dehydrogenase is largely unresponsive to low regulatory levels of hydrogen peroxide in Saccharomyces cerevisiae', *BMC Biochem*, 11, p. 49.
da Silva Dantas, A., Patterson, M.J., Smith, D.A., Maccallum, D.M., Erwig, L.P., Morgan, B.A. and Quinn, J. (2010) 'Thioredoxin regulates multiple hydrogen peroxide-induced signaling pathways in Candida albicans', *Mol Cell Biol*, 30(19), pp. 4550-63.
Dabir, D.V., Leverich, E.P., Kim, S.K., Tsai, F.D., Hirasawa, M., Knaff, D.B. and Koehler, C.M. (2007) 'A role for cytochrome c and cytochrome c peroxidase in electron shuttling from Erv1', *Embo j*, 26(23), pp. 4801-11.
Dahlkvist, A., Kanter-Smoler, G. and Sunnerhagen, P. (1995) 'The RCK1 and RCK2 protein kinase genes from Saccharomyces cerevisiae suppress cell cycle checkpoint mutations in Schizosaccharomyces pombe', *Mol Gen Genet*, 246(3), pp. 316-26.
Dalle-Donne, I., Rossi, R., Giustarini, D., Colombo, R. and Milzani, A. (2007) 'S-glutathionylation in protein redox regulation', *Free Radic Biol Med*, 43(6), pp. 883-98.
Dansen, T.B., Smits, L.M., van Triest, M.H., de Keizer, P.L., van Leenen, D., Koerkamp, M.G., Szypowska, A., Meppelink, A., Brenkman, A.B., Yodoi, J., Holstege, F.C. and Burgering, B.M. (2009) 'Redox-sensitive cysteines bridge p300/CBP-mediated acetylation and FoxO4 activity', *Nat Chem Biol*, 5(9), pp. 664-72.
Darby, N.J. and Creighton, T.E. (1995) 'Catalytic mechanism of DsbA and its comparison with that of protein disulfide isomerase', *Biochemistry*, 34(11), pp. 3576-87.
Darby, N.J., Penka, E. and Vincentelli, R. (1998) 'The multi-domain structure of protein disulfide isomerase is essential for high catalytic efficiency', *J Mol Biol*, 276(1), pp. 239-47.
Day, A.M., Brown, J.D., Taylor, S.R., Rand, J.D., Morgan, B.A. and Veal, E.A. (2012) 'Inactivation of a peroxiredoxin by hydrogen peroxide is critical for thioredoxin-mediated repair of oxidized proteins and cell survival', *Mol Cell*, 45(3), pp. 398-408.
Day, A.M. and Veal, E.A. (2010) 'Hydrogen peroxide-sensitive cysteines in the Sty1 MAPK regulate the transcriptional response to oxidative stress', *J Biol Chem*, 285(10), pp. 7505-16.
De Haes, W., Frooninckx, L., Van Assche, R., Smolders, A., Depuydt, G., Billen, J., Braeckman, B.P., Schoofs, L. and Temmerman, L. (2014) 'Metformin promotes lifespan through mitohormesis via the peroxiredoxin PRDX-2', *Proc Natl Acad Sci U S A*, 111(24), pp. E2501-9.
Degols, G., Shiozaki, K. and Russell, P. (1996) 'Activation and regulation of the Spc1 stress-activated protein kinase in Schizosaccharomyces pombe', *Mol Cell Biol*, 16(6), pp. 2870-7.
Delaunay, A., Isnard, A.D. and Toledano, M.B. (2000) 'H2O2 sensing through oxidation of the Yap1 transcription factor', *EMBO J*, 19(19), pp. 5157-66.

Delaunay, A., Pflieger, D., Barrault, M.B., Vinh, J. and Toledano, M.B. (2002) 'A thiol peroxidase is an H2O2 receptor and redox-transducer in gene activation', *Cell*, 111(4), pp. 471-81.
den Hertog, J., Groen, A. and van der Wijk, T. (2005) 'Redox regulation of protein-tyrosine phosphatases', *Arch Biochem Biophys*, 434(1), pp. 11-5.
Di, Y., Holmes, E.J., Butt, A., Dawson, K., Mironov, A., Kotiadis, V.N., Gourlay, C.W., Jones, N. and Wilkinson, C.R. (2012) 'H(2)O(2) stress-specific regulation of S. pombe MAPK Sty1 by mitochondrial protein phosphatase Ptc4', *EMBO J*, 31(3), pp. 563-75.
Duch, A., de Nadal, E. and Posas, F. (2012) 'The p38 and Hog1 SAPKs control cell cycle progression in response to environmental stresses', *FEBS Lett*, 586(18), pp. 2925-31.
Dudas, S.P. and Arking, R. (1995) 'A coordinate upregulation of antioxidant gene activities is associated with the delayed onset of senescence in a long-lived strain of Drosophila', *J Gerontol A Biol Sci Med Sci*, 50(3), pp. B117-27.
Durigon, R., Wang, Q., Ceh Pavia, E., Grant, C.M. and Lu, H. (2012) 'Cytosolic thioredoxin system facilitates the import of mitochondrial small Tim proteins', *EMBO Rep*, 13(10), pp. 916-22.
Farrell, S.R. and Thorpe, C. (2005) 'Augmenter of liver regeneration: a flavin-dependent sulfhydryl oxidase with cytochrome c reductase activity', *Biochemistry*, 44(5), pp. 1532-41.
Fernandes, A.P. and Holmgren, A. (2004) 'Glutaredoxins: glutathione-dependent redox enzymes with functions far beyond a simple thioredoxin backup system', *Antioxid Redox Signal*, 6(1), pp. 63-74.
Ferrari, D.M. and Soling, H.D. (1999) 'The protein disulphide-isomerase family: unravelling a string of folds', *Biochem J*, 339 (Pt 1), pp. 1-10.
Finkel, T. (2011) 'Signal transduction by reactive oxygen species', *J Cell Biol*, 194(1), pp. 7-15.
Finkel, T. and Holbrook, N.J. (2000) 'Oxidants, oxidative stress and the biology of ageing', *Nature*, 408(6809), pp. 239-47.
Freedman, R.B., Klappa, P. and Ruddock, L.W. (2002) 'Protein disulfide isomerases exploit synergy between catalytic and specific binding domains', *EMBO Rep*, 3(2), pp. 136-40.
Gabriel, K., Milenkovic, D., Chacinska, A., Muller, J., Guiard, B., Pfanner, N. and Meisinger, C. (2007) 'Novel mitochondrial intermembrane space proteins as substrates of the MIA import pathway', *J Mol Biol*, 365(3), pp. 612-20.
Gan, Z.R. (1991) 'Yeast thioredoxin genes', *J Biol Chem*, 266(3), pp. 1692-6.
Garrido, E.O. and Grant, C.M. (2002) 'Role of thioredoxins in the response of Saccharomyces cerevisiae to oxidative stress induced by hydroperoxides', *Mol Microbiol*, 43(4), pp. 993-1003.
Geiszt, M. and Leto, T.L. (2004) 'The Nox family of NAD(P)H oxidases: host defense and beyond', *J Biol Chem*, 279(50), pp. 51715-8.
Gonzalez Porque, P., Baldesten, A. and Reichard, P. (1970a) 'The involvement of the thioredoxin system in the reduction of methionine sulfoxide and sulfate', *J Biol Chem*, 245(9), pp. 2371-4.
Gonzalez Porque, P., Baldesten, A. and Reichard, P. (1970b) 'Purification of a thioredoxin system from yeast', *J Biol Chem*, 245(9), pp. 2363-70.
Gotoh, Y. and Cooper, J.A. (1998) 'Reactive oxygen species- and dimerization-induced activation of apoptosis signal-regulating kinase 1 in tumor necrosis factor-alpha signal transduction', *J Biol Chem*, 273(28), pp. 17477-82.
Grant, C.M. (2001) 'Role of the glutathione/glutaredoxin and thioredoxin systems in yeast growth and response to stress conditions', *Mol Microbiol*, 39(3), pp. 533-41.
Grant, C.M., Quinn, K.A. and Dawes, I.W. (1999) 'Differential protein S-thiolation of glyceraldehyde-3-phosphate dehydrogenase isoenzymes influences sensitivity to oxidative stress', *Mol Cell Biol*, 19(4), pp. 2650-6.
Grumbt, B., Stroobant, V., Terziyska, N., Israel, L. and Hell, K. (2007) 'Functional characterization of Mia40p, the central component of the disulfide relay system of the mitochondrial intermembrane space', *J Biol Chem*, 282(52), pp. 37461-70.
Guddat, L.W., Bardwell, J.C. and Martin, J.L. (1998) 'Crystal structures of reduced and oxidized DsbA: investigation of domain motion and thiolate stabilization', *Structure*, 6(6), pp. 757-67.

Gutteridge, J.M.C. and Halliwell, B. (1999) 'Free Radicals in Biology and Medicine', *Oxford, Oxford University Press*.
Halliwell, B. and Gutteridge, J.M. (1984a) 'Oxygen toxicity, oxygen radicals, transition metals and disease', *Biochem J*, 219(1), pp. 1-14.
Halliwell, B. and Gutteridge, J.M. (1984b) 'Role of iron in oxygen radical reactions', *Methods Enzymol*, 105, pp. 47-56.
Halliwell, B. and Gutteridge, J.M. (1985) 'The importance of free radicals and catalytic metal ions in human diseases', *Mol Aspects Med*, 8(2), pp. 89-193.
Hannig, G., Ottilie, S. and Erikson, R.L. (1994) 'Negative regulation of mitosis in fission yeast by catalytically inactive pyp1 and pyp2 mutants', *Proc Natl Acad Sci U S A*, 91(21), pp. 10084-8.
Hanzen, S., Vielfort, K., Yang, J., Roger, F., Andersson, V., Zamarbide-Fores, S., Andersson, R., Malm, L., Palais, G., Biteau, B., Liu, B., Toledano, M.B., Molin, M. and Nystrom, T. (2016) 'Lifespan Control by Redox-Dependent Recruitment of Chaperones to Misfolded Proteins', *Cell*, 166(1), pp. 140-51.
Hara, S., Nojima, T., Seio, K., Yoshida, M. and Hisabori, T. (2013) 'DNA-maleimide: an improved maleimide compound for electrophoresis-based titration of reactive thiols in a specific protein', *Biochim Biophys Acta*, 1830(4), pp. 3077-81.
Haridas, V., Ni, J., Meager, A., Su, J., Yu, G.L., Zhai, Y., Kyaw, H., Akama, K.T., Hu, J., Van Eldik, L.J. and Aggarwal, B.B. (1998) 'TRANK, a novel cytokine that activates NF-kappa B and c-Jun N-terminal kinase', *J Immunol*, 161(1), pp. 1-6.
Harman, D. (1956) 'Aging: a theory based on free radical and radiation chemistry', *J Gerontol*, 11(3), pp. 298-300.
Hartmuth, S. and Petersen, J. (2009) 'Fission yeast Tor1 functions as part of TORC1 to control mitotic entry through the stress MAPK pathway following nutrient stress', *J Cell Sci*, 122(Pt 11), pp. 1737-46.
Hayes, J.D., McLeod, R., Ellis, E.M., Pulford, D.J., Ireland, L.S., McLellan, L.I., Judah, D.J., Manson, M.M. and Neal, G.E. (1996) 'Regulation of glutathione S-transferases and aldehyde reductase by chemoprotectors: studies of mechanisms responsible for inducible resistance to aflatoxin B1', *IARC Sci Publ*, (139), pp. 175-87.
Herrmann, J.M. and Hell, K. (2005) 'Chopped, trapped or tacked--protein translocation into the IMS of mitochondria', *Trends Biochem Sci*, 30(4), pp. 205-11.
Herrmann, J.M. and Kohl, R. (2007) 'Catch me if you can! Oxidative protein trapping in the intermembrane space of mitochondria', *J Cell Biol*, 176(5), pp. 559-63.
Herrmann, J.M. and Riemer, J. (2010) 'The intermembrane space of mitochondria', *Antioxid Redox Signal*, 13(9), pp. 1341-58.
Hildebrandt, T., Knuesting, J., Berndt, C., Morgan, B. and Scheibe, R. (2015) 'Cytosolic thiol switches regulating basic cellular functions: GAPDH as an information hub?', *Biol Chem*, 396(5), pp. 523-37.
Hofmann, B., Hecht, H.J. and Flohe, L. (2002) 'Peroxiredoxins', *Biol Chem*, 383(3-4), pp. 347-64.
Holmes, E.J. (2013) *The Identification of Novel Targets of the Fission Yeast Sty1 MAP Kinase*. University of Manchester.
Holmgren, A., Johansson, C., Berndt, C., Lonn, M.E., Hudemann, C. and Lillig, C.H. (2005) 'Thiol redox control via thioredoxin and glutaredoxin systems', *Biochem Soc Trans*, 33(Pt 6), pp. 1375-7.
Holmgren, A. and Lu, J. (2010) 'Thioredoxin and thioredoxin reductase: current research with special reference to human disease', *Biochem Biophys Res Commun*, 396(1), pp. 120-4.
Hu, J., Dong, L. and Outten, C.E. (2008) 'The redox environment in the mitochondrial intermembrane space is maintained separately from the cytosol and matrix', *J Biol Chem*, 283(43), pp. 29126-34.
Ichijo, H., Nishida, E., Irie, K., ten Dijke, P., Saitoh, M., Moriguchi, T., Takagi, M., Matsumoto, K., Miyazono, K. and Gotoh, Y. (1997) 'Induction of apoptosis by ASK1, a mammalian MAPKKK that activates SAPK/JNK and p38 signaling pathways', *Science*, 275(5296), pp. 90-4.
Inoue, Y., Matsuda, T., Sugiyama, K., Izawa, S. and Kimura, A. (1999) 'Genetic analysis of glutathione peroxidase in oxidative stress response of Saccharomyces cerevisiae', *J Biol Chem*, 274(38), pp. 27002-9.

Ischiropoulos, H. and Beckman, J.S. (2003) 'Oxidative stress and nitration in neurodegeneration: cause, effect, or association?', *J Clin Invest*, 111(2), pp. 163-9.
Jacob, C., Holme, A.L. and Fry, F.H. (2004) 'The sulfinic acid switch in proteins', *Org Biomol Chem*, 2(14), pp. 1953-6.
Jamieson, D.J. (1998) 'Oxidative stress responses of the yeast Saccharomyces cerevisiae', *Yeast*, 14(16), pp. 1511-27.
Janero, D.R., Hreniuk, D. and Sharif, H.M. (1994) 'Hydroperoxide-induced oxidative stress impairs heart muscle cell carbohydrate metabolism', *Am J Physiol*, 266(1 Pt 1), pp. C179-88.
Jang, H.H., Lee, K.O., Chi, Y.H., Jung, B.G., Park, S.K., Park, J.H., Lee, J.R., Lee, S.S., Moon, J.C., Yun, J.W., Choi, Y.O., Kim, W.Y., Kang, J.S., Cheong, G.W., Yun, D.J., Rhee, S.G., Cho, M.J. and Lee, S.Y. (2004) 'Two enzymes in one; two yeast peroxiredoxins display oxidative stress-dependent switching from a peroxidase to a molecular chaperone function', *Cell*, 117(5), pp. 625-35.
Janssen-Heininger, Y.M., Mossman, B.T., Heintz, N.H., Forman, H.J., Kalyanaraman, B., Finkel, T., Stamler, J.S., Rhee, S.G. and van der Vliet, A. (2008) 'Redox-based regulation of signal transduction: principles, pitfalls, and promises', *Free Radic Biol Med*, 45(1), pp. 1-17.
Jara, M., Vivancos, A.P., Calvo, I.A., Moldon, A., Sanso, M. and Hidalgo, E. (2007) 'The peroxiredoxin Tpx1 is essential as a H2O2 scavenger during aerobic growth in fission yeast', *Mol Biol Cell*, 18(6), pp. 2288-95.
Jarvis, R.M., Hughes, S.M. and Ledgerwood, E.C. (2012) 'Peroxiredoxin 1 functions as a signal peroxidase to receive, transduce, and transmit peroxide signals in mammalian cells', *Free Radic Biol Med*, 53(7), pp. 1522-30.
Jin, J., Chen, X., Zhou, Y., Bartlam, M., Guo, Q., Liu, Y., Sun, Y., Gao, Y., Ye, S., Li, G., Rao, Z., Qiang, B. and Yuan, J. (2002) 'Crystal structure of the catalytic domain of a human thioredoxin-like protein', *Eur J Biochem*, 269(8), pp. 2060-8.
Kadokura, H. and Beckwith, J. (2009) 'Detecting folding intermediates of a protein as it passes through the bacterial translocation channel', *Cell*, 138(6), pp. 1164-73.
Kamata, H., Honda, S., Maeda, S., Chang, L., Hirata, H. and Karin, M. (2005) 'Reactive oxygen species promote TNFalpha-induced death and sustained JNK activation by inhibiting MAP kinase phosphatases', *Cell*, 120(5), pp. 649-61.
Kang, S.W., Chang, T.S., Lee, T.H., Kim, E.S., Yu, D.Y. and Rhee, S.G. (2004) 'Cytosolic peroxiredoxin attenuates the activation of Jnk and p38 but potentiates that of Erk in Hela cells stimulated with tumor necrosis factor-alpha', *J Biol Chem*, 279(4), pp. 2535-43.
Karin, M. (1995) 'The regulation of AP-1 activity by mitogen-activated protein kinases', *J Biol Chem*, 270(28), pp. 16483-6.
Kil, I.S., Lee, S.K., Ryu, K.W., Woo, H.A., Hu, M.C., Bae, S.H. and Rhee, S.G. (2012) 'Feedback control of adrenal steroidogenesis via H2O2-dependent, reversible inactivation of peroxiredoxin III in mitochondria', *Mol Cell*, 46(5), pp. 584-94.
Kim, D.U., Hayles, J., Kim, D., Wood, V., Park, H.O., Won, M., Yoo, H.S., Duhig, T., Nam, M., Palmer, G., Han, S., Jeffery, L., Baek, S.T., Lee, H., Shim, Y.S., Lee, M., Kim, L., Heo, K.S., Noh, E.J., Lee, A.R., Jang, Y.J., Chung, K.S., Choi, S.J., Park, J.Y., Park, Y., Kim, H.M., Park, S.K., Park, H.J., Kang, E.J., Kim, H.B., Kang, H.S., Park, H.M., Kim, K., Song, K., Song, K.B., Nurse, P. and Hoe, K.L. (2010) 'Analysis of a genome-wide set of gene deletions in the fission yeast Schizosaccharomyces pombe', *Nat Biotechnol*, 28(6), pp. 617-23.
Klappa, P., Ruddock, L.W., Darby, N.J. and Freedman, R.B. (1998) 'The b' domain provides the principal peptide-binding site of protein disulfide isomerase but all domains contribute to binding of misfolded proteins', *Embo j*, 17(4), pp. 927-35.
Koehler, C.M. and Tienson, H.L. (2009) 'Redox regulation of protein folding in the mitochondrial intermembrane space', *Biochim Biophys Acta*, 1793(1), pp. 139-45.
Kowalczyk, K.M., Hartmuth, S., Perera, D., Stansfield, P. and Petersen, J. (2013) 'Control of Sty1 MAPK activity through stabilisation of the Pyp2 MAPK phosphatase', *J Cell Sci*, 126(Pt 15), pp. 3324-32.

Kudo, N., Taoka, H., Toda, T., Yoshida, M. and Horinouchi, S. (1999) 'A novel nuclear export signal sensitive to oxidative stress in the fission yeast transcription factor Pap1', *J Biol Chem*, 274(21), pp. 15151-8.
Kurz, M., Martin, H., Rassow, J., Pfanner, N. and Ryan, M.T. (1999) 'Biogenesis of Tim proteins of the mitochondrial carrier import pathway: differential targeting mechanisms and crossing over with the main import pathway', *Mol Biol Cell*, 10(7), pp. 2461-74.
Kwon, J., Lee, S.R., Yang, K.S., Ahn, Y., Kim, Y.J., Stadtman, E.R. and Rhee, S.G. (2004) 'Reversible oxidation and inactivation of the tumor suppressor PTEN in cells stimulated with peptide growth factors', *Proc Natl Acad Sci U S A*, 101(47), pp. 16419-24.
Kyriakis, J.M. and Avruch, J. (2001) 'Mammalian mitogen-activated protein kinase signal transduction pathways activated by stress and inflammation', *Physiol Rev*, 81(2), pp. 807-69.
Lackner, D.H., Schmidt, M.W., Wu, S., Wolf, D.A. and Bahler, J. (2012) 'Regulation of transcriptome, translation, and proteome in response to environmental stress in fission yeast', *Genome Biol*, 13(4), p. R25.
Lawrence, C.L., Maekawa, H., Worthington, J.L., Reiter, W., Wilkinson, C.R. and Jones, N. (2007) 'Regulation of Schizosaccharomyces pombe Atf1 protein levels by Sty1-mediated phosphorylation and heterodimerization with Pcr1', *J Biol Chem*, 282(8), pp. 5160-70.
Lee, S.L., Wang, W.W., Finlay, G.A. and Fanburg, B.L. (1999) 'Serotonin stimulates mitogen-activated protein kinase activity through the formation of superoxide anion', *Am J Physiol*, 277(2 Pt 1), pp. L282-91.
Lee, S.R., Yang, K.S., Kwon, J., Lee, C., Jeong, W. and Rhee, S.G. (2002) 'Reversible inactivation of the tumor suppressor PTEN by H2O2', *J Biol Chem*, 277(23), pp. 20336-42.
Lee, S.Y., Song, J.Y., Kwon, E.S. and Roe, J.H. (2008) 'Gpx1 is a stationary phase-specific thioredoxin peroxidase in fission yeast', *Biochem Biophys Res Commun*, 367(1), pp. 67-71.
Lee, Y.Y., Jung, H.I., Park, E.H., Sa, J.H. and Lim, C.J. (2002b) 'Regulation of Schizosaccharomyces pombe gene encoding copper/zinc superoxide dismutase', *Mol Cells*, 14(1), pp. 43-9.
Linke, K. and Jakob, U. (2003) 'Not every disulfide lasts forever: disulfide bond formation as a redox switch', *Antioxid Redox Signal*, 5(4), pp. 425-34.
Little, C. and O'Brien, P.J. (1969) 'Mechanism of peroxide-inactivation of the sulphydryl enzyme glyceraldehyde-3-phosphate dehydrogenase', *Eur J Biochem*, 10(3), pp. 533-8.
Liu, X.P., Liu, X.Y., Zhang, J., Xia, Z.L., Liu, X., Qin, H.J. and Wang, D.W. (2006) 'Molecular and functional characterization of sulfiredoxin homologs from higher plants', *Cell Res*, 16(3), pp. 287-96.
Lo, Y.Y., Wong, J.M. and Cruz, T.F. (1996) 'Reactive oxygen species mediate cytokine activation of c-Jun NH2-terminal kinases', *J Biol Chem*, 271(26), pp. 15703-7.
Lopez-Aviles, S., Grande, M., Gonzalez, M., Helgesen, A.L., Alemany, V., Sanchez-Piris, M., Bachs, O., Millar, J.B. and Aligue, R. (2005) 'Inactivation of the Cdc25 phosphatase by the stress-activated Srk1 kinase in fission yeast', *Mol Cell*, 17(1), pp. 49-59.
Lopez-Aviles, S., Lambea, E., Moldon, A., Grande, M., Fajardo, A., Rodriguez-Gabriel, M.A., Hidalgo, E. and Aligue, R. (2008) 'Activation of Srk1 by the mitogen-activated protein kinase Sty1/Spc1 precedes its dissociation from the kinase and signals its degradation', *Mol Biol Cell*, 19(4), pp. 1670-9.
Lou, Y.W., Chen, Y.Y., Hsu, S.F., Chen, R.K., Lee, C.L., Khoo, K.H., Tonks, N.K. and Meng, T.C. (2008) 'Redox regulation of the protein tyrosine phosphatase PTP1B in cancer cells', *Febs j*, 275(1), pp. 69-88.
Lu, H., Allen, S., Wardleworth, L., Savory, P. and Tokatlidis, K. (2004) 'Functional TIM10 chaperone assembly is redox-regulated in vivo', *J Biol Chem*, 279(18), pp. 18952-8.
Marguerat, S., Schmidt, A., Codlin, S., Chen, W., Aebersold, R. and Bahler, J. (2012) 'Quantitative analysis of fission yeast transcriptomes and proteomes in proliferating and quiescent cells', *Cell*, 151(3), pp. 671-83.
Marshall, C.J. (1994) 'MAP kinase kinase kinase, MAP kinase kinase and MAP kinase', *Curr Opin Genet Dev*, 4(1), pp. 82-9.

Maundrell, K., Hutchison, A. and Shall, S. (1988) 'Sequence analysis of ARS elements in fission yeast', *Embo j*, 7(7), pp. 2203-9.
Meister, A. (1988) 'Glutathione metabolism and its selective modification', *J Biol Chem*, 263(33), pp. 17205-8.
Mesecke, N., Terziyska, N., Kozany, C., Baumann, F., Neupert, W., Hell, K. and Herrmann, J.M. (2005) 'A disulfide relay system in the intermembrane space of mitochondria that mediates protein import', *Cell*, 121(7), pp. 1059-69.
Mi, H., Poudel, S., Muruganujan, A., Casagrande, J.T. and Thomas, P.D. (2016) 'PANTHER version 10: expanded protein families and functions, and analysis tools', *Nucleic Acids Res*, 44(D1), pp. D336-42.
Michiels, C., Raes, M., Toussaint, O. and Remacle, J. (1994) 'Importance of Se-glutathione peroxidase, catalase, and Cu/Zn-SOD for cell survival against oxidative stress', *Free Radic Biol Med*, 17(3), pp. 235-48.
Milenkovic, D., Gabriel, K., Guiard, B., Schulze-Specking, A., Pfanner, N. and Chacinska, A. (2007) 'Biogenesis of the essential Tim9-Tim10 chaperone complex of mitochondria: site-specific recognition of cysteine residues by the intermembrane space receptor Mia40', *J Biol Chem*, 282(31), pp. 22472-80.
Milenkovic, D., Ramming, T., Muller, J.M., Wenz, L.S., Gebert, N., Schulze-Specking, A., Stojanovski, D., Rospert, S. and Chacinska, A. (2009) 'Identification of the signal directing Tim9 and Tim10 into the intermembrane space of mitochondria', *Mol Biol Cell*, 20(10), pp. 2530-9.
Millar, J.B., Buck, V. and Wilkinson, M.G. (1995) 'Pyp1 and Pyp2 PTPases dephosphorylate an osmosensing MAP kinase controlling cell size at division in fission yeast', *Genes Dev*, 9(17), pp. 2117-30.
Millar, J.B., Russell, P., Dixon, J.E. and Guan, K.L. (1992) 'Negative regulation of mitosis by two functionally overlapping PTPases in fission yeast', *EMBO J*, 11(13), pp. 4943-52.
Moon, J.C., Hah, Y.S., Kim, W.Y., Jung, B.G., Jang, H.H., Lee, J.R., Kim, S.Y., Lee, Y.M., Jeon, M.G., Kim, C.W., Cho, M.J. and Lee, S.Y. (2005) 'Oxidative stress-dependent structural and functional switching of a human 2-Cys peroxiredoxin isotype II that enhances HeLa cell resistance to H2O2-induced cell death', *J Biol Chem*, 280(31), pp. 28775-84.
Moreno, S., Klar, A. and Nurse, P. (1991) 'Molecular genetic analysis of fission yeast Schizosaccharomyces pombe', *Methods Enzymol*, 194, pp. 795-823.
Morgan, B. and Lu, H. (2008) 'Oxidative folding competes with mitochondrial import of the small Tim proteins', *Biochem J*, 411(1), pp. 115-22.
Morigasaki, S., Shimada, K., Ikner, A., Yanagida, M. and Shiozaki, K. (2008) 'Glycolytic enzyme GAPDH promotes peroxide stress signaling through multistep phosphorelay to a MAPK cascade', *Mol Cell*, 30(1), pp. 108-13.
Muller, E.G. (1991) 'Thioredoxin deficiency in yeast prolongs S phase and shortens the G1 interval of the cell cycle', *J Biol Chem*, 266(14), pp. 9194-202.
Muller, J.M., Milenkovic, D., Guiard, B., Pfanner, N. and Chacinska, A. (2008) 'Precursor oxidation by Mia40 and Erv1 promotes vectorial transport of proteins into the mitochondrial intermembrane space', *Mol Biol Cell*, 19(1), pp. 226-36.
Mutah, N., Nakagawa, C.W. and Yamada, K. (1999) 'The role of catalase in hydrogen peroxide resistance in fission yeast Schizosaccharomyces pombe', *Can J Microbiol*, 45(2), pp. 125-9.
Nadeau, P.J., Charette, S.J., Toledano, M.B. and Landry, J. (2007) 'Disulfide Bond-mediated multimerization of Ask1 and its reduction by thioredoxin-1 regulate H(2)O(2)-induced c-Jun NH(2)-terminal kinase activation and apoptosis', *Mol Biol Cell*, 18(10), pp. 3903-13.
Naoe, M., Ohwa, Y., Ishikawa, D., Ohshima, C., Nishikawa, S., Yamamoto, H. and Endo, T. (2004) 'Identification of Tim40 that mediates protein sorting to the mitochondrial intermembrane space', *J Biol Chem*, 279(46), pp. 47815-21.
Netto, L.E. and Antunes, F. (2016) 'The Roles of Peroxiredoxin and Thioredoxin in Hydrogen Peroxide Sensing and in Signal Transduction', *Mol Cells*, 39(1), pp. 65-71.

Nguyen, A.N., Lee, A., Place, W. and Shiozaki, K. (2000) 'Multistep phosphorelay proteins transmit oxidative stress signals to the fission yeast stress-activated protein kinase', *Mol Biol Cell*, 11(4), pp. 1169-81.
Nguyen, A.N. and Shiozaki, K. (1999) 'Heat-shock-induced activation of stress MAP kinase is regulated by threonine- and tyrosine-specific phosphatases', *Genes Dev*, 13(13), pp. 1653-63.
Nogae, I. and Johnston, M. (1990) 'Isolation and characterization of the ZWF1 gene of Saccharomyces cerevisiae, encoding glucose-6-phosphate dehydrogenase', *Gene*, 96(2), pp. 161-9.
Ogur, M., St. John, R. and Nagai, S. (1957) 'Tetrazolium overlay technique for population studies of respiration deficiency in yeast', *Science*, 125(3254), pp. 928-9.
Okazaki, S., Naganuma, A. and Kuge, S. (2005) 'Peroxiredoxin-mediated redox regulation of the nuclear localization of Yap1, a transcription factor in budding yeast', *Antioxid Redox Signal*, 7(3-4), pp. 327-34.
Olahova, M., Taylor, S.R., Khazaipoul, S., Wang, J., Morgan, B.A., Matsumoto, K., Blackwell, T.K. and Veal, E.A. (2008) 'A redox-sensitive peroxiredoxin that is important for longevity has tissue- and stress-specific roles in stress resistance', *Proc Natl Acad Sci U S A*, 105(50), pp. 19839-44.
Ottilie, S., Chernoff, J., Hannig, G., Hoffman, C.S. and Erikson, R.L. (1991) 'A fission-yeast gene encoding a protein with features of protein-tyrosine-phosphatases', *Proc Natl Acad Sci U S A*, 88(8), pp. 3455-9.
Pedrajas, J.R., Miranda-Vizuete, A., Javanmardy, N., Gustafsson, J.A. and Spyrou, G. (2000) 'Mitochondria of Saccharomyces cerevisiae contain one-conserved cysteine type peroxiredoxin with thioredoxin peroxidase activity', *J Biol Chem*, 275(21), pp. 16296-301.
Peralta, D., Bronowska, A.K., Morgan, B., Doka, E., Van Laer, K., Nagy, P., Grater, F. and Dick, T.P. (2015) 'A proton relay enhances H2O2 sensitivity of GAPDH to facilitate metabolic adaptation', *Nat Chem Biol*, 11(2), pp. 156-63.
Perez-Jimenez, R., Li, J., Kosuri, P., Sanchez-Romero, I., Wiita, A.P., Rodriguez-Larrea, D., Chueca, A., Holmgren, A., Miranda-Vizuete, A., Becker, K., Cho, S.H., Beckwith, J., Gelhaye, E., Jacquot, J.P., Gaucher, E.A., Sanchez-Ruiz, J.M., Berne, B.J. and Fernandez, J.M. (2009) 'Diversity of chemical mechanisms in thioredoxin catalysis revealed by single-molecule force spectroscopy', *Nat Struct Mol Biol*, 16(8), pp. 890-6.
Petersen, J. and Nurse, P. (2007) 'TOR signalling regulates mitotic commitment through the stress MAP kinase pathway and the Polo and Cdc2 kinases', *Nat Cell Biol*, 9(11), pp. 1263-72.
Pollak, N., Niere, M. and Ziegler, M. (2007) 'NAD kinase levels control the NADPH concentration in human cells', *J Biol Chem*, 282(46), pp. 33562-71.
Putker, M. (2014) *Redox control of cellular signalling*. Utrecht University.
Putker, M., Madl, T., Vos, H.R., de Ruiter, H., Visscher, M., van den Berg, M.C., Kaplan, M., Korswagen, H.C., Boelens, R., Vermeulen, M., Burgering, B.M. and Dansen, T.B. (2013) 'Redox-dependent control of FOXO/DAF-16 by transportin-1', *Mol Cell*, 49(4), pp. 730-42.
Quinn, J., Findlay, V.J., Dawson, K., Millar, J.B., Jones, N., Morgan, B.A. and Toone, W.M. (2002) 'Distinct regulatory proteins control the graded transcriptional response to increasing H(2)O(2) levels in fission yeast Schizosaccharomyces pombe', *Mol Biol Cell*, 13(3), pp. 805-16.
Ralser, M., Heeren, G., Breitenbach, M., Lehrach, H. and Krobitsch, S. (2006) 'Triose phosphate isomerase deficiency is caused by altered dimerization--not catalytic inactivity--of the mutant enzymes', *PLoS One*, 1, p. e30.
Ralser, M., Wamelink, M.M., Kowald, A., Gerisch, B., Heeren, G., Struys, E.A., Klipp, E., Jakobs, C., Breitenbach, M., Lehrach, H. and Krobitsch, S. (2007) 'Dynamic rerouting of the carbohydrate flux is key to counteracting oxidative stress', *J Biol*, 6(4), p. 10.
Reiter, W., Watt, S., Dawson, K., Lawrence, C.L., Bahler, J., Jones, N. and Wilkinson, C.R. (2008) 'Fission yeast MAP kinase Sty1 is recruited to stress-induced genes', *J Biol Chem*, 283(15), pp. 9945-56.
Rhee, S.G. (2006) 'Cell signaling. H2O2, a necessary evil for cell signaling', *Science*, 312(5782), pp. 1882-3.

Rhee, S.G., Bae, Y.S., Lee, S.R. and Kwon, J. (2000) 'Hydrogen peroxide: a key messenger that modulates protein phosphorylation through cysteine oxidation', *Sci STKE*, 2000(53), p. pe1.
Rhee, S.G., Chae, H.Z. and Kim, K. (2005) 'Peroxiredoxins: a historical overview and speculative preview of novel mechanisms and emerging concepts in cell signaling', *Free Radic Biol Med*, 38(12), pp. 1543-52.
Rhee, S.G., Chang, T.S., Bae, Y.S., Lee, S.R. and Kang, S.W. (2003) 'Cellular regulation by hydrogen peroxide', *J Am Soc Nephrol*, 14(8 Suppl 3), pp. S211-5.
Rhee, S.G. and Woo, H.A. (2011) 'Multiple functions of peroxiredoxins: peroxidases, sensors and regulators of the intracellular messenger H(2)O(2), and protein chaperones', *Antioxid Redox Signal*, 15(3), pp. 781-94.
Riemer, J., Fischer, M. and Herrmann, J.M. (2011) 'Oxidation-driven protein import into mitochondria: Insights and blind spots', *Biochim Biophys Acta*, 1808(3), pp. 981-9.
Riemer, J., Bulleid, N. and Herrmann, J.M. (2009) 'Disulfide formation in the ER and mitochondria: two solutions to a common process', *Science*, 324(5932), pp. 1284-7.
Ristow, M. and Zarse, K. (2010) 'How increased oxidative stress promotes longevity and metabolic health: The concept of mitochondrial hormesis (mitohormesis)', *Exp Gerontol*, 45(6), pp. 410-8.
Rodriguez-Gabriel, M.A., Burns, G., McDonald, W.H., Martin, V., Yates, J.R., 3rd, Bahler, J. and Russell, P. (2003) 'RNA-binding protein Csx1 mediates global control of gene expression in response to oxidative stress', *EMBO J*, 22(23), pp. 6256-66.
Roveri, A., Maiorino, M. and Ursini, F. (1994) 'Enzymatic and immunological measurements of soluble and membrane-bound phospholipid-hydroperoxide glutathione peroxidase', *Methods Enzymol*, 233, pp. 202-12.
Sabio, G. and Davis, R.J. (2014) 'TNF and MAP kinase signalling pathways', *Semin Immunol*, 26(3), pp. 237-45.
Saitoh, M., Nishitoh, H., Fujii, M., Takeda, K., Tobiume, K., Sawada, Y., Kawabata, M., Miyazono, K. and Ichijo, H. (1998) 'Mammalian thioredoxin is a direct inhibitor of apoptosis signal-regulating kinase (ASK) 1', *EMBO J*, 17(9), pp. 2596-606.
Salmeen, A., Andersen, J.N., Myers, M.P., Meng, T.C., Hinks, J.A., Tonks, N.K. and Barford, D. (2003) 'Redox regulation of protein tyrosine phosphatase 1B involves a sulphenyl-amide intermediate', *Nature*, 423(6941), pp. 769-73.
Sanso, M., Vargas-Perez, I., Garcia, P., Ayte, J. and Hidalgo, E. (2011a) 'Nuclear roles and regulation of chromatin structure by the stress-dependent MAP kinase Sty1 of Schizosaccharomyces pombe', *Mol Microbiol*, 82(3), pp. 542-54.
Sanso, M., Vargas-Perez, I., Quintales, L., Antequera, F., Ayte, J. and Hidalgo, E. (2011b) 'Gcn5 facilitates Pol II progression, rather than recruitment to nucleosome-depleted stress promoters, in Schizosaccharomyces pombe', *Nucleic Acids Res*, 39(15), pp. 6369-79.
Sanz, A. (2016) 'Mitochondrial reactive oxygen species: Do they extend or shorten animal lifespan?', *Biochim Biophys Acta*, 1857(8), pp. 1116-26.
Savitsky, P.A. and Finkel, T. (2002) 'Redox regulation of Cdc25C', *J Biol Chem*, 277(23), pp. 20535-40.
Schwertassek, U., Haque, A., Krishnan, N., Greiner, R., Weingarten, L., Dick, T.P. and Tonks, N.K. (2014) 'Reactivation of oxidized PTP1B and PTEN by thioredoxin 1', *Febs j*, 281(16), pp. 3545-58.
Sevier, C.S. and Kaiser, C.A. (2006) 'Conservation and diversity of the cellular disulfide bond formation pathways', *Antioxid Redox Signal*, 8(5-6), pp. 797-811.
Shiozaki, K. and Russell, P. (1995) 'Cell-cycle control linked to extracellular environment by MAP kinase pathway in fission yeast', *Nature*, 378(6558), pp. 739-43.
Shiozaki, K. and Russell, P. (1996) 'Conjugation, meiosis, and the osmotic stress response are regulated by Spc1 kinase through Atf1 transcription factor in fission yeast', *Genes Dev*, 10(18), pp. 2276-88.
Shiozaki, K., Shiozaki, M. and Russell, P. (1998) 'Heat stress activates fission yeast Spc1/StyI MAPK by a MEKK-independent mechanism', *Mol Biol Cell*, 9(6), pp. 1339-49.

Sideris, D.P. and Tokatlidis, K. (2007) 'Oxidative folding of small Tims is mediated by site-specific docking onto Mia40 in the mitochondrial intermembrane space', *Mol Microbiol*, 65(5), pp. 1360-73.
Sies, H. (1993) 'Ebselen, a selenoorganic compound as glutathione peroxidase mimic', *Free Radic Biol Med*, 14(3), pp. 313-23.
Sirover, M.A. (2011) 'On the functional diversity of glyceraldehyde-3-phosphate dehydrogenase: biochemical mechanisms and regulatory control', *Biochim Biophys Acta*, 1810(8), pp. 741-51.
Smith, D.A., Toone, W.M., Chen, D., Bahler, J., Jones, N., Morgan, B.A. and Quinn, J. (2002) 'The Srk1 protein kinase is a target for the Sty1 stress-activated MAPK in fission yeast', *J Biol Chem*, 277(36), pp. 33411-21.
Sobotta, M.C., Liou, W., Stocker, S., Talwar, D., Oehler, M., Ruppert, T., Scharf, A.N. and Dick, T.P. (2015) 'Peroxiredoxin-2 and STAT3 form a redox relay for H2O2 signaling', *Nat Chem Biol*, 11(1), pp. 64-70.
Stojanovski, D., Milenkovic, D., Muller, J.M., Gabriel, K., Schulze-Specking, A., Baker, M.J., Ryan, M.T., Guiard, B., Pfanner, N. and Chacinska, A. (2008) 'Mitochondrial protein import: precursor oxidation in a ternary complex with disulfide carrier and sulfhydryl oxidase', *J Cell Biol*, 183(2), pp. 195-202.
Sundaresan, M., Yu, Z.X., Ferrans, V.J., Irani, K. and Finkel, T. (1995) 'Requirement for generation of H2O2 for platelet-derived growth factor signal transduction', *Science*, 270(5234), pp. 296-9.
Tavender, T.J. and Bulleid, N.J. (2010) 'Peroxiredoxin IV protects cells from oxidative stress by removing H2O2 produced during disulphide formation', *J Cell Sci*, 123(Pt 15), pp. 2672-9.
Tavender, T.J., Springate, J.J. and Bulleid, N.J. (2010) 'Recycling of peroxiredoxin IV provides a novel pathway for disulphide formation in the endoplasmic reticulum', *Embo j*, 29(24), pp. 4185-97.
Taylor, S.R. (2009) *The role of 2-Cys peroxiredoxins in regulating responses to peroxide*. Newcastle University.
Teige, M., Scheikl, E., Reiser, V., Ruis, H. and Ammerer, G. (2001) 'Rck2, a member of the calmodulin-protein kinase family, links protein synthesis to high osmolarity MAP kinase signaling in budding yeast', *Proc Natl Acad Sci U S A*, 98(10), pp. 5625-30.
Terziyska, N., Grumbt, B., Bien, M., Neupert, W., Herrmann, J.M. and Hell, K. (2007) 'The sulfhydryl oxidase Erv1 is a substrate of the Mia40-dependent protein translocation pathway', *FEBS Lett*, 581(6), pp. 1098-102.
Tobiume, K., Matsuzawa, A., Takahashi, T., Nishitoh, H., Morita, K., Takeda, K., Minowa, O., Miyazono, K., Noda, T. and Ichijo, H. (2001) 'ASK1 is required for sustained activations of JNK/p38 MAP kinases and apoptosis', *EMBO Rep*, 2(3), pp. 222-8.
Toda, T., Shimanuki, M. and Yanagida, M. (1991) 'Fission yeast genes that confer resistance to staurosporine encode an AP-1-like transcription factor and a protein kinase related to the mammalian ERK1/MAP2 and budding yeast FUS3 and KSS1 kinases', *Genes Dev*, 5(1), pp. 60-73.
Tokatlidis, K. (2005) 'A disulfide relay system in mitochondria', *Cell*, 121(7), pp. 965-7.
Tomalin, L.E., Day, A.M., Underwood, Z.E., Smith, G.R., Dalle Pezze, P., Rallis, C., Patel, W., Dickinson, B.C., Bahler, J., Brewer, T.F., Chang, C.J., Shanley, D.P. and Veal, E.A. (2016) 'Increasing extracellular H2O2 produces a bi-phasic response in intracellular H2O2, with peroxiredoxin hyperoxidation only triggered once the cellular H2O2-buffering capacity is overwhelmed', *Free Radic Biol Med*, 95, pp. 333-48.
Toone, W.M. and Jones, N. (1998) 'Stress-activated signalling pathways in yeast', *Genes Cells*, 3(8), pp. 485-98.
Turner-Ivey, B., Manevich, Y., Schulte, J., Kistner-Griffin, E., Jezierska-Drutel, A., Liu, Y. and Neumann, C.A. (2013) 'Role for Prdx1 as a specific sensor in redox-regulated senescence in breast cancer', *Oncogene*, 32(45), pp. 5302-14.
Valko, M., Izakovic, M., Mazur, M., Rhodes, C.J. and Telser, J. (2004) 'Role of oxygen radicals in DNA damage and cancer incidence', *Mol Cell Biochem*, 266(1-2), pp. 37-56.
Valko, M., Rhodes, C.J., Moncol, J., Izakovic, M. and Mazur, M. (2006) 'Free radicals, metals and antioxidants in oxidative stress-induced cancer', *Chem Biol Interact*, 160(1), pp. 1-40.

Veal, E. and Day, A. (2011) 'Hydrogen peroxide as a signaling molecule', *Antioxid Redox Signal*, 15(1), pp. 147-51.
Veal, E.A., Day, A.M. and Morgan, B.A. (2007) 'Hydrogen peroxide sensing and signaling', *Mol Cell*, 26(1), pp. 1-14.
Veal, E.A., Findlay, V.J., Day, A.M., Bozonet, S.M., Evans, J.M., Quinn, J. and Morgan, B.A. (2004) 'A 2-Cys peroxiredoxin regulates peroxide-induced oxidation and activation of a stress-activated MAP kinase', *Mol Cell*, 15(1), pp. 129-39.
Veal, E.A., Ross, S.J., Malakasi, P., Peacock, E. and Morgan, B.A. (2003) 'Ybp1 is required for the hydrogen peroxide-induced oxidation of the Yap1 transcription factor', *J Biol Chem*, 278(33), pp. 30896-904.
Veal, E.A., Tomalin, L.E., Morgan, B.A. and Day, A.M. (2014) 'The fission yeast Schizosaccharomyces pombe as a model to understand how peroxiredoxins influence cell responses to hydrogen peroxide', *Biochem Soc Trans*, 42(4), pp. 909-16.
Vivancos, A.P., Castillo, E.A., Biteau, B., Nicot, C., Ayte, J., Toledano, M.B. and Hidalgo, E. (2005) 'A cysteine-sulfinic acid in peroxiredoxin regulates H2O2-sensing by the antioxidant Pap1 pathway', *Proc Natl Acad Sci U S A*, 102(25), pp. 8875-80.
Vivancos, A.P., Castillo, E.A., Jones, N., Ayte, J. and Hidalgo, E. (2004) 'Activation of the redox sensor Pap1 by hydrogen peroxide requires modulation of the intracellular oxidant concentration', *Mol Microbiol*, 52(5), pp. 1427-35.
Vogtle, F.N., Burkhart, J.M., Rao, S., Gerbeth, C., Hinrichs, J., Martinou, J.C., Chacinska, A., Sickmann, A., Zahedi, R.P. and Meisinger, C. (2012) 'Intermembrane space proteome of yeast mitochondria', *Mol Cell Proteomics*, 11(12), pp. 1840-52.
Wagner, E.F. and Nebreda, A.R. (2009) 'Signal integration by JNK and p38 MAPK pathways in cancer development', *Nat Rev Cancer*, 9(8), pp. 537-49.
Warbrick, E. and Fantes, P.A. (1991) 'The wis1 protein kinase is a dosage-dependent regulator of mitosis in Schizosaccharomyces pombe', *EMBO J*, 10(13), pp. 4291-9.
Wheeler, G.L. and Grant, C.M. (2004) 'Regulation of redox homeostasis in the yeast Saccharomyces cerevisiae', *Physiol Plant*, 120(1), pp. 12-20.
Wilkinson, M.G., Samuels, M., Takeda, T., Toone, W.M., Shieh, J.C., Toda, T., Millar, J.B. and Jones, N. (1996) 'The Atf1 transcription factor is a target for the Sty1 stress-activated MAP kinase pathway in fission yeast', *Genes Dev*, 10(18), pp. 2289-301.
Winterbourn, C.C. (2008) 'Reconciling the chemistry and biology of reactive oxygen species', *Nat Chem Biol*, 4(5), pp. 278-86.
Winterbourn, C.C. and Hampton, M.B. (2008) 'Thiol chemistry and specificity in redox signaling', *Free Radic Biol Med*, 45(5), pp. 549-61.
Winterbourn, C.C. and Hampton, M.B. (2015) 'Redox biology: signaling via a peroxiredoxin sensor', *Nat Chem Biol*, 11(1), pp. 5-6.
Winterbourn, C.C. and Metodiewa, D. (1999) 'Reactivity of biologically important thiol compounds with superoxide and hydrogen peroxide', *Free Radic Biol Med*, 27(3-4), pp. 322-8.
Wisdom, R. (1999) 'AP-1: one switch for many signals', *Exp Cell Res*, 253(1), pp. 180-5.
Woo, H.A., Jeong, W., Chang, T.S., Park, K.J., Park, S.J., Yang, J.S. and Rhee, S.G. (2005) 'Reduction of cysteine sulfinic acid by sulfiredoxin is specific to 2-cys peroxiredoxins', *J Biol Chem*, 280(5), pp. 3125-8.
Woo, H.A., Kang, S.W., Kim, H.K., Yang, K.S., Chae, H.Z. and Rhee, S.G. (2003) 'Reversible oxidation of the active site cysteine of peroxiredoxins to cysteine sulfinic acid. Immunoblot detection with antibodies specific for the hyperoxidized cysteine-containing sequence', *J Biol Chem*, 278(48), pp. 47361-4.
Woo, H.A., Yim, S.H., Shin, D.H., Kang, D., Yu, D.Y. and Rhee, S.G. (2010) 'Inactivation of peroxiredoxin I by phosphorylation allows localized H(2)O(2) accumulation for cell signaling', *Cell*, 140(4), pp. 517-28.

Wood, Z.A., Poole, L.B. and Karplus, P.A. (2003a) 'Peroxiredoxin evolution and the regulation of hydrogen peroxide signaling', *Science*, 300(5619), pp. 650-3.
Wood, Z.A., Schroder, E., Robin Harris, J. and Poole, L.B. (2003b) 'Structure, mechanism and regulation of peroxiredoxins', *Trends Biochem Sci*, 28(1), pp. 32-40.
Yang, C.S., Lee, D.S., Song, C.H., An, S.J., Li, S., Kim, J.M., Kim, C.S., Yoo, D.G., Jeon, B.H., Yang, H.Y., Lee, T.H., Lee, Z.W., El-Benna, J., Yu, D.Y. and Jo, E.K. (2007) 'Roles of peroxiredoxin II in the regulation of proinflammatory responses to LPS and protection against endotoxin-induced lethal shock', *J Exp Med*, 204(3), pp. 583-94.
Yang, W. and Hekimi, S. (2010) 'A mitochondrial superoxide signal triggers increased longevity in Caenorhabditis elegans', *PLoS Biol*, 8(12), p. e1000556.
Zuin, A., Carmona, M., Morales-Ivorra, I., Gabrielli, N., Vivancos, A.P., Ayte, J. and Hidalgo, E. (2010) 'Lifespan extension by calorie restriction relies on the Sty1 MAP kinase stress pathway', *EMBO J*, 29(5), pp. 981-91.

Communications

Mol. Cells 2016; 39(1): 40-45
http://dx.doi.org/10.14348/molcells.2016.2327

Molecules and Cells
http://molcells.org
Established in 1990

Minireview

Peroxiredoxins in Regulation of MAPK Signalling Pathways; Sensors and Barriers to Signal Transduction

Heather R. Latimer, and Elizabeth A. Veal*

Peroxiredoxins are highly conserved and abundant peroxidases. Although the thioredoxin peroxidase activity of peroxiredoxin (Prx) is important to maintain low levels of endogenous hydrogen peroxide, Prx have also been shown to promote hydrogen peroxide-mediated signalling. Mitogen activated protein kinase (MAPK) signalling pathways mediate cellular responses to a variety of stimuli, including reactive oxygen species (ROS). Here we review the evidence that Prx can act as both sensors and barriers to the activation of MAPK and discuss the underlying mechanisms involved, focusing in particular on the relationship with thioredoxin.

INTRODUCTION

Reactive oxygen species (ROS) are damaging, highly reactive, reduced forms of oxygen, produced in a wide range of physiological processes, including as a by-product of aerobic respiration in the mitochondria, and following exposure of cells to environmental agents such as UV light and drugs/xenobiotics (Gutteridge and Halliwell, 1999). Over recent years, rather than simply acting as toxic agents, it has been established that less-reactive ROS, particularly H_2O_2, also play positive roles as signalling molecules. Key to ROS-signalling functions is the ability to selectively regulate the activity of specific proteins, for example, by oxidising deprotonated cysteine residues, such as are found in the catalytic sites of many enzymes. This selective reactivity is one of the features making H_2O_2 well-suited as a signalling molecule (Winterbourn, 2008). Indeed, H_2O_2 signals have been shown to promote diverse biological responses, from stomatal opening in plants to cell migration in wound healing [For reviews see (Veal and Day, 2011)] and (Holmstrom and Finkel, 2014). However, the most fundamental and universal response to increases in ROS is to limit organismal damage by increasing the levels of detoxification and repair enzymes or initiating apoptosis. Many of these protective responses are mediated by MAPK pathways (Fig. 1). As we discuss below, redox-active cysteines have been shown to play an important part in the activation of these pathways.

Cells have evolved a variety of enzymes which remove ROS before they are able to cause oxidative damage (Bokov et al., 2004; Gutteridge and Halliwell, 1999). Redox-active cysteines are involved in the activity of many of these enzymes. For example, peroxiredoxins (Prx) are a family of extremely abundant, thioredoxin peroxidase enzymes. Prx are themselves highly reactive with H_2O_2 using the reversible oxidation of cysteine residues to reduce peroxides, including H_2O_2. During the catalytic mechanism of typical 2-Cys Prx, the peroxidatic cysteine becomes oxidised to a sulphenic acid, which then reacts with the resolving cysteine of a neighbouring Prx molecule, forming an intermolecular disulphide bond. The resulting Prx disulphides are reduced by thioredoxin using electrons from NADPH (Fig. 2A) [For a review see (Wood et al., 2003)]. Thioredoxin family proteins are oxidoreductases with broad substrate specificity, acting as cofactors in the activity of many other enzymes and participating in the reduction of many transcription factors and signalling molecules (Holmgren and Lu, 2010). However, the abundance of Prx and the high affinity of thioredoxin for Prx disulphides can render Prx disulphides the prevalent thioredoxin substrate when H_2O_2 levels increase (Day et al., 2012). Hence, the activities of Prx and thioredoxin in H_2O_2 signalling are inextricably linked. Here we will discuss the different roles that have been identified for Prx and thioredoxin in the regulation of mitogen activated protein kinase (MAPK) pathways. In some cases, Prx and thioredoxin have been shown to act as barriers to signal transduction, whereas in others Prx and thioredoxin are required for effective signalling. We will discuss the underlying mechanisms that give rise to these apparent contradictions.

MAPK PATHWAYS

In eukaryotes, conserved MAPK pathways mediate responses to various stimuli. In unicellular eukaryotes these MAPK pathways promote changes in gene expression that are vital for adaptation and growth under changing environmental conditions (Toone and Jones, 1998). MAPK signalling pathways are also important mediators of growth factors and

Institute for Cell and Molecular Biosciences, Newcastle University, Framlington Place, Newcastle upon Tyne, NE2 4HH, UK
*Correspondence: e.a.veal@ncl.ac.uk

Received 30 November, 2015; accepted 3 December, 2015; published online 25 January, 2016

Keywords: kinase, peroxiredoxin, phosphatase, redox, thioredoxin

eISSN: 0219-1032

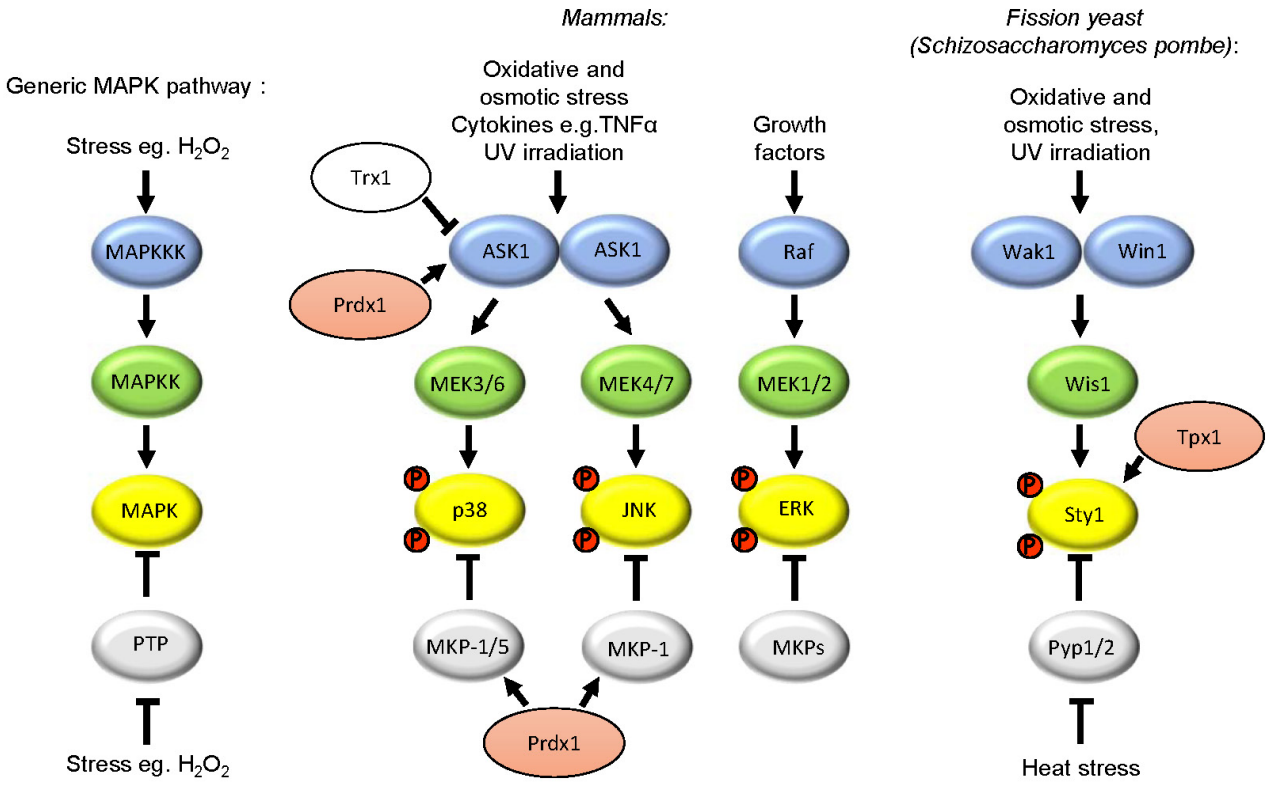

Fig. 1. Mitogen activated protein kinase (MAPK) signalling pathways mediate responses to a variety of stimuli, including ROS. MAPK pathways consist of a series of kinases: MAPKKK, MAPKK and MAPK, which are sequentially activated by phosphorylation. Three groups of MAPK, p38, JNK (c-Jun N-terminal kinase) and ERK (extracellular signal-regulated kinase), are preferentially activated by different MAPKK and MAPKKK. The activity of each kinase is also controlled by phosphatases. For example, to attenuate MAPK activity, protein tyrosine phosphatases (PTPs) dephosphorylate MAPK. Oligomerisation activates ASK1 by promoting autophosphorylation. Inactivation of phosphatases is an alternative mechanism to increase MAPK activity. For example, heat stress activation of the Sty1(Spc1) pathway in the fission yeast *Schizosaccharomyces pombe* involves inactivation of the PTP Pyp1 (Nguyen and Shiozaki, 1999). Steps in pathways which have been shown to be regulated by peroxiredoxins (pink) and/or thioredoxin (Trx1) are also indicated.

cytokine responses. For example, three MAPKs, JNK, p38 and ERK, all become activated following exposure to the cytokine, tumour necrosis factor-α (TNF-α). MAPK pathways consists of a series of protein kinases, which become sequentially activated by phosphorylation (Fig. 1) [For a review see (Marshall, 1994)]. Although some of the protein targets mediating the effects of MAPK remain unclear, MAPK have been found to phosphorylate a variety of target proteins, including transcription factors [For a review see (Sabio and Davis, 2014)]. Work to understand the activation of MAPK has largely focussed on how the phosphorylation of upstream kinases is triggered. However, there is some evidence that the regulation of dephosphorylation reactions, mediated by protein tyrosine phosphatases, doesn't just allow feedback control of kinase activity, but can also be involved in sensing stress stimuli (Nguyen and Shiozaki, 1999).

REGULATION OF MAPK ACTIVATION BY THIOREDOXIN

Although diverse stimuli activate MAPK pathways, in many cases, secondary generation of ROS/redox changes are responsible for increases in MAPK activity. Consequently, amongst the most studied mechanisms are those by which H_2O_2 stimulates MAPK activation. The MAPKKK ASK1(MAPKKK5) is important in the activation of both p38 and JNK MAPK in response to a variety of stimuli, including H_2O_2 which may also act as a second messenger downstream of other stimuli, such as TNF-α (Ichijo et al., 1997, Tobiume et al., 2001). Following identification in a two hybrid screen for ASK1 interactors, the thioredoxin, Trx1, was found to bind to the N-terminus of ASK1, directly inhibiting its activation under reducing conditions (Saitoh et al., 1998). In this study, treatment of cells with TNF-α, or for 20min with 1mM H_2O_2, was proposed to activate ASK1 by causing Trx1 to become oxidised, promoting its dissociation from ASK1 (Saitoh et al., 1998). ASK1 then oligomerises allowing autophosphorylation of a threonine residue in ASK1's activation loop that increases its kinase activity (Gotoh and Cooper, 1998; Tobiume et al., 2001). Hence this leads to the increased phosphorylation of p38 and JNK MAPK and apoptosis (Ichijo et al., 1997). More recent studies have suggested that ASK1 oligomerisation also involves the H_2O_2-induced formation of intermolecular disulphide bonds between cysteines in ASK1 which help stabilise the ASK1-ASK1 interactions required for autophosphorylation (Nadeau et al., 2007). This suggests that the ASK1-inhibitory role of Trx1 may be to reduce these oxidised, oligomeric forms of ASK1, preventing autophosphorylation (Nadeau et al., 2009).

ASK1 is critically involved in signal transduction to p38 and JNK MAPK in response to a variety of stimuli. In most cases the oxidation state of thioredoxin has not been examined. However, these studies suggest that many activating stimuli may act by causing increased oxidation of thioredoxin. In which case, this would render ASK1 an effective sensor of thioredoxin oxidation. Intriguingly, thioredoxin is actually required for the H_2O_2-induced activation of the p38/JNK-related Hog1 MAPK in the fungal pathogen *Candida albicans*, raising the possibility that, in some cases, oxidised thioredoxin might even play a positive role in MAPK activation (da Silva Dantas et al., 2010).

However, in addition to inhibiting the activity of MAPKKK, thioredoxins are also implicated in feedback mechanisms to reactivate protein tyrosine phosphatases (PTPs) which de-activate MAPK. The catalytic cysteine of PTP becomes oxidised by H_2O_2 generated in response to a variety of stimuli. In many cases, irreversible oxidation is prevented by the formation of a disulphide bond with another cysteine which may be reduced by thioredoxin Trx1 (Kwon et al., 2004; Schwertassek et al., 2014). Thioredoxin oxidation would therefore also be predicted to inhibit the reduction of oxidised, inactive PTPs, increasing the extent or duration of MAPK activation.

ROLES OF PRX IN H_2O_2 SIGNALLING AND ACTIVATION OF MAPK

Prx have been shown to have multiple roles in H_2O_2-signalling. Prx have been proposed to act as barriers to H_2O_2 signal transduction and indeed there is plenty of evidence to suggest that Prx inhibit the activation of ROS-activated signalling pathways, including MAPK (Cao et al., 2009; Choi et al., 2005; Kang et al., 2004; Kil et al., 2012; Woo et al., 2010; Yang et al., 2007). Given that antioxidants, such as N-acetyl cysteine (NAC) and catalase, inhibit MAPK activation, this has led to the conclusion that, in such cases, Prx inhibit activation by removing peroxides (Hashimoto et al., 2001; Yang et al., 2007) (Fig. 2A). Indeed, post-translational mechanisms to inhibit the thioredoxin peroxidase activity of Prx have been shown to be important for signal transduction (Kil et al., 2012; Woo et al., 2010).

Conversely, Prx have also been found to be important for H_2O_2 signal transduction. For instance, a genetic screen, using a LacZ reporter under the control of an H_2O_2-activated promoter, unexpectedly identified that the peroxiredoxin TSA1 was required for H_2O_2-induced gene expression in a commonly used laboratory strain of the budding yeast *Saccharomyces cerevisiae* (Ross et al., 2000) reflecting TSA1's involvement in the H_2O_2-induced activation of the AP1-like transcription factor Yap1 (Okazaki et al., 2005). Subsequent studies have established that the single 2-Cys Prx, Tpx1, is required for H_2O_2 signal transduction in the unrelated fission yeast *Schizosaccharomyces pombe*, suggesting a conserved function for Prx in promoting H_2O_2 signal transduction (Veal et al., 2004). Indeed, the thioredoxin peroxidase activity of Tpx1 is required for the H_2O_2-induced activation of the Pap1 transcription factor (Bozonet et al., 2005; Vivancos et al., 2005), that mediates the transcriptional response to low levels of H_2O_2. Moreover, Tpx1 is also required for the activation of the p38/JNK-related MAPK Sty1 (Spc1) that phosphorylates the Atf1 transcription factor, promoting the Atf1-dependent expression of an overlapping set of stress-protective genes (Veal et al., 2004). Intriguingly, in contrast to Pap1, the activation of Sty1 does not require the thioredoxin peroxidase activity of Tpx1 (Veal et al., 2004). Overexpression of Tpx1 also stimulates the increased phosphorylation of Sty1. Indeed, overexpression of Tpx1 restores inducible phosphorylation to cells expressing a constitutively partially active form of the MAPKK Wis1, indicating that Tpx1 acts downstream of the MAPKK to promote Sty1 activation (Veal et al., 2004) [For a review see (Veal et al., 2014)].

Although it was possible that positive ROS-signalling roles of Prx were confined to unicellular eukaryotes, there is increasing evidence that Prx promote ROS-signalling in animals too. For instance, Prx2 was recently found to act as an H_2O_2 receptor, transmitting oxidative signals to the redox-regulated transcription factor STAT3 (Sobotta et al., 2015) (Fig. 2). Prx have also been shown to promote ROS-induced activation of MAPK in animals. For instance, Prdx1 is required for oxidised Low Density Lipoprotein (oxLDL)-induced activation of p38 in macrophage-derived foam cells (Conway and Kinter, 2006), H_2O_2-induced p38 activation in mammalian cells (Jarvis et al., 2012), and for arsenite-induced activation of the PMK-1 MAPK in the nematode worm *Caenorhabditis elegans* (Olahova et al., 2008). Prdx1 has also been shown to promote p38 activity in pancreatic duct adenocarcinoma cells (Taniuchi et al., 2015). Although the mechanism/s by which Prx promote p38/JNK MAPK activation are not well-established there are a number of possibilities which are discussed below and illustrated in Fig. 2:

[1] As direct redox-transducers: Prdx1 has been found to form intermolecular disulphide bonds with ASK1 that were proposed to initiate the oxidation of ASK1 oligomers (Jarvis et al., 2012). This suggests that in this case Prdx1 is able to act as an H_2O_2 receptor transducing the signal to drive the oxidative activation of ASK1. This is reminiscent of the role of Prx2 in promoting the activation of the STAT3 transcription factor (Fig. 2) (Sobotta et al., 2015). STAT3 is activated by transient formation of disulphide-linked STAT3 oligomers which are subsequently reduced by thioredoxin. The detection of Prx2-STAT3 disulphides suggests that Prx2 participates directly in initiating STAT3 oxidation. Although the abundance and H_2O_2-reactivity of Prx has led to suggestions that such mechanisms must be prevalent in the H_2O_2-induced oxidation of target signalling proteins (Winterbourn, 2008), it remains to be determined whether such peroxidase-based redox relays are widely conserved H_2O_2-sensing mechanisms, or limited to specific situations. Intriguingly, in *S. pombe* Tpx1 also forms mixed disulphides with the Sty1 MAPK (Veal et al., 2004). Indeed, further cysteines in Sty1 have been identified which form an intracellular disulphide bond which is important for transcriptional responses to H_2O_2 (Day and Veal, 2010). However, it remains to be determined how Tpx1-Sty1 disulphide formation leads to increased phosphorylation of Sty1.

[2] As H_2O_2-dependent thioredoxin inhibitors: Given that thioredoxin is directly responsible for the reduction of Prx disulphides, it is impossible to separate the role of Prx in signalling from that of thioredoxin. For example, in *S. pombe* exposed to H_2O_2, Tpx1 disulphides become the main substrate for Trx1. Hence, as thioredoxin reductase (Trr1) levels are limiting, Trx1 becomes completely oxidised and the reduction of Tpx1 and other Trx1 substrates becomes inhibited (Brown et al., 2013, Day et al., 2012). It is yet to be determined whether this ability of Prx to inhibit the oxidoreductase activity of thioredoxin family proteins in response to H_2O_2 is generally an important function of Prx. However, the inhibition of the thioredoxin-like protein, Txl1, by H_2O_2-induced Tpx1 disulphides, underlays the role of the thioredoxin peroxidase activity of Tpx1 in the H_2O_2-induced activation of the AP-1-like transcription factor Pap1 and adaptation to growth under oxidative stress conditions (Brown et al., 2013). Given the important role of Trx1 in reduction of active, oxidised ASK1 oligomers and inactive, oxidised PTPs it is tempting to speculate that Prx might promote MAPK activation in yeast and animals by inhibiting the activity of thioredoxin

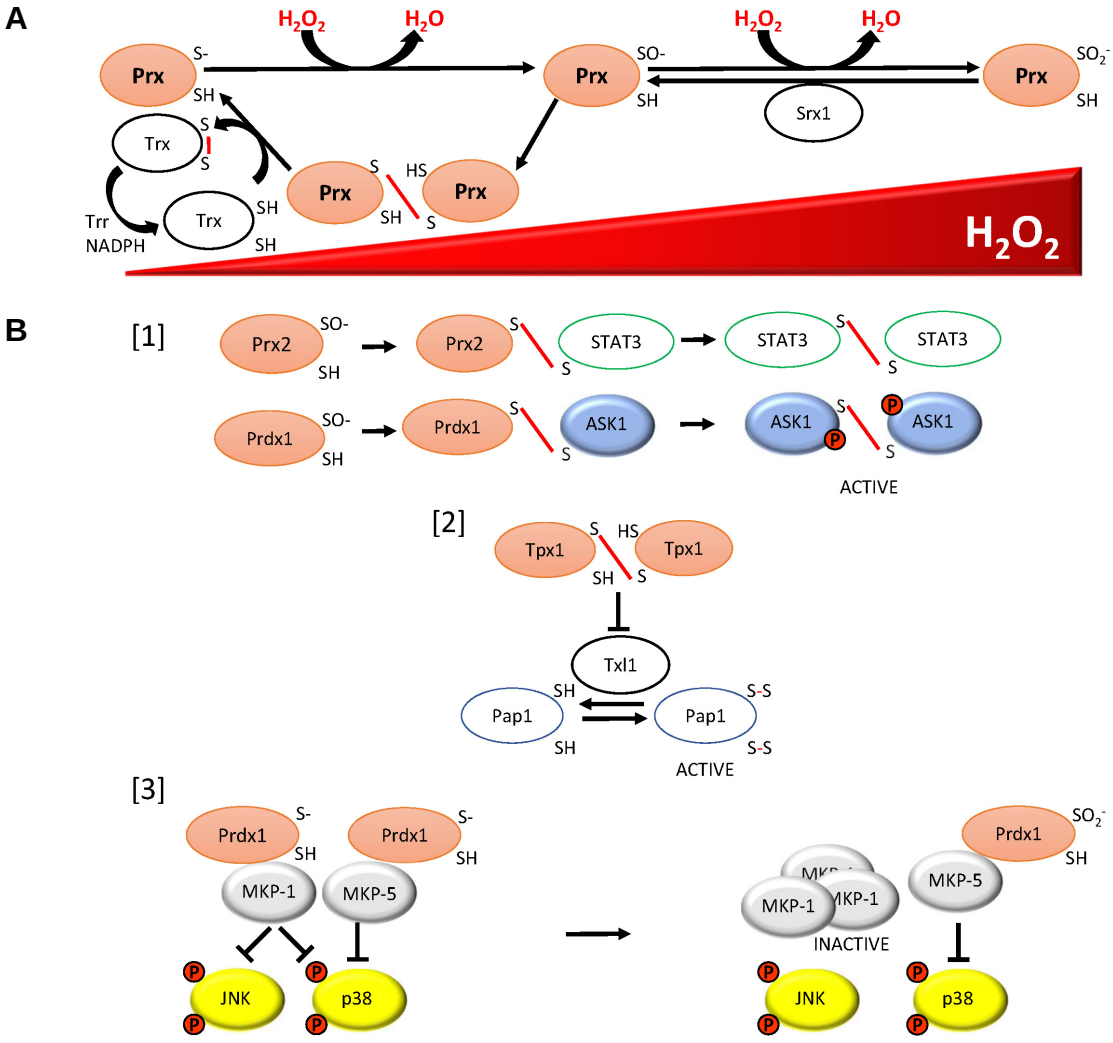

Fig. 2. Mechanisms underlying roles of peroxiredoxin and thioredoxin family proteins in responses to increasing concentrations of hydrogen peroxide, including MAPK activation. (A) Prx can inhibit H_2O_2 signalling, including activation of p38 MAPK, by reducing the levels of H_2O_2 available to activate these pathways: The peroxidatic cysteine residue of a peroxiredoxin (Prx) reacts with H_2O_2 to form a sulphenic acid derivative ($-SO^-$). In the catalytic cycle this is followed by the formation of a disulphide bond between this cysteine and the resolving cysteine of a neighbouring Prx. The resulting Prx disulphides are reduced by thioredoxin family proteins (Trx) by thioredoxin reductase (Trr) using electrons from NADPH. At high concentrations of H_2O_2, the peroxidatic cysteine can become hyperoxidised to a sulphinic acid ($-SO_2^-$), which can be reduced by sulphiredoxin (Srx1) back to the $-SO^-$ form. (B) Three mechanisms by which different redox forms of Prx have been shown to promote H_2O_2 signalling: [1] Prx2 is able to promote activation of STAT3 through transient formation of Prx2-STAT3 disulphides, which is followed by STAT3-STAT3 disulphide-linked oligomers, resulting in STAT3 activation (Sobotta et al., 2015). Similarly, Prdx1 forms disulphide bonds with ASK1, resulting in ASK1-ASK1 oligomers and ASK1 activation (Jarvis et al., 2012). [2] In *S. pombe*, Tpx1-Tpx1 disulphides are the main substrate for Trx1, therefore the presence of Tpx1 disulphides prevents the thioredoxin activity of Trx1 and Txl1 towards other substrates, such as the transcription factor Pap1 (Brown et al., 2013). [3] At low concentrations of H_2O_2 in human malignant breast epithelial cells, Prdx1 associates with two MAPK phosphatases, MKP-1 and MKP-5, inhibiting the activity of the MAPK p38, with MKP-1 also dephosphorylating JNK. However, at concentrations of H_2O_2 when Prdx1 is hyperoxidised, Prdx1 dissociates from MKP-1, resulting in oligomerisation and inactivation of MKP-1 towards p38 and JNK. The association between Prdx1 and MKP-5 is maintained even when Prdx1 is hyperoxidised, allowing MKP-5 to dephosphorylate p38 (Turner-Ivey et al., 2013).

towards these other substrates.

[3] Signalling activity/activities of hyperoxidised Prx: Following exposure of cells to high concentrations of H_2O_2, eukaryotic 2-Cys Prx are readily hyperoxidised to a sulphinic acid derivative that cannot be reduced by thioredoxin (Yang et al., 2002). This hyperoxidation is proposed to promote an alternative chaperone activity for Prx (Jang et al., 2004). Hyperoxidation of Tpx1 in *S. pombe* allows thioredoxins to reduce other oxidised proteins, and promote cell survival (Day et al., 2012). However, it also means that there is more reduced Txl1 available to reduce Pap1, inhibiting H_2O_2-induced Pap1 activation. Nevertheless, Sty1 MAPK becomes increasingly activated, in a Tpx1-dependent manner, as H_2O_2 concentrations increase suggesting that hyperoxidised Tpx1 is able to promote Sty1

activation (Veal et al., 2004). Intriguingly, in human malignant breast epithelial cells, hyperoxidation of Prdx1 has been shown to differentially affect the activity of two MAP kinase phosphatases (MKP), MKP-1 and MKP-5, that both dephosphorylate p38α MAPK, but which favour different substrates with MKP-1 also dephosphorylating JNK kinase (Turner-Ivey et al., 2013). Following exposure to high concentrations of H_2O_2, the peroxidatic cysteine of Prdx1 became hyperoxidised, causing it to dissociate from MKP-1. This results in the oligomerisation and inactivation of MKP-1, inhibiting the dephosphorylation of both p38α and JNK MAPKs. In contrast, the Prdx1:MKP-5 complex was maintained, even when Prdx1 was hyperoxidised, protecting MKP-5 from oligomerisation and maintaining its activity towards p38α MAPK. Accordingly, hyperoxidation of Prdx1 provides a mechanism for specifically increasing JNK activity more than p38α MAPK activity at high levels of ROS. Intriguingly, the ability of Prdx1 to protect MKP-1 and MKP-5 from inactivation is consistent with a potential chaperone function for Prdx1. Alternatively, parallels with our studies in yeast suggest that the hyperoxidation of Prdx1 may also increase the thioredoxin available to maintain MKP-5 in an active reduced state.

CONCLUSION

Peroxiredoxins and thioredoxin have multiple redox-signalling activities. Here we have attempted to rationalise the basis for both positive and negative effects of Prx on the activation of MAPK pathways. Some outstanding questions remain, for instance: Is the only role of Prx in promoting ASK1 activity due to a direct 'redox-transducing' role or does Prx also promote ASK1 activation by inhibiting thioredoxin from reducing ASK1? Do Prx participate directly in the oxidative inactivation of PTPs either as redox transducers or by promoting the oxidation of thioredoxin? Why, given the high degree of homology between Prdx1 and Prdx2, do they have apparently different effects on MAPK activation? In addition to maintaining MKP-5 activity, do hyperoxidised Prx have other positive signalling/chaperone activities that promote MAPK activation?

Although inhibiting Prx appears to have different effects on MAPK activation depending on the cell or stimuli, in some cases the use of different stimuli, or time-points at which MAPK activation is assessed, make comparisons between studies difficult. In any case, the consequence of inhibiting Prx in any given cell is likely to be determined by the levels of intracellular ROS and intrinsic features of the cell/compartment, such as the capacity to regenerate reduced Prx, using sulfiredoxin, or thioredoxin, using thioredoxin reductase and NADPH (Fig. 2A). For example, it was recently shown that the regulation of mitochondrial sulfiredoxin levels plays an important role in regulating mitochondrial Prx activity and consequently, cytosolic H_2O_2 levels and p38 activity (Kil et al., 2012; 2015). As several studies have illustrated, relative levels and localisation of Prx, thioredoxin and signalling pathway components will also play an important part (Taniuchi et al., 2015; Woo et al., 2010). Accordingly modelling approaches that take into account all these things, developed using quantitative data obtained in well-characterised systems, such as yeast, are likely to be extremely important for identifying key features regulating MAPK activity and predicting the response of these signalling pathways to changing redox conditions.

ACKNOWLEDGMENTS

We are grateful to Brian Morgan for comments on this manuscript and the BBSRC for funding.

REFERENCES

Bokov, A., Chaudhuri, A., and Richardson, A. (2004). The role of oxidative damage and stress in aging. Mech. Ageing Dev. *125*, 811-826.

Bozonet, S.M., Findlay, V.J., Day, A.M., Cameron, J., Veal, E.A., and Morgan, B.A. (2005). Oxidation of a eukaryotic 2-Cys peroxiredoxin is a molecular switch controlling the transcriptional response to increasing levels of hydrogen peroxide. J. Biol. Chem. *280*, 23319-23327.

Brown, J.D., Day, A.M., Taylor. S.R., Tomalin, L.E., Morgan, B.A., and Veal, E.A.. (2013). A peroxiredoxin promotes H2O2 signaling and oxidative stress resistance by oxidizing a thioredoxin family protein. Cell Rep. *5*, 1425-1435.

Cao, J., Schulte, J., Knight, A., Leslie, N.R., Zagozdzon, A., Bronson, R., Manevich, Y., Beeson, C., and Neumann, C.A. (2009). Prdx1 inhibits tumorigenesis via regulating PTEN/AKT activity. EMBO J. *28*, 1505-1517.

Choi, M.H., Lee, I.K., Kim, G.W., Kim, B.U., Han, Y.H., Yu, D.Y., Park, H.S., Kim, K.Y., Lee, J.S., Choi. C., et al. (2005). Regulation of PDGF signalling and vascular remodelling by peroxiredoxin II. Nature *435*, 347-353.

Conway, J.P., and Kinter, M. (2006). Dual role of peroxiredoxin I in macrophage-derived foam cells. J. Biol. Chem. *281*, 27991-28001.

da Silva Dantas, A., Patterson, M.J., Smith, D.A., Maccallum, D.M., Erwig, L.P., Morgan, B.A., and Quinn, J. (2010). Thioredoxin regulates multiple hydrogen peroxide-induced signaling pathways in Candida albicans. Mol. Cell. Biol. *30*, 4550-4563.

Day, A.M., and Veal, E.A. (2010). Hydrogen peroxide-sensitive cysteines in the Sty1 MAPK regulate the transcriptional response to oxidative stress. J. Biol. Chem. *285*, 7505-7516.

Day, A.M., Brown, J.D., Taylor, S.R., Rand, J.D., Morgan, B.A., and Veal EA. (2012). Inactivation of a peroxiredoxin by hydrogen peroxide is critical for thioredoxin-mediated repair of oxidized proteins and cell survival. Mol. Cell *45*, 398-408.

Gotoh, Y., and Cooper, J.A. (1998). Reactive oxygen species- and dimerization-induced activation of apoptosis signal-regulating kinase 1 in tumor necrosis factor-alpha signal transduction. J. Biol. Chem. *273*, 17477-17482.

Gutteridge, J.M.C., and Halliwell, B. (1999). Free Radicals in Biology and Medicine. (Oxford, UK: Oxford University Press).

Hashimoto, S., Gon, Y., Matsumoto, K., Takeshita, I., and Horie, T. (2001). N-acetylcysteine attenuates TNF-alpha-induced p38 MAP kinase activation and p38 MAP kinase-mediated IL-8 production by human pulmonary vascular endothelial cells. Br J. Pharmacol. *132*, 270-276.

Holmgren, A., and Lu, J. (2010). Thioredoxin and thioredoxin reductase: current research with special reference to human disease. Biochem. Biophys. Res. Commun. *396*, 120-124.

Holmström, K.M., and Finkel, T. (2014). Cellular mechanisms and physiological consequences of redox-dependent signalling. Nat. Rev. Mol. Cell Biol. *15*, 411-421.

Ichijo, H., Nishida, E., Irie, K., ten Dijke, P., Saitoh, M., Moriguchi, T., Takagi, M., Matsumoto, K., Miyazono, K., and Gotoh, Y. (1997). Induction of apoptosis by ASK1, a mammalian MAPKKK that activates SAPK/JNK and p38 signaling pathways. Science *275*, 90-94.

Jang, H.H., Lee, K.O., Chi, Y.H., Jung, B.G., Park, S.K., Park, J.H., Lee, J.R., Lee, S.S., Moon, J.C., Yun, J.W., et al. (2004). Two enzymes in one; two yeast peroxiredoxins display oxidative stress-dependent switching from a peroxidase to a molecular chaperone function. Cell *117*, 625-635.

Jarvis, R.M., Hughes, S.M., and Ledgerwood, E.C. (2012). Peroxiredoxin 1 functions as a signal peroxidase to receive, transduce, and transmit peroxide signals in mammalian cells. Free Radic. Biol. Med. *53*, 1522-1530.

Kang, S.W., Chang, T.S., Lee, T.H., Kim, E.S., Yu, D.Y., and Rhee, S.G. (2004). Cytosolic peroxiredoxin attenuates the activation of Jnk and p38 but potentiates that of Erk in Hela cells stimulated with tumor necrosis factor-alpha. J. Biol. Chem. *279*, 2535-2543.

Kil, I.S., Lee, S.K., Ryu, K.W., Woo, H.A., Hu, M.C., Bae, S.H., and Rhee, S.G. (2012). Feedback control of adrenal steroidogenesis via H2O2-dependent, reversible inactivation of peroxiredoxin III in mitochondria. Mol. Cell *46*, 584-594.

Kil, I.S., Ryu, K.W., Lee, S.K., Kim, J.Y., Chu, S.Y., Kim, J.H., Park,

S., and Rhee, S.G. (2015). Circadian oscillation of sulfiredoxin in the mitochondria. Mol. Cell *59*, 651-663.
Kwon, J., Lee, S.R., Yang, K.S., Ahn, Y., Kim, Y.J., Stadtman, E.R., and Rhee, S.G. (2004). Reversible oxidation and inactivation of the tumor suppressor PTEN in cells stimulated with peptide growth factors. Proc. Natl. Acad. Sci. USA *101*, 16419-16424.
Marshall, C.J. (1994). MAP kinase kinase kinase, MAP kinase kinase and MAP kinase. Curr. Opin. Genet. Dev. *4*, 82-89.
Nadeau, P.J., Charette, S.J., Toledano, M.B., and Landry, J. (2007). Disulfide Bond-mediated multimerization of Ask1 and its reduction by thioredoxin-1 regulate H(2)O(2)-induced c-Jun NH(2)-terminal kinase activation and apoptosis. Mol. Biol. Cell *18*, 3903-3913.
Nadeau, P.J., Charette, S.J., and Landry, J. (2009). REDOX reaction at ASK1-Cys250 is essential for activation of JNK and induction of apoptosis. Mol. Biol. Cell *20*, 3628-3637.
Nguyen, A.N., and Shiozaki, K. (1999). Heat-shock-induced activation of stress MAP kinase is regulated by threonine- and tyrosine-specific phosphatases. Genes Dev. *13*, 1653-1663.
Okazaki, S., Naganuma, A., and Kuge, S. (2005). Peroxiredoxin-mediated redox regulation of the nuclear localization of Yap1, a transcription factor in budding yeast. Antioxid. Redox Signal. *7*, 327-334.
Oláhová, M., Taylor, S.R., Khazaipoul, S., Wang, J., Morgan, B.A., Matsumoto, K., Blackwell, T.K., and Veal, E.A. (2008). A redox-sensitive peroxiredoxin that is important for longevity has tissue- and stress-specific roles in stress resistance. Proc. Natl. Acad. Sci. USA *105*, 19839-19844.
Ross, S.J., Findlay, V.J., Malakasi, P., and Morgan, B.A. (2000). Thioredoxin peroxidase is required for the transcriptional response to oxidative stress in budding yeast. Mol. Biol. Cell *11*, 2631-2642.
Sabio, G., and Davis, R.J. (2014). TNF and MAP kinase signalling pathways. Semin. Immunol. *26*, 237-245.
Saitoh, M., Nishitoh, H., Fujii, M., Takeda, K., Tobiume, K., Sawada, Y., Kawabata, M., Miyazono, K., and Ichijo, H. (1998). Mammalian thioredoxin is a direct inhibitor of apoptosis signal-regulating kinase (ASK) 1. EMBO J. *17*, 2596-2606.
Schwertassek, U., Haque, A., Krishnan, N., Greiner, R., Weingarten, L., Dick, T.P., and Tonks, N.K. (2014). Reactivation of oxidized PTP1B and PTEN by thioredoxin 1. FEBS J, *281*, 3545-3558.
Sobotta, M.C., Liou, W., Stöcker, S., Talwar, D., Oehler, M., Ruppert, T., Scharf, A.N., and Dick, T.P. (2015). Peroxiredoxin-2 and STAT3 form a redox relay for H2O2 signaling. Nat. Chem. Biol. *11*, 64-70.
Taniuchi, K., Furihata, M., Hanazaki, K., Iwasaki, S., Tanaka, K., Shimizu, T., Saito, M., and Saibara, T. (2015). Peroxiredoxin 1 promotes pancreatic cancer cell invasion by modulating p38 MAPK activity. Pancreas *44*, 331-340.
Tobiume, K., Matsuzawa, A., Takahashi, T., Nishitoh, H., Morita, K., Takeda, K., Minowa, O., Miyazono, K., Noda, T., and Ichijo, H. (2001). ASK1 is required for sustained activations of JNK/p38 MAP kinases and apoptosis. EMBO Rep. *2*, 222-228.
Toone, W.M., and Jones, N. (1998). Stress-activated signalling pathways in yeast. Genes Cells *3*, 485-498.
Turner-Ivey, B., Manevich, Y., Schulte, J., Kistner-Griffin, E., Jezierska-Drutel, A., Liu, Y., and Neumann, C.A. (2013). Role for Prdx1 as a specific sensor in redox-regulated senescence in breast cancer. Oncogene *32*, 5302-5314.
Veal, E., and Day, A. (2011). Hydrogen peroxide as a signaling molecule. Antioxid. Redox Signal. *15*, 147-151.
Veal, E.A., Findlay, V.J., Day, A.M., Bozonet, S.M., Evans, J.M., Quinn, J., and Morgan, B.A. (2004). A 2-Cys peroxiredoxin regulates peroxide-induced oxidation and activation of a stress-activated MAP kinase. Mol. Cell *15*, 129-139.
Veal, E.A., Tomalin, L.E., Morgan, B.A., and Day, A.M. (2014). The fission yeast Schizosaccharomyces pombe as a model to understand how peroxiredoxins influence cell responses to hydrogen peroxide. Biochem. Soc. Trans. *42*, 909-916.
Vivancos AP1, Castillo EA, Biteau B, Nicot C, Ayté J, Toledano MB, Hidalgo E. (2005). A cysteine-sulfinic acid in peroxiredoxin regulates H2O2-sensing by the antioxidant Pap1 pathway. Proc. Natl. Acad. Sci. USA *102*, 8875-8880.
Winterbourn, C.C. (2008). Reconciling the chemistry and biology of reactive oxygen species. Nat. Chem. Biol. *4*, 278-286.
Woo, H.A., Yim, S.H., Shin, D.H., Kang, D., Yu, D.Y., and Rhee, S.G. (2010). Inactivation of peroxiredoxin I by phosphorylation allows localized H(2)O(2) accumulation for cell signaling. Cell *140*, 517-528.
Wood, Z.A., Schröder, E., Robin Harris, J., and Poole, L.B. (2003). Structure, mechanism and regulation of peroxiredoxins. Trends Biochem. Sci. *28*, 32-40.
Yang, C.S., Lee, D.S., Song, C.H., An, S.J., Li, S., Kim, J.M., Kim, C.S., Yoo, D.G., Jeon, B.H., Yang, H.Y., et al. (2007). Roles of peroxiredoxin II in the regulation of proinflammatory responses to LPS and protection against endotoxin-induced lethal shock. J. Exp. Med. *204*, 583-594.
Yang, K.S., Kang, S.W., Woo, H.A., Hwang, S.C., Chae, H.Z., Kim, K., and Rhee, S.G. (2002). Inactivation of human peroxiredoxin I during catalysis as the result of the oxidation of the catalytic site cysteine to cysteine-sulfinic acid. J. Biol. Chem. *277*, 38029-38036.